ABSTRACT

Title of Dissertation:	TOWARDS ENERGY EFFICIENT AND ATOM ECONOMICAL CHEMICAL CYCLES FOR NITROGEN FIXATION
	Leila Margaret Duman, Doctor of Philosophy, 2018
Dissertation directed by:	Professor Lawrence R. Sita, Department of Chemistry and Biochemistry

Converting the abundant, but largely inert, dinitrogen (N_2) into the N-containing products upon which society relies (including proteins, explosives, and fertilizers) is a vital synthetic target as the worldwide population, and therefore demand for such commodities, continues to grow. The development of energetically and atomically efficient methods of cleaving, functionalizing, and releasing N_2 as other valuable N-containing products (a process known as fixation) is of the utmost importance to sustainably meet the global demand. Transition-metal-mediated examples of N_2 coordination, activation, cleavage, and N-atom product release are an attractive and active field of study in developing N_2 fixation cycle that operate under mild conditions and consume few resources. Herein, the effects of a sterically reduced pentamethylcyclopentadienyl, amidinate (CPAM) ligand framework around group 6 metal centers (M = Mo, W) are investigated as a means of lowering barriers to reaction

in order to complete a novel N_2 fixation cycle. The design and implementation of this set of reactions are reported, including synthesis and characterization of new dinitrogen and dinitrogen-derived organometallic compounds, as are the groundbreaking thermally mediated N≡N cleavage from dinuclear M(II) (μ-N_2) to M(V) (μ-N)$_2$ dinuclear complexes, N atom functionalization via silylation to form terminal Mo(IV) trimethylsilyl imidos, and a controlled, "dry hydrolysis" with Me_3SiCl and a readily available silanol or alcohol proton source (XOH) to releases hexamethyldisilazane ($HN(SiMe_3)_2$) and a silyl ether ($XOSiMe_3$) while regenerating the M(IV) dichloride starting material. Reactivities within and modifications to this cycle are explored, including the introduction of innovative reagents, and the versatility of the CPAM system is demonstrated while making strides towards more targeted and sustainable means of synthetic N_2 fixation.

TOWARDS ENERGY EFFICIENT AND ATOM ECONOMICAL CHEMICAL CYCLES FOR NITROGEN FIXATION

by

Leila Margaret Duman

Dissertation submitted to the Faculty of the Graduate School of the
University of Maryland, College Park, in partial fulfillment
of the requirements for the degree of
Doctor of Philosophy
2018

Advisory Committee:
Professor Lawrence R. Sita, Chair
Professor Daniel Falvey
Professor Efrain E. Rodriguez
Professor Andrei Vedernikov
Professor Ichiro Takeuchi, Dean's Representative

Dedication

For my parents, to whom I owe all.

Acknowledgements

I am extraordinarily lucky that many people have shared their expertise and encouragement with me in my time as a graduate student. Without this support, the work described in this dissertation would not have been possible.

First and foremost, I wish to thank my Research Advisor, Professor Lawrence Sita, whose direction has provided me with invaluable opportunities and helped me accomplish more than I knew myself capable of. I appreciate not only his guidance in research but also his support in my pursuit of careers outside the lab. His commitment to rigorous and impactful science has allowed me to contribute meaningfully to the field of organometallics and shaped me into the scientist I came to graduate school to be, for which I will always be grateful.

I am also grateful also to the other members of my Committee, Professor Ichiro Takeuchi for graciously serving as my Dean's Representative, and the faculty members of the Chemistry & Biochemistry Department, Professor Daniel Falvey, Professor Efrain Rodriguez, and Professor Andrei Vedernikov. I appreciate their time and attention to my thesis and, in the case of the Chemistry Faculty, their apt instruction and willing help throughout my time in the program.

My progress as a graduate student was made possible by multiple sources of financial support. From the UMD Chemistry & Biochemistry Department, I am thankful for having been awarded the Departmental Dean's Award Research Fellowship, the Graduate School Merit Fellowship, and the Graduate Assistance in Areas of National Need (GAANN) Fellowship. From the UMD Graduate School, I am privileged to have received the Graduate Student Summer Research Award, the All-S.T.A.R. Award, and the Lee Thronton Semester Dissertation Fellowship. Additionally, my research was supported by the National Science Foundation (CHE-1665421) for which I am grateful.

My work could not have been accomplished without the facilities and ready assistance of the department staff. Specifically, Dr. Yiu-Fai Lam, Dr. Yinde Wang, and Dr. Fu Chen for NMR maintenance and related advice, Dr. Yue Li for assistance on Mass Spec, and Dr. Peter Zavalij for expertly obtaining essential XRD data. I am indebted to them for their knowledge and help over the last four years. I would also like to thank Bill Griffin and LaVelle Robinson who kept our lab up and running with gas tanks, chemicals, deliveries, and supplies.

I am very thankful to have had the experiences of serving as a TA for Natalia White, Professor Lawrence Sita, Dr. Lee Friedman, and Dr. Bonnie Dixon, each of whom have shaped my pedagogical philosophy and helped me to grow as an instructor and scientific communicator. As a GAANN Fellow, I am further appreciative of the guidance of Program's Director, Professor Lyle Isaacs, and for the trust, cheer, and continuing support of my Master Teacher, Dr. Bonnie Dixon.

Mention must be made of my alma mater, Bard College, and its Chemistry Department which first fostered my interest in pursuing science professionally. Among the rest of the incomparable “Team Chem,” Professor Craig Anderson, who gave me the first chance to try my hand at research, and Professor Emily McLaughlin, whose good advice it was to start teaching, have been integral to my education and continue to be advisers and advocates for whom I am endlessly grateful.

My thanks go out in perpetuity to all the members of the Sita Lab, past and present, who have helped me through travail and triumph alike. When I began in the lab, I was given the great benefit being trained by now-Professor Wesley Farrell. His work ethic and dedication still motivate me, and I am remarkably lucky to have been his mentee as much of my success can be traced back to his capable tutelage and kind help. Dr. Andrew Keane was also a trailblazer for my research and I am thankful for his astute work and willing aid. Professor Kaitlyn Crawford, Dr. Tessy Ritchie, and Dr. Wonseok Hwang were each great sources of information and encouragement and I am truly grateful for their assistance and advice over the years. I am also thankful for the support of Kätchen Lachmayr, who has been a diligent co-worker and collaborator, and Mark Wallace, whose comradery and partnership on Team-Fix-It has been a buoy and a blessing. I am also glad to have worked with talented undergraduates in the lab, most especially my GAANN mentee, Jocelyn Baer, whose positive attitude and adaptability made many days brighter. Last, I would like to sincerely thank my lab/year-mate, Dr. (!) Samantha Nowak for her company on this journey. I would not have made it through the last four years without her solidarity, study-partnering, and varied diversions. The only thing I am more grateful for than her friendship, upon which I relied throughout grad school, is the certainty of its continuation, and continued growth, in post-grad life.

My deep thanks go to the rest of my friends, colleagues, and mentors. Though the stages of my life so far in Arizona, New York, and Maryland, I have been the recipient of steadfast support from the most wonderful people I could imagine. While too numerous to name individually in this document, I am forever thankful for their heartening presence in my life - I could neither have made it this far nor envision moving forward without them

Finally, thank you, thank you, thank you to my family. The gratitude and respect I have for them can only conceivably be matched by the boundless support and encouragement I receive from them. I am grateful for my extended family and their interest and patience, and for my siblings, Adam Duman, who has benevolently bestowed technological assistance, and Clara Duman, whose visits, enthusiasm, humor, and companionship I treasure. Above all, I appreciate the support of my generous and insightful parents, Denis Duman and Alix Shafer. Their absolute understanding and unconditional encouragement are the foundation upon which I’ve build everything else. “Some peoples’ children”, it transpires, are happily and eternally grateful to be so.

Before we are in the grip of actual dearth the chemist will step in and postpone the day of famine to so distant a period that we, and our sons and grandsons, may legitimately live without undue solicitude for the future…. It is through the laboratory that starvation may ultimately be turned into plenty.

– Sir William Crookes, *The Wheat Problem*

Table of Contents

List of Tables

List of Schemes

List of Figures

List of Abbreviations

° ..... degree
Å ..... angstrom
atm ..... standard atmospheric pressure
BAr^F ..... tetrakis(pentafluorophenyl)borate
BDE ..... bond dissociation energy
cm^{-1} ..... wavenumbers (inverse centimeters)
Cp ..... cyclopentadiene
Cp* ..... pentamethylcyclopentadiene
CPAM ..... petamethylcyclopentadienyl, amidinate
CPGU ..... petamethylcyclopentadienyl, guanidinate
Cy ..... cyclohexyl
depf ..... 1,1,'-bis(diethylphosphino)ferrocene
DME 1,2-dimethoxyethane
e^- ..... electron
ESI-MS ..... electrospray ionization mass spectrometry
Et ..... ethyl
equiv. ..... equivalent(s)
GC/MS ..... gas chromatography/mass spectrometry
H^+ ..... proton
h ..... hours
HOMO ..... highest occupied molecular orbital
iPr ..... isopropyl
kcal ..... kilocalorie
LUMO ..... lowest occupied molecular orbital
Me ..... methyl
mes ..... mesitylene
min ..... minutes
mol ..... mole
mV ..... milivolt
NaHg ..... 0.5% (w/w) sodium amalgam
napth ..... napthyl
NMR ..... nuclear magnetic resonance (spectroscopy)
vs ..... versus
Ph ..... phenyl
ppm ..... parts per million
psi ..... pounds per square inch
sec ..... seconds
tBu ..... tert-butyl
TCE 1,1,2,2-tetrachloroethane
THF ..... tetrahydrofuran
TMS ..... trimethylsilyl
tol ..... tolyl
UV-Vis ..... ultraviolet-visible
XRD ..... X-ray diffraction

Chapter 1: Introduction to Dinitrogen Fixation

1.1 Significance of N_2 Fixation

The reduction of dinitrogen (N_2) is among the most important and widely applicable chemical transformations in the world, converting the gas that composes 78% of the Earth's atmosphere into the atomic building blocks that make life possible. Nitrogen is an essential part of proteins, nucleic acids, pharmaceuticals, explosives, and many other commodity chemicals, but most importantly, it is the principal component of the fertilizers which enables modern agriculture to feed the world. The conversion of N_2 into other N-containing molecules is known as "fixation" and can be accomplished by natural or synthetic means. With the recognition that sustainable generation of N-containing products is critical to the continued growth and development of society on the global scale, chemists have long sought to improve existing methods of N_2 synthetic fixation and develop new ones.

Unfortunately, the principal challenge of N_2 fixation proves to be the inert nature of N_2 itself; for all that gaseous N_2 is a nearly infinite atomic resource that makes up most of the atmosphere, in its dimeric form the element is as inaccessible as it is abundant. Dinitrogen, which consists of two N atoms held together by a strong triple bond, has a high N-N bond dissociation energy (BDE) of 226 kcal/mol.[1] As a result, N_2 fixation is severely limited by the significant energy expenditure required to cleave the N≡N bond in order to incorporate N atoms into other molecules. Further exacerbating the situation, N_2 is non-polar, has low proton

affinity, has a high ionization potential, and has a large HOMO-LUMO gap that inhibits both oxidation and reduction because it is difficult both to remove electrons from the low HOMO or to add them to the much higher LUMO.[2, 3]

For the majority of the world's history, the only means by which any reasonable amount of N_2 was fixed at all was a natural process through bacteria that contain the nitrogenase enzyme, transforming atmospheric N_2, protons (H^+), and electrons (e^-) into bioavailable ammonia (NH_3) according to Scheme 1.1. This

Scheme 1.1

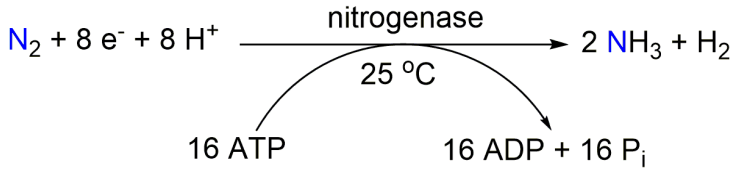

ubiquitous process has is responsible for the natural nitrogen cycle[4] and its importance cannot be overstated. That this transformation occurs under ambient conditions even more remarkable given that the only other natural fixation processes for N_2 occur infrequently, requiring volcanic eruptions or lightning strikes to provide the necessary energy to fix N_2.[5-8] Recent reports indicate that the active site of nitrogenase is the FeMo-cofactor of the enzyme. Its structure, elucidated with significant contribution from the work of Rees and co-workers[9-11] and which is shown in Figure 1.1, consists of an $\alpha_2\beta_2$ tetramer containing a pair of

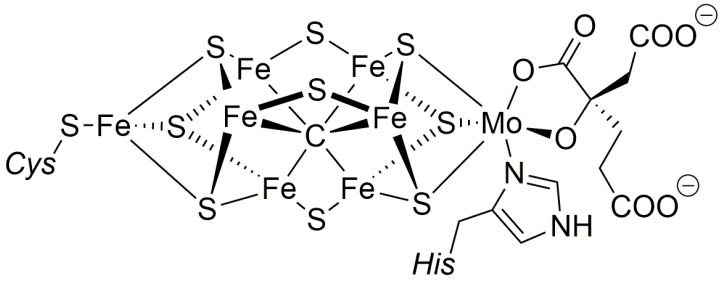

Figure 1.1. Structure of the FeMo cofactor, active site of the nitrogenase enzyme

polynuclear metalloproteins, Fe_4S_3 and $MoFe_3S_3$, which are joined by three S ligands and six internal Fe atoms that surround an interstitial C atom. Despite decades of study, and even the structural clarity of the FeMo-cofactor, the specific mechanism by which nitrogenase accomplishes N_2 fixation remains largely unknown. Some features of the black box reaction, such as the requirement of 16 equivalents of ATP to fuel electron transfer required for reaction and the recognition that evolution of 1 H_2 for each 2 NH_3 fixed, are recognized as key features of the process. Still, a step-by-step understanding of how nitrogenase binds and transforms N_2 remains elusive.[12-18]

Even before the role of nitrogenase was understood, its product, fixed nitrogen, has been recognized as a valuable commodity throughout human history. From agricultural soil fertilization increasing crop yields to the discovery and adoption of N-based explosives such as gunpowder, as human society has grown and developed, so too has the demand for N-containing products. Fixed nitrogen resources were so prized that in the 1800's, countries waged war over the ownership of nitrate-rich coastal lines and islands covered in nitrogen-rich guano.[19] By the turn of the century, the global economy was reliant upon stockpiles of naturally-fixed nitrogen to meet demands of food, explosives, dyes, and other commodities, but these resources were being consumed far more quickly than they could be replaced by nitrogenase alone. As the world's growing population threatened to outstrip ever-dwindling natural resources of fixed nitrogen, a global crisis loomed unless a scalable synthetic approach to dinitrogen fixation could be developed.[19-21]

The solution to this problem came from German chemist Fritz Haber and chemical engineer Carl Bosch who together developed an industrial analogue to nitrogenase, the Haber-Bosch process, which since its introduction a century ago has risen to prominence and re-defined the availability and role of nitrogen in society.[22] The Haber-Bosch process accomplishes the conversion of gaseous N_2 and H_2 into NH_3, shown in Scheme 1.2, by passing the gasses over beds of heterogeneous catalyst, which is typically Fe based, and operates on a massive scale, producing of 175 million metric tons of ammonia annually.[21] This is on par with the amount of nitrogen fixed by nitrogenase and accounts for roughly half of all nitrogen fixed annually on the planet, producing the necessary quantities of NH_3 to act as the industrial precursor to many other N-containing molecules that sustain society today.[23]

Scheme 1.2

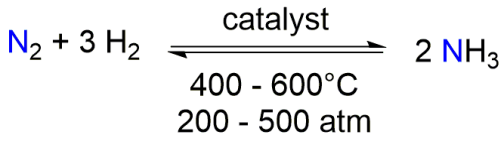

Though wildly successful by many measures, the Haber-Bosch Process is not without flaw. While the reaction is exothermic under standard temperature and pressure, it proceeds so slowly that NH_3 production cannot be observed under these conditions; therefore, while the nitrogenase enzyme fixes N_2 under ambient conditions, the Haber-Bosch Process requires much more harsh reaction conditions of up to 600 °C and 500 atm to proceed efficiently.[24] Furthermore, steam reformation, which generates the H_2 starting material from natural gas, is itself an incredibly costly endeavor, consuming and estimated 1% of the world's annual

energy supply and producing 450 million metric tons of CO_2 per year, accounting for 3% of the world's output.[23, 25, 26] Nevertheless, as the human population continues to grow, so too will the demand for fertilizers and N-containing products.[27, 28] To address this continuing challenge, research in synthetic dinitrogen fixation is founded on the effort to combine the best aspects of the natural N_2 fixation processes of the nitrogenase enzyme and with the highly efficient industrial Haber-Bosch process towards a better understanding of the fundamental reactions by which dinitrogen fixation can best be achieved.

1.2 Synthetic Approach to N_2 Coordination, Activation, and Fixation

1.2.1 Dinitrogen as a Ligand

Organometallic chemists have long sought new homogeneous methods to merge productivity with control, searching for systems that accomplish synthetic nitrogen fixation with high atom economy, chemical efficiency, and under mild conditions in order to minimize both energetic costs and the production of chemical waste. The connection between transition metals and dinitrogen fixation is well established, from Bortells linking Mo to the process of N_2 fixation by bacteria in 1930[29] to the use of Fe-based catalysts in the Haber-Bosch process. Despite the inert nature of N_2, which is neither a good donor nor acceptor, the first N_2 complex $[Ru(NH_3)_5(N_2)]^{2+}$ (**1.1**) was isolated in 1965 by Allen and Senoff,[30] followed in 1966 by the Shilov's discovery of the related $[Ru(NH_3)_4(N_2)]^{2+}$ (**1.2**) derived from the reduction of molecular dinitrogen.[31] Since then, electron rich transition metals have been demonstrated for

over half a century to bind, activate, and even facilitate the fixation of N_2, the study of which has been the subject of substantial review.[3, 32-41]

Transition metal centers can bind to dinitrogen in end-on, side-on, or end-on-side-on modes and if the N≡N bond can be cleaved, they can bind to single N-atoms as well, forming nitrides. Mononuclear and dinuclear configurations of dinitrogen and nitride binding have been reported and are illustrated in Figure 1.2. The extent of dinitrogen activation in a dinuclear organometallic complex is determined by the electron distribution across the M-N-N-M bonds. N_2 coordination ranges from the neutral, triply bonded N≡N, which hardly affects the oxidation state of the metal centers, to the anions of N_2^{2-} and N_2^{4-} which are already partially reduced. Weakly activated N_2 ligands can be displaced in a vacuum or by competition with more coordinating ligands while strongly activated N_2 units are more structurally robust and

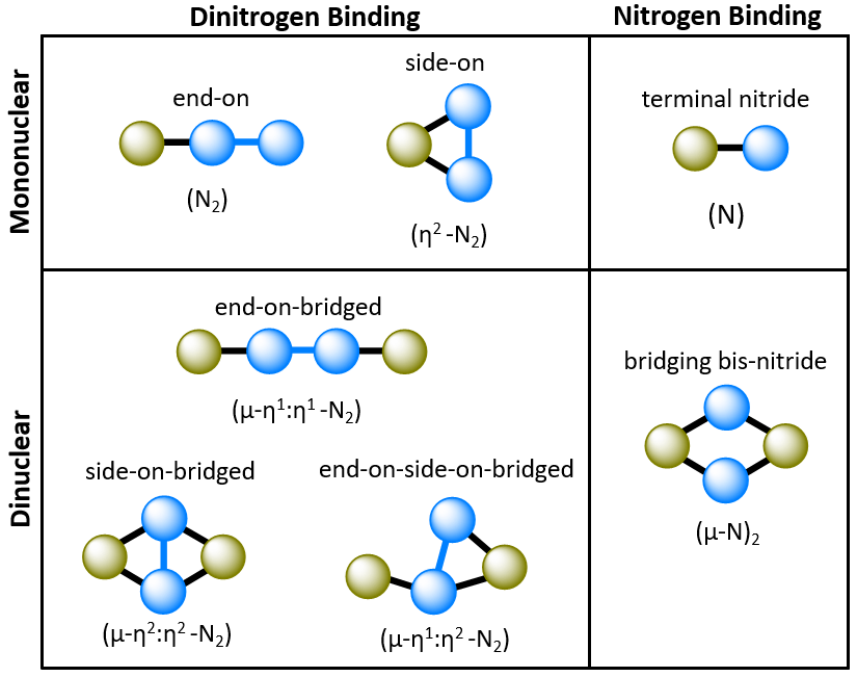

Figure 1.2 Binding modes of dinitrogen and nitrogen atoms (●) with the metal centers of mononuclear and dinuclear organometallic complexes (●)

more reactive towards functionalization. Structural parameters of dinitrogen complexes are typically judged in comparison to the characteristics of free N_2, such as the N-N bond length of 1.0968 Å and the Raman stretching frequency of 2331 cm^{-1}. End-on bridged (μ-η^1:η^1 -N_2) coordination of the N_2 unit to the transition metal centers results in smaller elongation, and thus less significant N≡N bond activation, than side-on (μ-η^2:η^2-N_2) or end-on-side-on (μ-η^2:η^1-N_2) coordination. This is due primarily to strong back-donation from d orbitals of the metal centers to the π^* orbital of the N_2. The stronger the M-N_2 interactions are, the more activated the N≡N bond will be, and the more easily N_2 will undergo functionalization.[3, 42, 43]

1.2.2 Transition Metal Centers

Complete scission of an N≡N bond requires 6 electrons, usually obtained either through external chemical reductants such as alkali metals or from the valence electrons of transition metal complexes, and as such, the identity of the metal center is of the utmost importance to successfully reducing N_2. Group 4 metals are very reducing, and metallocenes in particular have been successful in N_2 fixation, however with a maximum of M(0)d^4, they lack the 6 electrons sufficient to cleave the N≡N bond without added reagents.[38, 44, 45] Group 5 metals have also demonstrated significant activity in terms of N_2 activation and cleavage, though few examples of successful fixation are reported in the literature.[39, 40, 44, 46] Mid-valent group 6 metal centers are in many ways ideal for N_2 fixation. The group 6 metals tend to be more reducing than later transition metals, yet with a greater number of reducing equivalents and thus access to a greater range of oxidation states (of which at least 4 are required to facilitate the multielectron redox of N_2

reduction) than earlier metals.[47] These attributes make Cr, Mo, and W versatile in their scope of possible reactions, however it can also cause difficulties in controlling stability and limiting unproductive side reactions. This is most apparent with Cr, for which there are only a handful of isolated and characterized dinitrogen complexes[48-55] of which only one engages in catalytic N_2 fixation.[56] However, the recalcitrance of Cr to form dinitrogen complexes is in sharp contrast to the lower row metals Mo, which has biomimetic appeal due to its presence in the FeMo-cofactor of nitrogenase, and W, which often undergoes analogous reactivity, which are the subject of much study and even successful fixation. It is these metals, with flexible oxidation state and reductivity, upon which this dissertation will focus.

When designing a system for N_2 reduction, the d electron count of the metal center is among the most influential factors in determining the extent to which N_2 will be activated, reduced, or cleaved. The use of bimetallic complexes is a popular strategy as two metal centers inherently doubles the number of valence electrons available for N_2 reduction. Metals that begins in low oxidation states are more reducing and can access the higher oxidation states necessary to activate and reduce N_2. Care must be taken, however, to avoid the thermodynamic sink of the very strong, terminal M≡N bonds to metal centers of high oxidation state which are the result of N_2 cleavage as these are often unreactive and can hamstring the possibility of releasing N-containing products under mild conditions.[3] Formation of bridging bis-nitride structures, Figure 1.1, obviates this issue to some degree by avoiding the unreactive terminal metal nitride moieties, as does cleavage concomitant to N-atom functionalization which reduces the bond order of the M-N bond.

1.2.3 Impactful Homogeneous Fixation Systems

Though there have now been dozens of examples of catalytic N_2 fixation by organometallic complexes to NH_3 or other N-containing products, several are worthy of particular note. Early reports of stoichiometric N_2 fixation into NH_3 came from the groups of Chatt,[47, 57] Leigh,[58, 59] and Hidai,[60, 61] however the first example of catalytic NH_3 production from N_2 was first achieved in 2003 with Schrock's eponymous cycle, shown in Scheme 1.3. In it, the bulky trisamido amine supported

Scheme 1.3

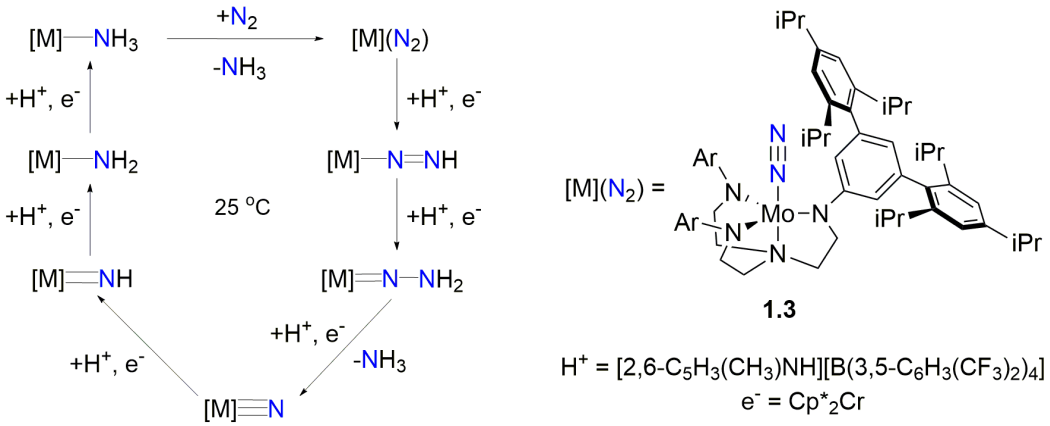

Mo center of {(HIPTNCH$_2$CH$_2$)$_3$NMo(N$_2$)} (HITP = 3,5-C$_6$H$_3$(2,4,6-C$_6$H$_2$iPr$_3$)) (**1.3**) catalyzes formation of 7.6 equiv. NH_3 per Mo through alternating protonation and reduction steps on Mo(III) to Mo(VI) centers. Isolation of 6 of the intermediates depicted in the cycle helped to inform the proposed mechanism in which the distal N atom is first protonated and released as NH_3 after which the nitride follows suit.[62] This is evocative of the Chatt cycle, a proposed progression of proton and electron addition to a coordinated dinitrogen unit (M-N≡N) which transforms through diazeniod (M-N=NH), hydrazido (M=N-NH$_2$), nitrido (M≡N), imido (M=NH), and amido (N-NH$_2$) functionalities to release 2 equiv. NH_3 but it typically envisioned

to operate between Mo(0) and Mo(IV) oxidation states.[13, 47] Building on this applied success, in 2011 the Peters group was able to demonstrate that iron, also present in the FeMo-cofactor of nitrogenase, is also catalytically active with their tris(phosphine)borane supported mononuclear complex [(TBP)Fe(N_2)][Na(12-crown-4)$_2$] (TBP = B(2-$C_6H_4PiPr_2$)$_3$) (**1.4**) that undergoes reductive protonation to yield 64 equiv. NH_3 at very low temperatures, shown in Scheme 1.4.[63, 64] Fe has tended to be less popular than Mo as a metal center for fixation, however, due primarily to a less flexible range of oxidation states.[59] Even more recently, the Nishibayashi group has made great strides in increasing the turnover of Mo complexes[65, 66] having developed an N-hetrerocyclic carbene and phosphine and based PCP-pincer supported dimolybdenum catalyst {(PCP)Mo(N_2)$_2$}(μ-η^1:η^1:N_2) (**1.5**) in 2017 that is able to catalytically form up to 115 equiv. NH_3 per Mo, shown in Scheme 1.4.[67] This is the highest reported yield of NH_3 directly produced by a transition metal catalyst, though there are other fruitful avenues have been investigated including the production of N($SiMe_3$)$_3$ in high turnover (*to be*

Scheme 1.4

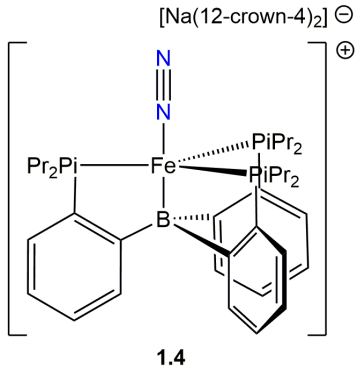

1.4

N_2 + 6 e^- + 6 H^+ —catalyst, -78 °C→ 2 NH_3

H^+ = $HBAr^F$· 2 Et_2O

e^- = KC_8

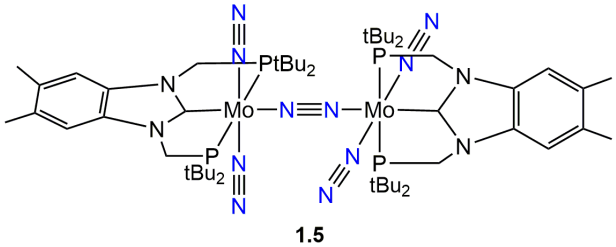

1.5

N_2 + 6 e^- + 6 H^+ —catalyst, 25 °C→ 2 NH_3

H^+ = [2,6-$C_5H_3(CH_3)NH$][CF_3SO_2]

e^- = Cp^*_2Cr

examined in Chapter 4), and demonstrates the significant progress that has been made in the field in only 15 years.

Not all N-fixation studies are focused directly on the production of NH_3, however; seminal work by Cummins in 1995 demonstrated the first example of thermally mediated N≡N cleavage in a group 6 complex. As is revealed in Scheme 1.5,

Scheme 1.5

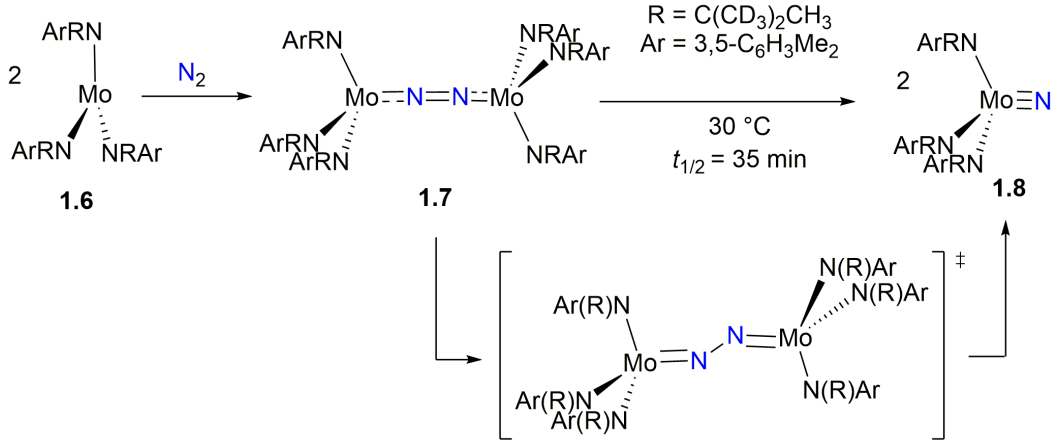

at sub-ambient temperatures a bulky tris amine supported molybdenum species{$(ArR)_3Mo$} (Ar = 3,5-$C_6H_3Me_2$, R = $C(CD_3)_2CH_3$) (**1.6**) can coordinate N_2 to become the dinuclear {$(ArR)_3Mo$}(μ-η^1:η^1:N_2) (Ar = 3,5-$C_6H_3Me_2$, R = $C(CD_3)_2CH_3$) (**1.7**). This Mo(III) complex moves through a proposed "zig-zag" transition state in the rate determining step to form a pair of terminal nitrides, {$(ArR)_3Mo(N)$} (**1.8**).[68, 69] While this was an unmatched accomplishment in terms of cleaving N_2 under mild conditions, the production of the strongly bound nitride **1.8** posed significant difficulty in its subsequent functionalization and release. Only upon its reaction with the strong electrophile trimethylsilyl triflate ([Me_3Si][CF_3SO_2]), benzoyl chloride, and a catalytic amount of pyridine could **1.8** be converted to an alkylimido salt $[(ArR)_3Mo(NC(O)Ph]^+$ (**1.9**) which could be reduced by magnesium anthracene and trimethylsilyl triflate to

the trimethylsilyl (TMS) substituted ketamide {(ArR)$_3$Mo(NC(OSiMe$_3$)R'} (**1.10**). Upon treatment with $SnCl_2$ or $ZnCl_2$, **1.10** returns to the chloride precursor {(ArR)$_3$MoCl} (**1.11**) while releasing a value-added nitriles, PhCN, according to Scheme 1.6. Other nitriles, MeCN and tBuCN, could be produced but only under

Scheme 1.6

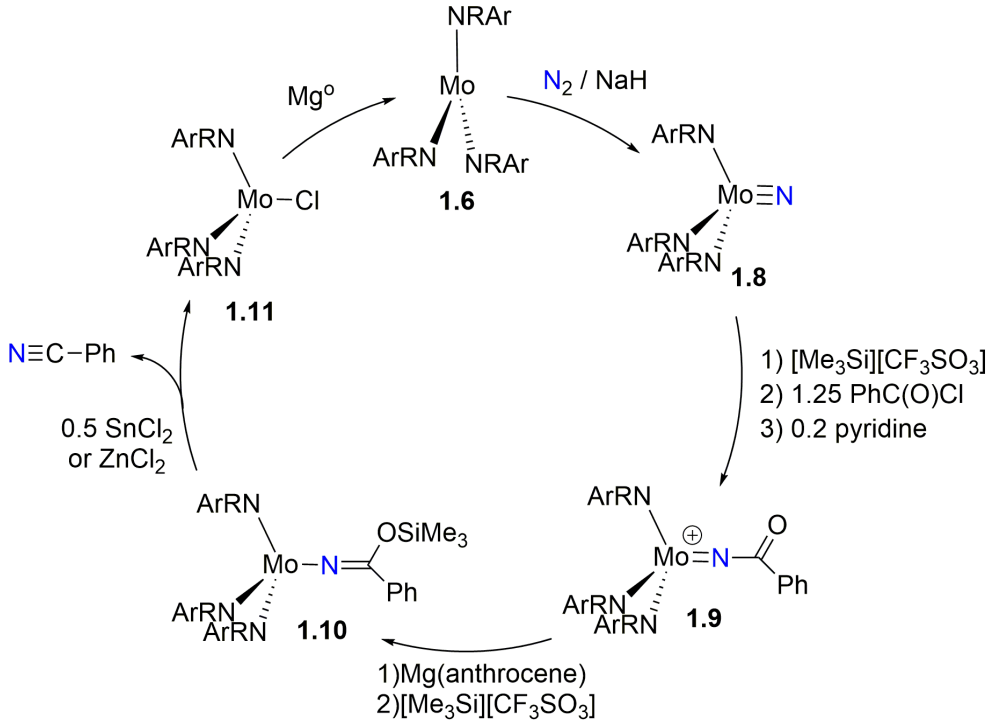

different conditions.[70] The formation of a N-C bond instead of an N-H bond to generate value-added organic nitriles is an important and different approach from the limited pursuit of NH_3 in that the it is the direct synthesis of a N-atom product that does not require protons, however this cycle requires specialized and harsh reagents and is not very adaptable towards substitution. Many other alternatives to NH_3 or even nitriles are produced in similarly complex synthetic pathways, including amines, carbodiimides, and isocyanates.

Finally, hough there is a dearth of examples in the literature of thermally mediated N_2 cleavage from group 6 centers besides Cummins's original example,[68] photolysis is a viable alternative route to overcoming the significant energy expenditure required to break the N_2 bond. Photolysis has been employed by the Florani,[71] Cummins,[72] and Nishibayashi[73] groups to cleave the N≡N bond of the respective dimolybdenum, end-on-bridged dinitrogen species $\{Mes_3Mo\}(\mu\text{-}\eta^1{:}\eta^1{:}N_2)$ (Mes = 2,4,6-$C_6H_2Me_3$) (**1.12**), (**1.7**), and $\{Cp^*Mo(depf)_2\}(\mu\text{-}\eta^1{:}\eta^1{:}N_2)$ (depf = 1,1,'-bis(diethylphosphino)- ferrocene)) (**1.13**) which upon photolysis form pairs of mononuclear terminal nitrides $\{Mes_3Mo(N)\}$ (**1.4**), $\{(ArR)_3Mo(N)\}$ (**1.8**), and $\{Cp^*Mo(depf)_2(N)\}$ (**1.15**), respectively, according to Scheme 1.7. This is an important strategy because it can employ photolysis in the difficult but necessary step of fixation, breaking the N_2 bond, in lieu of external reductants that can complicate subsequent reactivites.[74, 75]

Scheme 1.7

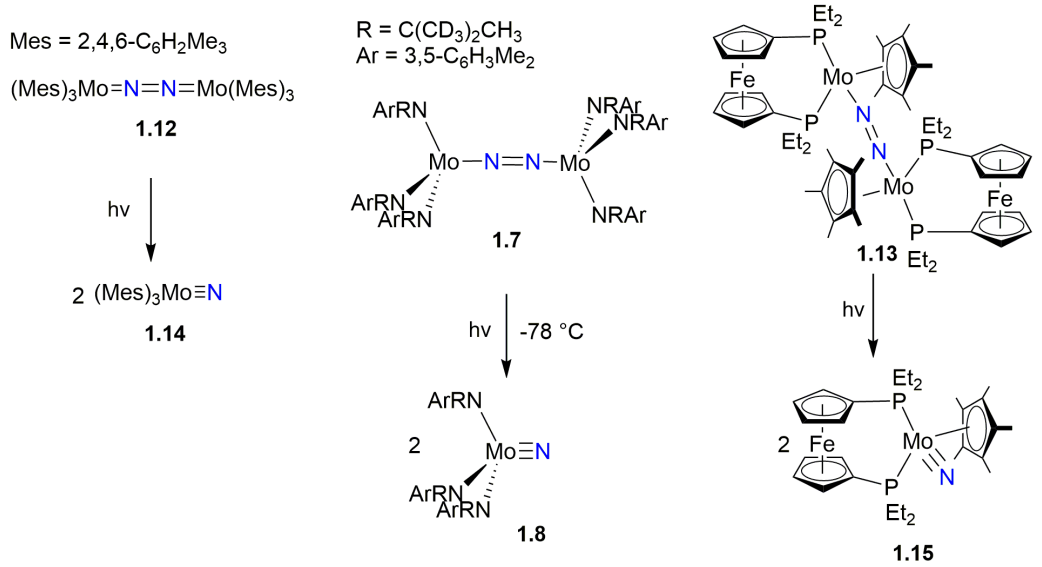

1.3 The CPAM Ligand Set

As is by now evident, successful N_2 activation and fixation is the result of a careful balance of many features including not only the identity of the metal and its oxidation state, but also, at least as importantly, the steric, electronic, and redox features of the supporting ligand platform. Certain trends (ranging from sandwich complexes to pincer ligands to electron donating moieties to name a few)[65, 67, 76-82] are popular in terms of supporting dinitrogen complexes. One oft-employed support for small molecule activation by transition metals is the monoanionic cyclopentadienyl (Cp) ligand. Usually coordinated in η^5 hapticity, it provides 6 e^- to the metal center and makes available a wide variety of derivates based on the substituents of the Cp ring, very commonly the sterically demanding pentamethylcyclopentadienyl (Cp*).[82, 83] Another commonly used class of ligands for early transition metals is the monoanionic, 4 electron-donating amidinate, [N(R')C(R)N(R")], which can be symmetrical or asymmetrical with regard to its ancillary, N-atom substituents (R' and R") and its distal C-atom substituent (R). These easily tunable moieties often coordinate in κ^1 or κ^2 denticity.[84-86] Still, for all of the examples of N_2 activation and fixation now in the literature, there are nearly as many unique ligand frameworks supporting the organometallic complexes, and the lack of ligand continuity from metal to metal and the many disparate ligand designs employed mean that there is a distinct and unfortunate lack of organized understanding with regards to the relationship between ligand design and resulting small molecule activation.[87]

Over the past decade, the Sita Research Group has systematically employed the pentamethylcyclopentadienyl, amidinate (CPAM) ligand set, shown in Figure 1.3, across the early transition metals to establish a series of analogous complexes

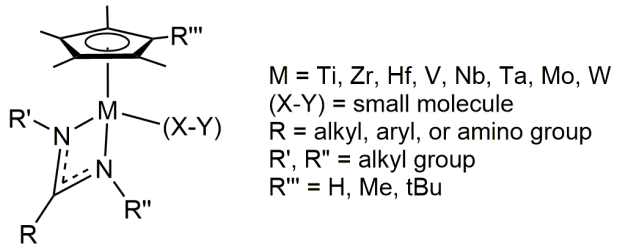

Figure 1.3. CPAM framework and possible substitutions

working towards a set of "first principles" for ligand design. The uncommon adaptability of this CPAM system is derived from the unique but complementary steric and electronic features of the Cp* and amidinate ligand environment; particularly, the ease with which the Cp* and amidinate substituents (R''', and R, R', or R'' respectively) can be modified to achieve desired structural results. Initially, the CPAM platform was used in Ziegler-Natta-type polyolefin synthesis where its ease of tuneability gave rise to chirality and asymmetric conversions.[88-92] More recently, the framework has also been employed on group 4, 5, and 6 metal centers to study the fundamental activation and cleavage of N_2 across the early transition metals, generating readily comparable dinuclear Ti, Zr, Hf, V, Nb, Ta, Mo, and W dinitrogen complexes,[45, 46, 93-96] selected examples of which are shown in Figure 1.4 ($\{Cp^*[N(iPr)C(Me)N(iPr)]Ti\}_2(\mu\text{-}\eta^1\text{:}\eta^1\text{-}N_2$) (**1.16**) for titanium, $\{Cp^*[N(iPr)C(NMe_2)N(iPr)]Zr\}_2(\mu\text{-}\eta^2\text{:}\eta^2\text{-}N_2$) (**1.17**) for zirconium, $\{Cp^*[N(iPr)C(Me)N(iPr)]Hf\}_2(\mu\text{-}\eta^2\text{:}\eta^2\text{-}N_2$) (**1.18a**) for hafnium, $\{Cp^*[N(iPr)C(Me)N(iPr)]V\}_2(\mu\text{-}\eta^1\text{:}\eta^1\text{-}N_2$) (**1.19**) for vanadium, $\{Cp^*[N(iPr)C(Ph)N(iPr)]Nb\}_2(\mu\text{-}\eta^1\text{:}\eta^1\text{-}N_2$) (**1.20**) for niobium,

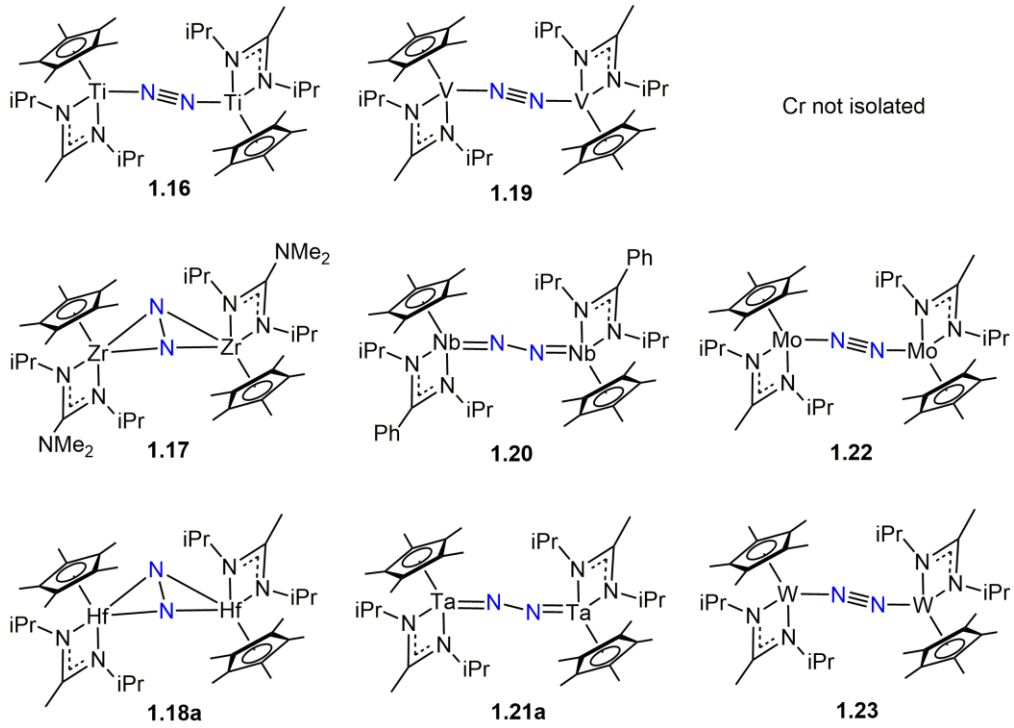

Figure 1.4. Selected isostructural dinuclear CPAM dinitrogen complexes spanning groups 4, 5, and 6

{Cp*[N(iPr)C(Me)N(iPr)]Ta}$_2$(μ-η^1:η^1-N$_2$) (**1.21a**) for tantalum, {Cp*[N(iPr)C(Me)N(iPr)]Mo}$_2$(μ-η^1:η^1-N$_2$) (**1.22**) for molybdenum, and {Cp*[N(iPr)C(Me)N(iPr)]W}$_2$(μ-η^1:η^1-N$_2$) (**1.16**) for tungsten). Within this remarkable isostructural series, it has been observed that decreases in the steric demands of the CPAM framework correspond to an increase in N$_2$ activation and reactivity (*this correlation is discussed in greater detail in Chapter 2.1*). Additionally, the compounds with heavier metal centers tend to be more stable than the earlier row counterparts. These findings illustrate how desired coordination, activation, and reactivity (including hydrogenation, hydrosilylation, bromination, alkylation, silylation, and cleavage of the N$_2$ unit) may be specifically targeted by tuning the CPAM ligand set and metal center combination.

1.4 CPAM N_2 Fixation Cycle

In 2015, the Sita group combined several well-characterized reactions into a chemical cycle for fixing N_2 by Mo or W CPAM complexes, shown in Scheme 1.8.[94] The first step is the dinitrogen reduction of dichloride

Scheme 1.8

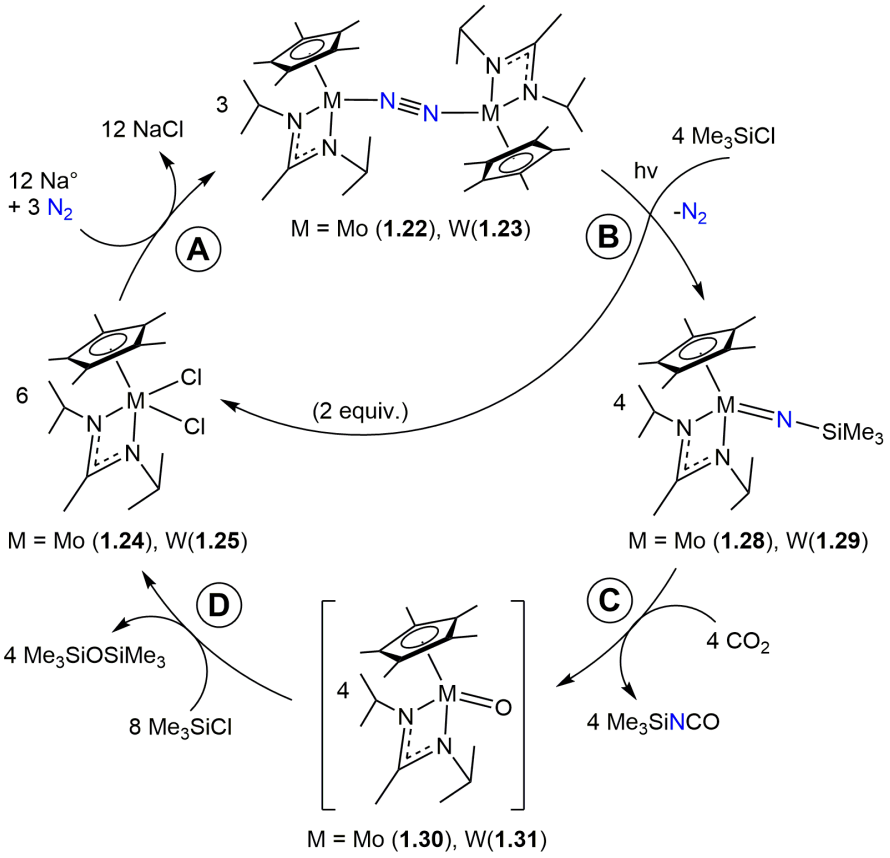

{Cp*[N(iPr)C(Me)N(iPr)]MCl_2}, M = Mo (**1.24**), W, (**1.25**), to end-on-bridged dinitrogen complexes {Cp*[N(iPr)C(Me)N(iPr)]M}$_2$(μ-η^1:η^1-N_2), M = Mo (**1.22**), W, (**1.23**) by sodium amalgam (NaHg) in Step A. These complexes are thermally stable but will undergo photolytic cleavage of the N≡N bond in a Rayonet® Photochemical Reactor containing medium-pressure Hg lamps according to Scheme 1.9. This is believed to be an intramolecular rearrangement and the structures of the resulting bridging bis-nitride complexes

Scheme 1.9

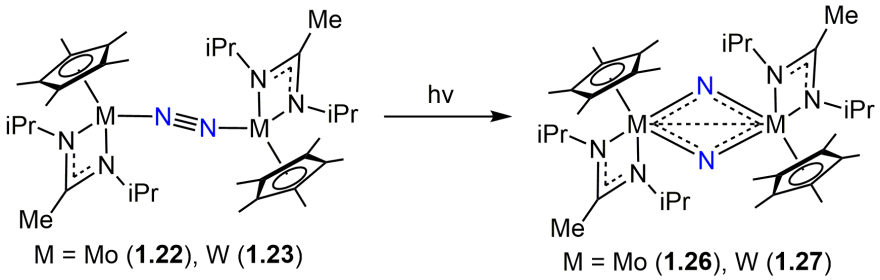

M = Mo (**1.22**), W (**1.23**)

M = Mo (**1.26**), W (**1.27**)

{Cp*[N(iPr)C(Me)N(iPr)]M(μ-N_2)}$_2$M = Mo (**1.26**), W, (**1.27**) are unique among reported group 6 nitrides. Functionalization of **1.26** or **1.27** can be accomplished through facile silylation by Me_3SiCl to form silylimidos {Cp*[N(iPr)C(Me)N(iPr)]M($NSiMe_3$)}, Mo (**1.28**), W, (**1.29**), in a 2 : 1 ratio with the dichloride starting materials, **1.24** or **1.25**, respectively. Step B, which combines the N_2 cleavage and silylation, is followed by Step C, release of the N-atom product facilitated by treatment of **1.28** or **1.29** with CO_2. This releases an isocyanate, $OCNSiMe_3$, through simultaneous oxygen atom and nitrene group transfer, while concomitantly converting the CPAM complex to a terminal oxo Cp*[N(iPr)C(Me)N(iPr)]M(O)}, Mo (**1.30**), W, (**1.31**). In step D, the oxo is cleanly converted back to the starting dichloride by reaction with Me_3SiCl to generate hexamethyldisiloxane ($O(SiMe_3)_2$).

This cycle produces an industrially valuable N-containing product in an alternative to typical ammonia-targeted fixation, and each step has been thoroughly investigated; however, there are a few notable ways in which the chemistry that drives Scheme 1.8 could be improved. First, the requirement of photolysis for N_2 cleavage is not ideal – the reaction requires many days and significantly more energy than thermal cleavage under ambient conditions would. Second, the use of

CO_2 to release the isocyanate inhibits further reaction; if any CO_2 lingers in the reaction vessel, it will compete with N_2 for coordination to the metal centers forming carbonyl complexes. Third, there a loss of N_2 in the silylation step B which lowers formal atom economy despite the fact that the N_2 could be re-reduced with the dichloride side product to re-enter the cycle. Overall, up to 50% of the metal could be recovered as the dichlorides and the cycle is certainly successful in fixing N_2 into a value-added product, but in its current form, it remains a series of chemical reactions and not yet a catalytic cycle.

1.5 Goals of the Thesis

The overall goal of this dissertation was to continue to map out the chemistry of CPAM Mo and W dinitrogen complexes to obviate or lessen the chemical challenges of Scheme 1.8 and thereby move closer to achieving a catalytic cycle. The work described herein has therefore aimed to 1) systematically substitute and reduce the sterics of the CPAM ligand framework to 2) increase reactivity at the Mo or W metal centers of these complexes, lowering the barriers to reaction in order to 3) investigate and optimize demonstrated cycles and 4) explore new chemical reagents to establish new fixation pathways. Beyond the scope of academic interest, the development of chemically and energetically efficient N_2 fixation processes is an imperative issue for modern life, and the better understanding chemists can acquire about how these reactions can be tuned, the more sustainable, energy efficient, and atom economical N_2 fixation processes will become in the long term.

References

1. Darwent, B. d. *Bond Dissociation Energies in Simple Molecules*. National Bureau of Standards: Washington, D. C, 1970.
2. Jia, H. P.; Quadrelli, E. A. Mechanistic aspects of dinitrogen cleavage and hydrogenation to produce ammonia in catalysis and organometallic chemistry: relevance of metal hydride bonds and dihydrogen. *Chem. Soc. Rev.* **2014,** *43*, 547-564.
3. Chatt, J. Molecular Nitrogen as a Ligand. *Pure. Appl. Chem.* **1970,** *24*, 425-441.
4. Simon, J.; Kroneck, P. M. H. The production of ammonia by multiheme cytochromes c. *Met Ions Life Sci.* **2014,** *14*, 211-236.
5. Navarro-González, R. M., M. J.; Molina, L. T. Nitrogen fixation by volcanic lightning in the early Earth. *Geophys. Res. Lett.* **1998,** *25*, 3123-3126.
6. Hill, R. D.; Rinker, R. G.; Wilson, H. D. Atmospheric Nitrogen Fixation by Lightining. *J. Atmospheric Sci.* **1980,** *37*, 179-192.
7. Drapcho, D. L.; Sisterson, D.; Kumar, R. Nitrogen fixation by lightning activity in a thunderstorm. *Atmospheric Environ.* **1983,** *17*, 729-734.
8. Aizawa, K.; Cimarelli, C.; Alatorre-Ibargüengoitia, M. A.; Yokoo, A.; Dingwell, D. B.; Iguchi, M. Physical properties of volcanic lightning: Constraints from magnetotelluric and video observations at Sakurajima volcano, Japan. *Earth Planet. Sci. Lett.* **2016,** *444*, 45-55.
9. Einsle, O.; Tezcan, F. A.; Andrade, S. L. A.; Schmid, D.; Yoshida, M.; Howard, J. B.; Rees, D. C. Nitrogenase MoFe-protein at 1.16 Å resolution: A central ligand in the FeMo-cofactor *Science* **2002,** *298*, 1696-1700.
10. Spatzal, T.; Aksoyoglu, M.; Zhang, L.; Andrade, S. L. A.; Schleicher, E.; Weber, S.; Rees, D. C.; Einsle, O. Evidence for interstitial carbon in nitrogenase FeMo cofactor. *Science* **2011,** *334*, 940.
11. Spatzal, T.; Perez, K. A.; Einsle, O.; Howard, J. B.; C., R. D. Ligand binding to the FeMo-cofactor: Structures of CO-bound and reactivated nitrogenase. *Science* **2014,** *345*, 1620-1623.
12. Burgess, B. K.; Lowe, D. J. Mechanism of Molybdenum Nitrogenase. *Chem. Rev.* **1996,** *96*, 2983-3011.
13. Pickett, C. J. The Chatt cycle and the mechanism of enzymic reduction of molecular nitrogen. *J. Biol. Inorg. Chem.* **1996,** *1*, 601-606.
14. Seefeldt, L. C.; Hoffman, B. M.; Dean, D. R. Mechanism of Mo-Dependent Nitrogenase. *Annual Review of Biochemistry* **2009,** *78*, 701-722.
15. Lukayanov, D.; Yang, Z. Y.; Barney, B. M.; Dean, D. R.; Seefeldt, L. C.; Hoffman, B. M. Unification of reaction pathway and kinetic scheme for N_2 reduction catalyzed by nitrogenase. *Proc. Natl. Acad. Sci. U.S.A.* **2012,** *109*, 5583-5587.
16. Howard, J. B.; Rees, D. C. How many metals does it take to fix N_2? A mechanistic overview of biological nitrogen fixation. *Proc. Natl. Acad. Sci. U.S.A.* **2014,** *103*, 17088-17093.
17. Lukayanov, D.; Khadka, N.; Yang, Z. Y.; Dean, D. R.; Seefeldt, L. C.; Hoffman, B. M., Reductive Elimination of H_2 Activates Nitrogenase to Reduce

the N≡N Triple Bond: Characterization of the E4(4H) Janus Intermediate in Wild-Type Enzyme *J. Am. Chem. Soc.* **2016,** *138*, 10674-10683.
18. Mus, F.; Alleman, A. B.; Pence, N.; Seefeldt, L. C.; Peters, J. W. Exploring the alternatives of biological nitrogen fixation. *Metallomics* **2018,** *10*, 523-538.
19. Farcau, B. W. *The ten cents war*. Praeger: Westprot, CT, **2000**.
20. Crookes, W. *The Wheat Problem*. Longmans, Green, and Co.: London, **1917**.
21. Smil, V. Detonator of the population explosion. *Nature* **1999,** *400*, 415.
22. Nørskov, J.; Chen, J. Sustainable Ammonia Synthesis: Exploring the scientific challenges associated with discovering alternative, sustainable processes for ammonia production. U.S. Department of Energy: Dulles, VA, **2016**.
23. Smil, V. *Enriching the Earth: Fritz Haber, Carl Bosch, and the Transformation of World Food Production*. MIT Press: Cambridge, MA, 2001.
24. Schlögl, R. Ammonia Synthesis. In *Handbook of Heterogeneous Catalysis*, Wiley Online Library: 2008.
25. MacKay, B. A.; Fryzuk, M. D. Dinitrogen Coordination Chemistry: On the Biomimetic Borderlands. *Chem. Rev.* **2004,** *104*, 385-401.
26. Bezdek, M. J.; Chirik, P. J. Expanding Boundaries: N_2 Cleavage and Functionalization beyond Early Transition Metals. *Angew. Chem. Int. Ed.* **2016,** *55*, 7892-7896.
27. Gruber, N.; Galloway, J. N. An Earth-system perspective of the global nitrogen cycle. *Nature* **2008,** *451*, 293-296.
28. *2017 Revision of World Population Prospects*; United Nations Population Division: **2017**.
29. Bortells, H. Molybdenum as a catalyst in biological nitrogen bonding. *Arch. Mikrobiol.* **1930,** *1*, 333-342.
30. Allen, A. D.; Senoff, C. W. Nitrogenpentammineruthenium(II) complexes. *Chem. Commun.* **1965**, 621-622.
31. Shilov, A. E.; Shilova, A.; Borod'ko, Y. G. *Kinetik i Kataliz* **1966,** *7*, 768.
32. Allen, A. D.; Senoff, C. V. Nitrogenopentammineruthenium(II) complexes. *Chem. Commun.* **1965,** *0*, 621-622.
33. Tanabe, Y.; Nishibayashi, Y. Catalytic Dinitrogen Fixation to Form Ammonia at Ambient Reaction Conditions Using Transition Metal-Dinitrogen Complexes. **2016,** *16*, 1549-1577.
34. Stucke, N.; Flöser, B. M.; Weirich, T.; Tuczek, F. Nitrogen Fixation Catalyzed by Transition Metal Complexes: Recent Developments. *Eur. J. Inorg. Chem.* **2018**, 1337–1355.
35. Y., R.; Duboc, C.; Gennari M. Molecular Catalysts for N_2 Reduction :State of the Art, Mechanism, and Challenges. *Chem. Phys. Chem.* **2017,** *18*, 2606-2617.
36. Fryzuk, M. D.; Johnson, S. A. The continuing story of dinitrogen activation. *Coord. Chem. Rev.* **2000,** *200-202*, 379-409.
37. Tanabe, Y.; Nishibayashi, Y. Developing more sustainable processes for ammonia synthesis. *Coord. Chem. Rev.* **2013,** *257*, 2551-2564.
38. Ohki, Y.; Fryzuk, M. D. Dinitrogen activation by group 4 metal complexes. *Angew. Chem. Int. Ed.* **2007,** *46*, 3180-3183.

39. Duman, L. M.; Sita, L. R. Group 5 transition metal-dinitrogen complexes. In *Transition Metal-Dinitrogen Complexes: Preparation and Reactivity*, Nishibayashi, Y., Ed. Wiley-VCH: Weinheim, **2018**; Vol. Accepted.
40. Nishibayashi, Y. E. *Topics in Organometallic Chemistry*. Springer Verlag: Berlin/Heidelberg, **2017**; Vol. 60.
41. Poveda, A.; Perilla, I. C.; Perez, C. R. Review: Some considerations about coordination compounds with end-on dinitrogen. *J. Coord. Chem.* **2001,** *54*, 427-440.
42. Zhang, W. C.; Tang, Y. H.; Lei, M.; Morokuma, K.; Musaev, D. G. Ditantalum Dinitrogen Complex: Reaction of H2 Molecule with "End-on-Bridged" [Ta(IV)2(μ-η(1): η(1)-N2) and Bis(μ-nitrido) [Ta(V)]2(μ-N)2 Complexes. *Inorganic Chemistry* **2011,** *50* (19), 9481-9490.
43. Burford, R. J.; Fryzuk, M. D. Examining the relationship between coordination mode and reactivity of dinitrogen. *Nat. Rev. Chem.* **2017,** *1*, 26.
44. Burford, R. J.; Yeo, A.; Fryzuk, M. D. Dinitrogen activation by group 4 and group 5 metal complexes supported by phosphine-amido containing ligand manifolds. *Coord. Chem. Rev.* **2017,** *334*, 84-99.
45. Hirotsu, M.; Fontaine, P. P.; Zavalij, P. Y.; Sita, L. R. Extreme N equivalent to N bond elongation and facile N-atom functionalization reactions within two structurally versatile new families of group 4 bimetallic "Side-on-Bridged" dimitrogen complexes for zirconium and hafnium. *J. Am. Chem. Soc.* **2007,** *129*, 12690-12692.
46. Keane, A. J.; Yonke, B. L.; Hirotsu, M.; Zavalij, P. Y.; Sita, L. R. Fine-Tuning the Energy Barrier for Metal-Mediated Dinitrogen N≡N Bond Cleavage. *J. Am. Chem. Soc.***2014,** *136*, 9906-9909.
47. Chatt, J.; Dilworth, J. R.; Richards, R. L. Recent advances in the chemistry of nitrogen fixation. *Chem. Rev.* **1978,** *78*, 589-625.
48. Mock, M. T.; Chen, S.; Rousseau, R.; O'Hagan, M. J.; Dougherty, W. G.; Kassel, W. S.; DuBois, D. L.; Bullock, R. M. A rare terminal dinitrogen complex of chromium. *Chem. Commun.* **2011,** *47*, 12212-12214.
49. Vidyaratne, I.; Scott, J.; Gambarotta, S.; Budzelaar, P. H. M. Dinitrogen Activation, Partial Reduction, and Formation of Coordinated Imide Promoted by a Chromium Diiminepyridine Complex. *Inorg. Chem.* **2007,** *46*, 7040-4049.
50. Sellman, D. M., G. Systematic Synthesis of N_2-Complexes: Further N_2-Complexes of Chromium. *Z. Naturforsch.* **1972,** *27B*, 718-719.
51. Denholm, S.; Hunter, G.; Weakley, T. J. R. Dinitrogen complexes derived from tricarbonyl(η^6-hexaethylbenzene)chromium(0): crystal and molecular structure of μ-dinitrogenbis[dicarbonyl(η^6-hexaethylbenzene)chromium(0)]-toluene (1/1). *J. Chem. Soc., Dalton Trans* **1987**, 2789-2792.
52. Monillas, W. H.; Yap, G. P. A.; MacAdams, L. A.; Theopold, K. H. Binding and Activation of Small Molecules by Three-Coordinate Cr(I). *J. Am. Chem. Soc.* **2007,** *129*, 8090-8091.
53. Berben, L. A.; Kozimor, S. A. Dinitrogen and Acetylide Complexes of Low-Valent Chromium. *Inorg. Chem.* **2008,** *47*, 6438-4647.
54. Hoffert, W. A.; Rappe, A. K.; Shores, M. P. Unusual Electronic Effects Imparted by Bridging Dinitrogen: an Experimental and Theoretical Investigation. *Inorg. Chem.* **2010,** *49*, 9497-9507.

55. López-Alcalá, J. M.; Puerta, M. C.; González-Vílchez, F. Dinitrogen complexes of chromium(III) with chelating agents. *Transition Met. Chem.* **1985,** *10*, 247-248.
56. Kendall, A. J.; Johnson, S. I.; Bullock, R. M.; Mock, M. T. Catalytic Silylation of N_2 and Synthesis of NH_3 and N_2H_4 by Net Hydrogen Atom Transfer Reactions Using a Chromium P_4 Macrocycle. *J. Am. Chem. Soc.* **2018,** *140*, 2528-2536.
57. Chatt, J.; Pearman, A. J.; Richards, R. L. The reduction of mono-coordinated molecular nitrogen to ammonia in a protic environment. *Nature* **1975,** *253*, 39-40.
58. Leigh, G. J.; Prietoalcon, R.; Sanders, J. R. The Protonation of Bridging Dinitrogen to Yield Ammonia. *ChemComm.* **1991,** *0*, 921-922.
59. Leigh, G. J. Protonation of coordinated dinitrogen. *Acc. Chem. Res.* **1992,** *25*, 177-181.
60. Hidai, M. Chemical nitrogen fixation by molybdenum and tungsten complexes. *Coord. Chem. Rev.* **1999,** *185-186*, 99-108.
61. Hidai, M.; Mizobe, Y. Recent Advances in the Chemistry of Dinitrogen Complexes. *Chem. Rev.* **1995,** *95*, 1115-1133.
62. Yandulov, R. R.; Schrock, R. R. Catalytic Reduction of Dinitrogen to Ammonia at a Single Molybdenum Center. *Science* **2003,** *301*, 67-78.
63. Anderson, J. S.; Rittle, J.; Peters, J. C. Catalytic conversion of nitrogen to ammonia by an iron model complex. *Nature* **2013,** *501*, 84-87.
64. Del Castillo, T. J.; Thompson, N. B.; Peters, J. C. A Synthetic Single-Site Fe Nitrogenase: High Turnover, Freeze-Quench 57Fe Mössbauer Data, and a Hydride Resting State. *J. Am. Chem. Soc.* **2016,** *138*, 5341–5350.
65. Arashiba, K.; Miyake, Y.; Nishibayashi, Y. A molybdenum complex bearing PNP-type pincer ligands leads to the catalytic reduction of dinitrogen into ammonia. *Nat. Chem.* **2011,** *3*, 120-125.
66. Arashiba, K.; Kinoshita, E.; Kuriyama, S.; Eizawa, A.; Nakajima, K.; Tanaka, H.; Yoshizawa, K.; Nishibayashi, Y. Catalytic Reduction of Dinitrogen to Ammonia by Use of Molybdenum–Nitride Complexes Bearing a Tridentate Triphosphine as Catalysts. *J. Am. Chem. Soc.* **2015,** *137*, 5666–5669.
67. Eizawa, A.; Arashiba, K.; Tanaka, H.; Kuriyama, S.; Matsuo, Y.; Nakajima, K.; Yoshizawa, K.; Nishibayashi, Y. Remarkable catalytic activity of dinitrogen-bridged dimolybdenum complexes bearing NHC-based PCP-pincer ligands toward nitrogen fixation. *Nat. Commun.* **2017,** *8*, 14874.
68. Laplaza, C. E.; Cummins, C. C. Dintrogen Cleavage by a 3-Coordinate Molybdenum(III) Complex. *Science* **1995,** *268*, 861-863.
69. Laplaza, C. E.; Johnson, M. J. A.; Peters, J. C.; Odom, A. L.; Kime, E.; Cummins, C. C.; George, G. N.; Pickering, I. J. *J. Am. Chem. Soc.* **1996,** *118*, 8623-8638.
70. Curley, J. J.; Sceats, E. L.; Cummins, C. C. A Cycle for Organic Nitrile Synthesis via Dinitrogen Cleavage. *J. Am. Chem. Soc.* **2006,** *128*, 14036-14037.
71. Solari, E.; Da Silva, C.; Iacono, B.; Hesschenbrouck, J.; Rizzoli, C.; Scopelliti, R.; Floriani, C. Photochemical activation of the N≡N bond in a dimolybdenum - dinitrogen complex: formation of a molybdenum nitride. *Angew. Chem. Int. Ed.* **2001,** *40*, 3907-3909.

72. Curley, J. J.; Cook, T. R.; Reece, S. Y.; Muller, P.; Cummins, C. C. Shining Light on Dinitrogen Cleavage: Structural Features, Redox Chemistry, and Photochemistry of the Key Intermediate Bridging Dinitrogen Complex. *J. Am. Chem. Soc.* **2008,** *130*, 9394-9405.
73. Miyazaki, R.; Tanaka, H.; Tanabe, Y.; Yuki, M.; Nakajima, K.; Yoshizawa, K.; Nishibayashi, Y. Cleavage and Formation of Molecular Dinitrogen in a Single System Assisted by Molybdenum Complexes Bearing Ferrocenyldiphosphine. *Angew. Chem. Int. Ed.* **2014,** *53*, 11488-11492.
74. Rebreyend, C.; de Bruin, B. Photolytic N_2 Splitting: A Road to Sustainable NH_3 Production? A*ngew. Chem. Int. Ed.* **2015,** *54*, 42-44.
75. Krewald, V. Dinitrogen photoactivation: status quo and future perspectives. *Dalton Trans.* **2018,** *47*, 10320-10329.
76. Hanna, T. E.; Lobkovsky, E.; Chirik, P. J. Dinitrogen Complexes of Bis(cyclopentadienyl) Titanium Derivatives: Structural Diversity Arising from Substituent Manipulation. *Organometallics* **2009,** *28*, 4079-4088.
77. Chirik, P. J. Group 4 Transition Metal Sandwich Complexes: Still Fresh after Almost 60 Years. *Organometallics* **2010,** *29*, 1500-1517.
78. Tanaka, H.; Arashiba, K.; Kuriyama, S.; Sasada, A.; Nakajima, K.; Yoshizawa, K.; Nishibayashi, Y. Unique behaviour of dinitrogen-bridged dimolybdenum complexes bearing pincer ligand towards catalytic formation of ammonia. *Nat. Commun.* **2014,** *5*, 3737.
79. Imayoshi, R.; Nakajima, K.; Takaya, J.; Iwasawa, N.; Nishibayashi, Y. Synthesis and Reactivity of Iron- and Cobalt-Dinitrogen Complexes Bearing PSiP-Type Pincer Ligands toward Nitrogen Fixation. *Eur. J. Inrog. Chem.* **2017,** *32*, 3769-3778.
80. Kinoshita, E.; Arashiba, K.; Kuriyama, S.; Miyake, Y.; Shimazaki, R.; Nakanishi, H.; Nishibayashi, Y. Synthesis and Catalytic Activity of Molybdenum–Dinitrogen Complexes Bearing Unsymmetric PNP-Type Pincer Ligands. *Organometallics* **2012,** *31*, 8437-8443.
81. Nishibayashi, Y.; Kuriyama, S.; Arashiba, K.; Nakajima, K.; Tanaka, H.; Yoshizawa, K. Azaferrocene-Based PNP-type Pincer Ligand: Synthesis of Molybdenum, Chromium, and Iron Complexes and Reactivity toward Nitrogen Fixation. *Eur. J. Inorg. Chem.* **2016,** *30*, 4856-4861.
82. Pool, J. A.; Lubkovsky, E.; Chirik, P. J. Hydrogenation and cleavage of dinitrogen to ammonia with a zirconium complex. *Nature* **2004,** *327*, 527-530.
83. Peng, Y.; Ramos-Garces, M. V.; Lionetti, D.; Blakemore, J. D. Structural and Electrochemical Consequences of [Cp*] Ligand Protonation. *Inorg. Chem.* **2017,** *56*, 10824-10831.
84. Berno, P.; Hao, S. K.; Minhas, R.; Gambarotta, S. Dinitrgen Fixation versus Metal-Metal Bond Formation in the Chemistry of Vanadium(II) Amidinates. *J. Am. Chem. Soc.* **1994,** *116*, 7417-7418.
85. Barry, S. T. Amidinates, guanidinates and iminopyrrolidinates: Understanding precursor thermolysis to design a better ligand. *Coord. Chem. Rev.* **2013,** *257*, 3192-3201.
86. Barker, J.; Kilner, M. The coordination chemistry of the amidine ligand. *Coord. Chem. Rev.* **1994,** *133*, 219-300.

87. MacLeod, K. C.; Holland, P. L. Recent Developments in Homogeneous Dinitrogen Reduction by Molybdenum and Iron. *Nat. Chem.* **2013,** *5*, 559-565.
88. Sita, L. R. Ex Uno Plures ("Out of One, Many"): New Paradigms for Expanding the Range of Polyolefins through Reversible Group Transfers. *Angew. Chem. Int. Ed.* **2009,** *48*, 2464-2472.
89. Babcock, J. R.; Sita, L. R. Facile Preparation of Unsymmetric Carbodiimides via i*n Situ* Tin(II)-Mediated Heterocumulene Metathesis. *Organometallics* **1998,** *120*, 5585-5586.
90. Koterwas, L. A.; Fettinger, J. C.; R., S. L. Stereospecific Syntheses, Metal Configurational Stabilities, and conformational Analyses of m*eso*-(R,*S)*- and (R,*R)*-(η^5-C_5R_5)Ti(CH_3)$_2$-N,*N'*-bis(1-phenylethyl)acetamidinates for R = H and Me. *Organometallics* **1999,** *18*, 4183-4190.
91. Jayaratne, K. C.; Keaton, R. J.; Henningsen, D. A.; Sita, L. R. Living Ziegler−Natta Cyclopolymerization of Nonconjugated Dienes: New Classes of Microphase-Separated Polyolefin Block Copolymers via a Tandem Polymerization/Cyclopolymerization Strategy. *J. Am. Chem. Soc.* **200,** *122*, 10490-10491.
92. Jayaratne, K. C.; Sita, L. R. Stereospecific Living Ziegler−Natta Polymerization of 1-Hexene. *J. Am. Chem. Soc.* **2000,** *122*, 958-959.
93. Fontaine, P. P.; Yonke, B. L.; Zavalij, P. Y.; Sita, L. R. Dinitrogen Complexation and Extent of N≡N Activation within the Group 6 "End-On-Bridged" Dinuclear Complexes, {(η^5-C_5Me_5)M N(i-Pr)C(Me)N(i-Pr)}$_2$(μ-η^1:η^1-N_2) (M = Mo and W). *J. Am. Chem. Soc.* **2010,** *132*, 12273-12285.
94. Production of Isocyanates, R_3EN=C=O from Dinitrogen, Carbon Dioxide, and R_3ECl. *Angew. Chem. Int. Ed.* **2015,** *54*, 10220-10224.
95. Duman, L. M.; Farrell, W. S.; Zavalij, P. Y.; Sita, L. R. Steric Switching from Photochemical to Thermal Reaction Pathways for Enhanced Efficiency in Metal-Mediated Nitrogen Fixation. *J. Am. Chem. Soc.* **2016,** *138*, 14856-14859.
96. Hirotsu, M.; Fontaine, P. P.; Epshteyn, A.; Zavalij, P. Y.; Sita, L. R. Dinitrogen activation at ambient temperatures: New modes of H(2) and PhSiH(3) additions for an "End-on-bridged" [Ta(IV)] (2)(μ-η(1):η(1)-N(2) complex and for the bis(μ-nitrido) [Ta(V)(μ-N)](2) product derived from facile N=N bond cleavage. *J. Am. Chem. Soc.* **2007,** *129*, 9284-9285.

Chapter 2: Dintirogen Coordination and Thermal Cleavage

2.1 Steric Reduction of the CPAM Ligand Set to Lower Reaction Barriers

The adaptability of the CPAM ligand framework is among its most attractive features. Variation of the substituents at the Cp* ligand as well as the ancillary N-atom and distal C-atom positions of the amidinate ligand has led to the ability to coordinate the N_2 ligand in dinuclear complexes spanning the early transition metals, tuning both reactivity and isolability.[1-6] Indeed, this control and its effects are clearly demonstrated in a series of isolated group 4 side-on-bridged dinitrogen complexes (**1.17 and 1.18a-e**). The group 4 metal centers [M(IV, d^0), $[N_2]^{4-}$] lack the two additional electrons necessary to complete N≡N bond cleavage, so the result is an extremely elongated N-N bond and which can be viewed as an "arrested" transition state along the cleavage pathway. As is illustrated in Figure 2.1, the wide variety of the R, R', and R" CPAM substituents display a clear trend regarding N_2 activation and bond length; namely, the less sterically demanding the CPAM framework is, the longer the N-N bond and thus the more activated the dinitrogen unit.[1]

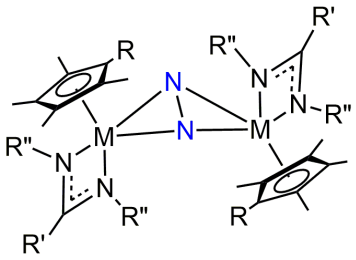

1.17: M = Zr, R = Me, R' = NMe_2, R" = iPr, d(NN) = 1.518(2) Å
1.18a: M = Hf, R = Me, R' = NMe_2, R" = iPr, d(NN) = 1.581(4) Å
1.18b: M = Hf, R = H, R' = NMe_2, R" = iPr, d(NN) = 1.600(6) Å
1.18c: M = Hf, R = Me, R' = Me, R" = iPr, d(NN) = 1.611(4) Å
1.18d: M = Hf, R = H, R' = Me, R" = iPr, d(NN) = 1.630(4) Å
1.18e: M = Hf, R = Me, R' = Me, R" = Et, d(NN) = 1.635(5) Å

Figure 2.1. Structural parameters for Group 4 side-on-bridged dinitrogen complexes **1.17** and **1.18a-e**

An extension of the observation is that for Group 5 dinuclear dinitrogen complexes $\{Cp^*[N(iPr)C(R)N(iPr)]Ta\}_2(\mu\text{-}\eta^1\text{:}\eta^1\text{-}N_2)$ where R = Me (**1.21a**), NMe_2 (**1.21b**), and Ph (**1.21c**), which undergo thermal N_2 cleavage from $(\mu\text{-}N_2)$ to $(\mu\text{-}N)_2$ complexes, $\{Cp^*[N(iPr)C(R)N(iPr)]Ta(\mu\text{-}N)\}_2$where R = Me (**2.1a**), NMe_2 (**2.1b**), and Ph (**2.1c**), shown in Scheme 2.1. There is marked relationship between the steric demands of the CPAM ligand set and the rate at which the N≡N bond is broken. Namely, cleavage is more facile in complexes with smaller amidinate C-atom substituents (Me > NMe_2 > Ph) because these less bulky complexes have smaller non-bonding steric interactions between the CPAM framework and the proximate metal centers and N_2 cores. That the sterics of the CPAM ligand set have such an effect upon reactivity is due in large part to the proposed mechanism for this cleavage process, an intramolecular isomerization wherein a dinuclear end-on bridged N_2 complex rearranges to a side-on bridged binding mode before cleaving the N-N bond fully resulting in a bridging bis-nitride structure.[2]

Scheme 2.1

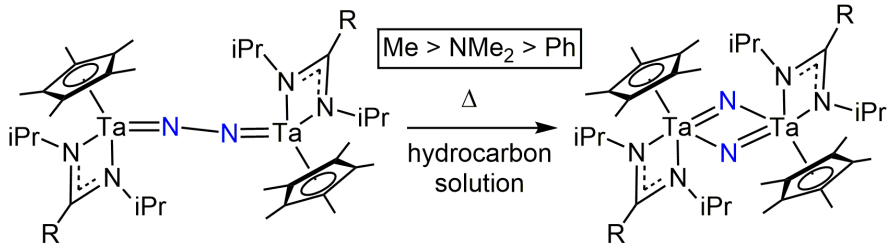

R = Me (**1.21a**), NMe_2 (**1.21b**), Ph (**1.21c**) R = Me (**2.1a**), NMe_2 (**2.b**), Ph (**2.1c**)

Further credence is given to the existence of a side-on bound intermediate through DFT studies by Morokuma for a simplified CPAM ligand framework of $\{Cp[N(Me)N(H)N(Me)Ta\}_2(\mu\text{-}N_2)$ (**2.2**). These computational studies explored the N≡N cleavage of a ditantalum dinitrogen complex, concluding that it likely transitions

from an end-on-bridged (μ-η^1:η^1-N_2), to an end-on/side-on (μ-η^2:η^1-N_2), to the side-on bridged ((μ-η^2:η^2-N_2) binding structure prior to total N_2 cleavage, as is depicted in Scheme 2.2.[7]

Scheme 2.2

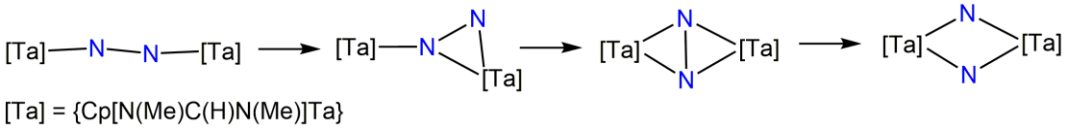

[Ta] = {Cp[N(Me)C(H)N(Me)]Ta}

If this is in fact the mechanism by which the N≡N bond is broken, then an increase in the steric crowding about the M-N_2-M core would inhibit the ability of the rearrangement to take place and thus slow the cleavage process. For group 6 [N(iPr)C(Me)N(iPr)] CPAM derivatives **1.22** and **1.23**, it is possible that the steric hindrance about the Mo and W centers of the (μ-N_2) is so great that in order to accommodate the necessary rearrangement and transition geometry of N_2 cleavage to make **1.26** and **1.27**, photolysis briefly reduce the binding of the amidinate ligand from κ^2 - to κ^1 -coordination which increases space about the core to accommodate N_2 rearrangement.[5] It follows then, that decreasing the barriers to N_2 activation and cleavage on Mo and W centers may be systematically accomplished by reducing the steric demands of the CPAM ligand set, even going so far as to undergo thermal N_2 cleavage instead of photolytic. Interestingly, this approach is in opposition to the general approach of the field which tends to eschew unencumbered ligand sets in favor of bulkier frameworks in the pursuit of catalytic N_2 fixation. Indeed, the use of sterically demanding ligand sets not only provides shielding from the formation of undesirable M-M bonds, it can also enforce rigid geometries on complexes, direct reactivity to desirable positions, and stabilize reactive intermediates.[8-17] Still, given the

value of continuing to expand the CPAM library of N_2 complexes and the prescient of increasing reactivity, the pursuit of undemanding ligands was deemed to be a potentially fruitful avenue of research.

This chapter will report the synthesis and characterization of various sterically reduced Mo and W CPAM complexes, their subsequent chemical reduction to coordinate dinitrogen between two centers in an (μ-N_2) end-on-bridged dinuclear fashion, and finally investigate the groundbreaking, thermally-mediated cleavage of the N≡N bond to form a dinuclear (μ-N)$_2$ species.

2.2 Diethyl, Phenyl CPAM-Facilitated Dinitrogen Reduction

The foundation of this thesis rests upon the initial design of a new diethyl, phenyl amidinate, [N(Et)C(Ph)N(Et)] (Et_2Ph). With the substitution of smaller ethyl groups for the established isopropyl group at the ancillary N-atom positions, once coordinated, the steric demands of this ligand about a metal center are significantly less than those of the previous [N(iPr)C(Me)N(iPr)] amidinate. The use of the phenyl substituent in place of a methyl group at the distal C-atom increases the crystallinity of the resulting products. Due to the vertical orientation the Ph can adopt with less

Scheme 2.3

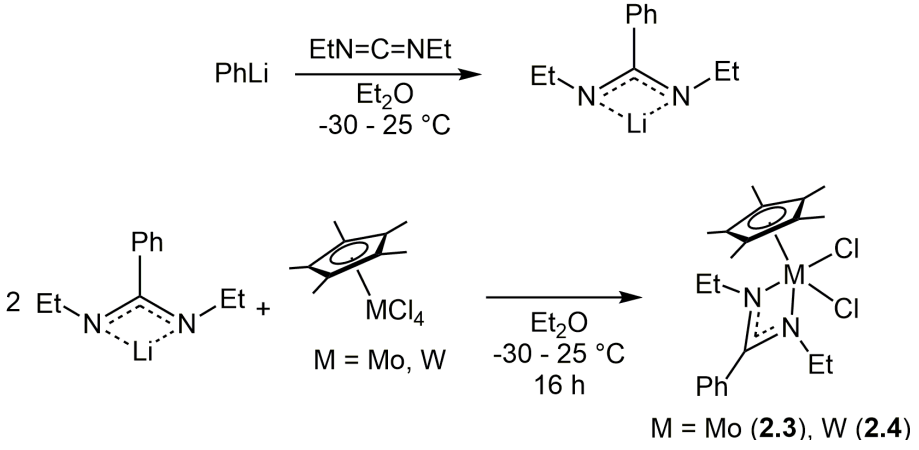

interference from the ethyl ligands, it does not in fact add significantly to non-bonding steric interactions at the metal centers. According to Scheme 2.3, the amidinate salt is synthesized by treating diethyl carbodiimide with phenyl lithium at -30 °C and can either be isolated by removing the solvent under reduced pressure and rinsing the resulting precipitate with pentane or generated in solution to be used *in situ* in the subsequent reactions. Next, the addition of a solution of the lithium amidinate salt to Cp^*MCl_4 (M = Mo or W) at -30 °C results in isolable CPAM group 6 dichloride compounds, $\{Cp^*[N(Et)C(Ph)N(Et)]MCl_2\}$, which are either paramagnetic (M = Mo (**2.3**)) or diamagnetic (W (**2.4**)).[4] Two equivalents of the salt are used for each equivalent of the tetrachloride as one serves as an *in situ* sacrificial reductant while the other adds the amidinate onto the metal center.[3]

In a glovebox atmosphere of N_2, **2.3** and **2.4** successfully undergo chemical reduction by 0.5% NaHg to form the corresponding end-on-bridged dinitrogen complexes $\{Cp^*[N(Et)C(Ph)N(Et)]M\}_2(\mu\text{-}\eta^1\text{:}\eta^1\text{-}N_2)$ where M = Mo (**2.5**) in 85% yield and W (**2.6**) in 80% yield. This reduction, shown in Scheme 2.4, occurs more quickly

Scheme 2.4

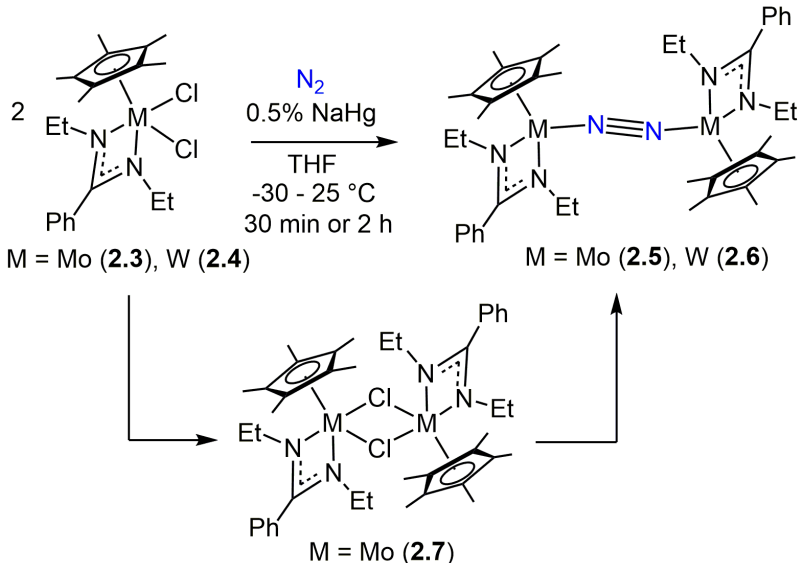

than in the corresponding diisopropyl, methyl complexes under identical conditions; reduction of **2.3** requires only 30 minutes while the comparable reduction of iPr_2Me dichloride **1.24** requires 2 hours.[3, 4] The mixtures were chilled to -30 °C and allowed to warm to room temperature over the course of reaction. Studies running the reduction of **2.3** at room temperature determined that the lowered temperature was not necessary for successful reduction, as **2.5** could be observed by proton nuclear magnetic resonance (^{1}H NMR) of the products, but that the low temperature reactions were cleaner. Further, by beginning the reaction chilled, it was easier to gauge the progress of the reaction by its distinct color changes. Specifically, these reductions pass through intermediate monochloride species, noted by sharp changes in color throughout the reactions (for Mo, dark maroon **2.3** quickly becomes navy blue before changing to orange-brown **2.5** while for W, dark orange **2.4** changes to deep purple before settling in the forest-green of **2.6**). The structure of these intermediate species is depicted in the lower portion of Scheme 2.3 and solid-state structure of the Mo species was confirmed by XRD as is shown in Figure 2.2, a dinuclear configuration of the monochloride $\{Cp^*[N(Et)C(Ph)N(Et)]MoCl\}_2$ (**2.7**).

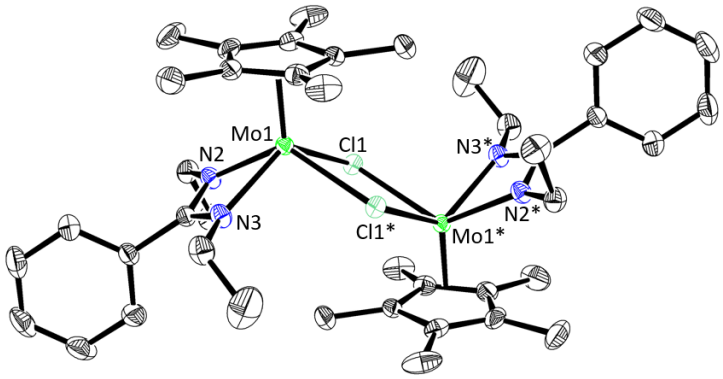

Figure 2.2. Crystal structure of **2.7** with hydrogen atoms omitted for clarity, ellipsoids for the non-hydrogen atoms are shown at the 30% probability level

In terms of structural parameters for the dinuclear end-on-bridged dinitrogen products, crystalline material of each **2.5** and **2.6** was obtained which was suitable for crystallographic analysis, the structures of which are shown in Figure 2.3. Both of diamagnetic these species have slightly transoid, though nearly linear, M-N-N-M core structures that can be formally viewed as of M(II,d^4) centers with a neutral (μ-N_2) unit or M(IV,d^2) centers with an anionic $[N_2]^{4-}$ bridging unit. The structurally determined lengths of these N_2 bonds are only slightly longer than the length of a bridging dinitrogen double bond, 1.25 Å,[18] and so in reality the oxidation state is likely somewhere between the two extremes.[3] The XRD demonstrates that the respective N≡N bonds for **2.5** and **2.6** are 1.288(3) Å and 1.299(5) Å,[4] respectively, each of which exhibit longer N_2 units than are found in the comparable cases of the bulkier iPr_2Me (μ-N_2) complexes, **1.22** at 1.267(2) Å and **1.23** at 1.277(8) Å.[3] The longer N≡N bond

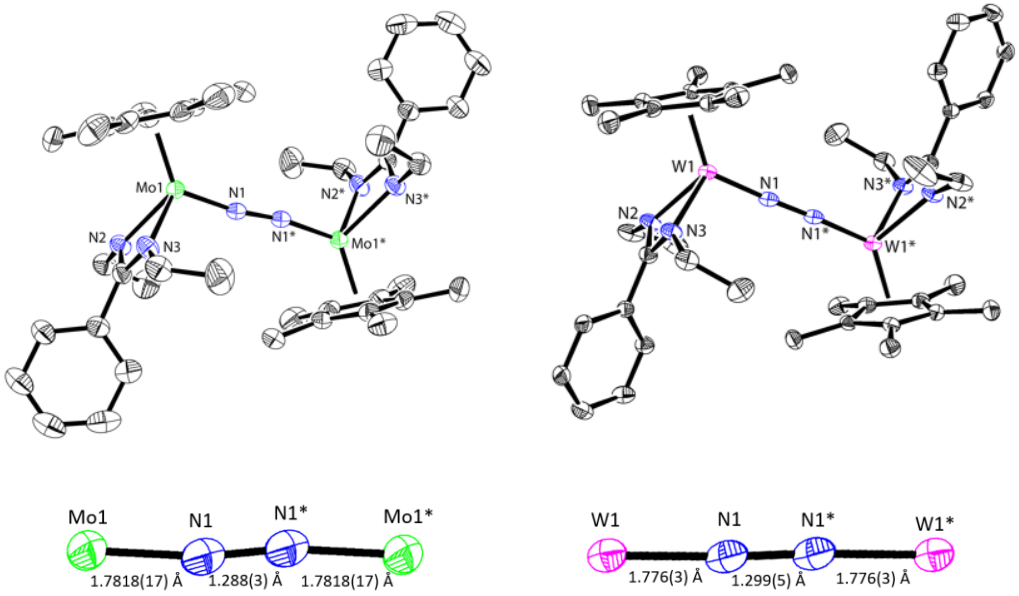

Figure 2.3. Top: Crystal structures of **2.5** (right) and **2.6** (left) with hydrogen atoms omitted for clarity, ellipsoids for the non-hydrogen atoms are shown at the 30% probability level. Bottom: Expanded view and bond lengths of M-N_2-M cores of **2.5** (right) and **2.6** (left)

lengths of **2.5** and **2.6** indicate that a higher degree of N_2 activation is indeed achieved with parring back the sterics of the CPAM ligand.

2.3 Thermal Dinitrogen Cleavage

The sensitive nature of these end-on-bridged N_2 complexes is demonstrated not only in the shorter times required for their synthesis and more activated dinitrogen cores but is exemplified in the observation that a solution of **2.5** in benzene-d_6 undergoes slow reaction at room temperature under ambient lighting. When tracked by ^{1}H NMR, a new species appeared very cleanly as the signals for **2.5** gradually lessened in intensity. Figure 2.4 shows a solution of **2.5** that was prepared in a J. Young tube and

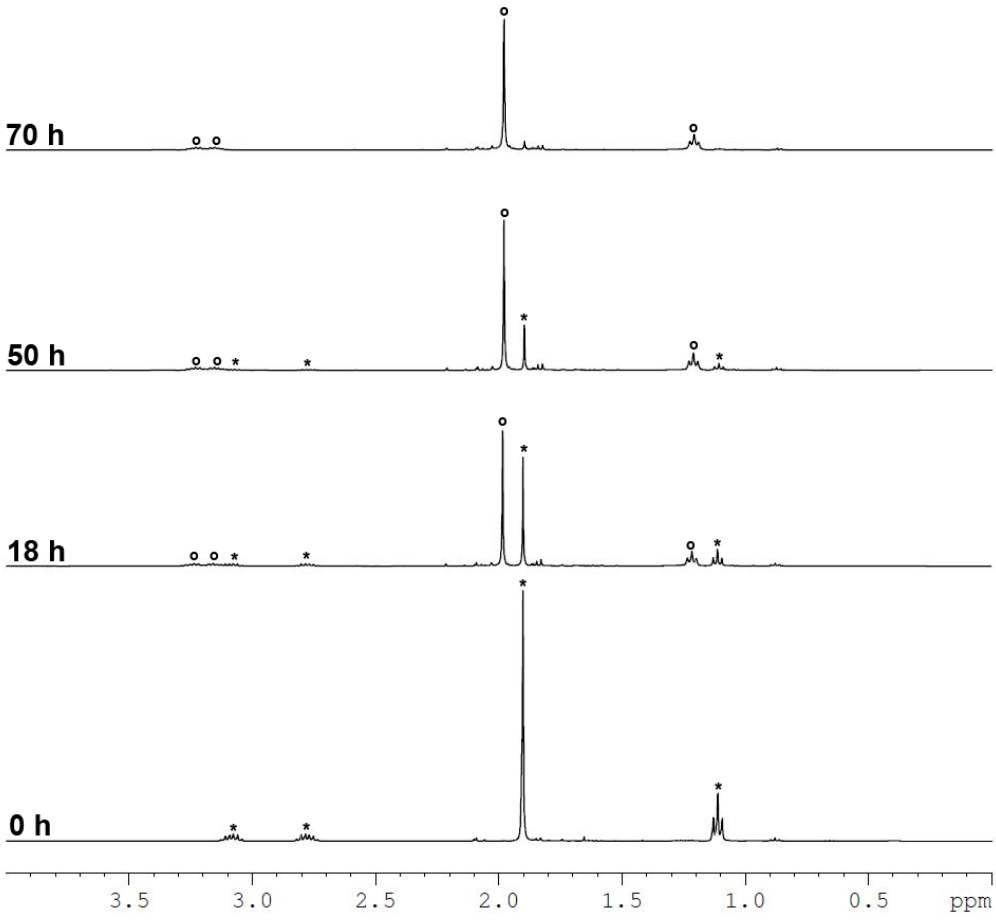

Figure 2.4. Partial ^{1}H NMR (400 MHz, C_6D_6, 25 °C) demonstrating the conversion of **2.5** (*****) to **2.8** (**o**) upon thermolysis at 60 °C

monitored by periodic ^{1}H NMR while heating at 60 °C on an oil bath, covered with aluminum foil to block ambient light. Over three days, this sample demonstrated the same clean and quantitive reaction taking place at an accelerated rate when compared to the room temperature sample, and confirmed that the reaction is induced thermally, even in the absence of light. As is shown in Scheme 2.5, performing the thermolysis on a preparatory scale in toluene and recrystallizing from THF produced the dimolybdenum bridging bis-nitrido species {Cp*[N(Et)C(Ph)N(Et)]Mo(μ-N)}$_2$ (**2.8**), in 80% isolated yield. Similarly, the ditungsten species {Cp*[N(Et)C(Ph)N(Et)]W(μ-N)}$_2$ (**2.9**), could be cleanly isolated in 77% yield from the thermolysis of **2.6**, albeit on a slightly longer time scale.

Scheme 2.5

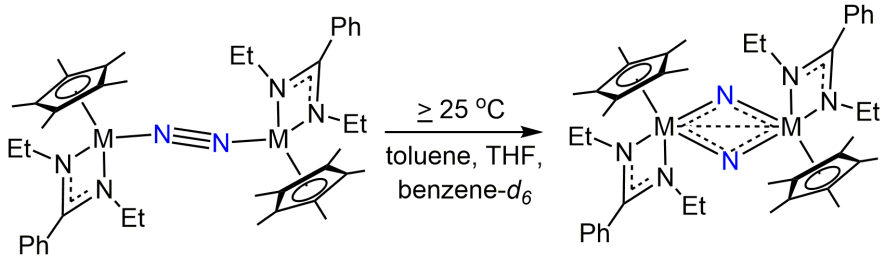

M = Mo (**2.5**), W (**2.6**)

M = Mo (**2.8**), W (**2.9**)

Solid-state structures of dinuclear M(V) complexes **2.8** and **2.9** are shown in Figure 2.5 and exhibit planar, 4-membered cores in which the N-N distance where the N_2 bond has been completely cleaved at *d*(N1N1*) = 2.752 Å for **2.8** and 2.777 Å for **2.9**. On the other hand, M-M bonds have been formed where *d*(Mo1Mo1*) = 2.6480(3) Å and *d*(W1W1*) = 2.6480(3) Å,[4] each of which are within twice the respective Pauling's covalent bond radius of 1.371 Å for Mo or 1.378 Å for W.[19] The M-N bonds are slightly asymmetric with a 'short' and 'long' bond distorting the diamond formation of the core, *d*(Mo1N1) = 1.8917(12) Å for and *d*(Mo1N1*) = 1.9269(12) Å for **2.8** or

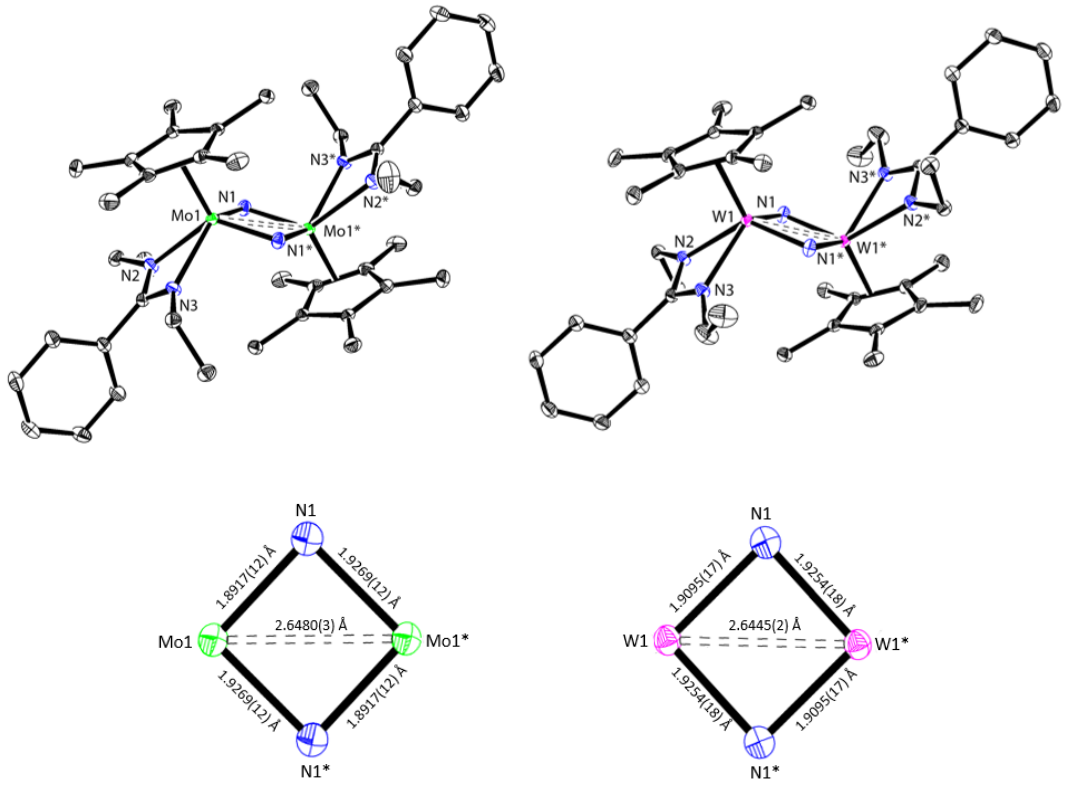

Figure 2.5. Top: Crystal structures of **2.8** (right) and **2.9** (left) with hydrogen atoms omitted for clarity, ellipsoids for the non-hydrogen atoms are shown at the 30% probability level. Bottom: Expanded view and bond lengths of M_2N_2 cores of **2.8** (right) and **2.9** (left)

d(W1N1) = 1.9095(17) Å for and *d*(W1N1*) = 1.9254(18) Å for **2.9**. However, all of the M-N bonds are elongated in the bis (μ-N) structures of **2.8** and **2.9** as compared to the M-N bonds of the (μ-N_2) complexes **2.5** and **2.6**.

2.3.1 Mechanism of Thermolytic N_2 Cleavage

There are two distinct pathways by which the N_2 cleavage might be proceed in the cases of **2.5** and **2.6**, each of which are shown in Scheme 2.6. Mechanism A is inspired by the "zig-zag" transition state from Cummins's seminal work (*detailed in Chapter 1.2.3*), in which the cleavage of a bulky trisamido-supported dinuclear Mo end-on-bridged N_2 complex **1.7** passes through a "zig-zag" transition state to form a pair of terminal nitrides **1.8** at ambient temperatures.[20, 21] Structurally, the dinuclear (μ-

Scheme 2.6

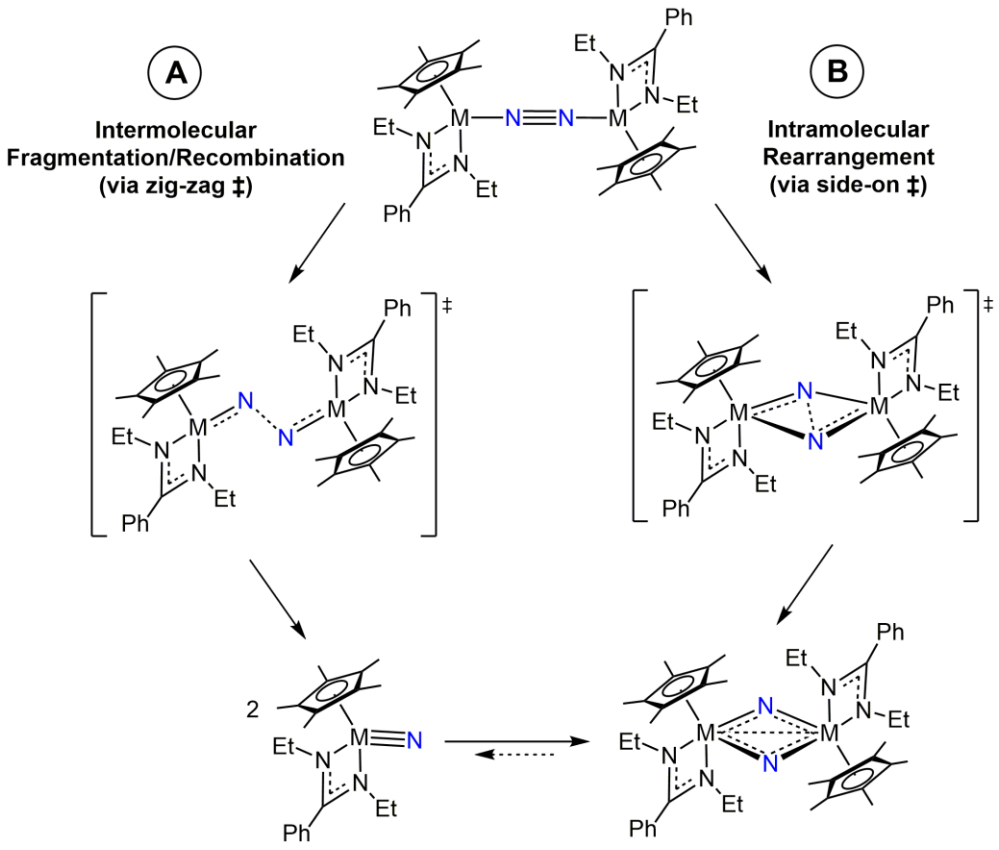

N)$_2$ products **2.8** and **2.9** are markedly different from the mononuclear terminal molybdenum nitride **1.8** isolated by Cummins, which is, incidentally, the only previous example of thermal N_2 cleavage from a dinitrogen complex to a nitride mediated by a group 6 metal center. The alternative pathway, mechanism B of Scheme 2.6, is an intramolecular isomerization of the bridging N_2 unit through a side-bound (μ-η^2:η^2-N_2) intermediate, of similar structure to the isolated group 4 CPAM dinitrogen complexes **1.17** and **1.18a-e**[1] and proposed as intermediates in the cleavage of group 5 CPAM dinitrogen complexes **1.20** and **1.21a-c**,[5] after which the N-N bond is fully broken to result in a dinuclear, (μ-N)$_2$ that could conceivably fragment into a pair of mononuclear, terminal nitrides which themselves could potentially recombine back into to the dimer.

In general, experimental evidence suggests that it is the intramolecular rearrangement pathway, Mechanism B, which is responsible for the N_2 cleavage of these CPAM complexes. For instance, the conversion from **2.5** to **3.8** was tracked in THF-d_8 or in benzene-d_6 spiked with dimethoxymethane (DME). In both cases, the process proceeded unimpeded by the presence of coordinating molecules that would likely have trapped a mononuclear nitrido species before recombining to form the dinuclear product if an intermolecular fragmentation process was taking place. Additionally, treatment of **2.8** with 2,3-dimethyl-butadiene yielded no reaction by ^{1}H NMR, even after heating for 24 h at 80 °C in benzene-d_6.

Further support for the rearrangement mechanism was garnered by UV-vis studies for the transformation of **2.5** to **2.8** in methylcyclohexane, the electronic spectra of which are shown in Figure 2.6.[4] The well-defined isosbestic point at λ = 757 nm

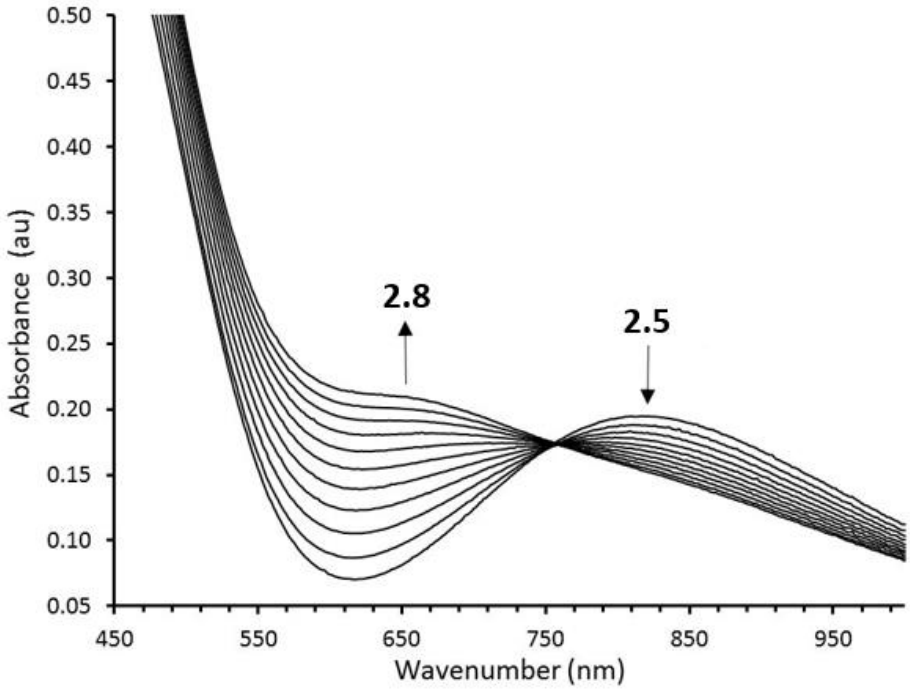

Figure 2.6. Partial display of a series of electronic spectra showing the initial thermolytic conversion of **2.5** to **2.8** recorded by scanning UV-vis spectroscopy at 70 °C (MCH, c = 0.38 mM) with isosbestic point at λ = 757 nm[4, 5]

indicates that there are only two species in solution, **2.5** to **2.8**, at any given point during the quantitative conversion. The presence of any other compound, such as a mononuclear nitrido intermediate, would prevent the observation of an isosbestic point.[22] It should be noted, however, that only the initial UV-vis data could be used in this study due to the disparate solubilities of (μ-N_2) and the bis (μ-N) complexes. While the brown **2.5** and green **2.6** are quite soluble in most organic solvents, including alkanes such as pentane, the dark brown compounds **2.8** and **2.9** are only sparingly soluble methylcyclohexane, THF, toluene, and benzene-d_6. As a result, during the thermolytic conversion of **2.5** to **2.8** or **2.6** to **2.9**, the increasing concentration of the product causes the bis (μ-N) complexes to precipitate or crystallize out of solution, causing the isosbestic point to become less resolved and making it impossible to track their production to completion using UV-vis, the accuracy of which depends on the reliable concentration measurements of both reactants and products.

2.3.2 Kinetic Studies of Thermolytic N_2 Cleavage

In order to obtain dependable kinetics of the thermolysis process which could help elucidate the mechanism of cleavage as well as draw comparisons between the Mo and W processes, the reactions were monitored by ^{1}H NMR at 60, 65, 70, 75, and 80 °C. Rather than monitoring the appearance of the signals for **2.8** or **2.9** − the integration values of which would not have been reliable once reaching the point of saturation − kinetic data was obtained by tracking the initial rate of the disappearance of the Cp* signals of **2.5** or **2.6** relative to an internal durene standard. Data points were collected every 10 minutes for 4 hours while the instrument was heated and the resulting decrease in concentration of the (μ-N_2) dinitrogen species are shown in Figure 2.7. Subsequent

Eyring analysis, shown in Figure 2.8, provided the activation parameters presented in Table 2.1.

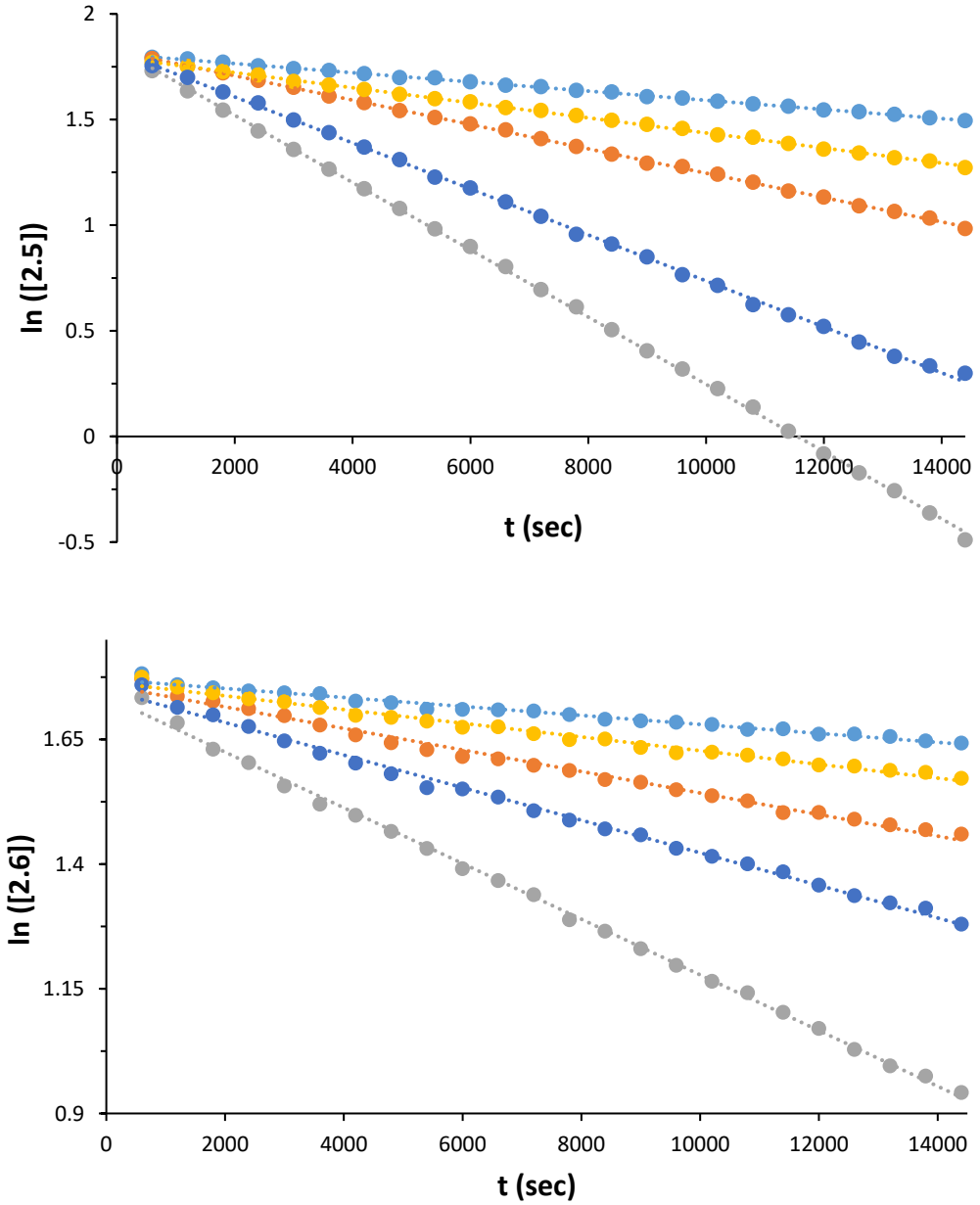

Figure 2.7. Time dependent ln([**3**]) (top) or ln([**4**]) (bottom) obtained by tracking the decrease in ^{1}H NMR signal for **3** or **4** in the thermal conversion to **6** or **7** respectively at 60 (●), 65 (●), 70 (●), 75 (●), and 80 (●) °C

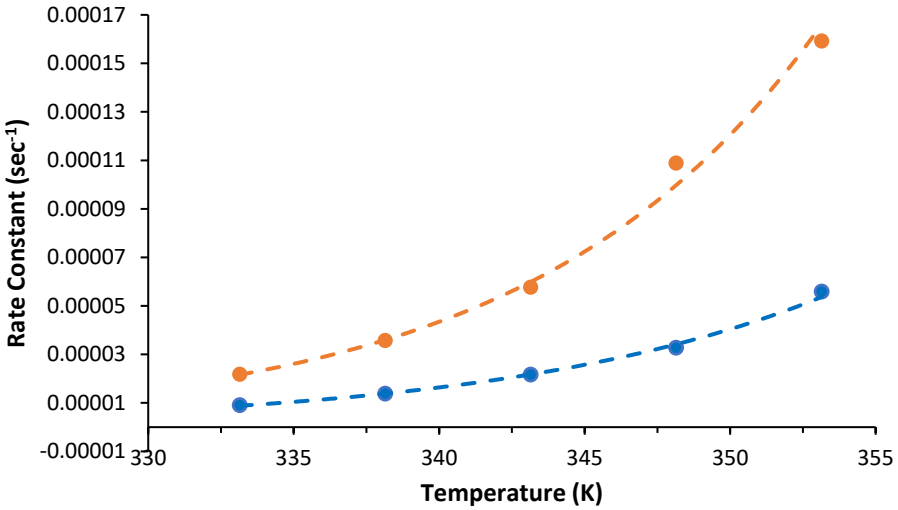

Figure 2.8. Temperature-dependent first-order rate constants with least-squares fit to the Eyring equation $k = (k_BT/h)\ \exp(\Delta S^{\ddagger}/R)\ \exp(-\Delta H^{\ddagger}/RT)$ for the thermal conversion of **2.5** to **2.8** (●) and **2.6** to **2.9** (●) at 60, 65, 70, 75, and 80 °C

Activation Parameters[4, 5]	**[Mo]**	**[W]**
$\Delta G^{\ddagger}_{calc}$ (338.15 K) (kcal mol^{-1})	26.8	27.4
$\Delta H^{\ddagger}$ (kcal mol^{-1})	23.2	20.4
$\Delta S^{\ddagger}$ (cal K^{-1} mol^{-1})	-10.6	-20.6

Table 1. Experimentally-derived activation parameters obtained by Eyring analysis of the conversion from **2.5** to **2.8** (Mo) and **2.6** to **2.9** (W).

First, the qualitative observation that cleavage of the molybdenum dinitrogen complex is faster than that of the tungsten is supported by the free energies of activation for **2.5** ($\Delta G^{\ddagger}_{calc}$ at 338.15 K of 26.8 kcal mol^{-1}) and **2.6** (**$\Delta G^{\ddagger}_{calc}$** at 338.15 K of 27.4 kcal mol^{-1}) which quantitively favor the Mo-mediated cleavage over W by 0.6 kcal mol^{-1}.[4] In addition to the more diffuse d orbitals of W, which tend to contribute to higher barriers to activation for W than Mo,[23] this is in keeping with the trend previously observed for group 5 where the third-row Ta CPAM dinitrogen complex **1.21** had higher barriers to N_2 cleavage by 2.2 kcal mol^{-1} than the second-row Nb complex **1.20**.[2] Rationale for this difference in reactivity is found upon closer examination of the bond

distances between the metal centers and the amidinate ligands. For both the (μ-N_2) and bis (μ-N) species, as shown in Figure 2.3 and Figure 2.5, the amidinate ligand is more closely bound to the W centers, *d*(W1N2) = 2.130(3) and *d*(W1N3) = 2.135(3) Å for (μ-N_2) **2.6** or *d*(W1N2) = 2.1975(17) and *d*(W1N3) = 2.2217(18) Å for bis (μ-N) **2.9**, than to the Mo centers, *d*(Mo1N2) = 2.1457(18) and *d*(Mo1N3) = 2.147(2) Å for (μ-N_2) **2.5** or *d*(Mo1N2) = 2.2023(12) and *d*(Mo1N3) = 2.2435(13) Å for bis (μ-N) **2.8**. The more closely the amidinate ligands are bound to the metal center, the more non-bonding steric interactions surround the bridging N_2 unit and, in turn, the slower the rate of N_2 rearrangement and cleavage according to an intramolecular mechanism. The atomic radius of Mo (which, at 1.45 Å, is larger than that of W, at 1.35 Å) may contribute to the longer distance between the Mo metal center and the amidinate ligand than the W center.[24] Further, W is more oxophilic than Mo,[25] which may also affect its proclivity to more tightly bind to the amidinate, thus increasing steric congestion near the dinitrogen moiety and slowing reactivity.

Second, the negative values and large magnitudes of the entropies of activation suggest the presence of *highly ordered transition states*, indicative of a contraction of the core in the transition state. This again supports an intramolecular N_2 cleavage pathway as opposed to a fragmentation and recombination pathway that would yield positive entropies of activation. That the $\Delta S^{\ddagger}$ parameter for W **(**$\Delta S^{\ddagger}$ = -20.6 cal mol^{-1} K^{-1}) is nearly twice the size of that for Mo ($\Delta S^{\ddagger}$ = -10.6 cal mol^{-1} K^{-1}) can once again likely be attributed the steric congestion of the W complex's N_2 core, where rearrangement would require more disorder of to accomplish the same transformation that be achieved more easily by the less sterically encumbered Mo-N_2-Mo core. Taken together, these

data strongly support the likelihood of N_2 cleavage through a intramolecular rearrangement pathway.[4]

2.4 Distal Substitutions of the Diethyl CPAM Ligand Set

To further expand the scope of the study for the sterically reduced CPAM system, several new derivatives were designed through the modification at the distal position of the amidinate in order to gain additional insight into the mechanism by which this groundbreaking thermal dinitrogen cleavage process occurs. By changing identity of the organolithium (RLi) reacted with the *N,N*-diethylcarbodiimide, new amidinate salts Li[N(Et)C(R)N(Et)] were produced that could be reacted with Cp^*MCl_4 to once again produce mononuclear dichloride complexes to undergo chemical reduction with N_2 and, ideally, thermally-mediated N_2 cleavage.

2.4.1 Distal Phenyl Substitution: CPAM Complexes

The first line of inquiry in altering the diethyl, phenyl CPAM framework was adding substituents to the phenyl group. In addition to the pursuit of a crossover experiment, which could definitively rule out an intermolecular mechanism of N_2 cleavage, these modifications were motivated by the potential of running a Hammett analysis[26, 27] which could yield a systematic study of the electronic effects of substituted phenyl groups and their subsequent contributions to the reactivities of the metal centers.[28] According to Scheme 2.7, targeted alterations to the ligand set consisted of a deuterated phenyl isotopologues – {Cp*[N(Et)C(C_6D_5)N(Et)]$MoCl_2$} (**2.10**), {Cp*[N(Et)C(C_6D_5)N(Et)]Mo}$_2$(μ-η^1:η^1-N_2) (**2.11**), and {Cp*[N(Et)C(C_6D_5)N(Et)]Mo(μ-N)}$_2$ (**2.12**) – the substitution of a p-tolyl group for the phenyl –{Cp*[N(Et)C(*p*-tol)N(Et)]MCl_2} (**2.13**) and {Cp*[N(Et)C(*p*-

Scheme 2.7

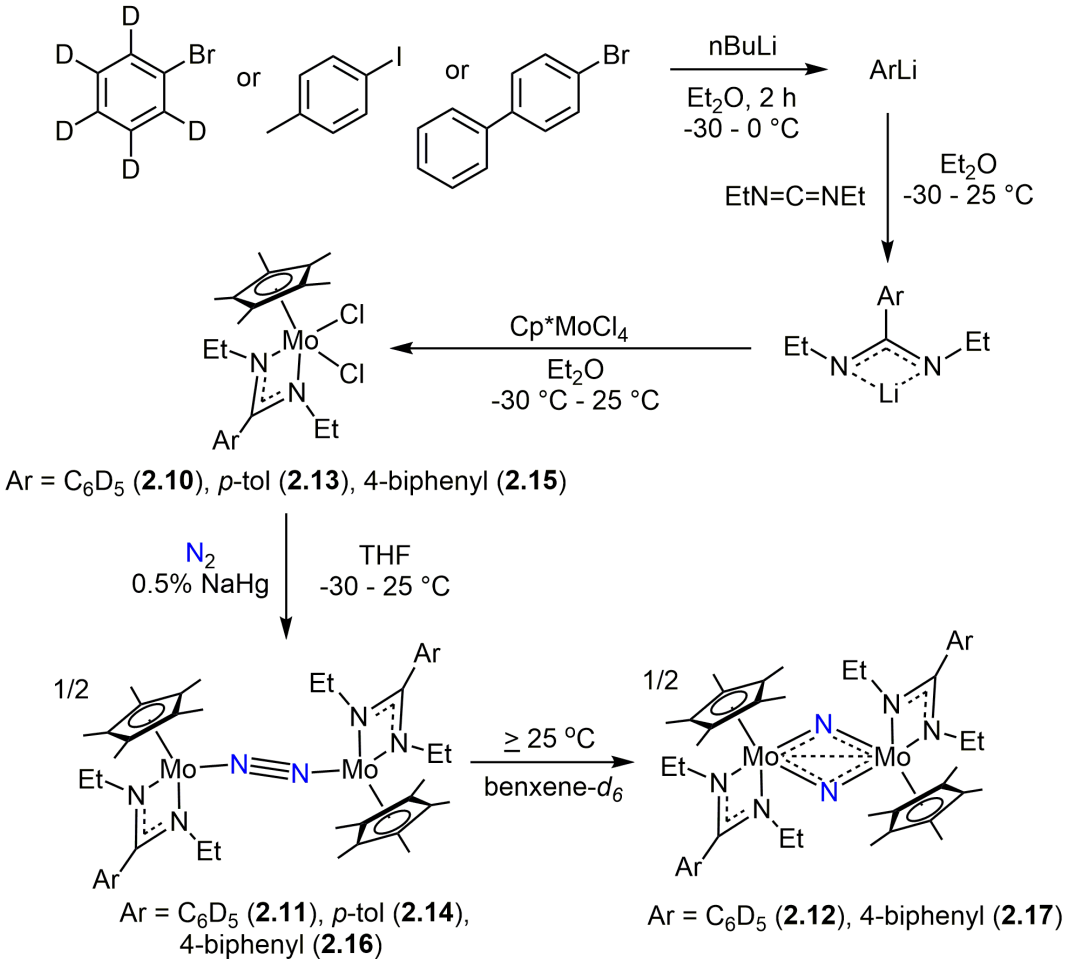

tol)N(Et)]Mo}$_2$(μ-η^1:η^1-N$_2$) (**2.14**) – or the addition of another phenyl to make a bi-phenyl moiety – {Cp*[N(Et)C(4-biphenyl)N(Et)]MoCl$_2$} (**2.15**), {Cp*[N(Et)C(4-biphenyl)N(Et)]Mo}$_2$(μ-η^1:η^1-N$_2$) (**2.16**), and {Cp*[N(Et)C(4-biphenyl)N(Et)]Mo(μ-N)}$_2$) (**2.17**). Unfortunately, each of these modified phenyl designs proved unsuitable for the crossover study: The deuterated **2.12** did not differ enough to provide conclusive evidence of the existence of a crossover species, the p-tolyl (μ-N$_2$) species **2.14** could not be isolated for clean thermolysis, and the bi-phenyl systems bis (μ-N) **2.17** could not be cleanly isolated leading to ambiguity as to its characterization.

2.4.2 Distal Dimethylamino Substitution: CPGU Complexes

In lieu of distal Ph alterations, and inspired by previous successful work with the more sterically demanding, diisopropyl ligand set in group 5[2, 3] and group 6,[3] the distal substituent of the diethyl, phenyl amidinate was modified. The phenyl group was replaced with a dimethylamino to make a Cp*, guanidinate (CPGU) ligand set. Group 5 CPGU derivates are have previously been shown to react in a comparable manner to the classical CPAM compounds, and may even have extra electron density bestowed upon the metal center by the electron donating amine moiety, potentially stabilizing the transition state during N_2 cleavage.[2] The group 6 dimolybdenum (μ-N_2) CPGU complex, meanwhile, has better crystallinity than its CPAM counterpart.[3] As Scheme 2.8 demonstrates, reacting *N*,*N*-diethylcarbodiimide with lithium dimethylamide produced a white salt, Li[N(Et)C(NMe_2)N(Et)]. Once isolated, two equivalents could be reacted with Cp*MCl_4 (M = Mo or W) to produce the M(IV) dichloride complexes

Scheme 2.8

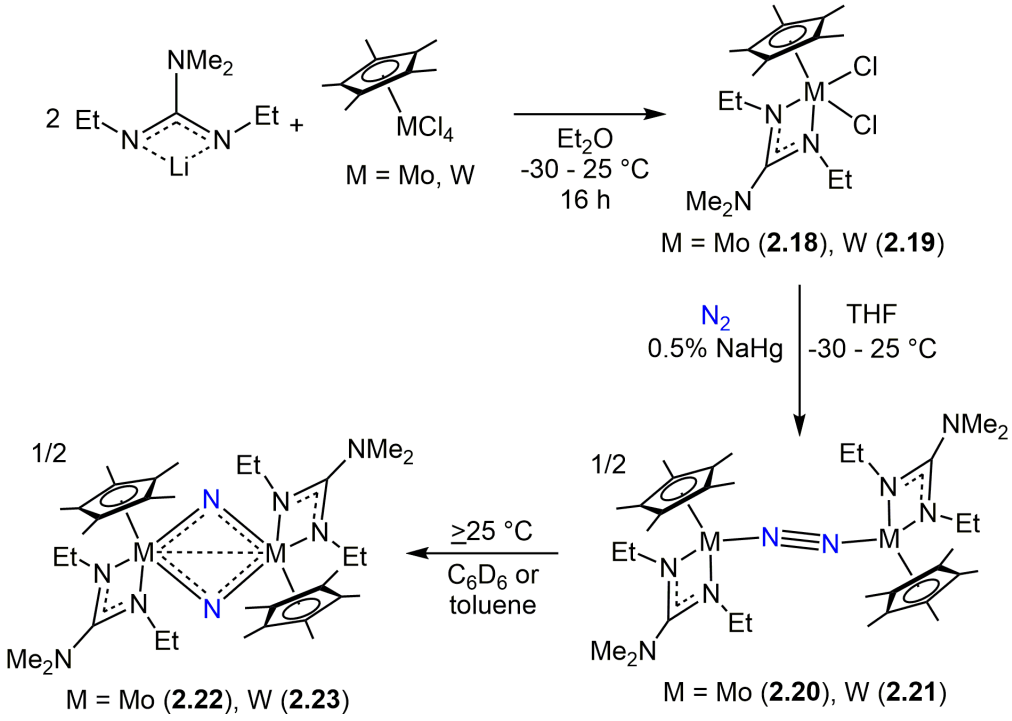

{Cp*[N(Et)C(NMe$_2$)N(Et)]MCl$_2$} (M = Mo (**2.18**), W (**2.19**)). Chemical reduction by NaHg in THF at under an atmosphere of N_2 once again yielded the desired dinuclear end-on-bridged dinitrogen compounds {Cp*[N(Et)C(NMe$_2$)N(Et)]Mo}$_2$(μ-η^1:η^1-N_2) (**2.20**) in 95% yield and {Cp*[N(Et)C(NMe$_2$)N(Et)]W}$_2$(μ-η^1:η^1-N_2) (**2.21**) in 25% yield as is illustrated in Scheme 2.8. Single crystals of each compound were obtained for X-Ray diffraction and are shown in Figure 2.9. The lengths of the N≡N and Mo-N bonds of **2.20**, at *d*(NN) = 1.275(2), *d*(MoN1) = 1.8008(17), *d*(MoN2) = 2.1382(16), and *d*(MoN3) = 2.1400(18) Å, are similar (if exhibiting a slightly less activated core and slightly closer amidinate proximity) to those of **2.5**, at *d*(NN) = 1.2883(2), *d*(MoN1) = 1.7818(17), *d*(MoN2) = 2.1457(16), and *d*(MoN3) = 2.147(2). Unfortunately, though several different crystals of **2.21** were submitted for XRD, the quality of their diffraction was too poor to be refined to a level from which structural parameters could be obtained, however the results were conclusive enough with regards

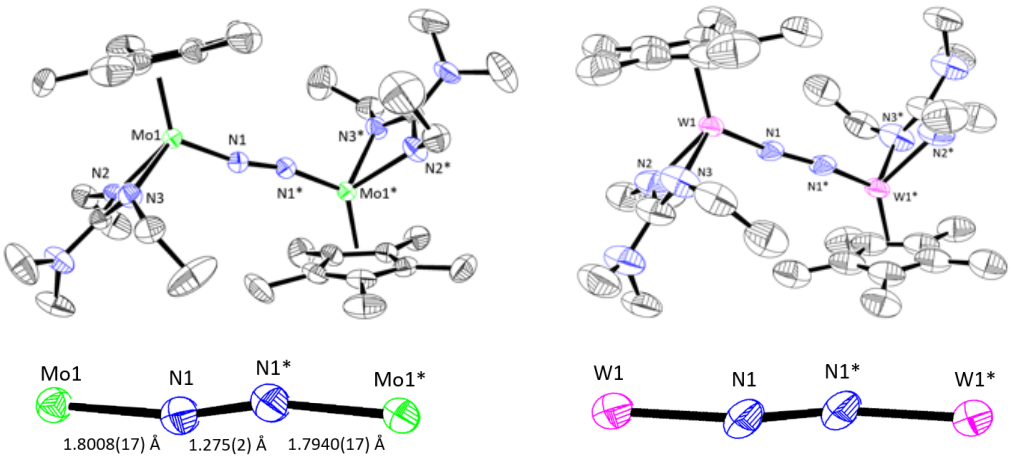

Figure 2.9. Top: Crystal structures of **2.20** (right) and **2.21** (left) with hydrogen atoms omitted for clarity, ellipsoids for the non-hydrogen atoms are shown at the 30% probability level. Bottom: Expanded view and bond lengths of M-N$_2$-M core of **2.20** (right) and expanded view of M-N$_2$-M core **2.21** (left)

to the overall structure of **2.21**, confirming connectivity of the dinitrogen in an end-on-bridged fashion between the two W centers.

Like **2.5** and **2.6**, the brown **2.20** and the green **2.21** proved to be thermally sensitive in hydrocarbon solutions and convert to new, dark brown species identified as the dinuclear bridging bis-nitride compounds isolated as {Cp*[N(Et)C(NMe$_2$)N(Et)]Mo(μ-N)}$_2$ (**2.22**) in 37% yield and {Cp*[N(Et)C(NMe$_2$)N(Et)]W(μ-N)}$_2$ (**2.23**) in 68% yield, respectively, shown in Scheme 2.8. This process is qualitatively observed to be very similar in rate to that of the CPAM complexes. Though W **2.23** seems to have slightly better solubility than **2.8** and **2.9**, Mo **2.22** is markedly more soluble than any others of its cohort, dissolving even in room temperature pentane. Crystalline material suitable for XRD confirmed the connectivity of the CPGU bis (μ-N) complexes and is detailed in Figure 2.10. the structural parameters of the planar M_2N_2 cores of the amidinate and the guanidinate species are very similar as is presented in Table 2.2 which details the compiled bond lengths of the sterically bulkier **1.22**, and **1.23**. Notably, the CPGU complexes **2.22** and **2.23** both have more asymmetric rhomboid cores with longer 'long' and shorter 'short'

Ligand Set	Complex	[M]	*d*(M1N1) Å	*d*(M1N1*) Å	*d*(M1M1*) Å
Et$_2$Ph[4]	**2.8**	Mo	1.8917(12)	1.9269(12)	2.6480(3)
	2.9	W	1.9095(17)	1.9254(18)	2.6445(2)
Et$_2$NMe$_2$[6]	**2.22**	Mo	1.8564(10)	1.9696(10)	2.6655(3)
	2.23	W	1.9095(17)	1.9254(18)	2.6445(2)
iPr$_2$Me[3]	**1.22****	Mo	1.8495(13)	1.9636(13)	2.6764(3)
	1.23	W	1.908(2)	1.912(2)	2.6560(3)

**puckered core: Mo-N bond lengths reflect *d*(M1N1)/*d*(M1N1*) or *d*(M1*N1)/*d*(M1*N1*)

Table 2.2. Bond lengths of M_2N_2 cores of dinuclear Mo and W (μ-N)$_2$ complexes **2.8**, **2.9**, **2.22**, **2.23**, **1.22**, and **1.23** obtained from XRD analysis.

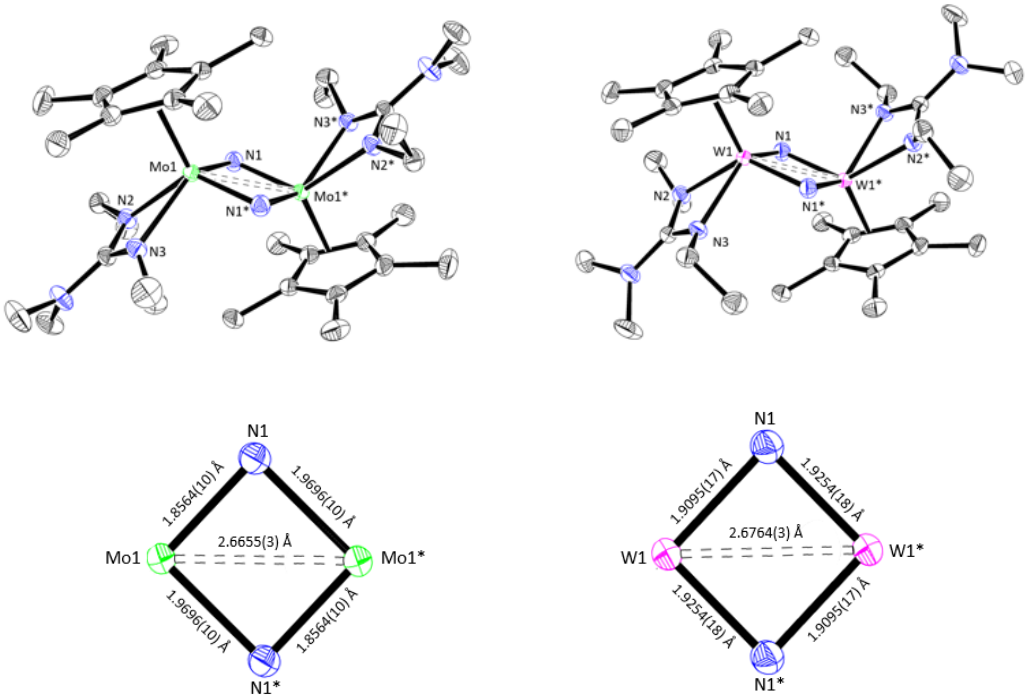

Figure 2.10. Top: Crystal structures of **2.22** (right) and **2.23** (left) with hydrogen atoms omitted for clarity, ellipsoids for the non-hydrogen atoms are shown at the 30% probability level. Bottom: Expanded view and bond lengths of M_2N_2 cores of **2.22** (right) and **2.23** (left)

bonds than the CPAM species, but both the sterically reduced diethyl CPAM ligand sets of **2.8**, **2.9**, **2.22**, **2.23**, have more disparate M-N bond lengths than the bulky diisopropyl set **1.22**, and **1.23**.[29]

2.5 Crossover and Scrambling Studies

With a complete set new dinitrogen-derived complexes **2.20** – **2.23** for the CPGU ligand set as well as the CPAM based **2.5**, **2.6**, **2.8**, and **2.9** now also in hand, crossover studies were undertaken with the goal of ruling out an intermolecular N_2 cleavage mechanism through crossover experiments.

2.5.1 ^{1}H NMR Experiments

To begin, a 1 : 1 mixture of the Mo amidinate **2.5** and guanidinate **2.20** was prepared in benzene-d_6 and heated at 55 °C, monitored by ^{1}H NMR as shown in Figure 2.11a. If intramolecular isomerization was occurring, the result of this experiment would be only a clean, 1 : 1 mixture of **2.8** and **2.22**. While these bridging bis-nitride species were observed over the course of the thermolysis, surprisingly, a number of ^{1}H NMR signals were also observed that corresponded neither to **2.8** nor **2.22**. These new signals are interpreted to belong to the crossover product of the amidinate and guanidinate complexes, {Cp*[N(Et)C(Ph)N(Et)]Mo}(μ-N)$_2${Cp*[N(Et)C(NMe$_2$)N(Et)]Mo} (**2.24**), as shown in Scheme 2.9. It is important to note, however, that the appearance of **2.24** does not necessarily mean that the mechanism of N_2 cleavage is fragmentation and recombination: It was discovered that a similar 1 : 1 mixture of pure **2.8** and **2.22** immediately began to react at room

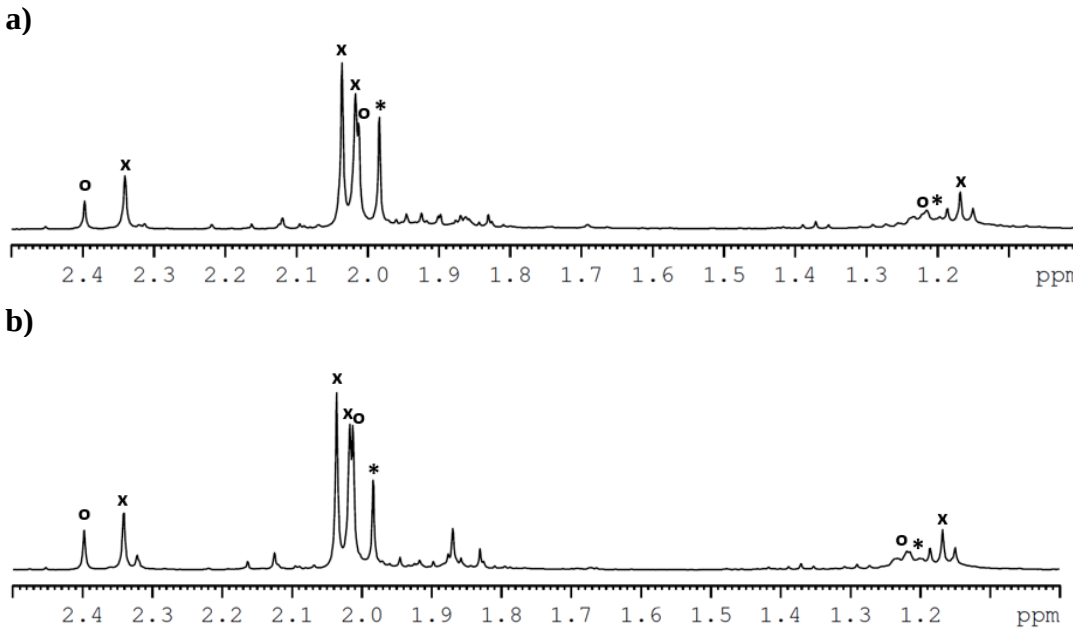

Figure 2.11. Partial ^{1}H NMR (400 MHz, benzene-d_6, 25 °C) spectra showing a mix of products **2.8** (*****), **2.22** (**o**), and **2.24** (**x**) from **a)** the thermolysis of **2.5** and **2.20** at 55 °C over 44 h or **b)** from the scrambling of **2.8** and **2.22** for 2 h at 65 °C

Scheme 2.9

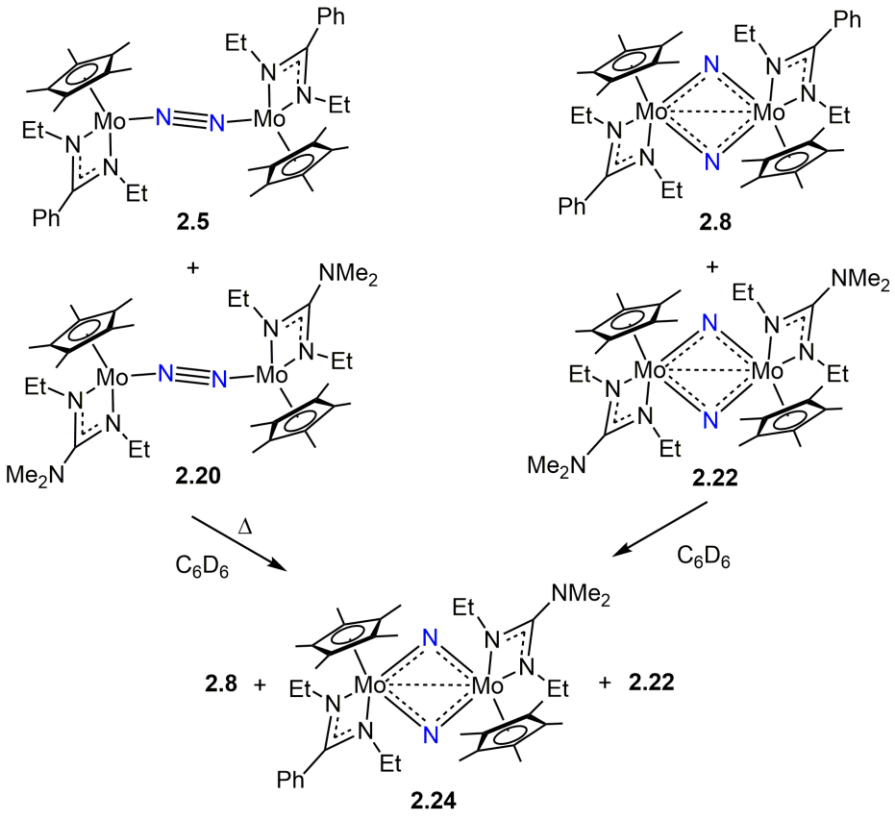

temperature to show the same ^{1}H NMR signals attributed to the crossover species **2.24**, shown in Figure 2.11b, and that therefore the bis (μ-N) complexes undergo scrambling indicative of a dynamic interchange, potentially even as soon as they are formed. For comparison, an authentic sample of **2.24** was prepared by the chemical reduction of a 1 : 1 mixture of **1** and **16** by NaHg under N_2 to make a mixture of **2.5**, **2.20**, and what is presumed to be the mixed-ligand end-on-bridged complex {Cp*[N(Et)C(Ph)N(Et)]Mo}(μ-η^1:η^1-N_2){Cp*[N(Et)C(NMe_2)N(Et)]Mo} (**2.25**). As is shown in Figure 2.12, this mixture was then heated to undergo thermal N_2 cleavage, the resulting ^{1}H NMR spectrum of which was nearly identical to the result of thermalizing only **2.5** and **2.20**, both showing a mixture of **2.8**, **2.22**, and **2.24**. While the results of the crossover experiment can now be explained without ruling out the

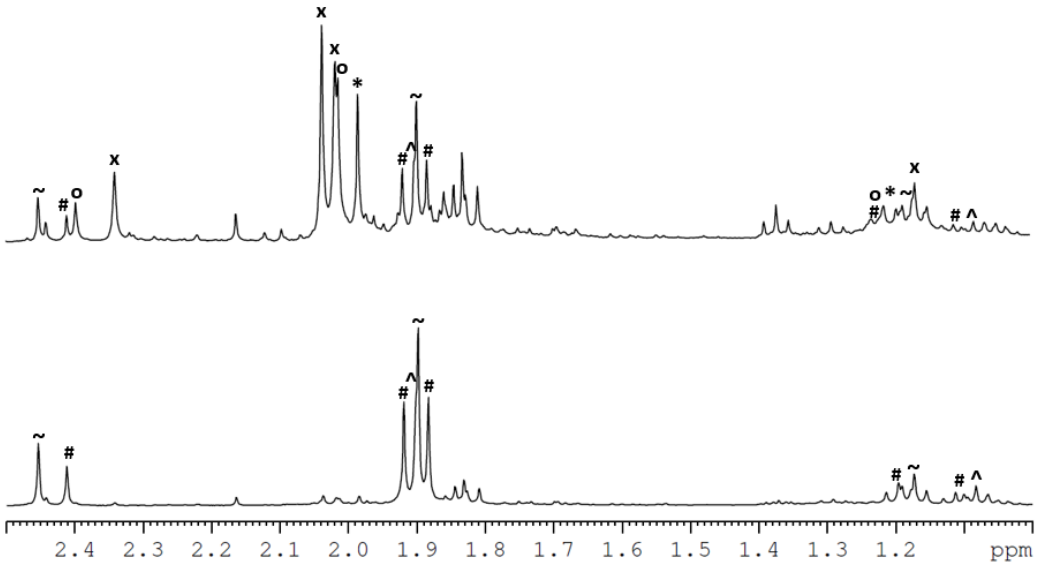

Figure 2.12. Partial ^{1}H NMR (400 MHz, benzene-d_6, 25 °C) spectra demonstrating the conversion of a mixture of **2.5** (^), **2.20** (~), and **2.25** (#) (bottom) to **2.8** (*), **2.22** (**o**), and **2.24** (**x**) (top) upon thermolysis for 15.5 h at 65 °C

possibility of intramolecular rearrangement taking place, it unfortunately means that for the experimental study of Mo, neither can a fragmentation mechanism cannot be definitively ruled out. [30]

Having already noted that the identity of the metal center has major impact upon the reactivity of the system, the same set of experiments was undertaken with W dinitrogen complexes. As is illustrated in Scheme 2.10, these studies had much more definitive results. A 1 : 1 benzene-d_6 mixture of CPAM **2.6** and CPGU **2.21** bis (μ-N) complexes was prepared and monitored by ^{1}H NMR throughout thermolysis at 80 °C, this time showing *only* the established products **2.9** and **2.23** as is displayed in Figure 2.13. Similarly, a 1 : 1 mixture of **2.9** and **2.23** showed no evidence of scrambling by ^{1}H NMR, remaining unchanged even upon heating the THF-d_8 sample, the result of which is illustrated in Figure 2.14. Authentic samples of the unobserved mixed-ligand dinitrogen complexes were prepared by the N_2 reduction of equimolar **2.4** and **2.19** by

Scheme 2.10

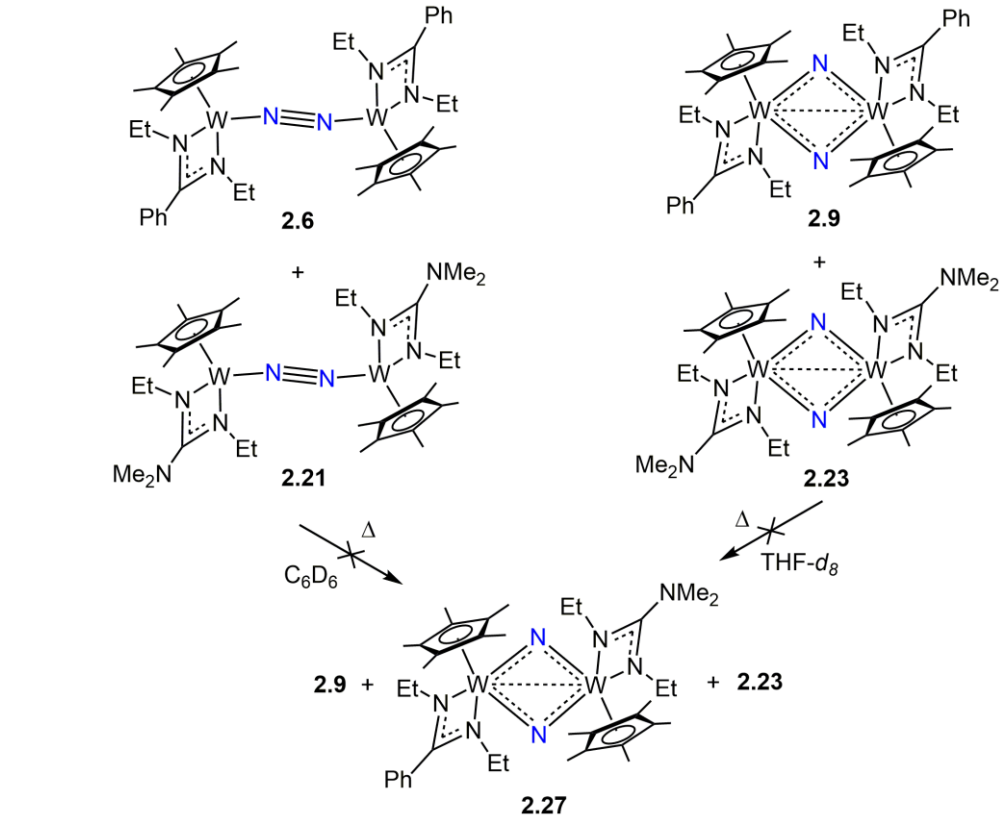

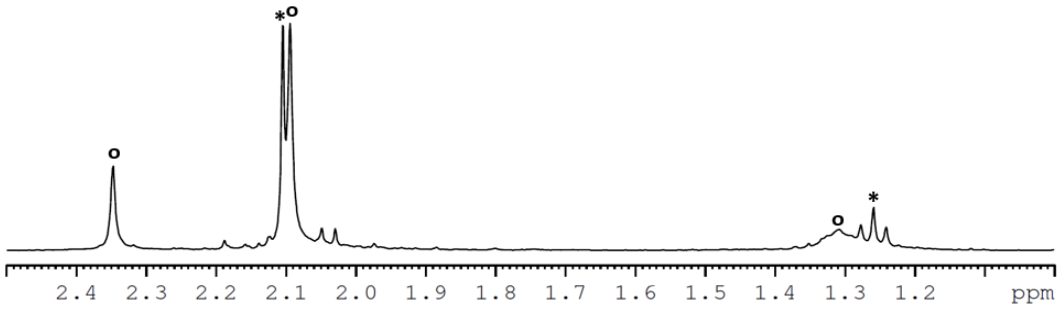

Figure 2.13. Partial ^{1}H NMR (400 MHz, benzene-d_6, 25 °C) showing mix of products **2.9** (*****) and **2.23** (**o**) from the thermolysis of **2.6** and **2.21** at 80 °C for 53 h

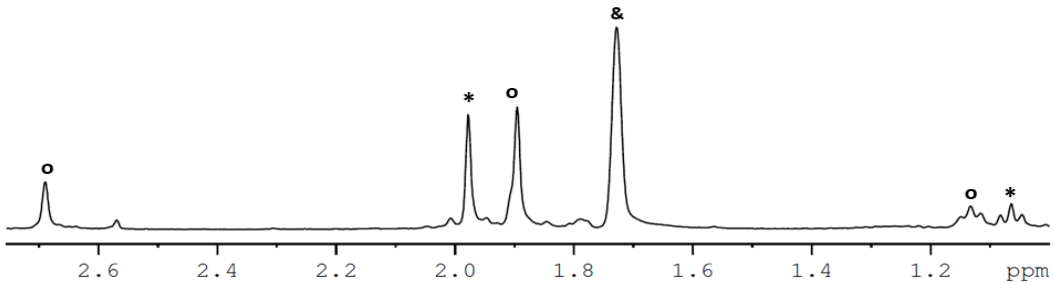

Figure 2.14. Partial ^{1}H NMR (400 MHz, THF-d_8, 25 °C) spectrum showing non-scrambled **2.9** (*****) and **2.23** (**o**) after heating for 17 h at 80 °C in THF-d_8 (**&**)

NaHg in THF to make a mixture of **2.6**, **2.21**, and what is again presumed to be the mixed-ligand end-on-bridged complex {Cp*[N(Et)C(Ph)N(Et)]W}(μ-η^1:η^1-N_2){Cp*[N(Et)C(NMe_2)N(Et)]W} (**2.26**). This mixture was then heated, resulting in a ^{1}H NMR spectrum showing a mixture of **2.9**, **2.23**, and signals attributed to the mixed-ligand bis (μ-N) product {Cp*[N(Et)C(Ph)N(Et)]W}(μ-$N)_2${Cp*[N(Et)C(NMe_2)N(Et)]W} (**2.27**), shown in Figure 2.15. When this spectrum was compared with the results of the crossover experiment, **2.27** was totally absent from the latter, indicating that *neither crossover nor scrambling is taking place* for the (μ-$N)_2$ W complexes. These experiments provide significant insight into the cleavage process. That no crossover product is observed rules out the possibility of fragmentation and recombination as the mechanism of N_2 cleavage by W CPAM

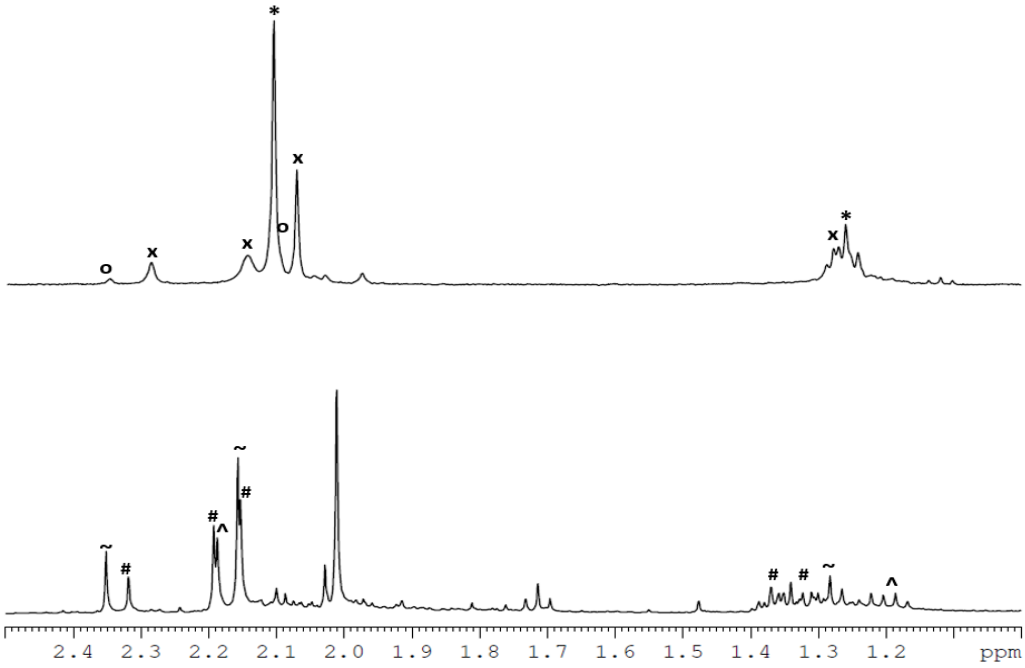

Figure 2.15. Partial ^{1}H NMR (400 MHz, benzene-d_6, 25 °C) spectra demonstrating the conversion of a mixture of **2.6** (^), **2.21** (~), and **2.26** (#) (bottom) to a pentane-washed mixture of **2.9** (*), **2.23** (**o**), and **2.27** (**x**) (top) upon heating for 18 h at 80 °C

complexes while that no scrambling occurs indicates that the dinuclear structures obtained for the solid state are not the result of the combination of mononuclear nitrides when in solution which would result in the presence of **2.27**.

2.5.2 ESI(+)-MS Experiments

Finally, to confirm that there are no stray, mixed-ligand W species in solution for these reactions (which could, based on the solubility problems of many of the bis (μ-N) species, conceivably be insoluble in benzene-d_6 and therefore not apparent by ^{1}H NMR), positive-mode electro-spray ionization mass spectrometry (ESI-MS) was used to confirm the masses of the products within the mixtures of **2.9** and **2.23** or **2.9**, **2.23**, and **2.27**. Like the ^{1}H NMR spectrum from Figure 2.13, Figure 2.16 depicts the ESI-MS(+) taken of the result of the "crossover" thermolysis of **2.6** and **2.21** which tellingly

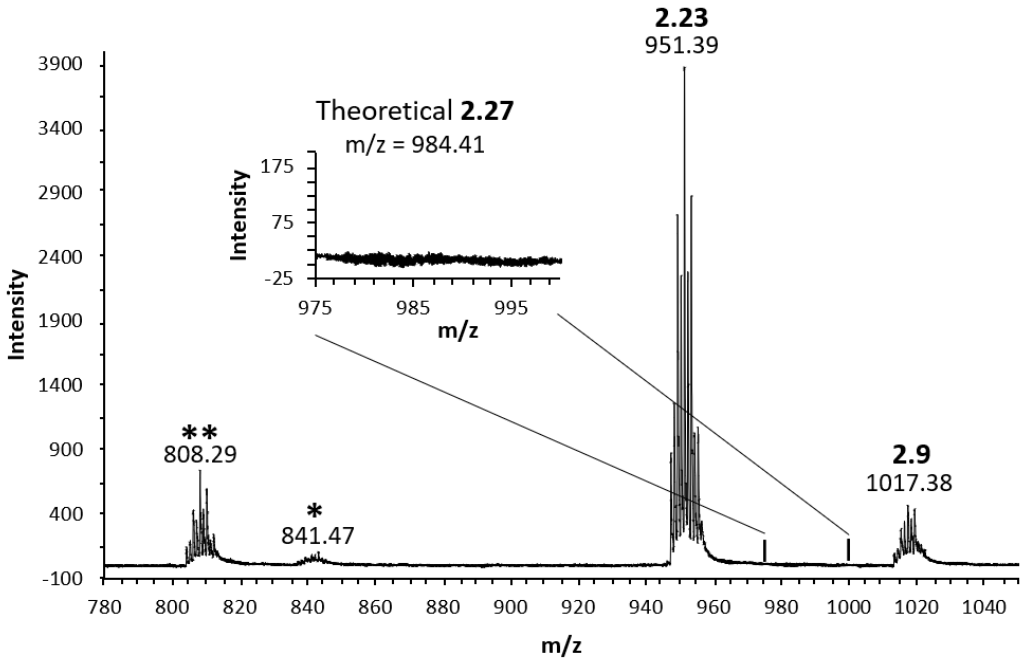

Figure 2.16. ESI-MS(+) in THF of the products of heating a mixture of **2.6** and **2.21** in benzene-d_6 at 80 °C for 53 h. No theoretical crossover product **2.27** was observed, only **2.9** and **2.23**. Fragments resulting from the loss of an amidinate or guanidinate are noted, {Cp*[N(Et)C(Ph)N(Et)]W(μ-N)}{Cp*W(μ-N)} ($[M]^+$ m/z = 841.21) (*****) or {Cp*[N(Et)C(NMe_2)N(Et)]W(μ-N)}{Cp*W(μ-N)} ($[M]^+$ m/z = 808.18) (******)

shows signal sets corresponding *only* to **2.9** ($[M + H]^+$ = 1017.38 m/z) and **2.23** ($[M + H]^+$ = 951.39 m/z) and their fragments. The fragments of lower mass in the spectrum correspond neatly to the loss of either an amidinate or guanidinate ligand from a W center, and there is no evidence of any signal anywhere else that would belong to the crossover species **2.27**. To limit the exposure of the sample to air and moisture, care was taken to seal the THF solutions in GPC vials while inside the glovebox and rinse the spectrometer lines with dry solvent prior to injection. Importantly, Figure 2.17 shows the ESI(+) under the same conditions of the authentic sample of the crossover product, **2.27** with **2.6** and **2.21**, which clearly displays the same fragments and peaks for each species i*ncluding* **2.27** ($[M + H]^+$ m/z = 984.41), even more clearly demonstrating the absence of **2.27** form Figure 2.16.

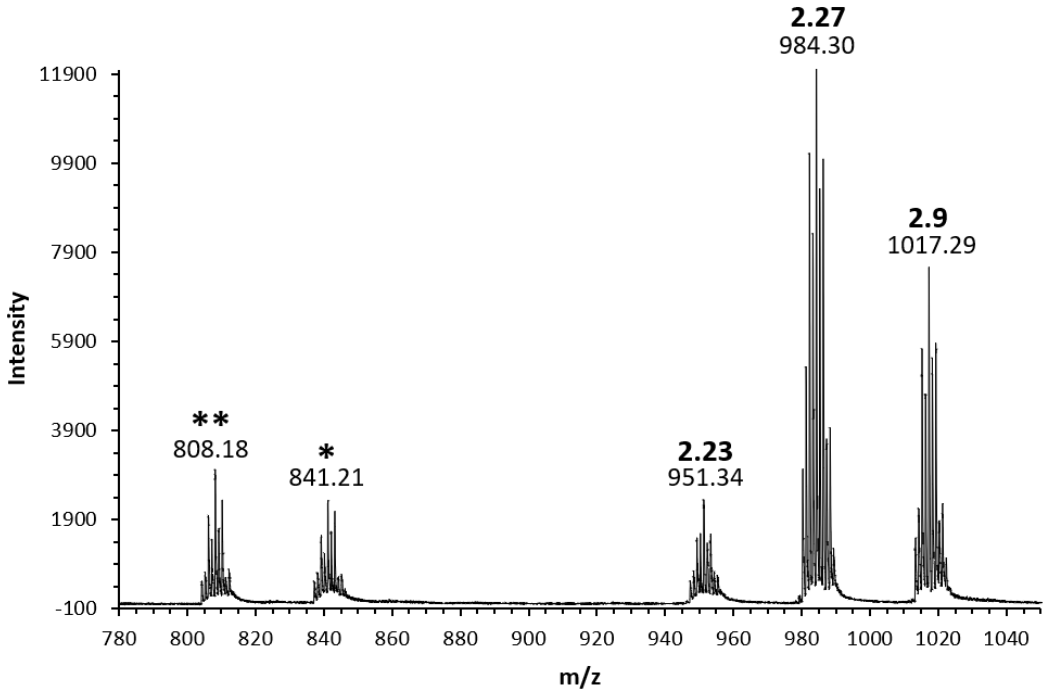

Figure 2.17. ESI-MS(+) of THF solution of **2.9**, **2.23**, **2.27**, the products of heating a mixture of **2.6**, **2.21**, and **2.26** in benzene-d_6 at 80 °C for 18 h. Fragments resulting from the loss of an amidinate or guanidinate are noted, {Cp*[N(Et)C(Ph)N(Et)]W(μ-N)}{Cp*W(μ-N)} ($[M]^+$ m/z = 841.21) (*****) or {Cp*[N(Et)C(NMe_2)N(Et)]W(μ-N)}{Cp*W(μ-N)} ($[M]^+$ m/z = 808.18) (******)

2.6 Conclusions

The correlation between the reduced steric demands of the CPAM ligand set and the reduced barriers to N_2 coordination and cleavage is both clear and gratifying. The above diethyl, phenyl CPAM and diethyl, dimethylamino CPGU complexes represent a significant step forward in the field, both in terms of successful examples of coordination and cleavage and in terms of mechanistic understanding what is accessible for group 6 dinitrogen complexes. Decreasing of the CPAM sterics via amidinate or guanidinate derivates was unequivocally shown to facilitate more facile N_2 cleavage and this, importantly, suggests that subsequent heteroatom transfer might also be more easily accessible.

This series of new transformations from Group 6 dinuclear (μ-N_2) to the dinuclear bis (μ-N) complexes is remarkable in its rarity, its adaptability, and its unique mechanism. **2.5** to **2.8** is only the second report of thermally mediated cleavage for Mo while **2.6** to **2.9** is the first ever reported example for W-mediated thermal cleavage. Moreover, these amidinate complexes are the first example of thermolytic N_2 cleavage in a *pair of congeners* of the heavier group 6 metals that are supported by the same ligand set. This importance is only magnified by the additional pair of guanidinate congeners and their transformations of Mo **2.20** to **2.22** and W **2.21** to **2.23**. Their presence nearly doubles the total number of examples of well characterized thermolytic group 6 N_2 cleavage. This allows for the unprecedented ability to directly compare either the two metal centers or ligand frameworks with regard to their structural and mechanistic similarities and differences, continuing to tease out and map N_2 reactivity in the early transition metals. Additionally, experimental studies now conclusively

confirm that, at least in the case of W, the thermal cleavage of N≡N is an intramolecular rearrangement. Though the results have been long hypothesized, the crossover experiments still shed light on this unique mechanism which is so unlike the only previous example of a "zig-zag" transition state and an intermolecular cleavage. However, a computational analysis of likely intermediates, including the proposed side-on-bridged species, would be of interest, especially with regards to explaining the dynamic behavior noted for the Mo complexes.

Finally, besides the diisopropyl, methyl CPAM complexes **1.22** and **1.23**,[5] no other group 6 complexes have been reported that display a 4-membered M_2N_2 core. This unique geometry is of interest not only because of its rarity within Group 6 dinitrogen activation and fixation studies, but also because of it's potential to undergo further functionalization reactions to be discussed in Chapters 3 and 5 of this document.

2.7 Experimental Details

2.7.1 General Considerations

All manipulations of air and moisture sensitive compounds were carried out under N_2 or Ar atmospheres with standard Schlenk or glovebox techniques. Et_2O and THF were distilled from Na/benzophenone under N_2 prior to use. Toluene and pentane were dried and deoxygenated by passage over activated alumina and GetterMax® 135 catalyst (purchased from Research Catalysts, Inc.) within a PureSolv solvent purification system manufactured by Innovative Technologies (model number PS-400-4-MD) and collected under N_2 prior to use. Benzene-d_6, toluene-d_8, THF-d_8, and methylcyclohexane were dried over Na/K alloy and isolated by vacuum transfer prior to use. Celite© was oven dried (150 °C for several days) prior to use. Cooling was

performed in the internal freezer of a glovebox maintained at -30 °C. Trimethylsilyl azide, trimethylsilyl chloride, bromobenzene-d_5, lithium dimethylamide, 4-bromobisphenyl, 4-iodotoluene, and *n*-butyllithium (2.5 M in hexanes) were purchased from Sigma Aldrich and used as received. Cp*$MoCl_4$,[31-33] Cp*WCl_4,[31-33] N,N'-diethylcarbodiimide,[1] were prepared according to the previously reported procedures in similar yield and purity. All room temperature ^{1}H NMR were recorded at 400.13 MHz and referenced to $SiMe_4$ using residual ^{1}H chemical shifts of benzene-d_6, toluene-d_8, or THF-d_8. High temperature ^{1}H NMR studies were recorded at 500 MHz with temperature calibration involving methanol standard. ^{13}C NMR spectra were recorded at 125.76 MHz and calibrated to residual ^{13}C chemical shifts of benzene-d_6, toluene-d_8, or THF-d_8. Scanning UV-Vis spectra were collected on an Agilent Cary 60 Spectrophotometer equipped with a Quantum Northwest temperature-controlled cuvette holder. ESI Mass Spectra were acquired at a rate of one spectrum per second with the m/z range of 400 to 2000 and were obtained from an atmospheric pressure ionization Time-of-Flight mass spectrometer (AccuTOF, JEOL, USA, Inc.) that was coupled with an Agilent 1100 HPLC system. The AccuTOF was equipped with an ESI ion source at a resolving power of 6000 (FWHM). The AccuTOF MS settings are as follows: needle voltage = 2100 V, desolvating chamber temperature = 250 °C, orifice 1 temperature = 100 °C, orifice 1 V= 30 V, orifice 2 = 5 V, ring V= 10 V. Elemental analyses were carried out by Midwest Microlab, LLC.

2.7.2 Synthesis of New Compounds

Cp*[N(Et)C(Ph)N(Et)]$MoCl_2$ (2.3). A solution of N,N'-diethylcarbodiimide (821.0 g, 8.366 mmol) in 25 mL Et_2O was added dropwise to a stirring solution of 15

mL Et_2O with phenyllithium (4.9 mL, 8.3 mmol) chilled to -30° C. After stirring for 1 h, the now white salt suspension was transferred via canula to a purple suspension of Cp*$MoCl_4$ (1.5212 g, 4.079 mmol) in 20 mL Et_2O cooled to -30° C and the mixture was stirred, warming to 0° C over 1 h. After further warming to room temperature, the solvent was removed *in vacuo* to afford a dark red solid that was dissolved in toluene and filtered through a frit with celite, concentrated, and recrystallized in toluene and pentane at -30° C to yield maroon crystals of **2.3** (1.8725 g, 96% yield). Anal. calc'd for $C_{21}H_{30}Cl_2N_2Mo$: C, 52.84; H, 6.33; N, 5.87; Found: C, 53.07; H, 6.15; N, 6.02. ^{1}H NMR (400 MHz, C_6D_6, 25 °C) -9.24 (2H, br s, CH_2(CH_3)), 2.42 (2H, br s, CH_2(CH_3)), 3.08 (1H, br s, C(C_6H_5)), 5.58 (6H, br s, CH_2(CH_3)), 9.87 (15H, br s, C_5(CH_3)$_5$)), 13.59 (2H, br s, C(C_6H_5)).

Cp*[N(Et)C(Ph)N(Et)]WCl_2 (2.4). A solution of **Li[N(Et)C(Ph)N(Et)]** (611.1 mg, 4.620 mmol) in 15 mL Et_2O was cooled to -30° C and added dropwise to a stirring brown suspension of Cp*WCl_4 (980.6 mg, 2.128 mmol) in 25 mL Et_2O cooled to -30° C. The mixture was allowed to stir for 15 h while warming to room temperature and volatiles were removed *in vacuo*. The resulting brunneous, dark red oil was dissolved in toluene and filtered through a frit with celite and the collected filtrate was dried under reduced pressure before being washed in pentane and recrystallized in toluene layered with pentane at -30° C to produce dark red-orange crystals of **2.4** (510.8 mg, yield = 41%). Anal. calc'd for $C_{21}H_{30}Cl_2N_2W$: C, 44.62; H, 5.35; N, 4.95; Found: C, 44.51; H, 5.19; N, 5.15. ^{1}H NMR (400 MHz, benzene-d_6): 0.81 (6H, t, J = 7.4 Hz, CH_2(CH_3)), 2.15 (15H, s, C_5(CH_3)$_5$), 3.24 – 3.33 (2H, m, CH_2(CH_3)), 3.86 – 3.95 (2H, m, CH_2(CH_3)), 6.92 – 7.14 (m, C(C_6H_5)). ^{13}C{H} NMR (125 MHz, C_6D_6, 25° C): 13.25

($C_5(CH_3)_5$), 17.80 ($CH_2(CH_3)$), 45.96 ($CH_2(CH_3)$), 106.96 ($C_5(CH_3)_5$), 125.70 ($C(C_6H_5)$), 128.57 ($C(C_6H_5)$), 129.34 ($C(C_6H_5)$), 130.96 ($C(C_6H_5)$), 168.68 ([(N(Et)*C*(Ph)N(Et)]).

Li[N(Et)C(Ph)N(Et)]. Phenyllithium (16.0 mL, 0.0329 mol) was added dropwise to a solution of N,N'-diethylcarbodiimide (3.9439 g, 0.03459 mol) in 30 mL Et_2O chilled previously to -30° C. The mixture was allowed to warm to room temperature while stirring for 16 h after which volatiles were removed *in vacuo* to yield a brown-orange, oily solid that was washed in pentane to yield a white, auburn tinged solid (4.2629 g, yield = 71 %) dried under reduced pressure. ^{1}H NMR (400 MHz, benzene-d_6): 1.72 (3H, t, J = 7.2 Hz, $CH_2(CH_3)$), 3.55 (1H, m, $CH_2(CH_3)$), 3.69 (1H, m, $CH_2(CH_3)$), 7.20 – 7.24 (5H, m, ($C(C_6H_5)$).

{Cp*[N(Et)C(Ph)N(Et)]Mo}$_2$(μ-η^1:η^1-N$_2$) (2.5). 2.3 (0463.1 g, 0.9702 mmol) was dissolved in 40 mL THF and cooled to -30° C. To this was added 0.5% (w/w) Na/Hg (13.3841 g, 2.911 mmol Na) and stirred under a N_2 atmosphere for 2 h while warming to 25 °C changing in color from maroon, to navy blue, to brown. Volatiles were removed *in vacuo* yielding a brown solid dissolved in pentane and filtered through a frit with celite. The collected filtrate was dried under reduced pressure and recrystallized in pentane and toluene at -30° C to produce dark golden-orange crystals **2.5** (345.5 mg, 85%). Anal. calc'd for $C_{42}H_{60}N_6Mo_2$: C, 60.00; H, 7.19; N, 9.99; Found: C, 59.93; H, 7.30; N, 9.78. ^{1}H NMR (400 MHz, C_6D_6, 25 °C): 1.11 (6H, t, J = 7.1 Hz, $CH_2(CH_3)$), 1.90 (15H, s, $C_5(CH_3)_5$), 2.74 – 2.82 (2H, m, $CH_2(CH_3)$), 3.04 – 3.13 (2H, m, $CH_2(CH_3)$), 6.99 – 7.13 (m, $C(C_6H_5)$). ^{13}C{H} NMR (125 MHz, C_6D_6, 25° C): 12.44 ($C_5(CH_3)_5$), 18.63 ($CH_2(CH_3)$), 44.69 ($CH_2(CH_3)$), 106.11 ($C_5(CH_3)_5$), 128.64

(C(C_6H_5)), 128.81 (C(C_6H_5)), 132.51 (C(C_6H_5)), 177.39 ([(N(Et)*C*(Ph)N(Et)]). UV-Vis (methylcyclohexane) λ (nm) (ε): 806 (429), 461 (1121), 342 (1562).

{Cp*[N(Et)C(Ph)N(Et)]W}$_2$(μ-η^1:η^1-N$_2$) (2.6). An orange solution of **2.4** (219.0 g, 0.3875 mmol) in 30 mL THF was cooled to -30° C and 0.5% (w/w) Na/Hg (5.4112 g, 1.177 mmol Na) was added. After stirring for 2 h passing through a dark purple in color while warming to 25° C, volatiles were removed *in vacuo* to yield a dark green solid that was dissolved in pentane and filtered through a frit with celite. The collected filtrate was dried under reduced pressure and recrystallized in pentane with acetonitrile at -30° C to produce dark green crystals of **2.6** (152.2 mg, 80%). Anal. calc'd for $C_{42}H_{60}N_2W_2$: C, 49.62; H, 5.95; N, 8.26; Found: C, 49.39; H, 5.70; N, 8.05. ^{1}H NMR (400 MHz, benzene-d_6): 1.22 (6H, t, J = 7.1 Hz, CH_2(C*H*$_3$)), 2.19 (15H, s, C_5(C*H*$_3$)$_5$), 2.74 – 2.82 (2H, m, C*H*$_2$(CH_3)), 3.04 – 3.13 (2H, m, C*H*$_2$(CH_3)), 7.07 – 7.24 (m, C(C_6*H*$_5$)). ^{13}C{H} NMR (125 MHz, C_6D_6, 25° C): 14.00 (C_5(*C*H$_3$)$_5$), 19.47 (CH_2(*C*H$_3$)), 45.43 (*C*H$_2$(CH_3)), 103.08 (*C*$_5$(CH_3)$_5$), 128.96 ((C(*C*$_6$H$_5$)), 134.14 ((C(*C*$_6$H$_5$)), 183.07 ([(N(Et)*C*(Ph)N(Et)]).

{Cp*[N(Et)C(Ph)N(Et)]Mo(μ-Cl)}$_2$ (2.7). A solution of **1** (198.2 mg, 0.4152 mmol) in 15 mL THF was cooled to -30° C to which 0.5% (w/w) Na/Hg (5.7555 g, 1.252 mmol Na) was added. After the reaction was and stirred for 30 minutes while warming to 25° C under a N_2 atmosphere, volatiles were removed *in vacuo* to yield a brown solid from which brown **2.5** was removed by washing with pentane. A navy blue solid remained that was then dissolved in toluene and filtered through a frit with celite. The collected filtrate was dried on vacuum and dissolved in toluene to recrystallize at -30° C producing purple-navy blue crystals of **2.7** (40.2 mg, yield = 23 %). ^{1}H NMR

(400 MHz, C_6D_6, 25 °C): -2.90 (2H, br s, C*H*$_2$(CH_3)), -2.19 (2H, br s, C*H*$_2$(CH_3)), 0.339 (15H, br s, C_5(C*H*$_3$)$_5$)), 0.95 (6H, br s, CH_2(C*H*$_3$)), 5.51 (2H, br s, C(C_6*H*$_5$)), 5.65 (1H, br s, C(C_6*H*$_5$)), 8.95 (2H, br s, C(C_6*H*$_5$)).

{Cp*[N(Et)C(Ph)N(Et)]Mo(μ-N)}$_2$ (2.8). 2.5 (80.3 mg, 95.5 μmol) was dissolved in 3.5 mL toluene in a heavy wall pressure vessel. The orange solution was heated at 65° C for 16 h causing brown crystals to crash out. The solvent was then removed *in vacuo* and the resulting brown crystalline solid was rinsed in pentane before being recrystallized in THF to yield brown crystals of **2.8** (63.9 mg, 80% yield). $C_{42}H_{60}N_2Mo_2$: C, 60.00; H, 7.19; N, 9.99; Found: C, 59.86; H, 7.33; N, 9.65. ^{1}H NMR (400 MHz, C_6D_6, 25 °C): 1.22 (6H, t, J =7.2 Hz, CH_2(C*H*$_3$)), 1.99 (15H, s, C_5(C*H*$_3$)$_5$), 3.11 – 3.20 (2H, m, C*H*$_2$(CH_3)), 3.20 – 3.29 (2H, m, C*H*$_2$(CH_3)), 7.08 – 7.33 (5H, m, C(C_6*H*$_5$)). ^{13}C{H} NMR (125 MHz, C_6D_6, 25° C): 12.03 (C_5(*C*H_3)$_5$), 17.90 (CH_2(*C*H_3)), 42.47 (*C*H_2(CH_3)), 111.26 (*C*$_5$(CH_3)$_5$), 127.38 (C(*C*$_6$H$_5$)), 128.45 (C(*C*$_6$H$_5$)), 128.57 (C(*C*$_6$H$_5$)), 134.72 (C(*C*$_6$H$_5$)), 175.48 ([(N(Et)*C*(Ph)N(Et)]). UV-Vis (methylcyclohexane) λ (nm) (ε): 632 (535), 464 (1486), 348 (8486).

{Cp*[N(Et)C(Ph)N(Et)]W(μ-N)}$_2$ (2.9) A green solution of **2.6** (32.4 mg, 31.9 μmol) in 1 mL benzene-*d*$_6$ was heated to 60 °C on an oil bath for 187 hours causing brown crystalline material to crash out. The solvent was removed *in vacuo* and pentane was used to wash the dark brown crystalline product **2.9** (25.0 mg, 77%). Anal. calc'd for $C_{42}H_{60}N_2W_2$: C, 49.26; H, 5.95; N, 8.26; Found: C, 49.67; H, 6.16; N, 8.24. ^{1}H NMR (400 MHz, benzene-*d*$_6$): 1.26 (6H, t, J = 7.2 Hz, CH_2(C*H*$_3$)), 2.11 (15H, s, C_5(C*H*$_3$)$_5$), 3.15 – 3.26 (4H, m, C*H*$_2$(CH_3)), 7.00 – 7.13 (5H, m, C(C_6*H*$_5$)). ^{13}C{H} NMR (125 MHz, C_6D_6, 25° C): 12.84 (C_5(*C*H_3)$_5$), 18.06 (CH_2(*C*H_3)), 41.58

($CH_2(CH_3)$), 108.72 ($C_5(CH_3)_5$), 127.43 (C(C_6H_5)), 128.35 (C(C_6H_5)), 128.62 (C(C_6H_5)), 135.35 (C(C_6H_5)), 177.77 ([(N(Et)*C*(Ph)N(Et)]).

{Cp*[N(Et)C(C_6D_5)N(Et)]$MoCl_2$} (2.10). A solution of **Li[N(Et)C(C_6D_5)N(Et)]** (0.3380 g, 1.805 mmol) in 10 mL Et_2O chilled to -30° C was added dropwise to a stirring purple suspension of Cp*$MoCl_4$ (0.3235 g, 0.8673 mmol) in 25 mL Et_2O at -30° C. The resulting red brown solution was and allowed to come to room temperature and stirred for 15.5 h before the volatiles were removed *in vacuo* yielding a brown solid filtered through a frit with celite in toluene. The collected filtrate was concentrated and recrystallized in toluene and pentane at -30° C to produce dark red crystals of **2.10** (0.2084 g, 49%). ^{1}H NMR (400 MHz, C_6D_6, 25 °C) -9.10 (2H, br s, C*H*$_2(CH_3)$), 5.55 (6H, br s, CH_2(C*H*$_3$)), 9.88 (15H, br s, C_5(C*H*$_3$)$_5$)).

Li[N(Et)C(C_6D_5)N(Et)]. *n*-Butyllithium (3.45 mL, 9.04 mmol) added dropwise to bromobenzene-d_5 (1.6116 g, 9.946 mmol) in 30 mL Et_2O chilled to -30° C. Colorless solution let warm to 0° C and stirred for 2 h, cooled to -30° C and N-N, diethylcarbodiimide (0.8988 g, 9.158 mmol) was added dropwise and stirred for 20 min before warming to room temperature and removing solvent *in vacuo.* White oily solid washed in -30° C pentane to produce a white powder **Li[N(Et)C(C_6D_5)N(Et)]** (0.8253 g, 49%).

{Cp*[N(Et)C(C_6D_5)N(Et)]Mo}$_2$(μ-η^1:η^1-N_2) (2.11). 7 (0.2048 g, 0.4246 mmol) in 20 mL THF was cooled to -30° C to which was added sodium amalgam (0.5% w/w) (5.8580 g, 1.2746 mmol Na) and stirred for 4 h under a N_2 atmosphere while warming to 25 °C. Volatiles removed *in vacuo* yielding brown solid dissolved in pentane and filtered through a frit with celite. The collected filtrate was dried on

vacuum and dissolved in pentane and toluene at -30° C to produce dark brown/golden orange crystals **2.11** (47.7 mg, yield = 26 %). ^{1}H NMR (400 MHz, benzene-d_6, 25° C): 1.11 (6H, t, J = 14.3 Hz, $CH_2(CH_3)$), 1.90 (15H, s, $C_5(CH_3)_5$), 2.79 (2H, m, $CH_2(CH_3)$), 3.08 (2H, m, $CH_2(CH_3)$).

{Cp*[N(Et)C(C_6D_5)N(Et)]Mo(μ-N)}$_2$ (2.12). **7** (11.0 mg, 12.9 μmol) was dissolved in 0.6 mL C_6D_6 in a J Young NMR tube and heated to 70 °C on an oil bath. Monitoring by ^{1}H NMR showed clean conversion to a set of peaks very similar to those for **2.8** but lacking aromatic resonances. ^{1}H NMR (400 MHz, benzene-d_6, 25° C): 1.28 (6H, t, J = 7.24 Hz, $CH_2(CH_3)$), 2.05 (15H, s, $C_5(CH_3)_5$), 3.18 – 3.35 (4H, m, $CH_2(CH_3)$).

{Cp*Mo[N(Et)C(C_6D_5)N(Et)]Cl_2} (2.13). A solution of **Li[N(Et)C(*p*-tol)N(Et)]** (0.4326 g, 2.204 mmol) in 20 mL Et_2O chilled to -30° C was added dropwise to a stirring purple suspension of Cp*$MoCl_4$ (0.3895 g, 1.044 mmol) in 15 mL Et_2O at -30° C. The resulting brown solution was and allowed to come to room temperature and stirred for 22 h before the volatiles were removed *in vacuo* yielding a brown solid filtered through a frit with celite in toluene. The collected filtrate was concentrated and recrystallized in toluene and pentane at -30 °C to produce dark brown crystals of **2.13** (0.4347 g, 85%). ^{1}H NMR (400 MHz, C_6D_6, 25 °C) -8.96 (2H, br s, $CH_2(CH_3)$), 5.68 (6H, br s, $CH_2(CH_3)$), 9.99 (15H, br s, $C_5(CH_3)_5$)).

Li[N(Et)C(*p*-tol)N(Et)]. *n*-butyllithium (3.22 mL, 7.224 mmol) was added dropwise to a clear, stirring solution of 4-iodotoluene (1.801 g, 8.260 mmol) in 25 mL Et_2O chilled to -30 °C. The solution was let warm to 0 °C and stirred for 2 h becoming white after which it was cooled back to -30 °C and diethylcarbodiimide (0.7090 g, 7.224

mmol) in 15 mL Et_2O was added dropwise. The foggy mixture was allowed to stir for 30 minutes, the gradually warmed to 25 °C and the solvent removed *in vacuo.* Pale yellow solid washed in -30° C pentane to produce a pale yellow powder **Li[N(Et)C(*p*-tol)N(Et)]** (1.3291 g, 94%).

{Cp*[N(Et)C(*p*-tol)N(Et)]Mo}$_2$(μ-η^1:η^1-N_2) (2.14). 2.13 (0.4243 g, 0.8636 mmol) in 35 mL THF was cooled to -30° C to which was added sodium amalgam (0.5% w/w) (12.1312 g, 2.638 mmol Na) and stirred for 2 h under a N_2 atmosphere while warming to 25 °C. Volatiles removed *in vacuo* yielding brown solid dissolved in pentane and filtered through a frit with celite. The collected filtrate was dried on vacuum and dissolved in pentane and toluene at -30° C to produce dark red oily solid recrystallized in toluene and pentane to yield small red crystals which were not shown to be clean by ^{1}H NMR and which could not be isolated without impurity.

{Cp*[N(Et)C(4-biphenyl)N(Et)]$MoCl_2$} (2.15). A solution of **Li[N(Et)C(4-biphenyl)N(Et)]** (0.4726 g, 1.660 mmol) in 10 mL Et_2O chilled to -30° C was added dropwise to a stirring purple suspension of Cp*$MoCl_4$ (0.3256 g, 0.8730 mmol) in 20 mL Et_2O at -30° C. The resulting brown solution was and allowed to come to room temperature and stirred for 16 h before the volatiles were removed *in vacuo* yielding a brown solid filtered through a frit with celite in toluene. The collected filtrate was concentrated and recrystallized in toluene and pentane at -30° C to produce reddish-brown crystals of **2.15** (0.4206 g, 87%). ^{1}H NMR (400 MHz, C_6D_6, 25 °C) -9.86 (2H, br s, C*H*$_2$(CH_3)), 1.93 (2H, br s, C*H*$_2$(CH_3)), 5.78 (6H, br s, CH_2(C*H*$_3$)), 7.95 (1H, br s, C(C_6H_4)(C_6*H*$_5$), 10.04 (15H, br s, C_5(C*H*$_3$)$_5$)), 14.43 (2H, br s, C(C_6*H*$_4$)).

Li[N(Et)C(4-biphenyl)N(Et)]. *n*-butyllithium (3.00 mL, 7.944 mmol) was added dropwise to a clear, stirring solution of 4-bromobiphenyl (2.037 g, 8.789 mmol) in 30 mL Et_2O chilled to -30 °C. The solution was let warm to 0 °C and stirred for 2 h becoming foggy grey after which it was cooled back to -30 °C and N,N'-diethylcarbodiimide (0.7814 g, 7.962 mmol) in 20 mL Et_2O was added dropwise. The foggy mixture was allowed to stir for 30 minutes becoming white, then the gradually warmed to 25 °C and the solvent removed *in vacuo.* White solid washed in -30° C pentane to produce a white powder **Li[N(Et)C(4-biphenyl)N(Et)]** (2.0447 g, 99%).

{Cp*[N(Et)C(4-biphenyl)N(Et)]Mo}$_2$(μ-η^1:η^1-N_2) (2.16). 2.15 (0.1677 g, 0.3030 mmol) in 35 mL THF was cooled to -30° C to which was added sodium amalgam (0.5% w/w) (4.1658 g, 0.9060 mmol Na) and stirred for 30 min under a N_2 atmosphere while warming to 25 °C. Volatiles removed *in vacuo* yielding brown solid dissolved in pentane and filtered through a frit with celite. The collected filtrate was dried on vacuum and dissolved in pentane and toluene at -30° C to produce brownish-black crystals of **2.16** (67.0 mg, 45%). ^{1}H NMR (400 MHz, benzene-d_6, 25° C): 1.19 (6H, t, J = 7.15 Hz, $CH_2(CH_3)$), 1.94 (15H, s, $C_5(CH_3)_5$), 2.80 – 2.89 (2H, m, $CH_2(CH_3)$), 3.14 – 3.23 (2H, m, $CH_2(CH_3)$), 7.11 – 7.54 (m, $C(C_6H_4)(C_6H_5)$).

{Cp*[N(Et)C(4-bipheneyl)N(Et)]Mo(μ-N)}$_2$ (2.17). 2.16 (3.8 mg, 3.8 μmol) was dissolved in 0.6 mL C_6D_6 in a J Young NMR tube and heated to 70 °C on an oil bath. Monitoring by ^{1}H NMR showed conversion of peaks but also appearance of impurities; **2.16**, therefore, could not be cleanly produced.

{Cp*[N(Et)C(NMe_2)N(Et)]$MoCl_2$} (2.18). Cp*$MoCl_4$ (0.4803 g, 1.288 mol) was suspended in 25 mL Et_2O and cooled to -30° C. To this was added a suspension of

Li[N(Et)C(NMe$_2$)N(Et)] (0.4091 g, 2.743 mol) in 15 mL Et$_2$O pre-cooled to -30° C and the mixture was warmed to room temperature while stirring 16.5 h, changing in color from purple to brown. The solvent was removed *in vacuo* to afford a dark orange-brown solid that was dissolved in toluene and filtered through a frit with celite. The resulting filtrate was dried under reduced pressure and recrystallized in toluene and pentane at -30° C to yield dark brown crystals of **2.18** (0.5133 g, 93% yield). Anal. calc'd for $C_{17}H_{31}Cl_2N_3Mo$ • 1/10 toluene: C, 46.90; H, 7.02; N, 9.27; Found: C, 46.98; H, 7.34; N, 9.44. ^{1}H NMR (400 MHz, C_6D_6, 25 °C) -4.53 ((2H, br s, C*H*$_2$(CH$_3$))), 9.25 (6H, br s, CH$_2$(C*H*$_3$)), 14.14 (15H, br s, C$_5$(C*H*$_3$)$_5$).

{Cp*[N(Et)C(NMe$_2$)N(Et)]WCl$_2$} (2.19). Cp*WCl$_4$ (0.2051 g, 0.5612 mol) was suspended in 25 mL Et$_2$O and cooled to -30° C. To this was added a suspension of **Li[N(Et)C(NMe$_2$)N(Et)]** (0.1760 g, 1.180 mol) in 20 mL Et$_2$O pre-cooled to -30° C and the mixture was warmed to room temperature while stirring for 4 h, changing in color from purple to brown. The solvent was removed *in vacuo* to afford a dark orange-brown solid that was dissolved in toluene and filtered through a frit with celite, the resulting filtrate was dried under reduced pressure and recrystallized in toluene and pentane at -30° C to yield dark brown crystals of **2.19** (0.2557 g, 85.6% yield). Anal. calc'd for $C_{17}H_{31}Cl_2N_3W$: C, 38.35; H, 5.87; N, 7.90; Found: C, 38.20; H, 5.98; N, 7.91. ^{1}H NMR (400 MHz, C_6D_6, 25 °C): 1.05 (6H, t, J = 7.1 Hz, CH$_2$(C*H*$_3$)), 2.45 (3H, s, N(C*H*$_3$)$_2$), 2.51 (15H, s, C$_5$(C*H*$_3$)$_5$)), 3.42 – 3.51 (2H, m, C*H*$_2$(CH$_3$)), 3.60 – 3.70 (2H, m, C*H*$_2$(CH$_3$)). ^{13}C{H} NMR (125 MHz, C_6D_6, 25° C): 15.84 (C$_5$(*C*H$_3$)$_5$), 17.80 (CH$_2$(*C*H$_3$)), 39.35 (N(*C*H$_3$)$_2$), 49.20 (*C*H$_2$(CH$_3$)), 108.67 (*C*$_5$(CH$_3$)$_5$).

Li[N(Et)C(NMe$_2$)N(Et)]. Lithium dimethylamide (0.6081 mg, 11.92 mmol) was suspended in 20 mL Et$_2$O and chilled to -30° C before being added dropwise a -30° C solution of N,N'-diethylcarbodiimide (1.2283 g, 12.516 mmol) in 25 mL Et$_2$O. The mixture was stirred for 15 h warming to room temperature and becoming foggy yellow. Volatiles were removed *in vacuo* to yield a solid that was washed in pentane to yield a yellow-white powdery solid dried under reduced pressure (1.3721 g, 77% yield).

{Cp*[N(Et)C(NMe$_2$)N(Et)]Mo}$_2$(μ-η^1:η^1-N$_2$)} (2.20). 2.18 (259.4 mg, 0.5839 mmol) dissolved in 20 mL THF was cooled to -30° C. 0.5% (w/w) Na/Hg (8.1240 g, 1.767 mmol Na) was added and the reaction was allowed to warm to 25° C while stirring under a N_2 atmosphere for 1 h, changing in color from brown, to deep purple, back to brown. Volatiles were removed *in vacuo* to yield a brown solid dissolved in pentane and filtered through a frit with celite. The collected filtrate was dried under reduced pressure and recrystallized in pentane and toluene at -30° C to produce dark brown crystals **2.20** (0.2157 g, yield = 95%). Anal. calc'd for $C_{34}H_{62}N_8Mo_2$: C, 52.71; H, 8.06; N, 14.46; Found: C, 52.75; H, 7.98; N, 14.18. ^{1}H NMR (400 MHz, C_6D_6, 25 °C): 1.74 (6H, t, J = 7.1 Hz, $CH_2(CH_3)$), 1.90 (15H, s, $C_5(CH_3)_5$)), 2.45 (3H, s, $N(CH_3)_2$), 2.66 – 2.74 (2H, m, $CH_2(CH_3)$), 3.25 – 3.33 (2H, m, $CH_2(CH_3)$). ^{13}C{H} NMR (125 MHz, C_6D_6, 25° C): 12.41 ($C_5(CH_3)_5$), 17.79 ($CH_2(CH_3)$), 38.57 ($N(CH_3)_2$), 44.32 ($CH_2(CH_3)$), 104.53 ($C_5(CH_3)_5$), 173.86 ([(N(Et)C(Ph)N(Et)]).

{Cp*[N(Et)C(NMe$_2$)N(Et)]W}$_2$(μ-η^1:η^1-N$_2$) (2.21). 2.19 (215.7 mg, 0.4054 mmol) dissolved in 10 mL THF was cooled to -30° C. 0.5% (w/w) Na/Hg (5.593 g, 1.216 mmol Na) was added and the reaction was allowed to warm to 25° C while stirring under a N_2 atmosphere for 30 min, changing in color from brown to a dark

yellow brown. Volatiles were removed *in vacuo* to yield a brown solid dissolved in pentane and filtered through a frit with celite. The collected filtrate was dried under reduced pressure and recrystallized in pentane at -30° C to produce dark green crystals **2.21** (0.0472 g, 25% yield). Anal. calc'd for $C_{34}H_{62}N_{8}W_2$: C, 42.94; H, 6.58; N, 11.79; Found: C, 43.06; H, 6.52; N, 11.52. ^{1}H NMR (400 MHz, C_6D_6, 25 °C): 1.28 (6H, t, J = 7.1 Hz, $CH_2(CH_3)$), 2.16 (15H, s, $C_5(CH_3)_5$)), 2.35 (3H, s, $N(CH_3)_2$), 2.71 – 2.79 (2H, m, $CH_2(CH_3)$), 3.28 – 3.36 (2H, m, $CH_2(CH_3)$). ^{13}C{H} NMR (125 MHz, C_6D_6, 25° C): 13.83 ($C_5(CH_3)_5$), 18.04 ($CH_2(CH_3)$), 37.67 ($N(CH_3)_2$), 45.69 ($CH_2(CH_3)$), 101.48 ($C_5(CH_3)_5$).

{Cp*[N(Et)C(Me$_2$)N(Et)]Mo(μ-N)}$_2$ (2.22). 2.20 (53.0 mg, 0.0684 mol) was dissolved in 1 mL benzene-d_6 and heated at 45 °C on an oil bath for 216 h. After removal of solvent *in vacuo*, the resulting brown powdery solid was rinsed in pentane and recrystallized in pentane to yield brown crystals of **2.22** (19.6 mg, 37%). ^{1}H NMR (400 MHz, C_6D_6, 25 °C): 1.22 (6H, t, J = 6.9 Hz, $CH_2(CH_3)$), 2.01 (15H, s, $C_5(CH_3)_5$), 2.40 (3H, s, $N(CH_3)_2$), 3.18 – 3.26 (2H, m, $CH_2(CH_3)$), 3.50 – 3.58 (2H, m, $CH_2(CH_3)$).^{13}C{H} NMR (125 MHz, C_6D_6, 25° C): 12.31 ($C_5(CH_3)_5$), 16.74 ($CH_2(CH_3)$), 38.35 ($N(CH_3)_2$), 43.08 ($CH_2(CH_3)$), 109.83 ($C_5(CH_3)_5$), 170.30 ([(N(Et)*C*(Ph)N(Et)]).

{Cp*[N(Et)C(NMe$_2$)N(Et)]W(μ-N)}$_2$ (2.23). 2.21 (35.1 mg, 0.0369 mmol) was dissolved in 0.6 mL benzene-d_6 and heated at 80 °C on an oil bath for 24 h. After removal of solvent *in vacuo*, the resulting brown powdery solid was rinsed in pentane to yield powder of **2.23** (23.9 mg, 68% yield). C, 42.94; H, 6.58; N, 11.79; Found: C, 43.09; H, 6.38; N, 11.64. ^{1}H NMR (400 MHz, C_6D_6, 25 °C): 1.31 (6H, br s, $CH_2(CH_3)$),

2.09 (15H, s, $C_5(CH_3)_5$), 2.35 (6H, s, $N(CH_3)_2$), 3.28 (2H, br s, $CH_2(CH_3)$), 3.54 (2H, br s, $CH_2(CH_3)$).$^{13}C\{H\}$ NMR (125 MHz, C_7D_8, 80° C): 13.07 ($C_5(CH_3)_5$), 17.11 ($CH_2(CH_3)$), 38.73 ($N(CH_3)_2$), 43.21 ($CH_2(CH_3)$), 108.62 ($C_5(CH_3)_5$), 170.30 ([(N(Et)*C*(Ph)N(Et)]). $^{13}C\{H\}$ NMR (125 MHz, C_6D_6, 25° C): 13.07 ($C_5(CH_3)_5$), 17.11 ($CH_2(CH_3)$), 30.73 ($N(CH_3)_2$), 43.21 ($CH_2(CH_3)$), 108.62 ($C_5(CH_3)_5$), 137.67 ([(N(Et)*C*(Ph)N(Et)]).

2.7.3 Supporting NMR, UV-Vis, and ESI-MS Experiments

Thermolysis of 2.5 followed by ^{1}H NMR. A solution of **2.5** (48.5 mg, 57.7 μmol) in 1.0 mL benzene-d_6 was prepared in a Teflon© sealed Pyrex© J. Young NMR tube. The tube was covered in aluminum foil to block exposure to ambient light and the sample was heated at 60 °C in an oil bath and periodically monitored by ^{1}H NMR. Over 70 h of heating, the clean conversion of **2.5** to **2.8** was noted as the solution changed in color from golden-orange to brown. See Figure 2.4 for corresponding spectra.

Thermolysis of 2.6 followed by ^{1}H NMR. A solution of **2.6** (32.4 mg, 31.9 μmol) in 1.0 mL benzene-d_6 was prepared in a Teflon© sealed Pyrex© J. Young NMR tube. Thermolysis of this material was monitored by ^{1}H NMR and, over 187 h of heating at 60 °C in an oil bath, the clean conversion of **2.6** to **2.9** was noted as the solution changed from dark green to dark brown. See Figure 2.18 for corresponding spectra.

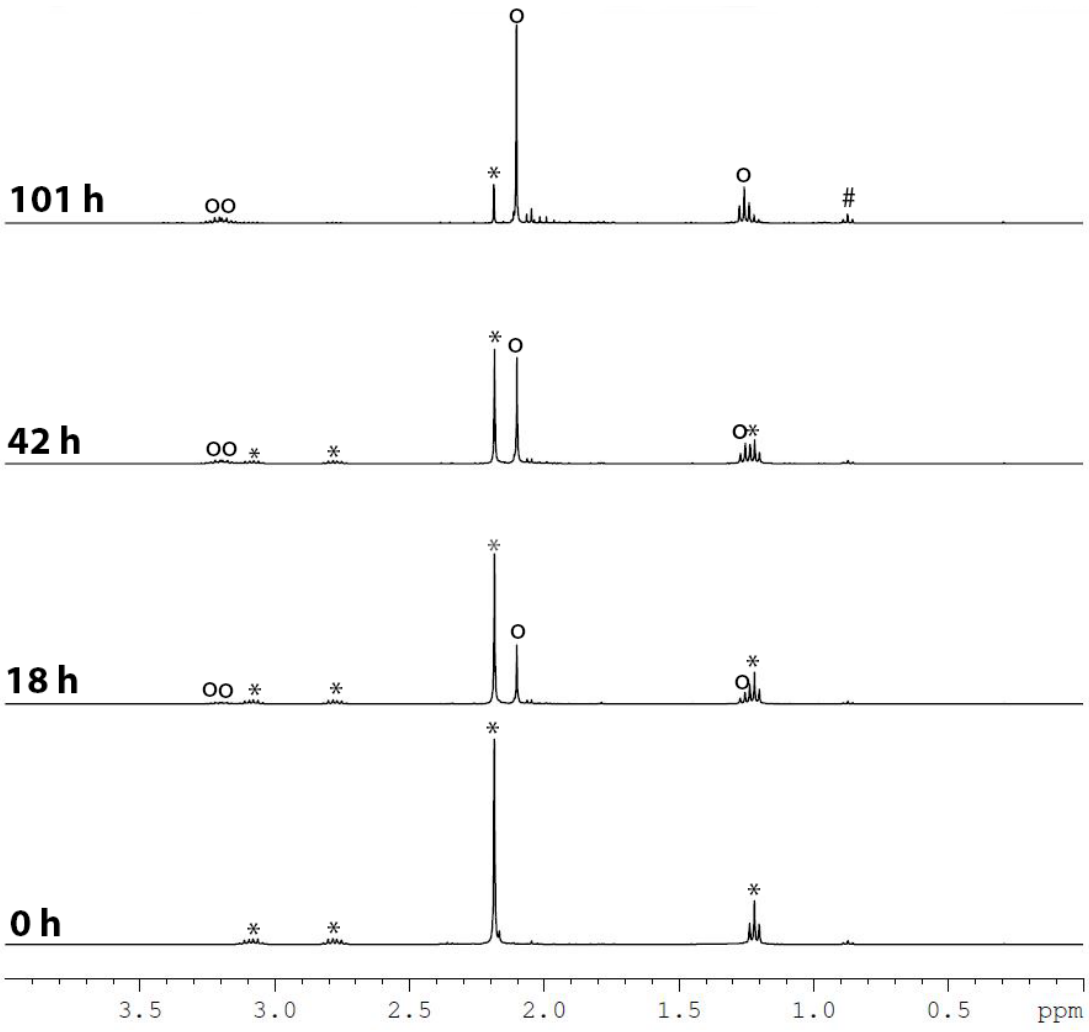

Figure 2.18. Partial ^{1}H NMR (400 MHz, C_6D_6, 25 °C) of a solution of **2.8** (*****) thermalized at 60 °C, converting cleanly to **2.9** (**o**) with pentane impurity noted (**#**)

Thermolysis of 2.5 in THF-*d*$_8$ followed by ^{1}H NMR. A solution of **2.5** (2.8 mg, 3.3 µmol) and durene (1.0 mg, 7.5 µmol) in 1.0 mL tetrahydrofuran-*d*$_8$ was prepared in a Teflon© sealed Pyrex© J. Young NMR tube. Thermolysis of this material was monitored by ^{1}H NMR and throughout 190 h of heating at 45 °C on an oil bath the color changed from golden to brown and the clean conversion of **2.5** to **2.8** was noted. See Figure 2.19 for corresponding spectra.

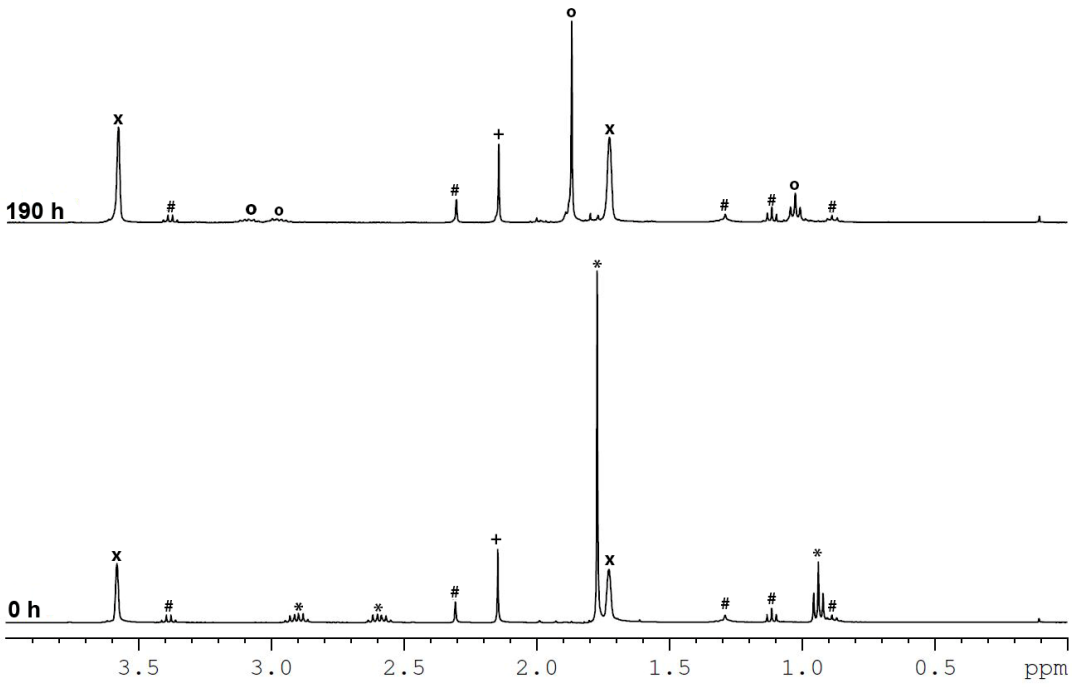

Figure 2.19. Partial ^{1}H NMR (400 MHz, THF-d_8, 25 °C) showing the conversion of **2.5** (*****) to **2.8** (**o**) upon thermolysis at 45 °C with an internal standard of durene (**+**). Residual solvent peaks for thf-d_8 (**x**) and pentane, diethyl ether, and toluene (**#**) are noted

Thermolysis of 2.5 in the presence of DME followed by ^{1}H NMR. A solution of **2.5** (8.1 mg, 9.6 µmol) and durene (3.0 mg, 22 µmol) in 0.6 mL benzene-d_6 was prepared in a Teflon© sealed Pyrex© J. Young NMR tube. A micro syringe was used to add 1,2-dimethoxyethane (3.0 µL, 29 µmol) and thermolysis of the sample was monitored by ^{1}H NMR. Over 90 h of heating at 55 °C in an oil bath, the solution changed from orange to brown and the clean conversion of **2.5** to **2.8** was noted. See Figure 2.20 for corresponding spectra.

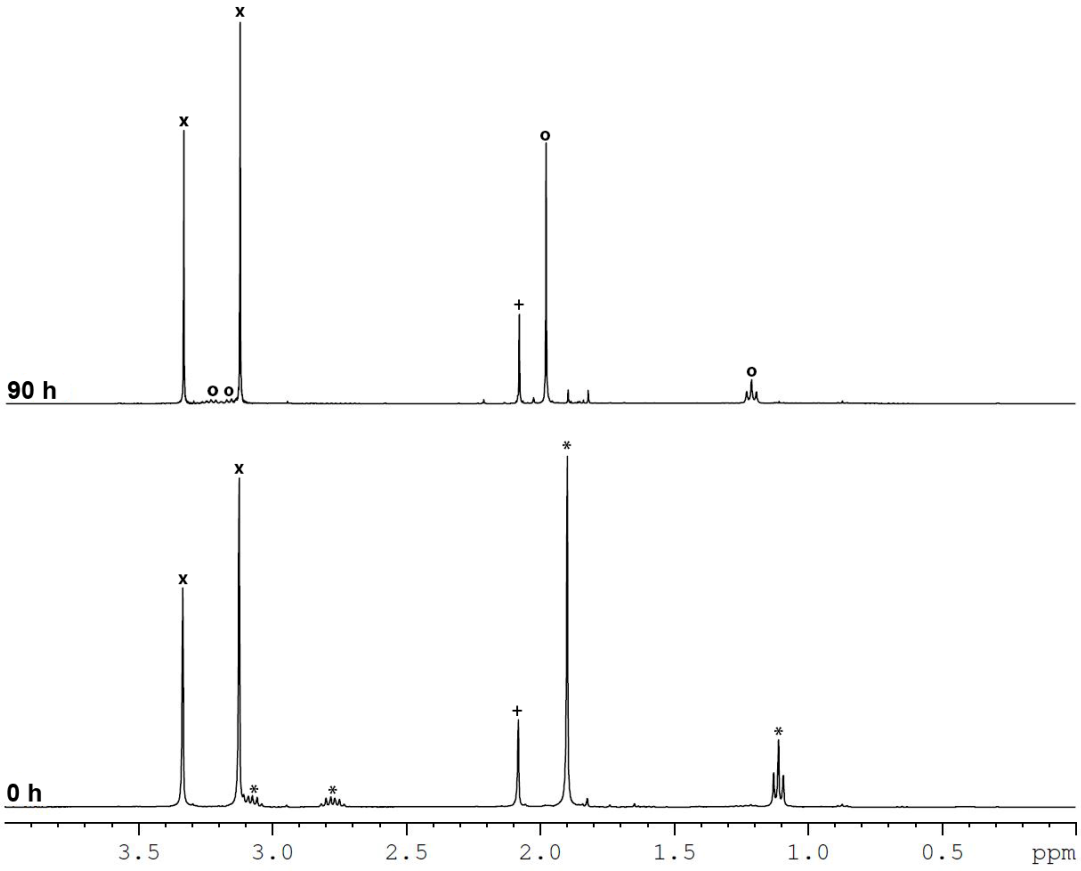

Figure 2.20. Partial ^{1}H NMR (400 MHz, benzene-d_6, 25 °C) demonstrating the conversion of **2.5** (*****) to **2.8** (**o**) with an internal durene standard (**+**) in the presence of excess DME (**x**) upon thermolysis at 55 °C

Reaction of 2.8 with 2,3-diemthyl-butadiene. A solution of **2.8** (8.0 mg, 9.5 µmol) and durene (4.0 mg, 30 µmol) in 0.6 mL benzene-d_6 was prepared in a Teflon© sealed Pyrex© J. Young NMR tube to which was added 2,3-dimethyl-butadiene (3.3 µL, 31 µmol) via micro syringe. No reaction besides a slight decomposition of the starting materials was observed by ^{1}H NMR after heating at 80 °C 24 h.

Thermolysis of 2.5 followed by UV-Vis. A 0.38 mM solution of **2.5** (3.2 mg, 3.8 µmol) was prepared in methylcyclohexane in a 10.00 mL volumetric flask, of which 3 mL was transferred to a Teflon© sealed quartz cuvette equipped with a magnetic sir bar. This sample was inserted into the cuvette holder of the UV-Vis which had been

pre-equilibrated to 70 °C and data acquisition began immediately. The cuvette solution was stirred for 22 h while scans from 400 – 1000 nm were collected over 2 minutes with a 5 minute delay between each collection (Δt = 7 minutes). The first set of data was excluded to account for temperature equilibration of the cuvette solution. The solution changed from pale golden to pale brown as **2.5** was observed to convert to **2.8** and 217 minutes are displayed with a clear isosbestic point (λ 757 nm). See Figure 2.6 for corresponding spectra.

Kinetic Studies for the Thermolysis of 2.5 followed by ^{1}H NMR. For Eyring analysis, a 12.0 mM solution of pre-cleaved N_2 complex **2.5** was prepared in a nitrogen filled glovebox by dissolving **2.5** (20.2 mg, 12.0 μmol) and durene (2.0 mg, 15.0 μmol) in 2.00 mL benzene-d_6 in a volumetric flask covered in aluminum foil to block ambient light. 0.50 mL samples of this orange-brown solution were transferred to Teflon© sealed Pyrex© J. Young NMR tubes covered in foil for transportation to the NMR which had been pre-calibrated to the desired temperature (65, 70, 75, or 80 °C). For the data collected at 60 °C, a comparable 12.1 mM solution of **2.5** (10.2 mg, 12.1 μmol) and durene (1.0 mg, 7.5 μmol) was prepared in 1.00 mL benzene-d_6 in a volumetric flask and likewise transported to the pre-heated NMR. ^{1}H NMR spectra of each sample were collected every 10 minutes for 4 hours, after an initial 10 minutes was allowed for each solution to equilibrate to the appropriate temperature. Each sample demonstrated the decrease in the intensity of the signals for **2.5** and the appearance and increase in the intensity of the signals for **2.8** over time. Due to the sparingly soluble nature of **2.8**, which tended to crystallize of solution upon reaching higher concentrations, only the disappearance of **2.5** was tracked for kinetic analysis whereby the integration value of

the **2.5** Cp* signal relative to the durene standard (set to 1) was converted to moles of **2.5**.

First-order rate constants for all kinetic runs were determined by a least-squares fit of the data for moles of **2.5** over time to the equation ln(**2.5**) = -*k*t + **2.5**$_0$ using the LINEST function in Excel. See Figures 2.7 and 2.8 for corresponding graphs. Standard linearity ($R^2 > 0.999$) for each kinetic run was obtained for 24 data points resulting in between 0.45 and 3.3 half-lives of first-order linear data for the temperature examined. Temperature dependent rate constants collected for each compound were least-squares fitted to the Eyring equation $k = (k_B T/h) \exp(\Delta S^{\ddagger}/R) \exp(-\Delta H^{\ddagger}/RT)$ using excel.

Kinetic Studies for the Thermolysis of 2.6 followed by ^{1}H NMR. For Eyring analysis, a 12.0 mM solution of pre-cleaved N_2 complex **2.6** was prepared in a nitrogen filled glovebox by dissolving **2.6** (12.2 mg, 12.0 μmol) and durene (1.0 mg, 7.5 μmol) in 1.00 mL benzene-*d*$_6$ in a volumetric flask covered in aluminum foil to block ambient light. Another 12.0 mM solution of pre-cleaved N_2 complex **2.6** was prepared by dissolving **2.6** (24.4 mg, 24.0 μmol) and durene (2.0 mg, 15 μmol) in 2.00 mL benzene-*d*$_6$ in a volumetric flask, also covered in aluminum foil to block ambient light. 0.50 mL samples of these dark green solution were transferred to Teflon© sealed Pyrex© J. Young NMR tubes covered in foil for transportation to the NMR which had been pre-calibrated to the desired temperature (60, 65, 70, 75, or 80 °C). ^{1}H NMR spectra of each sample were collected every 10 minutes for 4 hours, after an initial 10 minutes was allowed for each solution to equilibrate to the appropriate temperature. Each sample demonstrated the decrease in the intensity of the signals for **2.6** and the appearance and increase in the intensity of the signals for **2.9** over time. Due to the

sparingly soluble nature of **2.9**, which tended to crystallize of solution upon reaching higher concentrations, only the disappearance of **2.6** was tracked for kinetic analysis whereby the integration value of the **2.6** Cp* signal relative to the durene standard (set to 1) was converted to moles of **2.6**. First-order rate constants for all kinetic runs were determined by a least-squares fit of the data for moles of **2.6** over time to the equation $\ln(\mathbf{2.6}) = -kt + \mathbf{2.6}_0$ using the LINEST function in Excel. See Figures 2.6 and 2.7 for corresponding graphs. Standard linearity ($R^2 > 0.999$) for each kinetic run was obtained for 24 data points resulting in between 0.18 and 1.2 half-lives of first-order linear data for the temperature examined. Temperature dependent rate constants collected for each compound were least-squares fitted to the Eyring equation $k = (k_B T/h) \exp(\Delta S^{\ddagger}/R) \exp(-\Delta H^{\ddagger}/RT)$ using excel.

Initial Thermolysis of 2.20 followed by ^{1}H NMR. A 12.0 mM solution of **2.20** was prepared in a nitrogen filled glovebox by dissolving **2.20** (11.4 mg, 12.0 μmol) and durene (1.0 mg, 7.5 μmol) in 1.00 mL benzene-d_6 in a volumetric flask covered in aluminum foil to block ambient light. A 0.50 mL sample of this brown solution was transferred to Teflon© sealed Pyrex© J. Young NMR tubes covered in foil for transportation to the NMR which had been pre-calibrated to the 70 °C. The amount of **2.20** was measured over 3 h scaled to the durene standard while **2.22** formed as well. Relative to the cleavage of **2.5** under identical conditions,[4] **2.20** is observed to cleaves at a comparable, if very slightly faster, rate. See Figure 2.21 for corresponding plot.

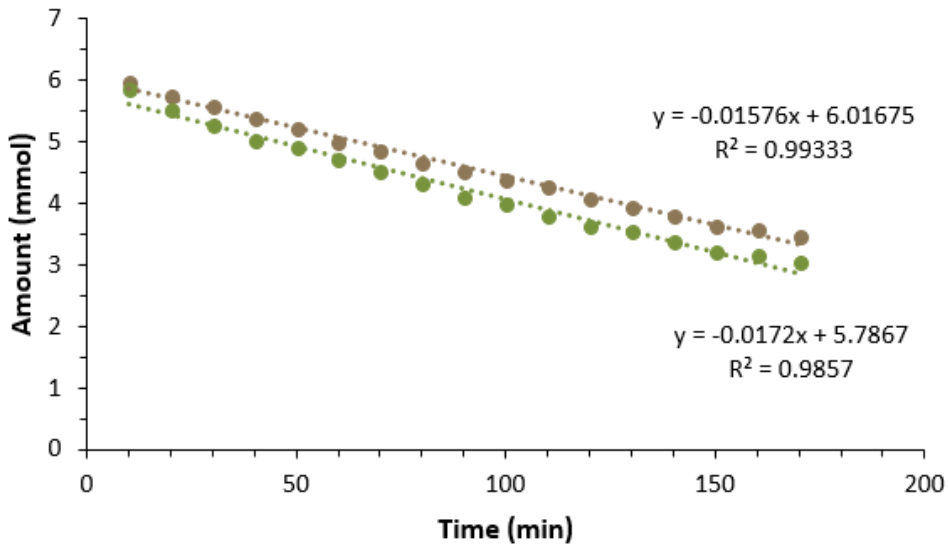

Figure 2.21. Comparison of the concentrations of **2.5** (●) compared **2.20** (●) during thermolysis at 70 °C relative to a durene standard

Crossover Thermolysis of 2.5 and 2.20 followed by ^{1}H NMR. 2.5 (4.4 mg, 5.2 µmol) and **2.20** (4.1 mg, 5.2 µmol) were dissolved in 0.6 mL benzene-d_6 in a Teflon© sealed Pyrex© J. Young NMR tube and an initial ^{1}H NMR was taken. The solution changed from orange to brown as it was heated on an oil bath at 65 °C and monitored by ^{1}H NMR over 44 h demonstrating consumption of **2.5** and **2.20** at comparable rates to produce a more complex mixture of products than can be attributed to the production of the observed **2.8** and **2.22** alone, indicating the formation of the **2.24**. See Figure 2.11a for corresponding for corresponding ^{1}H NMR spectrum.

Reaction of CPAM 2.8 and 2.22 followed by ^{1}H NMR. 2.8 (6.0 mg, 7.7 µmol) and **2.22** (6.4 mg, 7.6 µmol) were dissolved in 1 mL benzene-d_6 in a Teflon© sealed Pyrex© J. Young NMR tube. An initial ^{1}H NMR was immediately taken of the brown solution showing evidence of a more complex mixture of species than **2.8** and **2.22** alone which matched **2.24**. The product mixture reached equilibrium after 2 h at 65 °C

on an oil bath and did not change further upon continued heating the solution for 18 h. See Figure 2.11b for corresponding ^{1}H NMR spectrum.

Production of 2.25 and 2.24. 2.3 (31.9 mg, 0.0668 μmol) and **2.18** (30.3 mg, 0.0710 μmol) were dissolved together in 7 mL THF in a 50 mL Schlenk flask which was chilled to -30 °C. To this mixture was added 0.5% (w/w) Na/Hg (1.9481 g, 0.42368 mmol Na) and the solution was stirred for 1 h warming to room temperature during which point the brown starting mixture grew dark navy blue-purple before returning to brown. The mixture was dried under reduced pressure and extracted with pentane to filter through a pipet with a kimwipe and Celite® plug then solvent was removed *in vacuo*, then set up to recrystallize in pentane at -30 °C from which the mother liquor yielded a mixture of **2.5**, **2.20**, and **2.25**. This was then dissolved in 0.6 mL benzene-d_6 in a Teflon© sealed Pyrex© J. Young NMR tube to characterize the mixture by ^{1}H NMR. The solution which was heated on an oil bath at 65 °C growing darker brown over 15.5 h after which a ^{1}H NMR showed evidence of the starting material as well as **2.8**, **2.22**, and **2.24**. See Figure 2.12 for relevant spectra.

Crossover Thermolysis of 2.6 and 2.21 followed by ^{1}H NMR. 2.6 (4.2 mg, 4.4 μmol) and **2.21** (4.5 mg, 4.4 μmol) were dissolved in 0.6 mL benzene-d_6 in a Teflon© sealed Pyrex© J. Young NMR tube and an initial ^{1}H NMR was taken. The solution changed from green to brownish yellow as it was heated on an oil bath at 80 °C and monitored by ^{1}H NMR over 53 h demonstrating consumption of **2.6** and **2.21** along with the clean production of only **2.9** and **2.23** alone with no indication of the formation of the **2.27.** 7.5 mg of the product mixture was totally dissolved in 1.5 mL THF to produce a solution which was subjected to ESI-MS (positive ion mode). Only

peaks corresponding to **2.9** $[M + H]^+$ = 1017.38 m/z) and **2.23** ($[M + H]^+$ = 951.39 m/z) were present, along with peaks identified as fragments resulting from the loss of an amidinate or guanidinate off of one of the metal centers, {Cp*[N(Et)C(Ph)N(Et)]W(μ-N)}{Cp*W(μ-N)} ($[M]^+$ m/z = 841.47), or {Cp*[N(Et)C(NMe_2)N(Et)]W(μ-N)}{Cp*W(μ-N)} ($[M]^+$ m/z = 808.29). No crossover product, **2.27** ($[M + H]^+$ m/z = 984.41), was observed. See Figures 2.13 and 2.16 for corresponding spectra.

Reaction of 2.9 and 2.23 followed by ^{1}H NMR. 2.9 (4.4 mg, 4.3 μmol) **2.23** (4.0 mg, 4.2 μmol) were rinsed together with 1.2 mL THF-d_8 into a Teflon© sealed Pyrex© J. Young NMR tube. An initial ^{1}H NMR was immediately taken of the brown solution showing no evidence of any product other than the starting material. The mixture was heated on an oil bath at 80 °C for 17 h and another ^{1}H NMR showed only ^{1}H NMR with no evidence of **2.27**. See Figure 2.14 for corresponding spectra.

Production of 2.26 and 2.27. 2.4 (1025 mg, 0.1927 μmol) and **2.19** (0.1099 mg, 0.1945 μmol) were dissolved together in 10 mL THF in a 50 mL Schlenk flask which was chilled to -30 °C. To this mixture was added 0.5% (w/w) Na/Hg (4.9810 g, 1.0833 mmol Na) and the solution was stirred for 30 min h warming to room temperature during which point the orange starting mixture grew to a dark, yellow-brown. The mixture was dried under reduced pressure and extracted with pentane to filter through a pipet with a kimwipe and Celite® plug and then solvent was removed *in vacuo*. The resulting oily brown solid was then set up to recrystallize in pentane at -30 °C to yield **2.6**, **2.21**, and **2.26.** This was then dissolved in 1.5 mL toluene-d_8 in a Teflon© sealed Pyrex© J. Young NMR tube to characterize the mixture by ^{1}H NMR. The yellow-brown solution was then heated on an oil bath at 80 °C growing darker

brown over 18 h and followed by ^{1}H NMR after which the mixture was dried under reduced pressure, washed in pentane, and dried again to provide a brown solid which was determined by ^{1}H NMR to contain **2.9**, **2.23**, and **2.27**. 2.0 mg of the product mixture was totally dissolved in 0.66 mL THF to make solution which was subjected to ESI-MS (positive ion mode). Peaks corresponding to **2.9** ($[M + H]^+$ = 1017.29 m/z), **2.23** ($[M + H]^+$ = 951.34 m/z), and the mixed-ligand product, **2.27** ($[M + H]^+$ m/z = 984.30), were observed along with peaks identified as fragments resulting from the loss of an amidinate or guanidinate off of one of the metal centers, {Cp*[N(Et)C(Ph)N(Et)]W(μ-N)}{Cp*W(μ-N)} ($[M]^+$ m/z = 841.21), or {Cp*[N(Et)C(NMe$_2$)N(Et)]W(μ-N)}{Cp*W(μ-N)} ($[M]^+$ m/z = 808.18). See Figures 2.15 and 2.17 for corresponding spectra.

References

1. Hirotsu, M.; Fontaine, P. P.; Zavalij, P. Y.; Sita, L. R. Extreme N equivalent to N bond elongation and facile N-atom functionalization reactions within two structurally versatile new families of group 4 bimetallic "Side-on-Bridged" dimitrogen complexes for zirconium and hafnium. *J. Am. Chem. Soc.* **2007,** *129*, 12690-12692.
2. Keane, A. J.; Yonke, B. L.; Hirotsu, M.; Zavalij, P. Y.; Sita, L. R. Fine-Tuning the Energy Barrier for Metal-Mediated Dinitrogen N≡N Bond Cleavage. *J. Am. Chem. Soc.***2014,** *136*, 9906-9909.
3. Fontaine, P. P.; Yonke, B. L.; Zavalij, P. Y.; Sita, L. R. Dinitrogen Complexation and Extent of N≡N Activation within the Group 6 "End-On-Bridged" Dinuclear Complexes, {(η^5-C$_5$Me$_5$)M N(i-Pr)C(Me)N(i-Pr)}$_2$(μ-η^1:η^1-N$_2$) (M = Mo and W). *J. Am. Chem. Soc.* **2010,** *132*, 12273-12285.
4. Duman, L. M.; Farrell, W. S.; Zavalij, P. Y.; Sita, L. R. Steric Switching from Photochemical to Thermal Reaction Pathways for Enhanced Efficiency in Metal-Mediated Nitrogen Fixation. *J. Am. Chem. Soc.* **2016,** *138*, 14856-14859.
5. Keane, A. J.; Farrell, W. S.; Yonke, B. L.; Zavalij, P. Y.; Sita, L. R., Metal-Mediated Production of Isocyanates, R$_3$EN=C=O from Dinitrogen, Carbon Dioxide, and R$_3$ECl. *Angew. Chem. In. Ed.* **2015,** *54*, 10220-10224.
6. Duman, L. M.; Zavalij, P. Y.; Sita, L. R. An Intramolecular N2 Cleavage Mechanism for G6 CPAM/CPAM Dinuclear Complexes. *J. Am. Chem. Soc.* **2018,** *In Preperation*.

7. Zhang, W. C.; Tang, Y. H.; Lei, M.; Morokuma, K.; Musaev, D. G. Ditantalum Dinitrogen Complex: Reaction of H2 Molecule with "End-on-Bridged" [Ta(IV)2(μ-η(1): η(1)-N2) and Bis(μ-nitrido) [Ta(V)]2(μ-N)2 Complexes. *Inorganic Chemistry* **2011,** *50* (19), 9481-9490.
8. Wickramasinghe, L. A.; Ogawa, T.; Schrock, R. R.; Müller, P. Reduction of Dinitrogen to Ammonia Catalyzed by Molybdenum Diamido Complexes. *J. Am. Chem. Soc.* **2017,** *139*, 9132-9135.
9. Y., R.; Duboc, C.; Gennari, M. Molecular Catalysts for N_2 Reduction: State of the Art, Mechanism, and Challenges. *Chem. Phys. Chem.* **2017,** *18*, 2606-2617.
10. Yandulov, R. R.; Schrock, R. R. Catalytic Reduction of Dinitrogen to Ammonia at a Single Molybdenum Center. *Science* **2003,** *301*, 67-78.
11. Smythe, N. C.; Schrock, R. R.; Muller, P.; Weare, W. W. Synthesis of [(HIPTNCH$_2$CH$_2$)$_3$N]V compounds (HIPT=3,5-(2,4,6-i-Pr$_3$C$_6$H$_2$)$_2$C$_6$H$_3$) and an evaluation of vanadium for the reduction of dinitrogen to ammonia. *Inorganic Chemistry* **2006,** *45*, 9197-9205.
12. Arashiba, K.; Miyake, Y.; Nishibayashi, Y. A molybdenum complex bearing PNP-type pincer ligands leads to the catalytic reduction of dinitrogen into ammonia. *Nat. Chem.* **2011,** *3*, 120-125.
13. Kiriyama, S.; Arashiba, K.; Nakajima, K.; Tanaka, H.; Kamaru, N.; Youshizawa, K.; Nishibayashi, Y. Catalytic Formation of Ammonia from Molecular Dinitrogen by Use of Dinitrogen-Bridged Dimolybdenum–Dinitrogen Complexes Bearing PNP-Pincer Ligands: Remarkable Effect of Substituent at PNP-Pincer Ligand. *J. Am. Chem/. Soc.* **2014,** *27*, 9719-9731.
14. Tanaka, H.; Arashiba, K.; Kuriyama, S.; Sasada, A.; Nakajima, K.; Yoshizawa, K.; Nishibayashi, Y. Unique behaviour of dinitrogen-bridged dimolybdenum complexes bearing pincer ligand towards catalytic formation of ammonia. *Nat. Commun.* **2014,** *5*, 3737.
15. Tanaka, H.; Arashiba, K.; Kuriyama, S.; Sasada, A.; Nakajia, K.; Yoshizawa, K.; Nishibayashi, Y. Catalytic Nitrogen Fixation via Direct Cleavage of Nitrogen–Nitrogen Triple Bond of Molecular Dinitrogen under Ambient Reaction Conditions. *Bull. Chem. Soc. Jpn.* **2014,** *90*, 1111-1118.
16. Kinoshita, E.; Arashiba, K.; Kuriyama, S.; Miyake, Y.; Shimazaki, R.; Nakanishi, H.; Nishibayashi, Y. Synthesis and Catalytic Activity of Molybdenum–Dinitrogen Complexes Bearing Unsymmetric PNP-Type Pincer Ligands. *Organometallics* **2012,** *31*, 8437-8443.
17. Eizawa, A.; Arashiba, K.; Tanaka, H.; Kuriyama, S.; Matsuo, Y.; Nakajima, K.; Yoshizawa, K.; Nishibayashi, Y. Remarkable catalytic activity of dinitrogen-bridged dimolybdenum complexes bearing NHC-based PCP-pincer ligands toward nitrogen fixation. *Nat. Chem.* **2017,** *8*, 14874.
18. Holland, P. L. Metal–dioxygen and metal–dinitrogen complexes: where are the electrons? *Dalton Trans.* **2010,** *39*, 5415-5425.
19. Pauling, L.; Kamb, B. A revised set of values of single-bond radii derived from the observed interatomic distances in metals by correction for bond number and resonance energy. *Proc. Natl. Acad. Sci. U.S.A.* **1986,** *83*, 3569-3571.
20. Laplaza, C. E.; Cummins, C. C., Dinitrogen Cleavage by a 3-Coordinate Molybdenum9III) Complex. *Science* **1995,** *268*, 861-863.

21. Laplaza, C. E.; Johnson, M. J. A.; Peters, J. C.; Odom, A. L.; Kime, E.; Cummins, C. C.; George, G. N.; Pickering, I. J. *J. Am. Chem. Soc.* **1996,** *118*, 8623 - 8638.
22. Morrey, J. R. Isosbestic Points in Absorbance Spectra. *Phys. Chem.* **1963,** *67*, 1569–1569.
23. Hinrichsen, S.; Broda, H.; Gradert, C.; Söncksen, L.; Tucsek, F. Recent developments in synthetic nitrogen fixation. *Annu. Rep. Prog. Chem., Sect. A: Inorg. Chem.* **2012,** *108*.
24. Slater, J. C. Atomic Radii in Crystals. *J. Chem. Phys.* **1964,** *41*, 3199-3204.
25. Kepp, K. P. A Quantitative Scale of Oxophilicity and Thiophilicity. *Inorg. Chem.* **2016,** *55*, 9461–9470.
26. Hammett, L. P. The Effect of Structure upon the Reactions of Organic Compounds. Benzene Derivatives. *J. Am. Chem. Soc.* **1937,** *59*, 96-103.
27. Jaffé, H. H. A Reëxamination of the Hammett Equation. *Chem. Rev.* **1953,** *53*, 191–261.
28. Caro, C. A.; Cabello, G.; Landaeta, E.; Pérez, J.; González, M.; Zagal, J. H.; Lillo, L. Preparation, spectroscopic, and electrochemical characterization of metal(II) complexes with Schiff base ligands derived from chitosan: correlations of redox potentials with Hammett parameters. *J. Coord. Chem.* **2014,** *67*, 4114-4124.
29. Duman, L. M.; Sita, L. R., Closing the Loop on Transition-Metal-Mediated Nitrogen Fixation: Chemoselective Production of $HN(SiMe_3)_2$ from N_2, Me_3SiCl, and X—OH (X = R, R_3Si, or Silica Gel). *J. Am. Chem. Soc.* **2017,** *139*, 17241-17244.
30. Duman, L. M.; Zavalij, P. Y.; Sita, L. R. An Intramolecular Mechanism for N_2 Cleavage in Dinuclear Mo and W CPAM/CPGU Complexes. *J. Am. Chem. Soc.* **2018,** *In Preperation*.
31. Murray, R. C.; Blum , L.; Liu, A. H.; Schrock, R. R. Simple routes to mono(μ^5-pentamethylcyclopentadienyl) complexes of molybdenum(V) and tungsten(V). **1985,** *4*, 953-954.
32. Sal, P. G.; Jiménez, I.; Martín, A.; Pedraz, T.; Royo, P.; Sellés, A.; Vazquez de Miguel, A. Synthesis of chloro and methyl imido cyclopentadienyl molybdenum and tungsten complexes. X-ray molecular structures of [WCp^*Cl_3(NtBu)], [$MoCp^*C1Me_2$(NtBu)] and [WCp^*C1Me_2(NtBu)]. *Inrog. Chim. Acta.* **1998,** *273*, 270-278.
33. King, R. B.; Iqbal, M. Z.; King, A. J., Jr. Pentamethylcyclopentadienyl derivatives of transition metals: VI. Carbonylation of metal-metal tripple bonds: a high pressure infrared spectroscopic study. *J. Organomet. Chem.* **1979,** *15*, 53-63.

Chapter 3: Reactivity and Functionalization of Dinitrogen and Nitride Complexes

3.1 N-atom Functionalization

Having used the sterically reduced CPAM framework to support the facile thermal cleavage of the dinitrogen suspended between the two metal centers, the next step towards the goal of completing a cycle for dinitrogen fixation is *to functionalize the nitrogen atoms*. Without functionalization, a value-added N-atom-containing product will neither be formed on nor released from the metal center. Formation of dinuclear bridging bis-nitride species **2.8** and **2.9** are a promising route towards functionalization in that their structure inherently avoids the thermodynamic sink of formation of a mononuclear terminal nitride which are stereotypically stable and tend to require harsh reagents, conditions, or both in order to functionalize and release N-containing products. [1-9]

The formation of a N-R bond while an N-atom remains attached to the metal center produces a metal imido, [M]=NR (R = alkyl, aryl, silyl, etc.), functionalities that are useful both for modeling N-H bond behavior and in their own right as key intermediates in dinitrogen fixation reactivity.[10-13] For instance, when considering the Chatt cycle of dinitrogen fixation,[14] after the loss of the first equivalent of NH_3 by protonation and reduction of coordinated N_2 the resulting Mo(IV) or W(IV) nitrido or imido complexes undergo four reduction and three protonation steps to release a second equivalent of NH_3, passing through an imido structure before being recycled back to Mo(0) or W(0) $(N_2)_2$ starting materials.[15, 16] Alkylimido complexes are a useful means of elucidating the details of such reaction steps because, unlike non-alkylated species,

they do not undergo undesirable intermolecular acid-base reactions and H_2 evolution.[13, 17] Alternately, the significant library of nitrene group functionalization and transfer makes it an ideal area of study to merge with dinitrogen fixation, so long as the N-containing moieties are themselves derived from molecular dinitrogen.[2, 18-21] By this approach, a N_2-derived imido moiety itself can be a stepping stone to successful dinitrogen fixation, as was the case for the series of CPAM imidos {Cp*[N(iPr)C(Me)N(iPr)]Mo(NRR$_3$')}(R = C, R' = Me (**3.1**); R = Si, R' = Me (**1.28**); R = Si, R' = Ph (**3.2**); R = Ge, R' = Me (**3.3**)) which have been shown to lead to the formation of value-added isocyanates (OCNRR'$_3$) upon reaction with CO.[22-24] To that end, experiments were undertaken targeting the efficient formation of a sterically reduced CPAM imido, directly from the (μ-N_2) complexes or through the intermediacy of the (μ-N)$_2$ complexes. Further, experiments were conducted with regards to the general reactivity of the (μ-N_2) and (μ-N)$_2$ complexes to continue to map out their chemical reactivity and in pursuit of potentially useful functionalizations.

3.2 Silylation Reactions

3.2.1 Synthesis of Nitrido Chlorides and Silylimidos

The first step was to synthesize and analyze the targeted M(IV) silylimido products, a task that does not necessarily require an N-atom from molecular dinitrogen for the purposes of simple characterization. The synthetic pathway presented in Scheme 3.1 illustrates such a transformation from the Mo(IV) dichloride starting material **2.3**. Upon reaction with a slight excess of trimethylsilyl azide, N_3SiMe_3, a molybdenum

Scheme 3.1

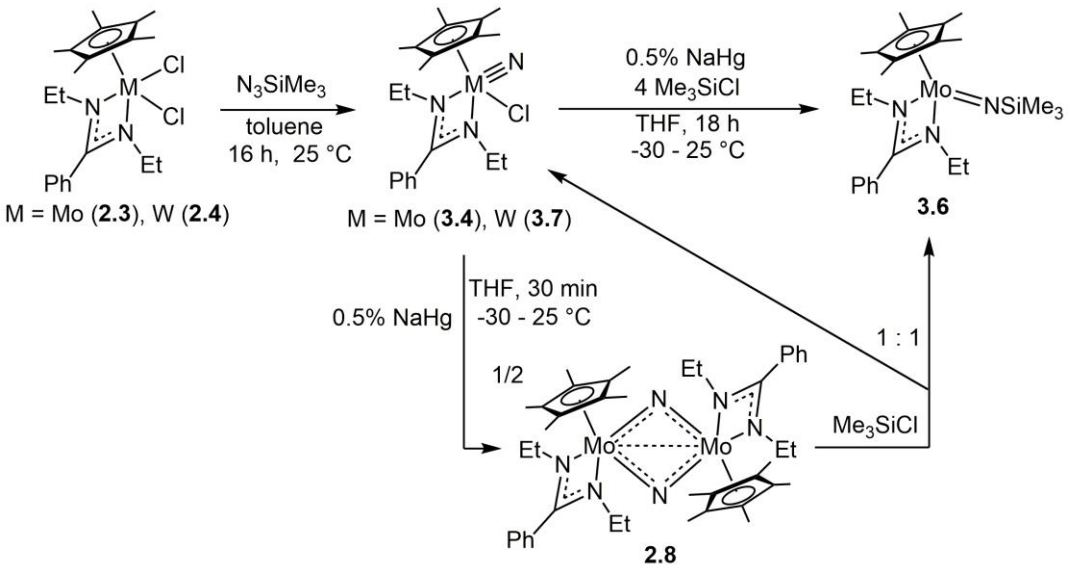

nitrido, chloride {Cp*[N(Et)C(Ph)N(Et)]Mo(N)Cl} (**3.4**) is produced in high yield (93 %) as a crystalline material in an olive green / gold color. The XRD structure, displayed in Figure 3.1, indicates that the nitride unit is very tightly bound with a Mo≡N bond length of 1.6792(18) Å.[25] This is very slightly longer than the analogous {Cp*[N(iPr)C(Me)N(iPr)]Mo(N)Cl} (**3.5**) M≡N bond length of 1.674(3) Å[22] but, as would be expected for a triply-bonded terminal nitride, it is more than 0.2 Å shorter in

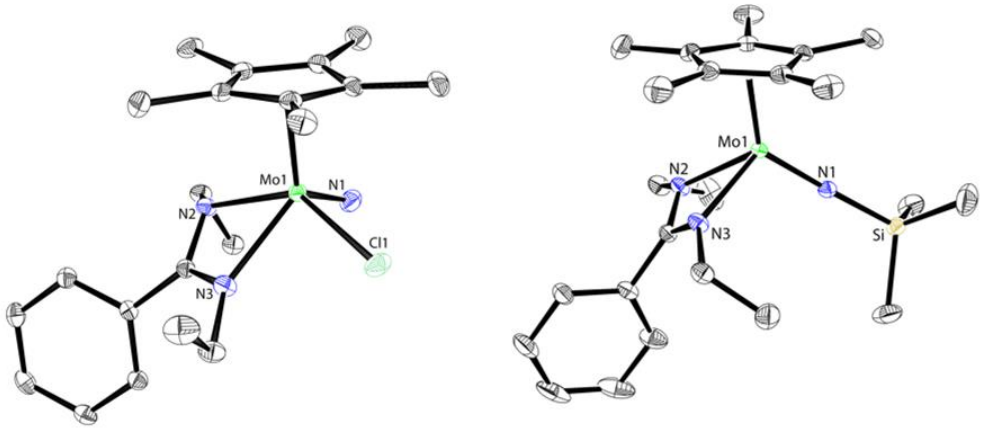

Figure 3.1. Crystal structures of **3.4** (right) and **3.6** (left) with hydrogen atoms omitted for clarity, ellipsoids for the non-hydrogen atoms are shown at the 30% probability level

comparison to either of the Mo-N bonds of the dinuclear $(\mu\text{-N})_2$ complex **2.8**. Already at the highest oxidation state accessible to Mo, the Mo(VI) complex **3.4** will undergo chemical reduction by NaHg in THF to cleanly generate **2.8** as the lower half of Scheme 3.1 also reveals. This proves to be an efficient alternative for the conversion from **2.5** to **2.8** and allows for the convenient preparation of larger scales of the $(\mu\text{-N})_2$ complex that are easily accessible and less time consuming than the thermolysis of **2.5**. When coupled with the presence of excess Me_3SiCl, this i*n situ* reduction from **3.4** to **2.8** will produce the desired Mo(IV) silylimido, {Cp*[N(Et)C(Ph)N(Et)]Mo($NSiMe_3$)} (**3.6**), in high yield as is shown in Scheme 3.1 (*Section 3.2.2 offers further mechanistic insight into this reaction*). Though generally isolated as an oil and thus not suitable for elemental analysis (EA), a sample stored in the glovebox freezer for several months produced a single crystal amenable to XRD, the structure of which is displayed in Figure 3.1. The imido Mo=N bond of **3.6** is 1.7562(12) Å,[25] slightly shorter than that of the more sterically bulky silylimido **1.28**, which has a Mo=N length of 1.758(3) Å, [22] and formally constitutes a double bond.

Though the different rates of dinitrogen cleavage exhibited by the Mo vs W complexes generally makes the Mo congeners more attractive targets due to their higher reactivities (*see Chapter 2.3.2*), whenever possible, W analogues were still created for the purposes of characterization and reactivity comparison.[22, 23, 25] For example, as is demonstrated in Scheme 3.1, the tungsten nitrido, chloride, {Cp*[N(Et)C(Ph)N(Et)]W(N)Cl} (**3.7**), can be synthesized by the same methods as **3.4** and isolated in 50 % yield; however, unlike its molybdenum counterparts, **3.7** cannot be successfully reduced by NaHg to the $(\mu\text{-N})_2$ **2.9**. This is a stark reminder of the

differences in reactivity (not desirable for every application) that result from varying the identity of the metal center, even by a single row in the periodic table. Scheme 3.2 depicts an alternate route for they synthesis of a silylated W complex,[26] forming the terminal silylimido, {Cp*[N(Et)C(Ph)N(Et)]W(NSiMe$_3$)} (**3.8**), in 95% yield by reacting **2.6** with an excess of N_3SiMe_3 to displace the bridging dinitrogen moiety. [25]

Scheme 3.2

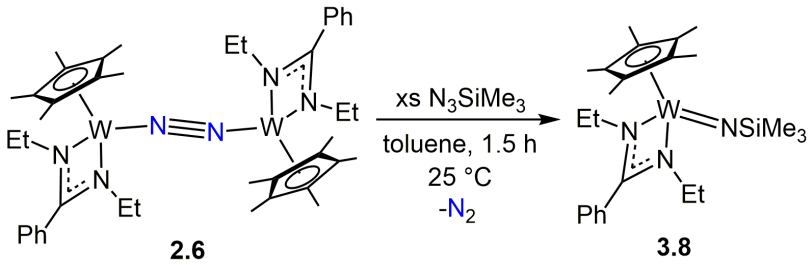

2.6 **3.8**

The CPGU Mo and W analogues {Cp*[N(Et)C(NMe$_2$)N(Et)]Mo(N)Cl} (**3.9**), {Cp*[N(Et)C(NMe$_2$)N(Et)]Mo(NSiMe$_3$)} (**3.10**), {Cp*[N(Et)C(NMe$_2$)N(Et)]-W(N)Cl} (**3.11**), and {Cp*[N(Et)C(NMe$_2$)N(Et)]W(NSiMe$_3$)} (**3.12**), could be prepared though very similar methods as those described for the CPAM complexes (*vide supra*) but were generally be more oily than their CPAM counterparts and thus less amenable to purification and isolation. However, the similar reactivities once again reaffirms the consistency between the CPAM/CPGU ligand pair, though the CPAM species were more crystalline and easier to isolate consistently.[27]

3.2.2 (μ-N)$_2$ and (μ-N$_2$) silylation by Me$_3$SiCl

Returning to the target goal of functionalizing N-atoms specifically derived from molecular dinitrogen, in practice, the molybdenum imido can be synthesized through several different reactions. The reactivities of the (μ-N$_2$) complex **2.5** and (μ-N)$_2$ complex **2.8** with Me$_3$SiCl are of significant interest because they are surprisingly

Scheme 3.3

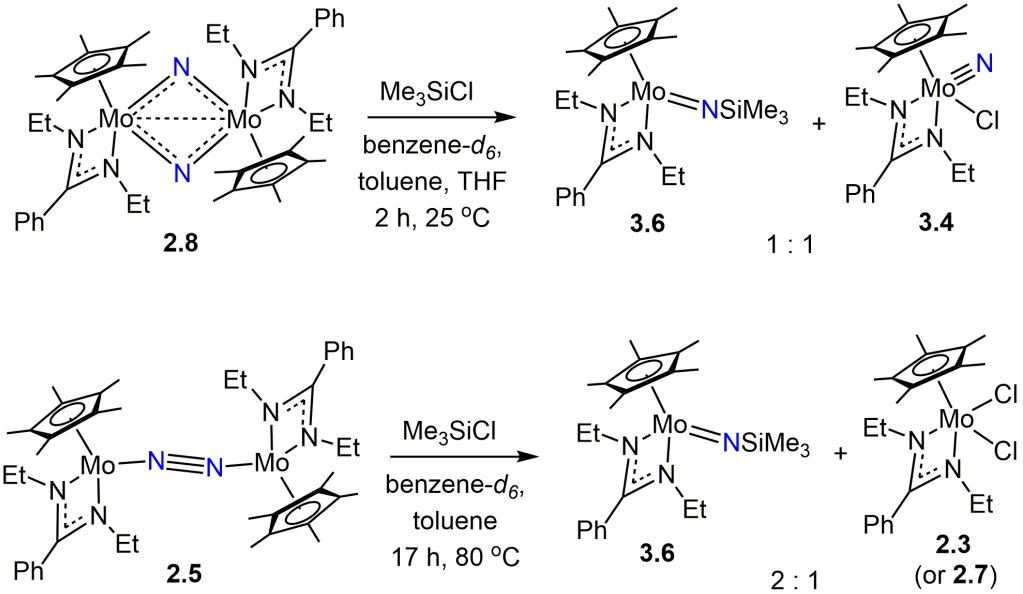

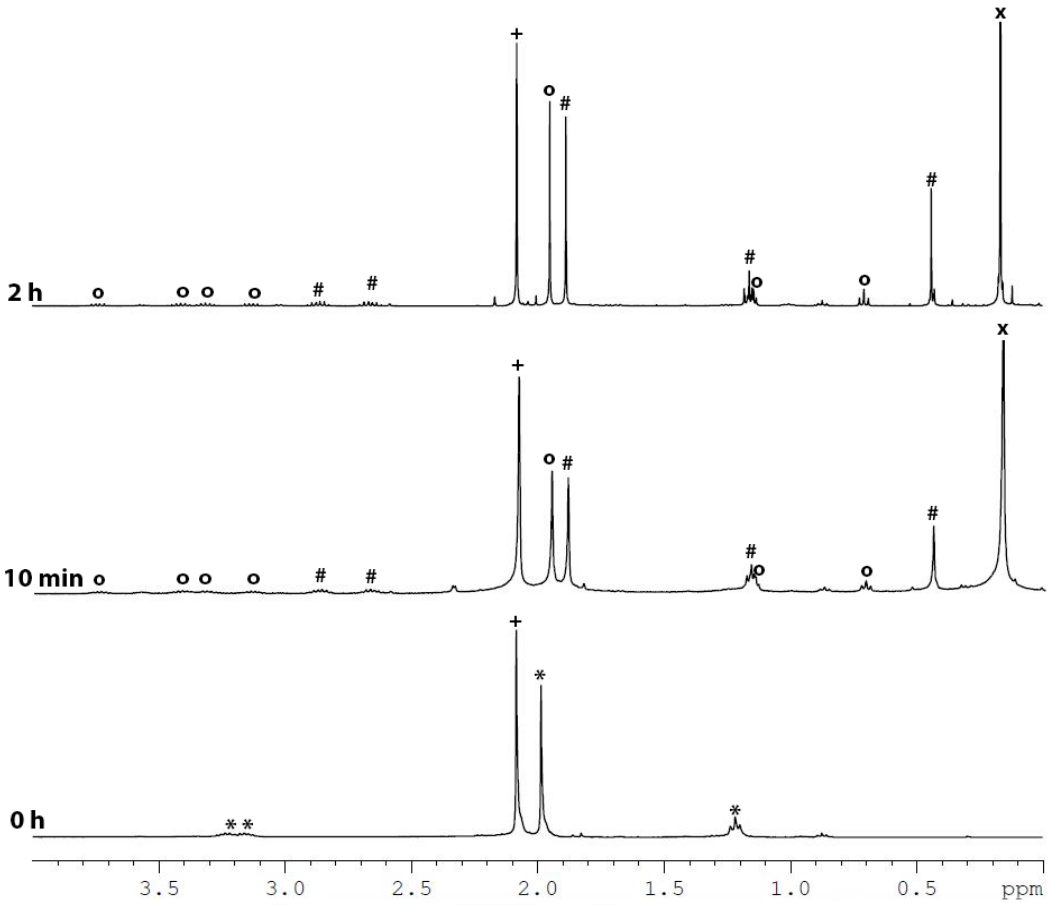

Figure 3.2. Partial ^{1}H NMR (400 MHz, C_6D_6, 25 °C) of a solution of **2.8** (*) with durene (+) and Me_3SiCl (**x**) reacting at 25 °C, converting to **3.4** (**o**) and **3.6** (#)

dissimilar from one another. First, the top of Scheme 3.3 depicts the addition of Me_3SiCl to **2.8** at room temperature which quickly and cleanly yields a 1 : 1 mixture of **3.4** and **3.6**. According to the ^1H NMR spectra shown in Figure 3.2, the reaction quickly consumes all the **2.8** initially available in solution within 10 minutes and as more of the sparingly soluble **2.8** dissolves and becomes accessible, the reaction continues to form an equimolar mixture of **3.4** and **3.6**. As is depicted earlier in Scheme 3.1, when excess NaHg and Me_3SiCl are present in addition to this equimolar mixture, subsequent chemical reduction of **3.4** by NaHg recycles the Mo center back to **2.8** and repetition of this process eventually quantitively forms **3.6**. On the other hand, the lower portion of Scheme 3.3 illustrates that **3.5** must be heated in order to react with

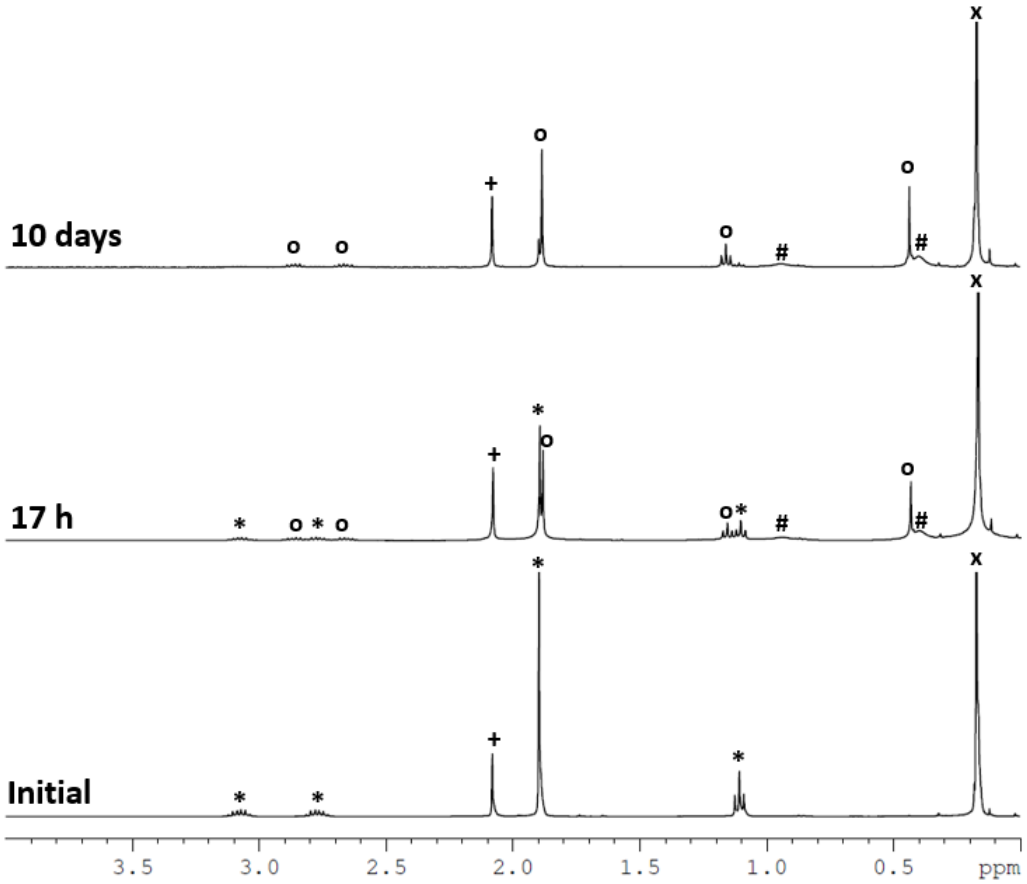

Figure 3.3. Partial ^1H NMR (400 MHz, benzene-d_6, 25 °C) of a solution of **2.5** (*****) with durene (+) and Me_3SiCl (**x**) heated at 55 °C to convert to **3.4** (**o**) and **2.7** (#)

Me_3SiCl, at which point a 2 : 1 product mixture of **3.6** and a Mo chloride species, see Figure 3.3; both **2.3** or **2.7** have been spectroscopically observed as chloride-containing products, the identity of which likely depends on the conditions under which the reaction is run. In this capacity, **2.5** apparently acts as a chloride atom trap. The different results upon reaction of the two dinuclear nitrogen-containing complexes **2.5** or **2.8** with the same reagent, Me_3SiCl, suggest that various mechanism must be in play, otherwise the reactions would result in the same products.

This disparity in reactivity can be explained by considering the complex mixture of Mo compounds present within each separate reaction, and the discovery of their *in situ* relationship as is depicted in Scheme 3.4. Specifically, **2.5** acts as a formal reductant upon **3.4**, abstracting its chloride atom and converting two equivalents of the remaining nitrido species in to **2.8** as is shown in Figure 3.4. Stoichiometrically, **2.5** thus becomes a chloride species, spectroscopically observed in the reaction of **2.5** with

Scheme 3.4

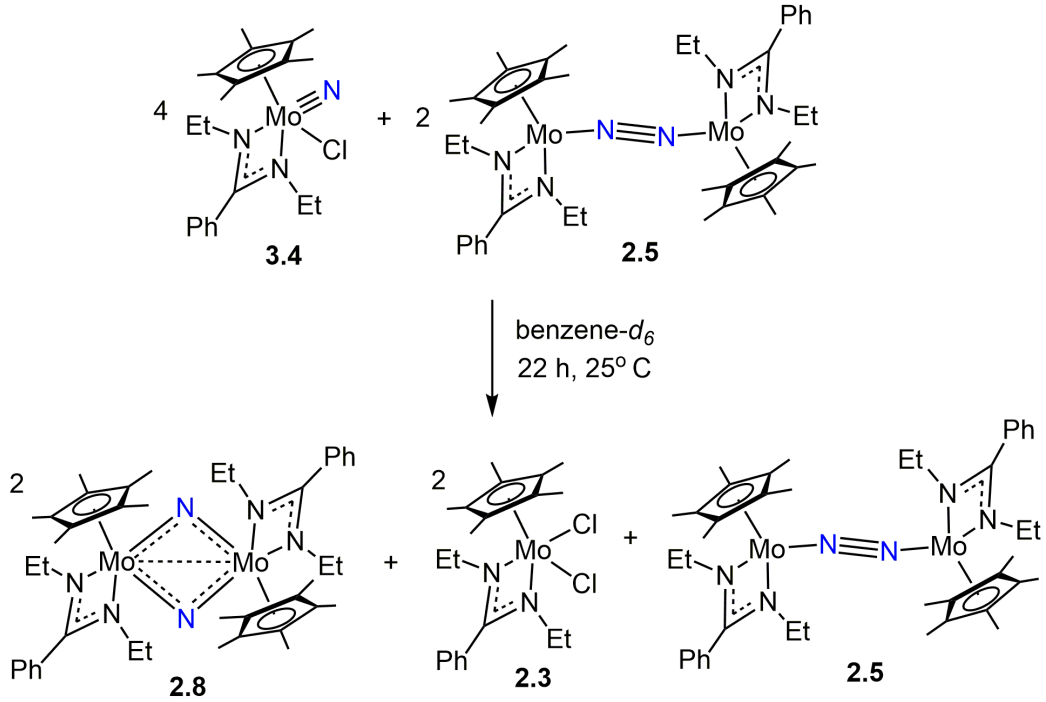

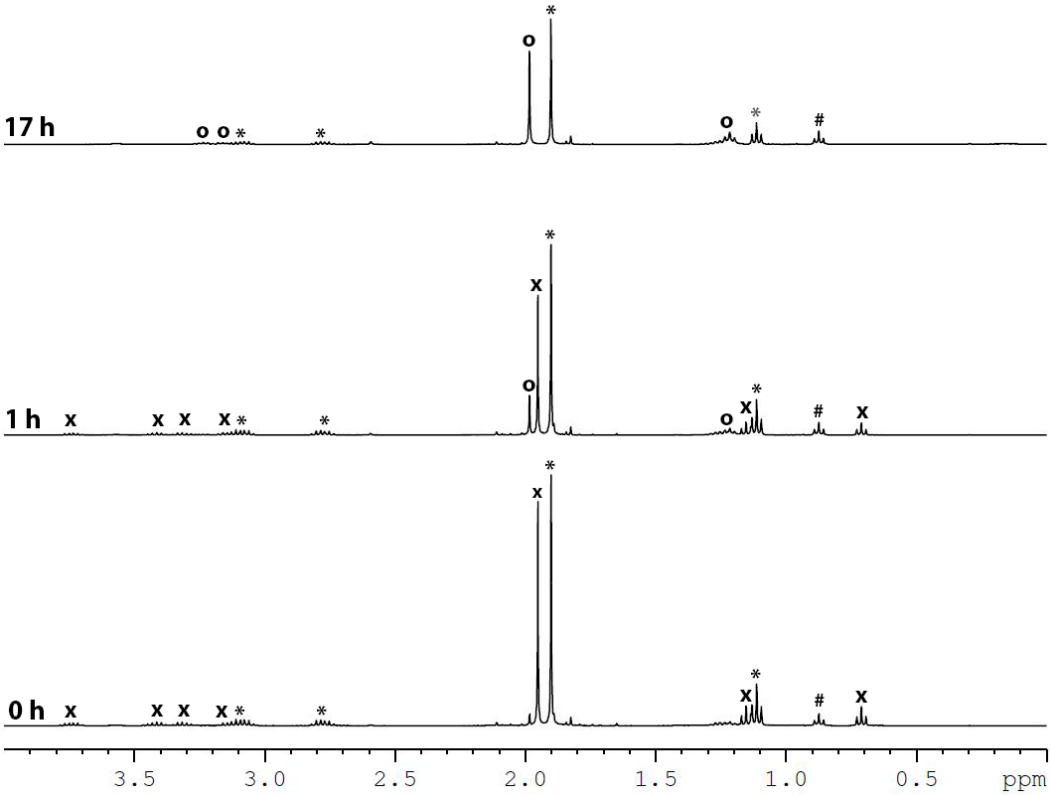

Figure 3.4. Partial ^{1}H NMR (400 MHz, C_6D_6, 25 °C) of a solution of **2.5** (*****) reacting with **3.4** (**x**) at 25 °C to produce organic products (remove under reduced pressure) and **2.7** (**o**). Pentane (**#**) impurity noted

Me_3SiCl; no evidence of a chloride species was observed by ^{1}H NMR during this reaction of **2.5** with **2.4**, but on a preparative scale an intractable species was produced that is presumed to contain the chloride atoms. It can then be extrapolated that the reactivity displayed in Scheme 3.3 is the result of the process shown in Scheme 3.5 where **2.5** thermally isomerizes to **2.8**, which reacts with Me_3SiCl producing **3.4** and **3.6**, at which point the newly formed **3.4** reacts immediately with remaining **2.5** to create **2.3** and more **2.8**, which repeats the above process ultimately generating only the silylimido **3.6** and a chloride species **2.3** or **2.7**. [25]

One final observation of note is that while the reactions of **2.8** or **2.5** with Me_3SiCl is successful when in a hydrocarbon solvent such as toluene or benzene-*d*$_6$, as

Scheme 3.5

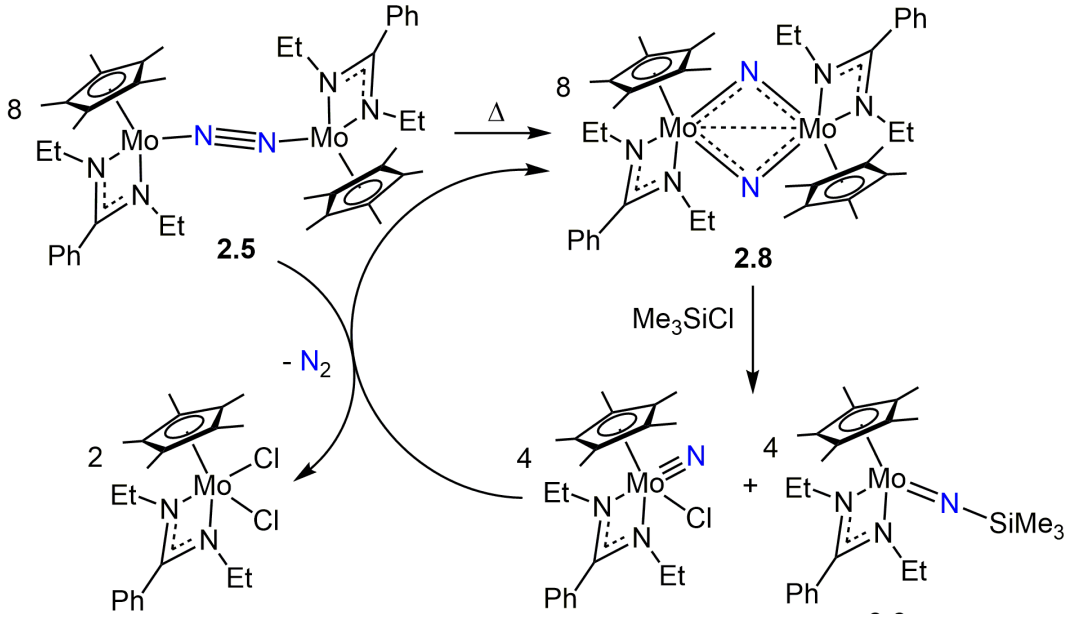

depicted in Scheme 3.3, the results when run in the etherial THF are more complicated. A solution of **2.8** in THF-d_8 became a vibrant green color upon the addition of excess Me_3SiCl but gradually faded to a brown color, all the while tracked by ^1H NMR to produce the expected 1 : 1 ratio of **3.4** and **3.6**. The green color is perhaps a result of a THF adduct with one of the metal complexes and Me_3SiCl as each **2.8**, **3.4**, and **3.6** are not bright green in THF solutions on their own. A similar THF-d_8 soltuion of **2.5** with excess Me_3SiCl however, did not proceed as expected: upon heating the mixure at 60 °C for 19 h, it grew to a very dark brown and while ^1H NMR revealed readily identifable **3.4**, there was no sign of **3.6** where a 1 : 2 ratio is expected for the two products. Because the reaction of **3.5** with Me_3SiCl relies on the complex set of *in situ* reactions illustrated in Scheme 3.4, it is likely that in the more polar solution of THF, the reduction potential of **2.5** is increased[28] which may interfere with its ability to productively reduce **3.4** back to **2.8**, thus inhibiting the reaction as depicted in the lower protion of Scheme 3.3.

3.2.3 (μ-N)$_2$ and (μ-N$_2$) Silylation by Hg(SiMe$_3$)$_2$

The better understanding of the reaction of Me$_3$SiCl with the dinitrogen complexes **2.5** and **2.8** allows for reconciliation of the reactivities which initially seemed irreconcilably unalike but are in fact simply distinct stages of the same overall silylation process. This is an important realization because they beg the question of the extent to which the reactivity of the end-on-bridged dinitrogen complex differ from, or are merely an extension of, the bridging bis-nitride species. To probe this question, **2.5** and **2.8** were reacted with bis trimethylsilyl mercury, Hg(Me$_3$Si)$_2$, a simultaneously reducing and silylating agent[22, 29] [*Note: though no known toxicology studies have been conducted, Hg(Me$_3$Si)$_2$ is handled with the utmost caution due to its resemblance to the infamous and pernicious reagent dimethyl mercury*[30]]. As is shown in Scheme 3.6, while heating the dinuclear nitrogen complexes **2.5** and **2.8** with an excess of Hg(Me$_3$Si)$_2$, two equivalents of **3.6** were produced along with a small amount of Hg$^\circ$ which collected at the bottom of the reaction vessel. Though the conditions of these

Scheme 3.6

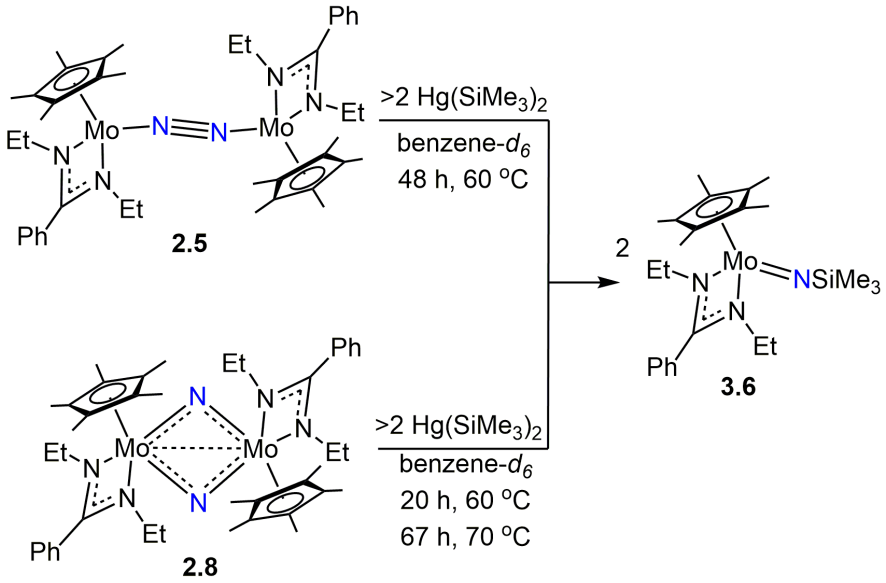

reactions vary slightly, the mercuric reagent (which can be conceptualized of as being generated *in situ* during the synthesis of **3.6** from **2.8**, NaHg, and Me_3SiCl as is depicted in Scheme 3.1) serves as a more direct means of incorporating the trimethylsilyl (TMS) moiety into the N-atom than Me_3SiCl on its own. Importantly, in the reaction with **2.5**, **2.8** was only briefly observed as an intermediate by ^1H NMR relative to an internal durene standard. The extent of the presence of **2.8** the depended on the initial concentration of reactants, shown in Figure 3.5; when only a slight stoichiometric excess of 2.6 equivalents $Hg(SiMe_3)_2$ was employed, the reaction proceeded more slowly and with more detectable **2.8** for longer than when a large excess of 9.7 equivalents was used. This indicates that although **2.8** is formed as a result of the expected dinitrogen cleavage of **2.5**, upon its appearance, it quickly reacts with the $Hg(SiMe_3)_2$. For instance, ^1H NMR spectra tracking the reaction of **2.5** with a large excess of $Hg(Me_3Si)_2$ are shown in Figure 3.6. Also of note is that **3.6** is produced from **2.5** under more mild conditions and in less time than from **2.8**, which could indicate that the mechanisms of the processes may differ, though the end result does not.

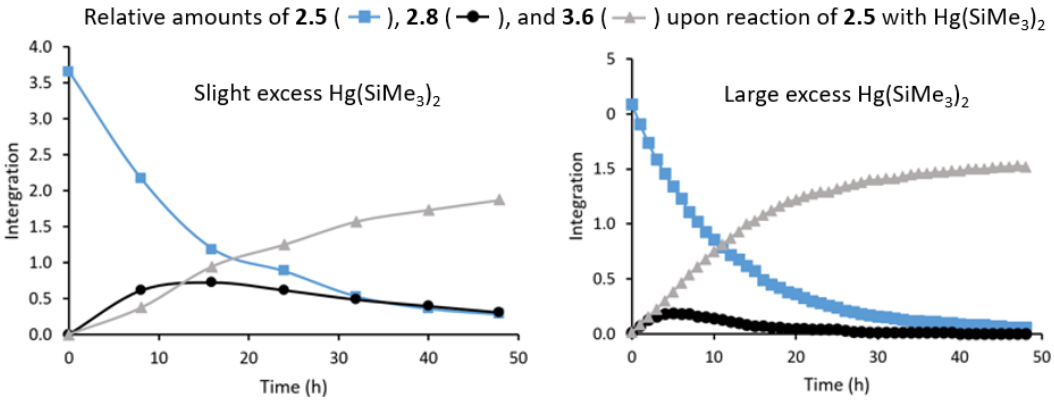

Figure 3.5. Integration signals of reactant **2.5**, intermediate **2.8**, and product **3.6**, with respect to a durene internal standard set to 1, heated at 60 °C over the course of 48 h. Left: slight excess of $Hg(Me_3Si)_2$, based on ^1H NMR data acquired every 8 h. Right: large excess of $Hg(Me_3Si)_2$, based on ^1H NMR data acquired every 1 h

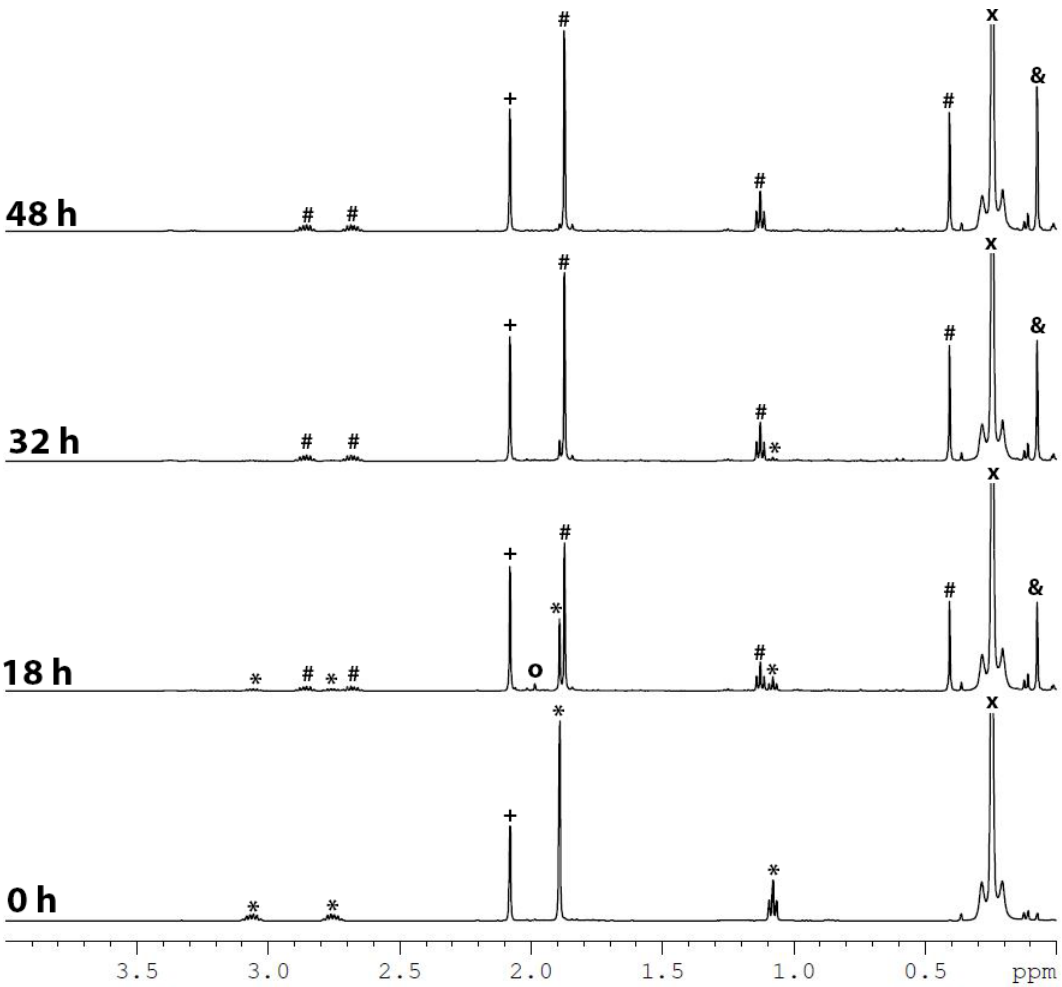

Figure 3.6: Partial ^{1}H NMR (400 MHz, C_6D_6, 60 °C) showing **2.5** (*****) with internal standard durene (**+**) reacting quickly with 9.7 eq $(Me_3Si)_2Hg$ (**x**) upon being heated at 60 °C to convert to intermediate **2.8** (**o**) and eventually **3.6** (**#**) with hexamethyldisilane (**&**), a by-product of $(Me_3Si)_2Hg$ decomposition

3.3 Other Reactivities

With the thermal cleavage of the N≡N bond accomplished in the formation of **2.8**, it is vitally important to gauge some of the chemical reactions that might feasibly be accomplished, both to gain more information about the reactivity of the nitride complex and, more directly, to functionalize the bridging nitrides so as to eventually release N-atom-containing products, bringing a complete fixation cycle to fruition. The silyl imido is an enormously valuable product, however there are many other potential

opportunities to trap or functionalize the nitride, and so a wide variety or lead reactions were conducted.

3.3.1 Attempted Alkylimido Formation

With multiple successful synthetic routes to the molybdenum silylimido, which prescient dictates can be released from the metal center from one of several reactions with other small molecules, it was intriguing to consider if a corresponding alkylimido could be synthesized and subsequently released in the form of a value-added N-atom product. Successful alkylimido formation has previously been demonstrated with the CPAM system.[22, 26 24] Several different synthetic routes to this goal were attempted, focusing on reaction of various alkyl halides with either the (μ-N_2) **2.5** or (μ-N)$_2$ **2.8**.

Initial interest was piqued by the reaction of **2.5** with methyl iodide (MeI), as shown in Scheme 3.7. The addition of MeI immediately consumes all available **2.8** to form what appears by ^{1}H NMR to be an equimolar mixture of a *C*$_1$ symmetric species and a *C*$_S$ symmetric species, as is shown in Figure 3.7. According to the established addition of Me_3SiCl to **2.8**,[25] these species are likely the nitrido iodo {Cp*[N(Et)C(Ph)N(Et)]Mo(N)I} (**3.13**) and the methylimido {Cp*[N(Et)C(Ph)N(Et)]Mo(NMe)} (**3.14**) (*For greater detail on the characterization of **3.13** as well as a more in depth investigation of the substitution of iodo ligands for*

Scheme 3.7

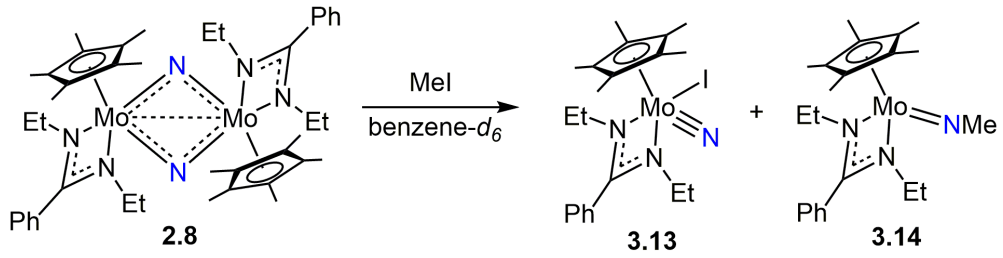

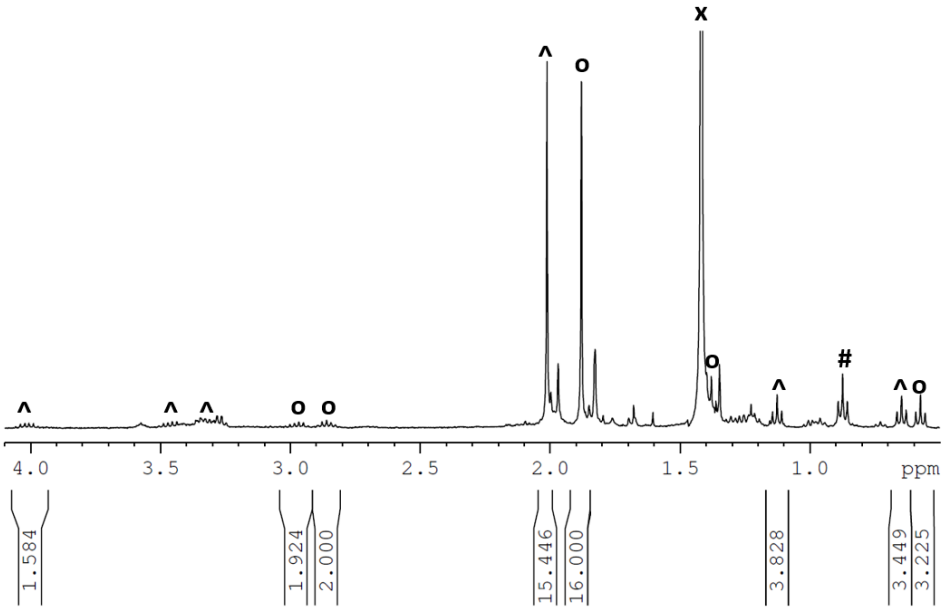

Figure 3.7. Partial ^{1}H NMR (400 MHz, C_6D_6, 25 °C) showing the immediate result of reacting a solution of **2.8** with MeI (**x**) at 25 °C to produce presumed **3.13** (^) and **3.14** (**o**). Pentane (#) impurity noted

chloride, see Chapter 5.2). Unfortunately, as time passed, a brown precipitate began to drop out of solution and the amount of (presumed) **3.14** decreased by ^{1}H NMR until nothing recognizable besides **3.13** remained in the spectrum after 17 h.

In response to this potentially promising result, the dinuclear $(\mu\text{-N})_2$ **2.8** was treated with various an alkyl halides, RX, in an attempt to generate an equimolar the respective alkylimido {Cp*[N(Et)C(Ph)N(Et)]Mo(NR)} (**3.15**) which might prove more stable than **3.14**, along with an even amount of the respective nitrido, halide {Cp*[N(Et)C(Ph)N(Et)]Mo(N)X} (X = Cl (**3.4**), I (**3.13**), or Br (**3.16**)), according to Scheme 3.8. MeI, PhCl, iPrCl, iPrBr, iPrI, iBuCl, tBuCl, tBuBr, and tBuI were all screened, but unfortunately despite numerous reactions varying temperature, time, and RX identity, at best all that could be identified by ^{1}H NMR was fleeting amounts of **3.13** upon the addition of tBuI and iPrI, and there was no successful recovery of any products that could be assigned as a terminal alkylimido.

Scheme 3.8

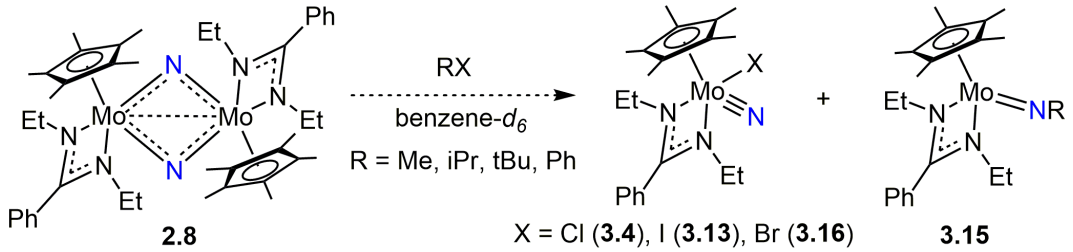

3.3.2 Attempted Protonation/Hydrogenation

If the ultimate goal of N_2 fixation is often cited as the formation of ubiquitous NH_3, then perhaps the most obvious reaction to attempt with the dinuclear bis nitride **2.8** is simple protonation. Though somewhat robust, at least in comparison to the pre-cleaved **2.5**, **2.8** remains extremely sensitive, prone to decomposition upon exposure to air or moisture. As a result, a gentle acid was sought to act as a productive proton donor. It was hoped that *N*,*N*-dimethylanilinium tetrakis(pentafluorophenyl)borate ($[(C_6H_5)N(H)(CH_3)_2][B(C_6F_5)_4]$) might be such a reagent, however an equimolar mixture of **2.8** with the analinium borate salt in toluene-d_8 immediately reacted to form an intractable brown precipitate from which no further information could be determined. Related, H_2 is known to add across metal-nitrogen bonds,[31] and so hydrogenation of **2.8** was also attempted by charging a benzene-d_6 solution of **2.8** with H_2 (10 psi) This also proved unproductive, showing no initial reaction at room temperature and, upon heating at 65 °C, decomposing into a complex mixture of products, at least one of which is likely the amidine from the protonation and loss of the amidinate ligand. (*For further insight into successful reaction of CPAM complexes with proton donors, see Chapter 4*)

3.3.3 Oxidation by Halides

It was also of interest to determine if the Mo(V) **2.8** could be returned to a Mo(VI) nitrido halide through oxidation, since the ability to move freely between oxidation states is of great importance to continuous processes. More specifically, since nitrido chloride **3.4** is demonstrated to undergo reduction by NaHg to form **2.8**, shown in Scheme 3.1, the natural extension of this is to wonder if **2.8** could be made to return to **3.4** via oxidation. As is laid out in Scheme 3.9, the addition of excess carbon tetrachloride (CCl_4), which may be considered radical-like in its behavior,[32-34] to a toluene solution of **2.8** cleanly forms **3.4** in 86% isolated yield. Interestingly, addition of CCl_4 to **2.9** did not follow the same facile reactivity to form **3.7**, and instead quickly formed a complex mixture of products, none of which were recognizable, that eventually decomposed over 16 h at room temperature. The success of an oxidation process of Mo was not limited to chloride derivates; indeed, addition of I_2 to **2.8** in THF yielded the nitrido iodo complex **3.13** according to Scheme 3.9 (*See Chapter 5.1 of this document for further exploration of the use of iodo ligands*). This interconversion between the Mo(V) and Mo(VI) oxidation states demonstrates the versatility of the ligand set and underlines its ability to facilitate successful reactions in the higher oxidation states, a trait that is very important to a complete chemical or catalytic cycle for dinitrogen fixation.

Scheme 3.9

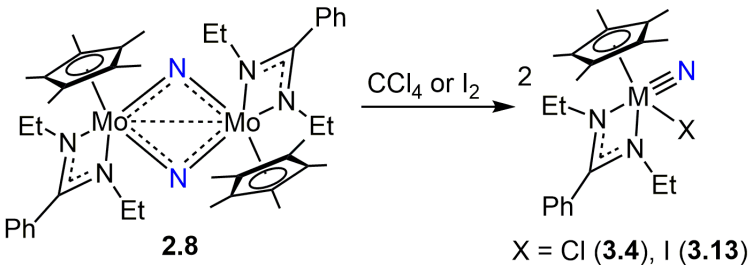

2.8

X = Cl (**3.4**), I (**3.13**)

3.3.4 Diphenyl Disulfide Reactivity with (μ-N)$_2$ and (μ-N$_2$) Complexes

A number of studies were conducted to gain more information about bridging bis-nitride itself. Some attempts to "trap" a terminal, mononuclear nitride from **2.8** have previously been reported in Chapter 2. However, the addition of diphenyl disulfide, PhSSPh, to the (μ-N)$_2$ complexes, and indeed, even the (μ-N$_2$) complexes, yielded unique, if preliminary, results in each instance depending on both the geometry of N$_2$ core and the identity of the metal centers. Varied results of the oxidative addition of disulfides and their S-S bond cleavage have been observed in many cases of transition-metal complexes spanning the periodic table and help to highlight both metal and ligand-dependent trends.[35-38]

First, addition of excess PhSSPh to a benzene-d_6 solution of **2.5** immediately causes a change in color from brown to dark red and is shown by ^{1}H NMR to produce a C_s symmetric product which, by integration, is determined to have two SPh units per each CPAM ligand set. Larger scale reactions in toluene could be isolated as a red oil out of which a single crystal was obtained that, by XRD, confirmed the structure to be a mononuclear bis thiolate {Cp*[N(Et)C(Ph)N(Et)]Mo(SPh)$_2$} (**3.17**), see Figure 3.8.

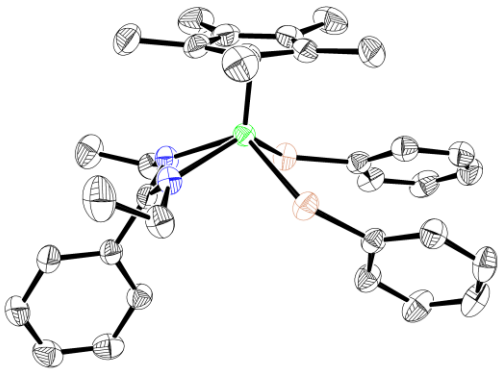

Figure 3.8. Crystal structure of **3.17** with hydrogen atoms omitted for clarity, ellipsoids for the non-hydrogen atoms are shown at the 30% probability level

This reaction, illustrated in Scheme 3.10, results in the immediate displacement of the bridging N_2 unit from the Mo(II) metal centers. When a substoichiometric amount of PhSSPh was added to a benzene-d_6 solution of **2.5** it produced no observable intermediates by ^{1}H NMR but only resulted in the incomplete conversion of **2.5** to **3.17**. Addition of more PhSSPh immediately consumed the remaining **2.5** to form **3.17**.

Scheme 3.10

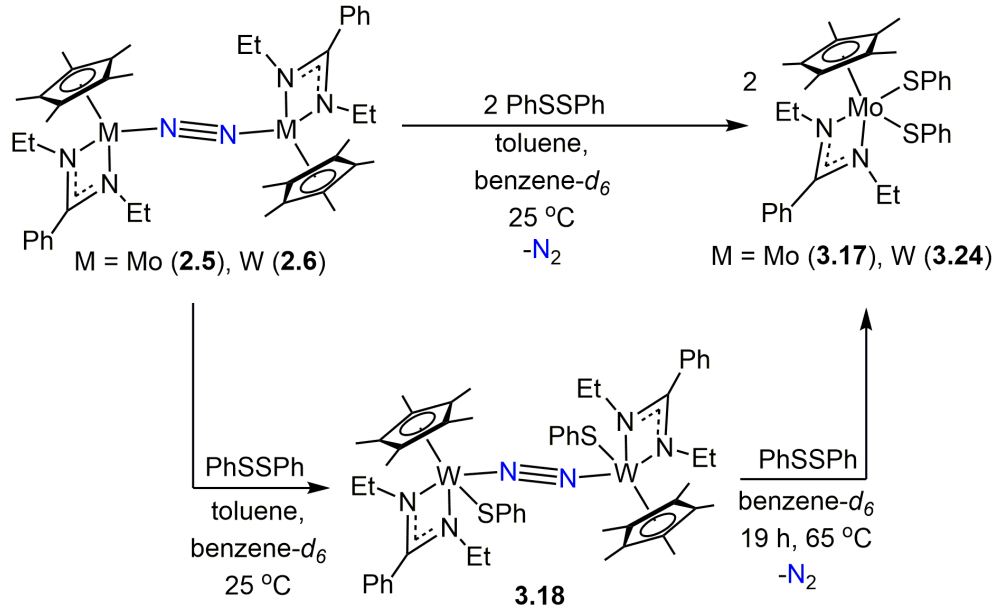

Alternately, the comparable addition of one equivalent of PhSSPh to a benzene-d_6 or toluene solution of **2.6** immediately changed in color from a deep forest green to a brown kaki solution out of which precipitate began to crash. ^{1}H NMR of this species indicated the formation of a C_i (or, in the case of a mononuclear product, potentially C_1) symmetric product that contains one SPh unit for each CPAM set. This is believed to be the product of 1,4-addition of PhSSPh across the W-N-N-W core to produce $\{Cp^*[N(Et)C(Ph)N(Et)]W(SPh)\}_2(\mu\text{-}\eta^1\text{:}\eta^1\text{-}N_2)$ (**3.18**) as Scheme 3.10 reveals. The identity of this species is bolstered by ESI-MS(+) analysis which reveals a series of peaks that match **3.18** ($[M + H]^+$ = 1234.53 m/z) as is shown in Figure 3.9. Unlike in

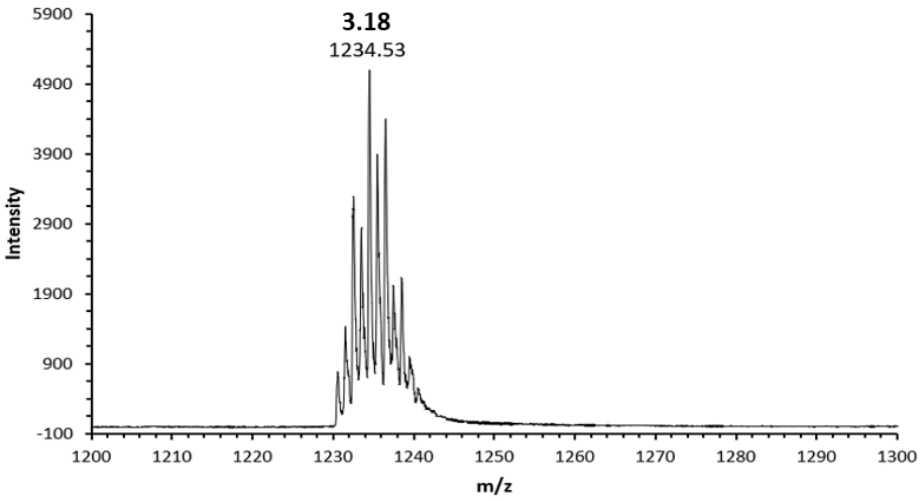

Figure 3.9. Partial ESI-MS(+) of THF solution of **3.18**, the product of a stoichiometric mixture of **2.6** and PhSSPh

the case of Mo, the bridging N_2 between W centers is not labile upon the addition of PhSSPh at room temperature. This is in keeping with reaction of PhSSPh with the group 5 ditantalum (μ-N_2) complex, {Cp*[N(iPr)C(Me)N(iPr)]Ta(μ-N)}$_2$ (**3.19**) with PhSSPh which reacts in the same 1,4-addition fashion to form {Cp*[N(iPr)C(Me)N(iPr)]Ta(SPh)}$_2$(μ-η^1:η^1-N_2) (**3.20**).[24] Several other disulfides (dicyclohexyl disulfide, 2-napthyl disulfide, and ditertbutyl disulfide) were screened in reactions with **2.6** and were judged by ^{1}H NMR as likely to be undergoing the same 1,4-addition with each equivalent of the disulfide to produce {Cp*[N(Et)C(Ph)N(Et)]W(SR)}$_2$(μ-η^1:η^1-N_2) (R = 2-Napthyl (**3.21**), Cy (**3.22**), tBu

Scheme 3.11

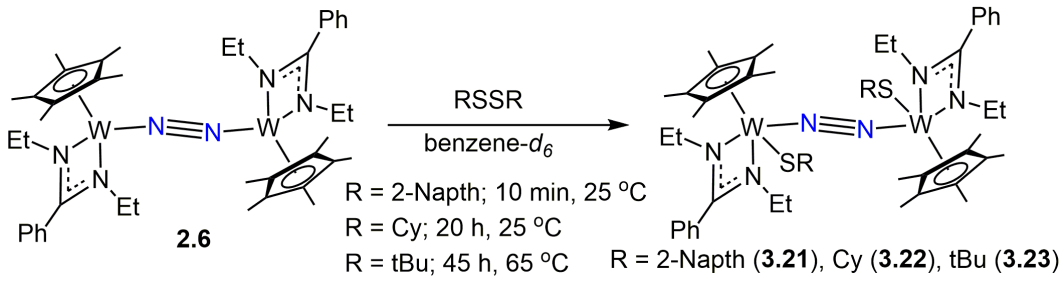

(**3.23**)) as shown in Scheme 3.11; however, the bulkier the alkyl or aryl substituent was, the slower the reaction proceeded, in the case of tBu even requiring an elevated temperature to react.

The disparity between the reactivity of Mo and W(μ-N_2) complexes when mixed with PhSSPh is striking, though not necessarily surprising. CPAM W complexes have been repeatedly shown to have higher barriers to reaction than their Mo counterparts[23, 25, 31] so the addition of PhSSPh to the W (μ-N_2) complex **2.6** through a 1,4-addition to make **3.18** is likely the same pathway by which the Mo (μ-N_2) complex **2.5** produces **3.17** - the Mo simply does so without an observable 1,4-addition intermediate. In support of this theory, while the addition of another equivalent of PhSSPh to a benzene-d_6 solution of **3.18** had no result at room temperature, upon heating the sample at 65 °C, the resulting ^{1}H NMR spectra was very similar to **3.17**, in that there appeared to be a C_s product with two SPh ligands to each CPAM set. Therefore, it is hypothesized that with the addition of heat, the W 1,4-addition product can add another equivalent of PhSSPh and displace its bridging N_2 unit, as Mo does immediately at room temperature, to convert to the bis thiolate {Cp*[N(Et)C(Ph)N(Et)]W(SPh)$_2$} (**3.24**) as shown in Scheme 3.10.

Preliminary studies of the reactivity of PhSSPh with the (μ-N)$_2$ complexes were also conducted. The addition of PhSSPh to **2.8** in toluene or benzene-d_6 results in the immediate transformation of the solution from brown to orange, from which feathery crystalline material precipitates at room temperature. ^{1}H NMR of this material demonstrates a C_i symmetric product judged likely to be the nitrido, thiolate {Cp*[N(Et)C(Ph)N(Et)]Mo(N)(SPh)} (**2.25**), illustrated in Scheme 3.12, but the fluffy

Scheme 3.12

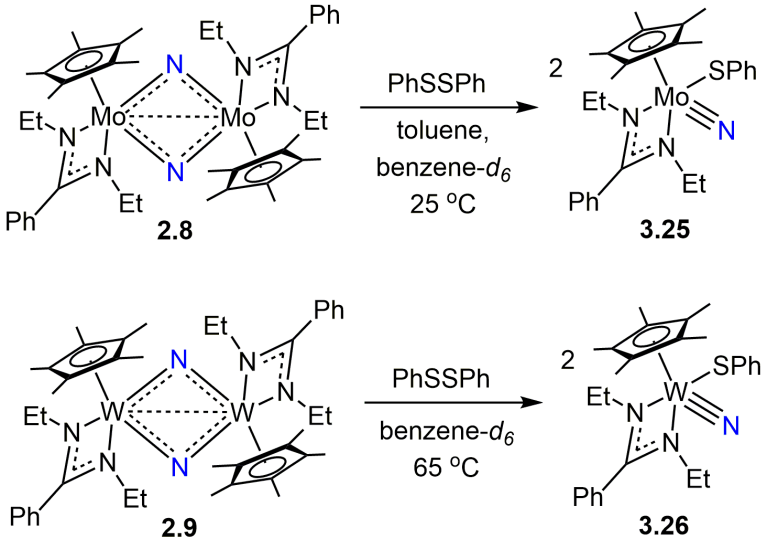

nature of the product and its low solubility even at room temperature made isolation for characterization by XRD or EA difficult. On the other hand, adding PhSSPh to a benzene-d_6 solution of **3.9** caused a slow reaction at room temperature to a product of undetermined structure, however upon heating, this material converted to a C_1 symmetric product which seemed by ^{1}H NMR to be very similar to **3.25** and was therefore tentatively identified as {Cp*[N(Et)C(Ph)N(Et)]W(N)(SPh)} (**3.26**) as is shown in Scheme 3.12.

Though these studies undoubtedly require further attention and corroboration, they once again suggest that the Mo reactions proceed quickly to the final product while W reactions pass through an observable intermediate. More importantly, these reactions of PhSSPh with the $(\mu\text{-N})_2$ complexes corroborate the more dynamic behavior of **2.8** than **2.9**, (*discussed in depth in Chapter 2.5*). Knowing that the Mo(V) centers of **2.8** engage in some sort of dynamic behavior, the observed formation of **3.25** makes sense if the cleaved disulfide is in effect "trapping" the mononuclear Mo(VI) complex. Further, especially given that the W(V) cores of **2.9** do not seem to engage in a

mononuclear/dinuclear conversion, even at elevated temperatures, should the intermediate of the transformation from **2.9** to **3.26** be identified, and the structure of **3.26** confirmed through complete characterization, it may provide significant insight into the fragmentation behavior of the (μ-N) complexes.

3.4 Conclusions

Key functionalization of the N-atom from N_2 has now been mapped for the sterically reduced CPAM series. Both Me_3SiCl and $Hg(SiMe_3)_2$ have been used to successfully convert **2.5** (or **2.8**) to **3.6**. As is shown in Scheme 3.13, the former produces a 2 : 1 mixture of **3.6** : **2.3** (where the **2.3** can be recycled back to **2.5** via

Scheme 3.13

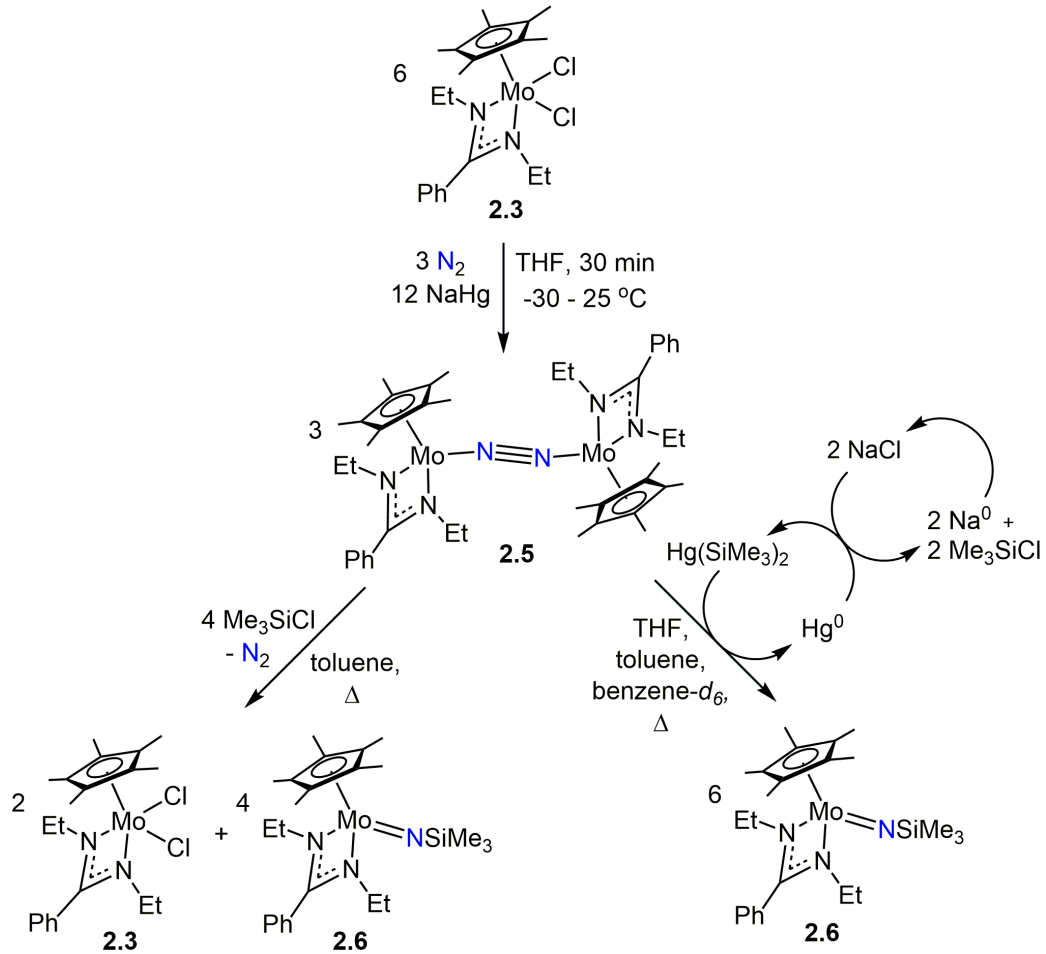

chemical reduction) while the latter quantitively produces **3.6** and could conceivably be created *in situ* with the production of the $Hg(SiMe_3)_2$. Generally speaking, these reactions confirm the observation that the W complexes tend to react more slowly or require more energy than their Mo counterparts. Similar to the rate of N_2 cleavage, this is likely due to greater steric crowding about the W centers than the Mo which inhibits reactivity. Though other reactions of the dinitrogen and nitride species have also been attempted, including the formation of alkylimidos by alkyl halides, oxidation by halides, and thiolation by disulfides, these are by no means a comprehensive investigation into every possible reactivity. The work with disulfides, in particular, is worth continuing with alternate sulfide substituents, reaction conditions, and complete characterization for a greater depth of understanding of the Mo and W reactivities. The silylation reactions, however, are so far the most successful and produces a well-characterized product, namely the silylimido **3.6**, which can be released off the metal center as a value-added N-containing product as is described in Chapter 4.

3.5 Experimental Details

3.5.1 General Considerations

All manipulations of air and moisture sensitive compounds were carried out under N_2 or Ar atmospheres with standard Schlenk or glovebox techniques. Et_2O and THF were distilled from Na/benzophenone under N_2 prior to use. Toluene and pentane were dried and deoxygenated by passage over activated alumina and GetterMax® 135 catalyst (purchased from Research Catalysts, Inc.) within a PureSolv solvent purification system manufactured by Innovative Technologies (model number PS-400-

4-MD) and collected under N_2 prior to use. Benzene-d_6, toluene-d_8, and THF-d_8 were dried over Na/K alloy and isolated by vacuum transfer prior to use. Celite© was oven dried (150 °C for several days) prior to use. Cooling was performed in the internal freezer of a glovebox maintained at -30 °C. Trimethylsilyl azide, trimethylsilyl chloride, trimethylsilyl iodide, iodine, methyl iodide, *N*,*N*-dimethylanilinium tetrakis(pentafluorophenyl)borate, diphenyl disulfide, 2-napthyl disulfide, dicyclohexyl disulfide, and ditertbutyl disulfide were purchased from Sigma Aldrich and used as received. $Hg(SiMe_3)_2$[39] was prepared according to the previously reported procedures in similar yield and purity [***Caution:*** *To the best of our knowledge, there have been no toxicology studies performed for* $Hg(SiMe_3)_2$ *to date. Therefore, extreme precautions should be taken during the synthesis, handling, and disposal of this crystalline material, and any solutions derived therefrom*]. All room temperature ^{1}H NMR were recorded at 400.13 MHz and referenced to $SiMe_4$ using residual ^{1}H chemical shifts of benzene-d_6, toluene-d_8, or THF-d_8. ^{13}C NMR spectra were recorded at 125.76 MHz and calibrated to residual ^{13}C chemical shifts of benzene-d_6. Elemental analyses were carried out by Midwest Microlab, LLC.

3.6.2 Synthesis of New Compounds

{Cp*[N(Et)C(Ph)N(Et)]Mo(N)Cl} (3.4). Me_3SiN_3 (41.0 µL, 0.331 mmol) was added in a dropwise fashion via micro syringe to a solution of **2.3** (98.1 mg, 0.206 mmol) in 3 mL toluene causing bubbles of N_2 to effervesce. After stirring at 25 °C for 17 hours, volatiles were removed *in vacuo* to produce a yellow-brown solid dissolved in toluene and filtered through a pipet with kimwipe and celite plug. The filtrate was dried under reduced pressure before being recrystallized in toluene and pentane and

chilled to -30 °C to yield golden-olive crystals of **3.4** (87.1 mg, yield = 93%). Anal. calc'd for $C_{21}H_{30}ClN_3Mo$: C, 55.33; H, 6.63; N, 9.22; Found: C, 55.10; H, 6.44; N, 9.22. ^{1}H NMR (400 MHz, C_6D_6, 25 °C): 0.71 (3H, t, J = 7.1 Hz, $CH_2(CH_3)$) 1.15 (3H, t, J = 7.0 Hz, $CH_2(CH_3)$), 1.95 (15H, s, $C_5(CH_3)_5$), 3.09 – 3.18 (1H, m, $CH_2(CH_3)$), 3.26 – 3.35 (1H, m, $CH_2(CH_3)$), 3.38 – 3.47 (1H, m, $CH_2(CH_3)$), 3.70 – 3.79 (1H, m, $CH_2(CH_3)$), 6.89 – 7.03 (5H, m, $C(C_6H_5)$). ^{13}C{H} NMR (125 MHz, C_6D_6, 25° C): 11.62 ($C_5(CH_3)_5$), 17.25 ($CH_2(CH_3)$), 18.15 ($CH_2(CH_3)$), 41.35 ($CH_2(CH_3)$), 44.65 ($CH_2(CH_3)$), 119.54 ($C_5(CH_3)_5$), 128.59 ($C(C_6H_5)$), 128.76 ($C(C_6H_5)$), 129.81 ($C(C_6H_5)$), 131.76 ($C(C_6H_5)$), 180.73 ([(N(Et)*C*(Ph)N(Et)]).

{Cp*[N(Et)C(Ph)N(Et)]Mo(NSiMe$_3$)} (3.6). A solution of **3.4** (70.7 mg, 0.155 mmol) in 2 mL THF was chilled to -30° C to which was added 0.5% (w/w) Na/Hg (2.8585 g, 0.62168 mmol Na) and let stir for 1 h coming to room temperature. Me_3SiCl (12.0 µL, 0.0956 mmol) was added via micro syringe and the green mixture was stirred for 1 hour at room temperature, becoming browner, at which point additional $SiMe_3Cl$ (6.0 µL, 0.047 mmol) was added, and the solution let stir for another hour. Following this, a final portion of $SiMe_3Cl$ (3.0 µL, 0.024 mmol) was added and the solution was then stirred for 15 hours. The solvent was removed *in vacuo* and the resulting brown oil was dissolved in pentane and filtered through a kimwipe and celite plug in a pipet. After drying under reduced pressure, the brown oil **3.6** (63.5 mg, 83%) was stored at -30 °C and formed crystals suitable for XRD though there were not enough crystals formed to acquire EA, for which oil not amenable. ^{1}H NMR (400 MHz, C_6D_6, 25 °C) 0.44 (9H, s, $Si(CH_3)_3$), 1.16 (6H, t, *J* = 7.1 Hz, $CH_2(CH_3)$), 1.89 (15H, s, $C_5(CH_3)_5$)), 2.62 – 2.71 (2H, m, $CH_2(CH_3)$), 2.83 – 2.91 (2H, m, $CH_2(CH_3)$), 7.06 (5H, m, $C(C_6H_5)$).

$^{13}C\{H\}$ NMR (125 MHz, C_6D_6, 25° C): 2.51 (Si(*C*H_3)$_3$), 13.15 (C_5(*C*H_3)$_5$), 18.17 (CH_2(*C*H_3)), 43.07 (*C*H_2(CH_3)), 105.70 (*C*$_5$(CH_3)$_5$), 127.24 (C(*C*$_6$H$_5$)), 128.86 (C(*C*$_6$H$_5$)), 128.93 (C(*C*$_6$H$_5$)), 131.15 (C(*C*$_6$H$_5$)), 181.29 ([(N(Et)*C*(Ph)N(Et)]).

{Cp*[N(Et)C(Ph)N(Et)]W(N)Cl} (3.7). 2.4 (128.4 mg, 0.2272 mmol) was dissolved in 6 mL toluene to which was added Me_3SiCl (31.8 µL, 0.240 mmol) via micro syringe. The mixture stirred for 45 min while the color changed immediately from orange to brown while N_2 bubbles effervesced. Volatiles were removed *in vacuo* and the resulting brown solid was re-dissolved in toluene and filtered through a pipet with a kimwipe and celite plug, then pumped down to yield a greyish-black solid which was recrystallized in toluene and pentane and cooled at -30° C to produce grey crystals **3.7** (49.5 mg, 40%). Anal. calc'd for $C_{21}H_{30}ClN_3W$: C, 46.38; H, 5.56; N, 7.73; Found: C, 46.15; H, 5.25; N, 7.63. ^1H NMR (400 MHz, C_6D_6, 25 °C): 0.66 (3H, t, J = 7.1 Hz, CH_2(C*H*$_3$)), 1.21 (3H, t, J = 7.0 Hz, CH_2(C*H*$_3$)), 2.06 (15H, s, C_5(C*H*$_3$)$_5$), 3.18 – 3.34 (2H, m, C*H*$_2$(CH_3)), 3.47 – 3.56 (1H, m, C*H*$_2$(CH_3)), 3.62 – 3.71 (1H, m, C*H*$_2$(CH_3)), 6.90 – 7.01 (m, C(C_6*H*$_5$)).

{Cp*[N(Et)C(Ph)N(Et)]W(NSiMe$_3$)} (3.8). 3.7 (83.3 mg, 0.0819 mmol) was dissolved in 5 mL toluene to which was added Me_3SiN_3 (43.5 µL, 0.327 mmol) and the dark green mixture was stirred at 25 °C for 1.5 h coming to a red brown solution before being pumped down. The oil was re-dissolved in toluene and filtered through a pipet with a kimwipe and celite plug and pumped down again to a red oil, **3.8** (86.4 mg, 95%), not amenable to EA. ^1H NMR (400 MHz, C_6D_6, 25 °C) 0.43 (9H, s, Si(C*H*$_3$)$_3$), 1.21 (6H, t, *J* = 7.1 Hz, CH_2(C*H*$_3$)), 2.08 (15H, s, C_5(C*H*$_3$)$_5$)), 2.60 – 2.69 (2H, m, C*H*$_2$(CH_3)), 2.86 – 2.94 (2H, m, C*H*$_2$(CH_3)), 7.04 (5H, m, C(C_6*H*$_5$)).

{Cp*[N(Et)C(NMe$_2$)N(Et)]Mo(N)Cl} (3.9). Me_3SiN_3 (87.0 µL, 0.662 mmol) was added in a dropwise fashion via micro syringe to a solution of **2.18** (195.4 mg, 0.4398 mmol) in 7 mL toluene causing bubbles of N_2 to effervesce. After stirring at 25 °C for 17 hours, volatiles were removed *in vacuo* to produce a yellow-green solid dissolved in toluene and filtered through a pipet with kimwipe and celite plug. The filtrate was dried under reduced pressure before being recrystallized in toluene and pentane and chilled to -30 °C to yield yellow-olive crystals of **3.9** (150.4 mg, 74 %). Anal. calc'd for $C_{17}H_{31}ClN_4Mo$: C, 48.27; H, 7.39; N, 13.25; Found: C, 48.13; H, 7.33; N, 13.29. ^{1}H NMR (400 MHz, C_6D_6, 25 °C): 0.84 (3H, t, J = 6.7 Hz, $CH_2(CH_3)$) 1.34 (3H, t, J = 6.7 Hz, $CH_2(CH_3)$), 1.90 (15H, s, $C_5(CH_3)_5$), 2.17 (6H, s, $(NCH_3)_2$), 3.06 – 3.14 (1H, m, $CH_2(CH_3)$), 3.54 – 3.52 (2H, m, $CH_2(CH_3)$), 3.64 – 3.73 (1H, m, $CH_2(CH_3)$). ^{13}C{H} NMR (125 MHz, C_6D_6, 25° C): 11.52 ($C_5(CH_3)_5$), 13.76 ($CH_2(CH_3)$), 16.98 ($CH_2(CH_3)$), 38.07 ($CH_2(CH_3)$), 40.23 ($CH_2(CH_3)$), 47.6 ($NCH_3)_2$), 118.48 ($C_5(CH_3)_5$), 169.36 ([(N(Et)*C*(Ph)N(Et)]).

{Cp*[N(Et)C(NMe$_2$)N(Et)]Mo(NSiMe$_3$)} (3.10). A solution of **3.9** (77.3 mg, 0.170 mmol) in 4 mL THF was chilled to -30° C to which was added 0.5% (w/w) Na/Hg (3.1602 g, 0.68730 mmol Na) and let stir for 1 h coming to room temperature. Me_3SiCl (13.0 µL, 0.102 mmol) was added via micro syringe and the brown mixture was stirred for 1 hour at room temperature, becoming darker brown, at which point additional $SiMe_3Cl$ (7.0 µL, 0.055 mmol) was added, and the solution let stir for another hour. Following this, a final portion of $SiMe_3Cl$ (4.5 µL, 0.035 mmol) was added and the solution was then stirred for 16 hours. The solvent was removed *in vacuo* and the resulting brown oil was dissolved in pentane and filtered through a kimwipe and celite

plug in a pipet. After drying under reduced pressure, the brown oil **3.10** was not amenable for EA but was stored at -30 °C (79.1 mg, 101 %). ^{1}H NMR (400 MHz, C_6D_6, 25 °C) 0.39 (9H, s, Si(C*H*$_3$)$_3$), 1.28 (6H, t, *J* = 7.1 Hz, CH$_2$(C*H*$_3$)), 1.87 (15H, s, C$_5$(C*H*$_3$)$_5$)), 2.28 (6H, s, (NC*H*$_3$)$_2$), 2.72 – 2.81 (2H, m, C*H*$_2$(CH$_3$)), 3.09 – 3.18 (2H, m, C*H*$_2$(CH$_3$)). ^{13}C{H} NMR (125 MHz, C_6D_6, 25° C): 2.58 (Si(*C*H$_3$)$_3$), 13.13 (C$_5$(*C*H$_3$)$_5$), 17.55 (CH$_2$(*C*H$_3$)), 38.46 (N*C*H$_3$)$_2$), 43.774 (*C*H$_2$(CH$_3$)), 104.69 (*C*$_5$(CH$_3$)$_5$), 127.24 (C(*C*$_6$H$_5$)), 128.86 (C(*C*$_6$H$_5$)), 128.93 (C(*C*$_6$H$_5$)), 131.15 (C(*C*$_6$H$_5$)), 173.14 ([(N(Et)*C*(NMe$_2$)N(Et)]).

{Cp*[N(Et)C(NMe$_2$)N(Et)]W(N)Cl} (3.11). 2.19 (76.0 mg, 0.143 mmol) was dissolved in 6 mL toluene to which was added Me$_3$SiCl (33.0 µL, 0.251 mmol) via micro syringe. The mixture stirred for 4 h while the color changed immediately from orange to grey-brown and N_2 bubbles effervesced. Volatiles were removed *in vacuo* and the resulting brown solid was re-dissolved in toluene and filtered through a pipet with a kimwipe and celite plug, then pumped down to yield a greyish-dark green oil that was washed in pentane repeatedly and dried under reduced pressure to yield the oil of **3.11** (50.2 mg, 71 %). ^{1}H NMR (400 MHz, C_6D_6, 25 °C): 0.83 (3H, t, J = 7.2 Hz, CH$_2$(C*H*$_3$)), 1.23 (3H, t, J = 7.2 Hz, CH$_2$(C*H*$_3$)), 2.00 (15H, s, C$_5$(C*H*$_3$)$_5$), 2.15 (6H, s, (NC*H*$_3$)$_2$), 3.11 – 3.20 (1H, m, C*H*$_2$(CH$_3$)), 3.45 – 3.67 (3H, m, C*H*$_2$(CH$_3$)).

{Cp*[N(Et)C(NMe$_2$)N(Et)]W(NSiMe$_3$)} (3.12). 3.11 (4.6 mg, 0.0048 mmol) was dissolved in 0.6 mL benzene-*d*$_6$ to which Me$_3$SiN$_3$ (2.5 µL, 0.019 mmol) was added via micro syringe and the dark green began to grow yellow then orange as it reacted at room temperature for 1 h. Volatiles were removed *in vacuo* to yield an orange oil, **3.12** (2.0 mg, 91 %). ^{1}H NMR (400 MHz, C_6D_6, 25 °C) 0.39 (9H, s, Si(C*H*$_3$)$_3$), 1.31 (6H, t,

J = 7.2 Hz, $CH_2(CH_3)$), 2.09 (15H, s, $C_5(CH_3)_5$)), 2.21 (6H, s, $(NCH_3)_2$), 2.27 – 2.81 (2H, m, $CH_2(CH_3)$), 3.14 – 3.23. $^{13}C\{H\}$ NMR (125 MHz, C_6D_6, 25° C): 3.08 ($Si(CH_3)_3$), 14.55 ($C_5(CH_3)_5$), 17.90 ($CH_2(CH_3)$), 37.89 ($CH_2(CH_3)$), 45.39 (($NCH_3)_2$), 102.99 ($C_5(CH_3)_5$), 178.36 ([(N(Et)*C*(Ph)N(Et)]).

{Cp*[N(Et)C(NMe$_2$)N(Et)]Mo(SPh)$_2$} (3.17). 2.5 (67.1 mg, 0.0798 mmol) was dissolved in 3 mL toluene to which was added PhSSPh (33.0 mg, 0.251 mmol). The mixture was stirred for 10 minutes changing from brown to maroon before volatiles were removed *in vacuo*. The resulting oil was rinsed with cold pentane and attempts to recrystallize yielded a single crystal amenable to XRD while the rest remained a red oil **3.17** (45.1 mg, 95%). ^1H NMR (400 MHz, C_6D_6, 25 °C): 0.83 (3H, t, J = 7.3 Hz, $CH_2(CH_3)$), 1.97 (15H, s, $C_5(CH_3)_5$), 2.85-2.94 (2H, m, $CH_2(CH_3)$), 3.30 – 3.39 (2H, m, $CH_2(CH_3)$), 6.70 (2H, t, J = 7.3, S*Ph*), 6.88 – 7.07 (5H, m, *Ar*), 7.12 (2H, d, J = 7.4, S*Ph*) 7.44 (4H, d, J = 7.4, S*Ph*). $^{13}C\{H\}$ NMR (125 MHz, C_6D_6, 25° C): 13.95 ($C_5(CH_3)_5$), 18.61 ($CH_2(CH_3)$), 42.95 ($CH_2(CH_3)$), 110.09 ($C_5(CH_3)_5$), 125.90 (S*Ph*), 126.86 (S*Ph*), 135.26 (S*Ph*).

{Cp*[N(Et)C(NMe$_2$)N(Et)]W(SPh)}(μ-η^1:η^1-N$_2$) (3.18). 2.6 (75.0 mg, 0.0738 mmol) was dissolved in 2 mL toluene to which was added PhSSPh (15.0 mg, 0.0687 mmol). The mixture was stirred for 10 minutes changing from a deep green to a kaki-orange. The solution was allowed to sit for 30 min at room temperature at which point precipitate began to drop out of solution. The precipitate was dried under reduced pressure and identified as **3.18** (71.2 mg, 82%). ^1H NMR (400 MHz, C_6D_6, 25 °C): 0.66 (3H, t, J = 7.1 Hz, $CH_2(CH_3)$), 1.06 (3H, t, J = 7.1 Hz, $CH_2(CH_3)$), 2.26 (15H, s, $C_5(CH_3)_5$), 3.09 – 3.34 (1H, m, $CH_2(CH_3)$), 4.23 – 4.32 (1H, m, $CH_2(CH_3)$), 7.03 –

7.14 (7H, m, *Ar*/S*Ph*) 7.23 (1H, br, S*Ph*), 7.56 (2H, d, J = 8.2, S*Ph*). ^{13}C{H} NMR (125 MHz, C_6D_6, 25° C): 11.85 ($C_5(CH_3)_5$), 18.13 ($CH_2(CH_3)$), 18.75 ($CH_2(CH_3)$), 41.95 ($CH_2(CH_3)$), 43.49 ($CH_2(CH_3)$), 105.44 ($C_5(CH_3)_5$), 122.45 (S*Ph*), 126.86 (S*Ph*), 133.13 (S*Ph*), 134.26 (S*Ph*), 151.40 (S*Ph*), 180.27 ([(N(Et)*C*(Ph)N(Et)]).

{Cp*[N(Et)C(NMe$_2$)N(Et)]Mo(N)(SPh)} (3.25). 2.8 (76.0 mg, 0.143 mmol) was dissolved in 0.6 mL benzene-*d*$_6$ to which was added PhSSPh (33.0 mg, 0.251 mmol). The mixture stirred for 4 h while the color changed immediately from orange to grey-brown and N_2 bubbles effervesced. Volatiles were removed *in vacuo* and the resulting brown solid was re-dissolved in toluene and filtered through a pipet with a kimwipe and celite plug, then pumped down to yield a greyish-dark green oil that was washed in pentane repeatedly and dried under reduced pressure to yield the oil of **3.25** (50.2 mg, 71 %). ^{1}H NMR (400 MHz, C_6D_6, 25 °C): 0.66 (3H, t, J = 7.1 Hz, $CH_2(CH_3)$), 1.26 (3H, t, J = 7.1 Hz, $CH_2(CH_3)$), 1.94 (15H, s, $C_5(CH_3)_5$), 2.92 – 3.01 (1H, m, $CH_2(CH_3)$), 2.32 – 3.47 (2H, m, $CH_2(CH_3)$), 3.48 – 3.57 (1H, m, $CH_2(CH_3)$), 7.23 (1H, t, J = 7.7, S*Ph*), 8.50 (2H, d, J = 7.7, S*Ph*). ^{13}C{H} NMR (125 MHz, C_6D_6, 25° C): 11.51 ($C_5(CH_3)_5$), 17.32 ($CH_2(CH_3)$), 18.59 ($CH_2(CH_3)$), 40.79 ($CH_2(CH_3)$), 44.39 ($CH_2(CH_3)$), 117.57 ($C_5(CH_3)_5$), 123.54 (S*Ph*), 129.65 (S*Ph*), 132.70 (S*Ph*), 146.04 (S*Ph*), 157.47(S*Ph*), 181.00 ([(N(Et)*C*(Ph)N(Et)]).

3.5.3 Supporting Syntheses and NMR Experiments

Reduction of 3.4 to 2.8 by NaHg. **3.4** (184.0 mg, 0.4036 mmol) was dissolved 5 mL THF and chilled to -30°C. To this olive-green solution was added 0.5% (w/w) Na/Hg (1.8633 g, 0.40524 mmol Na) and the mixture was allowed to stir for 1 h, warming to room temperature as the solution became dark brown. The solution was

filtered through a pipet with a kimwipe and celite plug and volatiles were removed *in vacuo* to yield a greyish-brown solid, rinsed repeatedly in chilled pentane and confirmed by ^{1}H NMR to be **2.8** (52.7 mg, 31 %).

Reactivity of 2.8 with Me_3SiCl followed by ^{1}H NMR. A mixture of **2.8** (3.3 mg, 3.9 µmol) and durene (1.0 mg, 7.5 µmol) in 1 mL benzene-d_6 was placed in a Teflon© sealed Pyrex© J. Young NMR tube of which an initial ^{1}H NMR was taken. Me_3SiCl (2.0 µL, 16 µmol) was added via micro syringe causing the sample to change rapidly in color from brown to olive within 10 minutes and showing production of comparable amounts of **3.4** and **3.6** along with the consumption of all the **2.8**, observable by ^{1}H NMR. Upon further reaction at room temperature for 2 h, the amount of **3.4** and **3.6** relative to the internal standard was observed to have increased as the **3.8** that had been insoluble initially (and therefore inaccessible) became available for reaction. See Figure 3.2 for corresponding spectra.

Reactivity of 2.5 with Me_3SiCl followed by ^{1}H NMR. **2.5** (5.5 mg, 6.5 µmol) and durene (2.0 mg, 15 µmol) were dissolved in in 0.6 mL benzene-d_6 in a Teflon© sealed Pyrex© J. Young NMR tube to which Me_3SiCl (1.6 µL, 12 µmol) was added via micro syringe. An initial ^{1}H NMR was taken of the orange solution and after being heated at 55 °C for 10 days, **2.5** had been consumed completely to produce diamagnetic **3.6** and paramagnetic **2.7** in the brown solution. See Figure 3.3 for corresponding spectra.

Preparative Scale Reaction of 2.5 with Me_3SiCl. **2.5** (78.5 mg, 93.4 µmol) was dissolved in in 6 mL benzene-d_6 in a heavy walled pressure vessel. Me_3SiCl (36.0 µL, 284 µmol) was added via micro syringe to the dark orange solution which was

heated at 80 °C on an oil bath for 17 h becoming a dark brown. After this, an aliquot was taken for ^{1}H NMR which showed that **2.5** had been consumed to produce diamagnetic **3.6** and paramagnetic **2.3**.

Reactivity of 2.5 with 3.4 followed by ^{1}H NMR. A mixture of **2.5** (3.8 mg, 4.5 µmol) and **3.4** (4.0 mg, 8.8 µmol) was dissolved in in 0.6 mL benzene-d_6 in a Teflon© sealed Pyrex© J. Young NMR tube. An initial ^{1}H NMR was taken and the orange solution was allowed to react at 25 °C over 21 h in which time the solution turned to brown then green and **3.4** was observed by ^{1}H NMR to disappear while **2.8** was produced. Some **2.5** meanwhile, remained observable throughout the reaction. See Figure 3.4 for corresponding spectra.

Preparative Scale Reaction of 2.5 with 3.4. **2.5** (18.5 mg, 22.0 µmol) and **3.4** (20.0 mg, 43.9 µmol) were rinsed into a Teflon© sealed Pyrex© J. Young NMR tube with 1.0 mL benzene-d_6. The golden-brown-orange solution quickly grew dark brown as the products reached saturation in the solution causing crystals and precipitate for form making the mixture sludge-like and unsuitable for NMR. The reaction was allowed to stand for 22 h at 25 °C, then filtered with benzene-d_6 through a pipet with a kimwipe and celite plug to separate the solids from solution. A sample of the filtrate was taken for ^{1}H NMR showing primarily **2.5** and **2.8**, with very slight paramagnetic peaks corresponding to a solid which could not be isolated.

Reactivity of 2.8 with Me_3SiCl followed by ^{1}H NMR in THF-d_8. A mixture of **2.8** (2.8 mg, 3.3 µmol) and durene (0.5 mg, 3.7 µmol) in 0.5 mL THF-d_8 was placed in a Teflon© sealed Pyrex© J. Young NMR tube of which an initial ^{1}H NMR was taken. Me_3SiCl (1.8 µL, 14 µmol) was added via micro syringe and the sample rapidly grew

from dark brown to a vibrant green. After sitting at room temperature for 2h, the solution had changed to a paler green and **3.4** and **3.6** were observable by ^{1}H NMR in even ratios.

Reactivity of 2.5 with Me_3SiCl followed by ^{1}H NMR in THF-d_8. **2.5** (4.9 mg, 5.8 µmol) and durene (1.0 mg, 7.5 µmol) were dissolved in in 0.5 mL THF-d_8 in a Teflon© sealed Pyrex© J. Young NMR tube to which Me_3SiCl (1.6 µL, 12 µmol) was added via micro syringe and the mixture heated at 60 °C on an oil bath and monitored by periodic ^{1}H NMR over 3 d during which time **3.4** was observed to form but there was no evidence of **3.6**, instead only unknown paramagnetic peaks.

Reactivity of 2.8 with excess $(Me_3Si)_2Hg$ followed by ^{1}H NMR. A mixture of **2.8** (2.2 mg, 2.6 µmol) and $(Me_3Si)_2Hg$ (2.4 mg, 6.9 µmol) in 0.6 mL benzene-d_6 was made in a Teflon© sealed Pyrex© J. Young NMR tube and an initial ^{1}H NMR was taken. The solution was heated to 60 °C in an oil bath for 20 h causing silver Hg° to drop out of solution and the conversion of **2.8** to **3.6** was observed. The temperature was increased to 70 °C and the reaction was allowed to continue for another 67 h yielding **3.6** as the major product.

Reactivity of 2.5 with slight excess $(Me_3Si)_2Hg$ followed by ^{1}H NMR. A solution of **2.5** (5.4 mg, 6.4 µmol) and durene (0.8 mg, 0.6 µmol) in 0.6 mL benzene-d_6 was made in a Teflon© sealed Pyrex© J. Young NMR tube with $(Me_3Si)_2Hg$ (5.9 mg, 17 µmol) and an initial ^{1}H NMR was taken. The solution was heated to 60 °C in an oil bath, causing silver Hg^0 to drop out of solution, and ^{1}H NMR taken every 8 h showed the consumption of **2.5** and simultaneous production of **2.8** and **3.6**. After 24 h, the amount of **2.8** had begun to decline in tandem with the continued disappearance of **2.5**,

while **3.6** grew in as the major product. See Figure 3.5 for graph tracking compound growth and decay.

Reactivity of 2.5 with large excess $(Me_3Si)_2Hg$ followed by ^1H NMR. A solution of **2.5** (7.2 mg, 8.6 μmol) and durene (1.0 mg, 7.5 μmol) in 0.5 mL benzene-d_6 was made in a Teflon© sealed Pyrex© J. Young NMR tube with $(Me_3Si)_2Hg$ (36.5 mg, 10.5 μmol) and an initial ^1H NMR was taken once the solution had equilibrated to 60 °C via high temperature NMR. ^1H NMR data was collected every hour, as the solution changed from orange to brown and silver Hg^0 dropped out, and showed the rapid consumption of **2.5** along with production of **2.8** and **3.6**. After 8 h, the amount of **2.8** was slight and continued to decline rapidly in keeping with the increase of **3.6** and the continued decrease of **2.5**. See Figure 3.6 for corresponding spectra and Figure 3.5 for graph tracking compound growth and decay.

Reactivity of 2.8 with MeI followed by ^1H NMR. **2.8** (3.5 mg, 4.2 μmol) was dissolved in in 0.6 mL benzene-d_6 in a Teflon© sealed Pyrex© J. Young NMR tube and an initial ^1H NMR was taken. To this was added MeI (1.0 μL, 17 μmol) and another ^1H NMR was immediately taken, showing even amounts of what is presumed to be **3.13** and **3.14**. While sitting at room temperature, a brown precipitate began to drop out of the yellow solution and the signals for **3.14** in the spectra began to decrease, until after 17 h, a ^1H NMR of the now green solution showed only **3.14** was left. See Figure 3.8 for corresponding spectrum.

Exposure of 2.8 to air followed by ^1H NMR. **2.8** (5.0 mg, 5.9 μmol) was placed in 0.6 mL benzene-d_6 in a Teflon© sealed Pyrex© J. Young NMR tube and an initial ^1H NMR was taken. The cap was removed outside of the glovebox for 5 seconds,

after which it was replaced. While an immediate ^{1}H NMR spectrum showed no significant change, after 2 h at room temperature, messy, new, unidentified products were growing in as the signal for **2.8** decreased.

Reaction of 2.8 with *N,N*-dimethylanilinium tetrakis(pentafluorophenyl) borate followed by ^{1}H NMR. **2.8** (10.0 mg, 12.0 μmol) was placed in 0.6 mL toluene-d_8 in a Teflon© sealed Pyrex© J. Young NMR tube with an internal durene standard (2.0 mg, 15 μmol) and an initial ^{1}H NMR was taken. To this was added *N,N*-dimethylanilinium tetrakis(pentafluorophenyl)borate (9.8 mg, 12.2 μmol) which immediately caused a brown precipitate to crash out of solution and collect at the bottom to the tube. Another ^{1}H NMR spectrum showed no more signals for **2.8** and no other identifiable features.

Reaction of 2.8 with H_2 followed by ^{1}H NMR. **2.8** (6.5 mg, 7.7 μmol) was placed in 0.6 mL benzene-d_6 in a Teflon© sealed Pyrex© J. Young NMR tube and an initial ^{1}H NMR was taken. The tube was charged with 10 psi H_2 and another ^{1}H NMR showed no change. Heating the tube at 65 °C over the course of 7 days resulted in a complex mixture of products of which none could be identified.

Oxidation of 2.8 by CCl_4. A suspension of **2.8** (23.0 mg, 27.4 μmol) was prepared in 10 mL toluene in a 25 mL Schlenk Flask. To this dark brown solution was added CCl_4 (14.0 μL, 144 μmol) via micro syringe causing the color to immediately change to an orange which settled to an olive-gold after stirring for 15 h at room temperature. Solvents were removed *in vacuo*, the reaction mixture was dissolved in toluene and filtered through a pipet with a kimwipe and Celite© plug, and then solvents were removed again to yield a slightly oily golden solid that was recrystallized in

toluene layered with pentane at -30 °C producing olive-golden crystals of **3.4** (21.8 mg, 86% yield).

Reaction of 2.9 with CCl_4. A solution of **2.9** (8.5 mg, 8.4 µmol) was prepared in 0.6 mL benzene-d_6 in a Teflon© sealed Pyrex© J. Young NMR tube to which was added CCl_4 (4.0 µL, 42 µmol) via micro syringe causing the solution to change from brown to yellows out of which beige precipitate began to form. ^{1}H NMR spectra showed not remaining **2.9** and only a complicated mixture of products, none of which are known species.

Reaction of 2.5 with PhSSPh. A solution of **2.5** (11.2 mg, 11.0 µmol) was prepared in 0.6 mL benzene-d_6 in a Teflon© sealed Pyrex© J. Young NMR tube to which was added PhSSPh (2.4 mg, 11.0 µmol) causing an immediate change in color from dark green to olive brown. ^{1}H NMR showed a C_i product judged likely to be **3.17**.

Reaction of 2.6 with PhSSPh. A solution of **2.6** (11.2 mg, 11.0 µmol) was prepared in 0.6 mL benzene-d_6 in a Teflon© sealed Pyrex© J. Young NMR tube to which was added PhSSPh (2.4 mg, 11.0 µmol) causing an immediate change in color from dark green to olive brown. ^{1}H NMR showed a C_i product judged likely to be **3.18**.

Reaction of 2.6 with 2-napthyl disulfide. A solution of **2.6** (10.1 mg, 9.94 µmol) was prepared in 0.6 mL benzene-d_6 in a Teflon© sealed Pyrex© J. Young NMR tube to which was added 2-napthyl disulfide (3.3 mg, 10.4 µmol) causing an immediate change in color from dark green to purple-maroon. ^{1}H NMR showed a C_i product judged likely to be **3.21**.

Reaction of 2.6 with dicyclohexyl disilane. A solution of **2.6** (10.2 mg, 10.0 µmol) was prepared in 0.6 mL benzene-d_6 in a Teflon© sealed Pyrex© J. Young NMR

tube to which was added dicyclohexyl disulfide (2.2 µL, 9.98 µmol). Reaction over 20 h at room temperature caused the solution to change from dark green to brown in color and a ^{1}H NMR showed around half the **2.6** remained while rest had converted to a new *C$_i$* product thought to be **3.22**.

Reaction of 2.6 with ditertbutyl disilane. A solution of **2.6** (10.0 mg, 9.84 µmol) was prepared in 0.6 mL benzene-*d$_6$* in a Teflon© sealed Pyrex© J. Young NMR tube to which was added ditertbutyl disulfide (1.9 µL, 9.83 µmol). Sitting for 20 h at room temperature had no effect on the mixture as judged by ^{1}H NMR and it remained a dark green in color, but heating at 65 °C for 45 h consumed all the starting **2.6** and produced a *C$_i$* product, likely **3.23**.

Reaction of 3.18 with PhSSPh. A solution of **3.18** (2.0 mg, 1.6 µmol) was prepared in 0.6 mL benzene-*d$_6$* in a Teflon© sealed Pyrex© J. Young NMR tube to which was added a large excess of PhSSPh (2.0 µL, 9.2 µmol). This mixture was stable for 19 h at room temperature, but upon heating at 65 °C for 42 h, converted completely to what is believed to be **3.24**.

Reaction of 2.8 with PhSSPh. A solution of **2.8** (6.5 mg, 7.7 µmol) was prepared in 0.6 mL benzene-*d$_6$* in a Teflon© sealed Pyrex© J. Young NMR tube to which was added PhSSPh (2.3 mg, 11 µmol) causing the solution to change immediately from dark brown to a kaki while feathery precipitate formed. The precipitate was dried *in vacuo* and identified as **3.25**.

Reaction of 2.9 with PhSSPh. A solution of **2.9** (29.5 mg, 29.0 µmol) was prepared in 0.6 mL benzene-*d$_6$* in a Teflon© sealed Pyrex© J. Young NMR tube to which was added PhSSPh (6.5 mg, 29.8 µmol) causing an immediate change in color from

dark brown to orange while a complex mixture of unknown products appeared by ^{1}H NMR after sitting at room temperature 18 h. After heating at 55 °C for 18 h, ^{1}H NMR showed a C_i product judged likely to be **2.26**.

References

1. Laplaza, C. E.; Cummins, C. C. Dintrogen Cleavage by a 3-Coordinate Molybdenum(III) Complex. *Science* **1995,** *268*, 861-863.
2. Curley, J. J.; Sceats, E. L.; Cummins, C. C. A Cycle for Organic Nitrile Synthesis via Dinitrogen Cleavage. *J. Am. Chem. Soc.* **2006,** *128*, 14036-14037.
3. MacLeod, K. C.; Holland, P. L. Recent Developments in Homogeneous Dinitrogen Reduction by Molybdenum and Iron. *Nat. Chem.* **2013,** *5*, 559-565.
4. Nishibayashi, Y. E. *Topics in Organometallic Chemistry*. Springer Verlag: Berlin/Heidelberg, 2017; Vol. 60.
5. Buss, J. A.; Cheng, C.; Agapie, T. A Low-Valent Molybdenum Nitride Complex: Reduction Promotes Carbonylation Chemistry. *Angew. Chem. Int. Ed.* **2018,** *57*, 9670-9674.
6. Y., R.; Duboc, C.; Gennari M. Molecular Catalysts for N_2 Reduction :State of the Art, Mechanism, and Challenges. *Chem. Phys. Chem.* **2017,** *18*, 2606-2617.
7. Stucke, N.; Flöser, B. M.; Weirich, T.; Tuczek, F. Nitrogen Fixation Catalyzed by Transition Metal Complexes: Recent Developments. *Eur. J. Inorg. Chem.* **2018**, 1337–1355.
8. Liao, Q.; Cavaillé, A.; Saffon-Merceron, N.; Mézailles, N. Direct Synthesis of Silylamine from N_2 and a Silane Mediated by a Tridentate Phosphine Molybdenum Fragment. *Angew. Chem. Int. Ed.* **2016,** *55*, 11212-11216.
9. Shaver, M. P.; Fryzuk, M. D. Activation of molecular nitrogen: Coordination, cleavage and functionalization of N_2 mediated by metal complexes. *Adv. Synth. Catal.* **2003,** *345*, 1061-1076.
10. Gade, L. H.; P., M. New transition metal imido chemistry withdiamido-donor ligands. *Coord. Chem. Rev.* **2001,** *216-217*, 65–97.
11. Bezdek, M. J.; Chirik, P. J. Interconversion of Molybdenum Imido and Amido Complexes by Proton-Coupled Electron Transfer. *Angew. Chem. Int. Ed.* **2018,** *57*, 2224-2228.
12. Ishii, Y.; Tokunaga, S.; Seino, H.; Hidai, M. Synthesis of Tungsten (1-Pyridinio)imido Complexes: Facile N-N Bond Cleavage To Form Pyridine from Coordinated Dinitrogen. *Inorg. Chem.* **1996,** *35*, 5118-5119.
13. Dreher, A.; Meyer, S.; Näther, C.; Westphal, A.; Broda, H.; Sarkar, B.; Kiam, W.; Kurz, P.; Tuczek, F. Reduction and Protonation of Mo(IV) Imido Complexes with depe Coligands: Generation and Reactivity of a S = 1/2 Mo(III) Alkylnitrene Intermediate. *Inrog. Chem.* **2013,** *52*, 2335-2352.
14. Chatt, J.; Dilworth, J. R.; Richards, R. L. Recent advances in the chemistry of nitrogen fixation. *Chem. Rev.* **1978,** *78*, 589-625.

15. Stephan, G. C.; Sivasankar, C.; Studt, F.; Tuczek, F. Energetics and Mechanism of Ammonia Synthesis through the Chatt Cycle: Conditions for a Catalytic Mode and Comparison with the Schrock Cycle. *Chem. Eur. J.* **2007,** *14*, 644-652.
16. Chatt, J.; Pearman, A. J.; Richards, R. L. The reduction of mono-coordinated molecular nitrogen to ammonia in a protic environment. *Nature* **1975,** *253*, 39-40.
17. Alias, Y.; Ibrahim, S. K.; Queiros, M. A.; Fonseca, A.; Talarmin, J.; Volant, F.; Pickett, C. J. Electrochemistry of molybdenum imides: cleavage of molybdenum–nitrogen triple bonds to release ammonia or amines. *J. Chem. Soc. Dalton. Trans.* **1997,** *26*, 4807-4815.
18. Yandulov, R. R.; Schrock, R. R. Catalytic Reduction of Dinitrogen to Ammonia at a Single Molybdenum Center. *Science* **2003,** *301*, 67-78.
19. Suess, D. L. M.; Peters, J. C., H–H and Si–H Bond Addition to Fe≡NNR$_2$ Intermediates Derived from N$_2$. *J. Am. Chem. Soc.* **2013,** *135*, 4938-4941.
20. Klopsch, I.; Finger, M.; Wurtele, C.; Milde, B.; Werz, D. B.; Schneider, S. Dinitrogen Splitting and Functionalization in the Coordination Sphere of Rhenium. *J. Am. Chem. Soc.* **2014,** *136*, 6881-6883.
21. MacLeod, K. C.; McWilliams, S. F.; Mercado, B. Q.; Holland, P. L. Stepwise N-H bond formation from N2-derived iron nitride, imide and amide intermediates to ammonia. *Chem. Sci.* **2016,** *7*, 5736-5746.
22. Keane, A. J.; Farrell, W. S.; Yonke, B. L.; Zavalij, P. Y.; Sita, L. R. Metal-Mediated Production of Isocyanates, R$_3$EN=C=O from Dinitrogen, Carbon Dioxide, and R$_3$ECl. *Angew. Chem. Int. Ed.* **2015,** *54*, 10220-10224.
23. Yonke, B. L.; Reeds, J. P.; Fontaine, P. P.; Zavalij, P. Y.; Sita, L. R. Catalytic Production of Isocyanates via Orthogonal Atom and Group Transfers Employing a Shared Formal Group 6 M(II)/M(IV) Redox Cycle. *Organometallics* **2014,** *33*, 3239-3242.
24. Keane, A. J. Early Transition Metal Sutdies of Dintirogen Cleavage and Metal-Nitrogen Bond Reactivity towards catalytic N$_2$ Fixation. Ph.D. Dissertation, *University of Maryland*, College Park, MD, **2015**.
25. Duman, L. M.; Farrell, W. S.; Zavalij, P. Y.; Sita, L. R. Steric Switching from Photochemical to Thermal Reaction Pathways for Enhanced Efficiency in Metal-Mediated Nitrogen Fixation. *J. Am. Chem. Soc.* **2016,** *138*, 14856-14859.
26. Yonke, B. L.; Reeds, J. P.; Zavalij, P. Y.; Sita, L. R. Atom- and Group Transfers to M^{IV} Oxo and Imido Complexes, (η^5-C$_5$Me$_5$)M[N(*i*Pr)C(Me)N(*i*Pr)](E) (M = Mo, W; E = O, NSiMe$_3$): Orthogonal Generation of a M^{VI} Terminal Nitride via Inter-ligand Silyl Group Migration. *Z. Anorg. Allg. Chem.* **2014,** *641*, 61 - 64.
27. Duman, L. M.; Zavalij, P. Y.; Sita, L. R. An Intramolecular Mechanism for N$_2$ Cleavage in Dinuclear Mo and W CPAM/CPGU Complexes. *J. Am. Chem. Soc.* **2018,** *In Preperation*.
28. Connelly, N. G.; Gieger, W. E. Chemical Redox Agents for Organometallic Chemistry. *Chem. Rev.* **1996,** *96*, 877-910.
29. Eaborn, C.; Jackson, R. A.; Walsingham, R. W. Organosilicon compounds. Part XLI. The reaction of bis(trimethylsilyl)mercury with some ethers. *J. Chem. Soc. C.* **1967,** *0*, 2188-2191

30. Blayney, M. B.; Winn, J. S.; Nierenberg, D. W. Handling dimethylmercury. *Chemical and Engineering News* **1997**.
31. Fontaine, P. P.; Yonke, B. L.; Zavalij, P. Y.; Sita, L. R. Dinitrogen Complexation and Extent of N≡N Activation within the Group 6 "End-On-Bridged" Dinuclear Complexes, $\{(\eta^5\text{-}C_5Me_5)M\ N(i\text{-}Pr)C(Me)N(i\text{-}Pr)\}_2(\mu\text{-}\eta^1\text{:}\eta^1\text{-}N_2)$ (M = Mo and W). *J. Am. Chem. Soc.* **2010,** *132*, 12273-12285.
32. Tarkhanova, I. G.; Gantman, M. G.; Chizhov, A. O.; Smirnov, V. V. Addition of tetrachloromethane to oct-1-ene initiated by amino alcohols. *Russ. Chem. Bull., Int. Ed.* **2006,** *55*, 1624-1630.
33. Saeki, A.; Yamamoto, N.; Yoshida, Y.; Kozawa, T., Geminate Charge Recombination in Liquid Alkane with Concentrated CCl_4: Effects of CCl_4 Radical Anion and Narrowing of Initial Distribution of Cl-. *J. Phys. Chem. A.* **2011,** *115*, 10166-10173.
34. Nair, R. P.; Kim, T. H.; Frost, B. J., Atom Transfer Radical Addition Reactions of CCl_4, $CHCl_3$, and p-Tosyl Chloride Catalyzed by Cp′Ru(PPh_3)(PR_3)Cl Complexes. **2009,** *28*, 4681-4688.
35. Zanella, R.; Ros, R.; Grazian, M. Sulfur-sulfur bond cleavage promoted by palladium(0) and Platinum(0) triphenylphosphine complexes. *Inorg. Chem.* **1973,** *12*, 2736-2738.
36. Blower, P. J.; Dilworth, J. R. Thioalto-Complexes of the Transition Metals. *Coord. Chem. Rev.* **1987,** *76*, 121-185.
37. Hossain, M. M.; Lin, H.-M.; Zhu, J.; Lin, Z.; Shyu, S.-G. Activation of the S-S Bonds of Alkyl Disulfides RSSR (R) Me, Et, Pr, Bun) by Heterodinuclear Phosphido-Bridged $CpW(CO)_2(\mu\text{-}PPh_2)Mo(CO)_5$. *Organometallics* **2006,** *25*, 440-446.
38. Aubart, M. A.; Bergman, R. G. Reaction of Organic Disulfides with Cobalt-Centered Metal Radicals. Use of the E- and C-Based Dual-Parameter Substituent Model and Quantitative Solvent Effect Analyses To Compare Outer-Sphere and Inner-Sphere Electron-Transfer Processes. *J. Am. Chem. Soc.* **1998,** *120*, 8755-8766.
39. Eaborn, C.; Jackson, R. A.; Walsingham, R. Organosilicon compounds. Part XLI. The reaction of bis(trimethylsilyl)mercury with some ethers. **1967,** *0*, 2188-2191.

Chapter 4: Closing the Cycle by Release of an N-atom Product, $HN(SiMe_3)_2$

4.1 Silylamine Products of Dinitrogen Fixation

Having now illustrated several routes to incorporate a TMS group to make a terminal silylimido **3.6** containing a fixed N atom via either **2.5** or **2.8**, the final challenge remaining in completing a chemical or catalytic cycle is *the release of an N-containing moiety from the metal center*. The specific identity of value-added N-containing products from dinitrogen fixation by group 6 metals runs the gamut, from hydrazine (N_2H_4) and ammonia (NH_3) to nitriles (RCN) and carbodiimides (RNCNR), naming just a few.[1-5] The products most relevant to the sterically reduced CPAM cycle under construction within this thesis, however, are the known production of a TMS isocyanate ($OCNSiMe_3$) by the bulkier CPAM system[6] and the well-established production of silylamines, mainly tris(trimethylsilyl)amine ($N(SiMe_3)_3$), from the reductive silylation of varied organometallic complexes with a reducing agent, such as Na, and excess Me_3SiCl in lieu of protons.[7-35] Nishibayashi has recently accomplished Mo-catalyzed N_2 fixation under ambient conditions forming $N(SiMe_3)_3$ at the impressive turnover number of 226.[16] This product is especially valuable in that upon acid workup, it can easily be converted to ammonium chloride (NH_4Cl) making it analogous pathway to the formation of NH_3.[36] Intriguingly, the early reports of synthetic $N(SiMe_3)_3$ production actually predate the first NH_3 fixation methods.[7, 8] Silylated amines are therefore as desirable, if an alternative, target of dinitrogen fixation as is ammonia itself, with the ability to be converted to ammonia or to be used in their own industrial applications.

Scheme 4.1

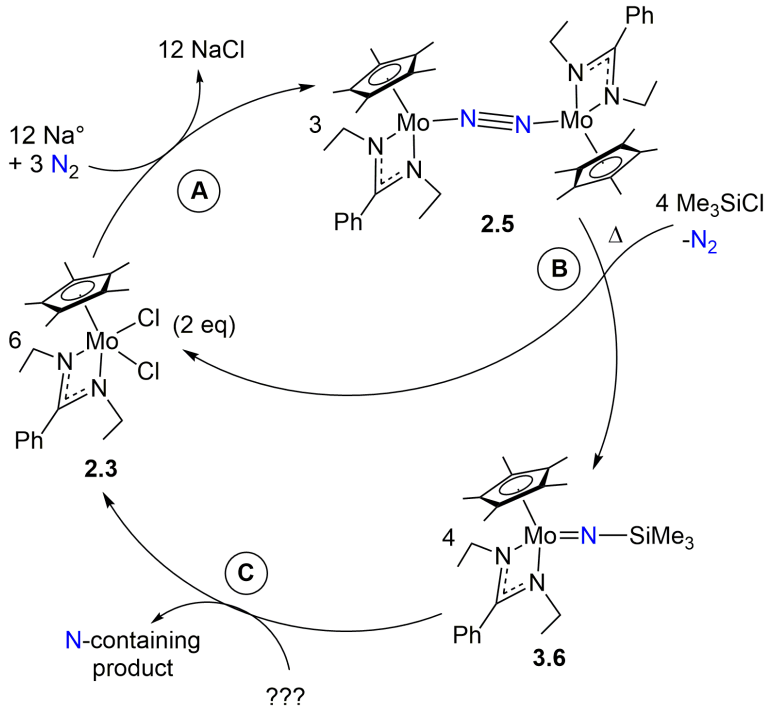

Ideally for the sterically reduced CPAM system so far described, illustrated in Scheme 4.1 (Step A, dinitrogen reduction and coordination and Step B, dinitrogen cleavage and functionalization), the final stage of the cycle (Step C) would be a process that, in addition to releasing an N-containing product from the Mo(IV) center of **3.6**, would also regenerate the Mo(IV) dichloride **2.3** from which the cycle may be repeated.

4.2 Silylamine Formation by the CPAM System

4.2.1 Targeted $H_2N(SiMe_3)$ Release

Several straightforward approaches to accomplishing this step and releasing a value-added product are illustrated in Scheme 4.2. The first would be the treatment of **3.6** with anhydrous HCl which stoichiometrically should yield an equivalent each of **2.3**, Me_3SiCl, and (upon *in situ* acidolysis of the initially formed TMS amine (H_2NSiMe_3)), H_4NCl. An alternate route could be a metathetical exchange between **3.6** and H_2O that would provide H_2NSiMe_3 and a terminal oxo species,

Scheme 4.2

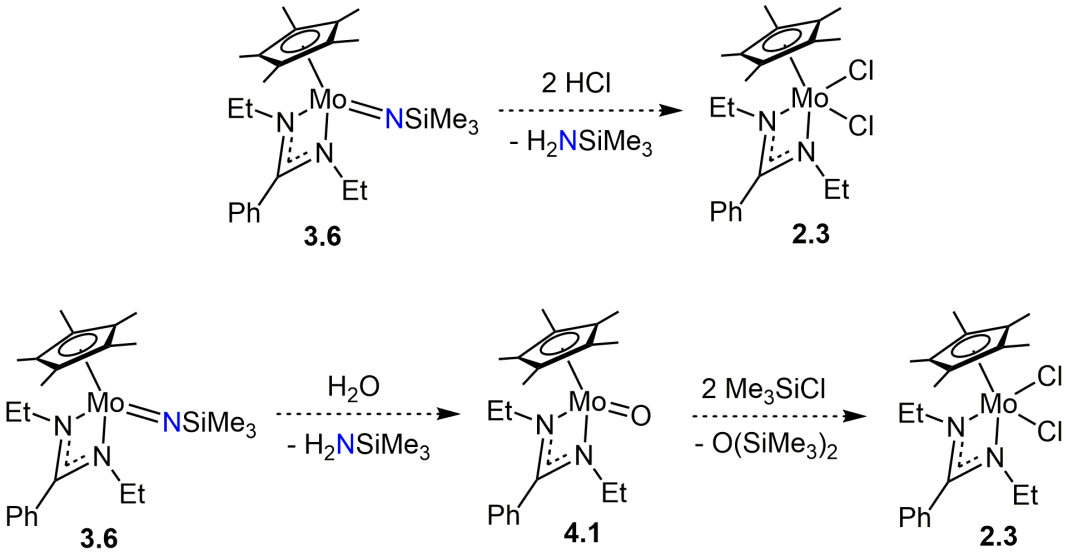

{Cp*[N(Et)C(Ph)N(Et)]Mo(O)} (**4.1**),[37-39] that could be recycled back to **2.3** upon treatment with Me_3SiCl to release hexamethydisiloxane[6] according to Scheme 4.2. Despite the attractiveness of these theoretical reaction pathways, in practice **3.6** proves to be very moisture sensitive, and the introduction of even trace amounts of H_2O in polar (THF) or nonpolar (benzene) solvent led to a complex mixture of unidentifiable products with no amine observed by ^1H NMR. Furthermore, because HCl and H_2O are unlikely to be compatible with the other reagents and complexes involved in a nitrogen fixation cycle supported by the CPAM framework (f*or instance, See Chapter 3 for incompatibility of **2.8** with air, moisture, and acid*), an alternate route was sought out to accomplish these goals.

A different, potentially milder route would be to employ an alcohol (ROH) as a proton source. Upon the addition of two equivalents of alcohol to **3.6**, a Mo(IV) bisalkoxide {Cp*[N(Et)C(Ph)N(Et)]Mo$(OR)_2$} (**4.2**) could be predicted to form in tandem with the release of the TMS amine organic product. Further reaction with

Scheme 4.3

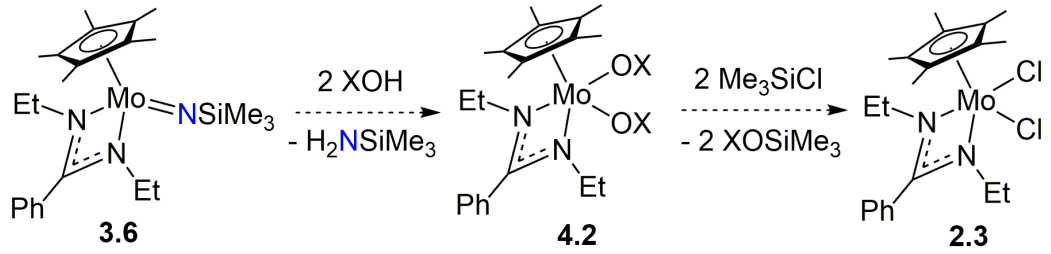

Me_3SiCl through metathesis could regenerate **2.3** and release a TMS ether, $ROSiMe_3$), as is shown in Scheme 4.3. Surprisingly, unlike exposure to H_2O, when a benzene-d_6 solution of **3.6** was observed by ^1H NMR it appeared to be to be unreactive to the addition of excess iPrOH after an extended period of time. In order to facilitate reaction, pinacol (2,3-dimethyl-2,3-butadiol) was employed in an attempt to form a cyclic bisalkoxide through chelation control.[40, 41] Again, however, a benzene-d_6 solution of **3.6** appeared unreactive to the diol when allowed to react over two days. As an alternative to an alcohol, trimethylsilanol (Me_3SiOH) was used next because triorganosilanols are more acidic than alcohols[42] and might therefore facilitate the desired reaction. Like the previous reactions, however, a benxene-d_6 solution of **3.6** was not observed by ^1H NMR to react when an excess of Me_3SiOH was added. Finally, upon the addition of excess phenol (PhOH) to a benxene-d_6 solution of **3.6**, a reaction did quickly take place, however it was the undesirable decomposition of **3.6** into an unidentifiable mixture of diamagnetic and paramagnetic products. That **3.6** appears not to react deleteriously in the presence of iPrOH, pinacol, and Me_3SiOH but does so when exposed to PhOH indicates that, though high, there may be an acidity wall to the uncontrolled reaction of **3.6** with protic reagents.

4.2.2 Observed $HN(SiMe_3)_2$ Release

With no seeming luck in the use of alcohols and silanols as protic reagents with **3.6**, the replication of the simultaneous oxygen-atom and nitrene-group transfer to produce TMS isocyanate, which proved successful in the case of the more sterically bulky CPAM ligand set (shown in Scheme 1.8),[6] was therefore attempted as is depicted in Scheme 4.4. In theory, this would consist of the reaction of **3.6** with CO_2 and Me_3SiCl. **3.6** is known not to react with an excess of Me_3SiCl, and when a benzene-d_6 mixture of the two was charged with CO_2, the expected hexamethydisiloxane ($O(SiMe_3)_2$) byproduct was immediately observed to grow in by ^{1}H NMR, δ = 0.12 ppm, as was paramagnetic **2.3**. However, even after extended periods of time, there was no evidence of the formation of the targeted isocyanate $OCNSiMe_3$ which would have appeared at δ = -0.14 ppm following the reactivity laid out in Scheme 4.4. Instead, a new, unfamiliar signal appeared as an upfield singlet in the ^{1}H NMR spectrum at δ = 0.10 ppm. This new peak was successfully identified as bis(trimethylsilyl)amine ($HN(SiMe_3)_2$) by spiking the reaction mixture with an authentic sample of the silylamine. Though metal-amides derived from $HN(SiMe_3)_2$ are known,[43, 44] and indeed, $HN(SiMe_3)_2$ has often been reported as a minor product of reductive silylation of dinitrogen, the reason for its presence (and seeming purity) in this reaction was not immediately apparent.

After this intriguing initial result, the experiment was repeated; however, on each subsequent attempt the reaction proceeded more and more slowly. It is likely that this inconsistency can be explained with the observation that in order for $HN(SiMe_3)_2$ to form, a proton must have been acquired from some source not previously accounted

for or present in the reaction of Scheme 4.4. It was therefore hypothesized that the manifold used to charge the reaction vessels with CO_2 gas could potentially have had residual moisture or some other proton-containing contaminant in it which, instead of resulting in the decomposition of **3.6**, fortuitously causing a new reaction by forming Me_3SiOH in situ which in turn reacted with **3.6** and Me_3SiCl.[45]

Scheme 4.4

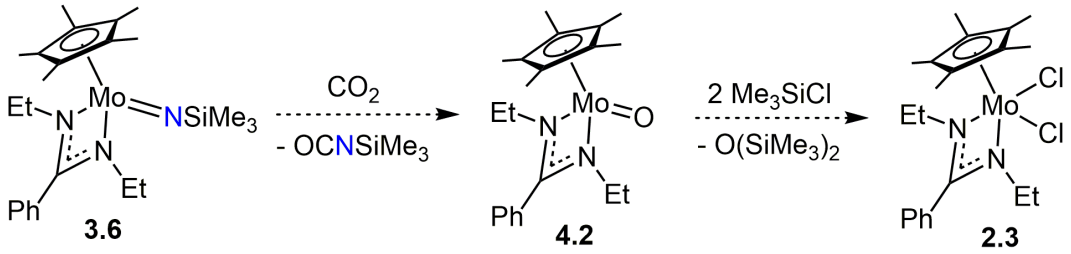

If such a hydrolysis were to be the mechanism of releasing the amine from the Mo center,[38] it was reasoned that this serendipitous reactivity from the manifold might be effectively emulated by adding one equivalent of commercially available Me_3SiOH to a mixture of **3.6** and Me_3SiCl in the absence of a moisture contaminate – a so-called "dry hydrolysis". Indeed, as is shown in Scheme 4.5, in the presence of Me_3SiOH with two equivalents of Me_3SiCl, **3.6** began to immediately convert to **2.3** while the expected organic products of the controlled hydrolysis, $O(SiMe_3)_2$ and $HN(SiMe_3)_2$, began to appear according to ^1H NMR, illustrated in Figure 4.1. The reaction was judged to have

Scheme 4.5

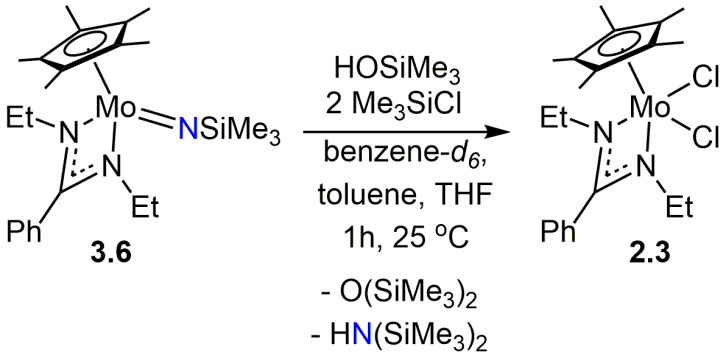

successfully run to completion upon the total consumption of **3.6** after 16 h at room temperature. Though the paramagnetic nature of the metal-product **2.3** makes it difficult to gauge the yield of the reaction spectroscopically, in comparison to an internal durene standard, the organic products are judged to form quantitively. By running the reaction on a preparative scale, 94% of the metal was recovered as **2.3** once volatiles were removed. By running the reaction in pentane (in which the dichloride **2.3**

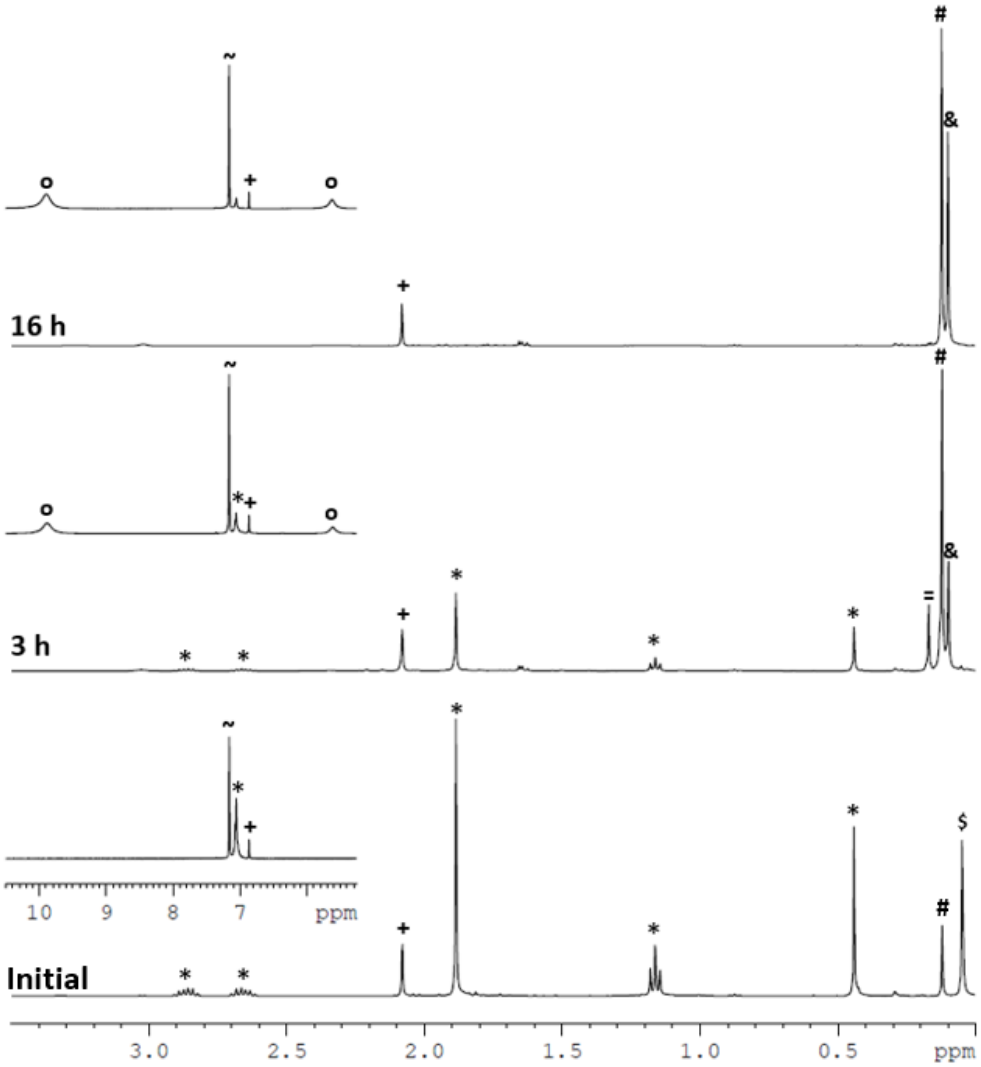

Figure 4.1. Partial ^{1}H NMR (400 MHz, C_6D_6, 25 °C) demonstrating the conversion of **3.6** (*****) and Me_3SiOH (**$**) (bottom spectrum, stable after 17 h), to **2.3** (**o**), $(Me_3Si)_2O$ (#), and $(Me_3Si)_2NH$ (**&**) upon the addition of Me_3SiCl (=) (middle and top spectra) at 25 °C with durene (+) standard in benzene-*d*$_6$ (~)

is insoluble and therefore crashes out of solution immediately upon its formation, leaving the solution free of any metal species), the reaction solution containing the organic products was subjected to Gas Chromatography - Mass Spectrometry (GC-MS), illustrated in Figure 4.2, which corroborated the identities of the organic products.

Upon further investigation of this reaction, it became apparent that the dry hydrolysis it is quite versatile with regards to the identity of the proton source, XOH,

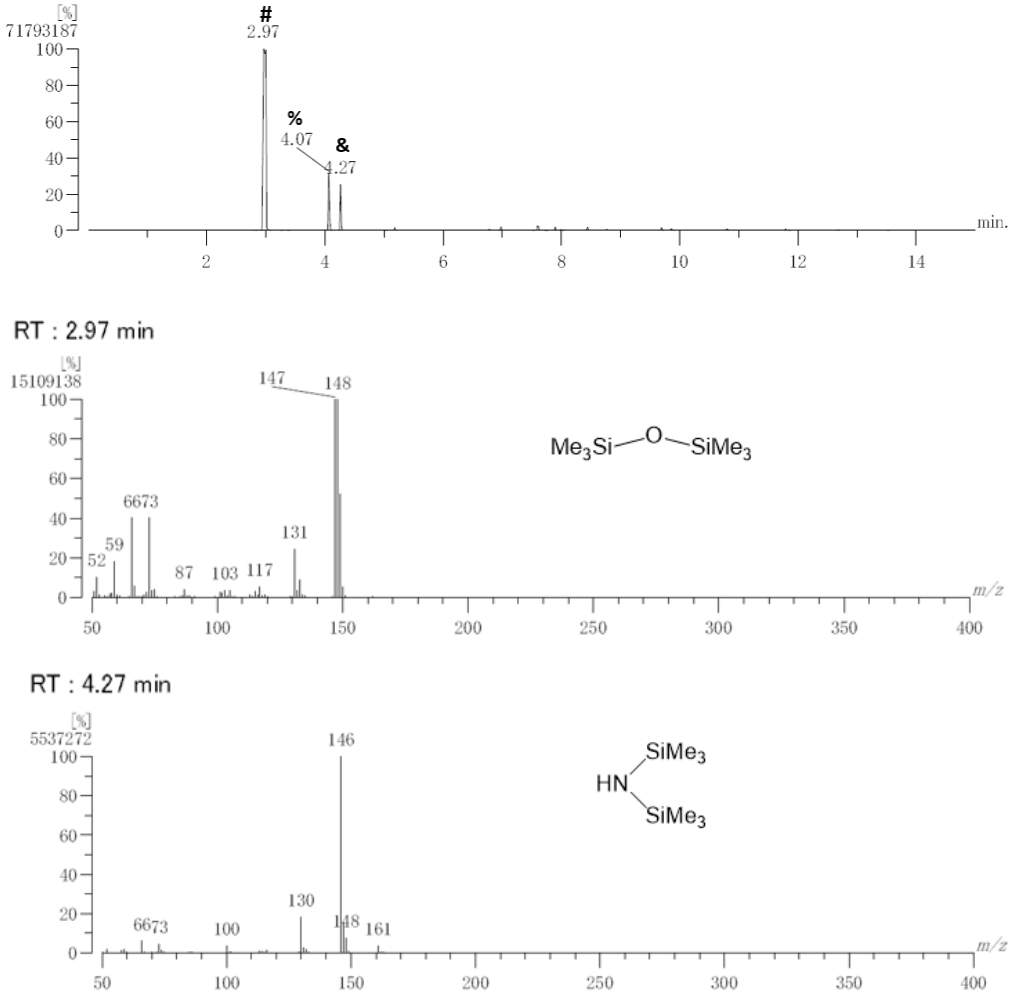

Figure 4.2. (Top) Chromatograph of pentane solution from the reaction of **3.6** with Me_3SiOH and Me_3SiCl at 25 °C to produce **2.3**, $(Me_3Si)_2O$ (#) at 2.97 min, and $(Me_3Si)_2NH$ (**&**) at 4.27 min. Slight toluene **(%)** impurity noted at 4.07 min. (Bottom) Mass spectra for $(Me_3Si)_2O$ (retention time 2.97 min) and $(Me_3Si)_2NH$ (retention time 4.27 min)

that can successfully be employed to drive the process forward. Far from being limited $HOSiMe_3$, the dry hydrolysis will proceed unimpeded by the use of the bulkier X = $SiEt_3$ and $SiPh_3$.[46] Silanols, unfortunately, tend to be prone to decomposition; any trace moisture can catalyze the formation of the related silyl ether and water[45] which were noticed as an impurity in the reagents that increased over time. It was gratifying, then, to discover that alcohols were also appropriate protic sources (X = iPr, tBu, and even Ph) because of their ready accessibility and stability as reagents. It important to note that in all cases, steric bulk of the silanols and alcohols did not seem to have an effect on the speed or yield of the reaction, changing only the identity of the ether product from hexamethyldisiloxane, $O(SiMe_3)_2$, to $XOSiMe_3$ as confirmed by ^1H NMR and GC-MS analysis which may be found in Section 4.5.

In one last surprise, it was discovered that even dehydrated silica gel (SiO_2) served to facilitate the dry hydrolysis reaction. Though thoroughly dried in an oven at 150 °C and stored under an inert glovebox atmosphere, the SiO_2 is presumed to contain some silanol groups that allow the reaction to proceed.[45] Practically, there are a number of advantages to the idea of using silica gel – it is easily replaceable and could be packaged in a column through which the reaction could run, making it of potential industrial interest. While attempting to collect **2.3** after running a THF solution of it through a small silica gel plug in a pipet, very little was recovered. However, a non-destructive pathway was discovered when the THF solution of **2.3** also contained excess Me_3SiCl. In this case, **2.3** was recoverable in 93% yield[46] indicating that the Me_3SiCl may act as a silylating agent on the silica gel[47, 48] which allows the metal species to travel through the $SiO_2/SiOSiMe_3$ column. Altogether, **2.3** could be

recovered from a silica gel-based dry hydrolysis reaction of **3.6** on a preparatory scale in 80% yield. While it is remarkable that so many proton sources are applicable for this dry hydrolysis, its mechanism required much more study to elucidate.

4.3 Mechanistic Details of "Dry Hydrolysis" Reaction

Though the dry hydrolysis of **3.6** with XOH and Me_3SiCl occurs nearly instantaneously as is depicted in Scheme 4.5, it is proposed to proceed through three distinct steps that are illustrated in Scheme 4.6: Step I is an initial association of XOH with **3.6**, followed quickly by Steps II and III; Me_3SiCl addition and product release.

4.3.1 Step I: Low Temperature ^1H NMR Studies and Signal "Marching"

As was noted at length in Section 4.2.1, it was initially observed that a mixture of **3.6** and various XOH proton sources appeared unreactive for extended periods of time, either at room temperature or elevated temperature. However, immediately upon the addition of Me_3SiCl to such a mixture, the dry hydrolysis reaction proceeds to

Scheme 4.6

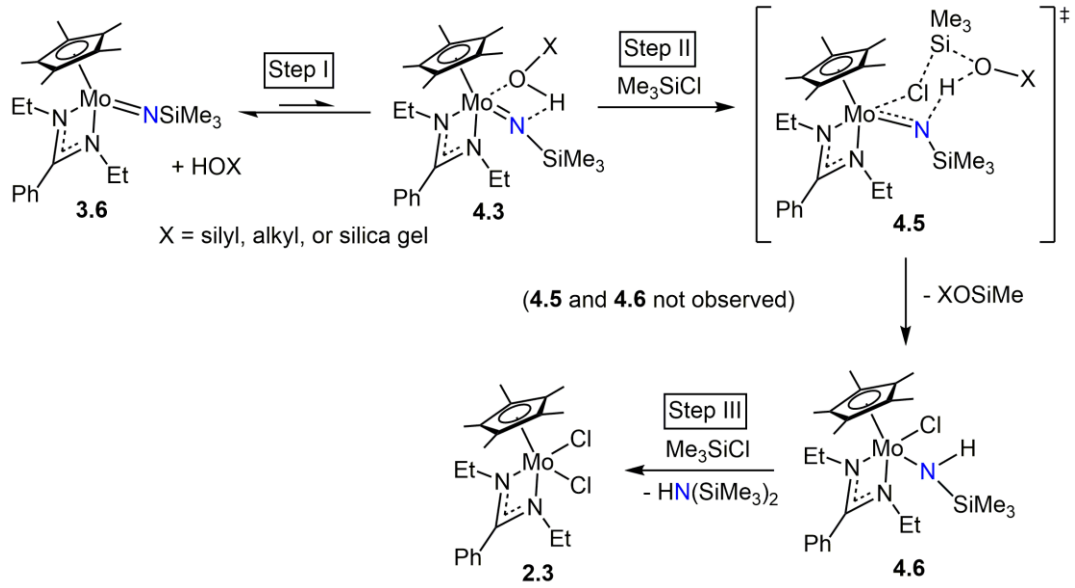

completion. It is proposed therefore that in Step I, prior to the addition of Me_3SiCl, the proton source and **3.6** form a 1 : 1 adduct between the Lewis Basic N-atom of the terminal imido[49] and Hydrogen-bond of XOH according to Scheme 4.6. This 1 : 1 association product of **3.6** and XOH, {Cp*[N(Et)C(Ph)N(Et)]Mo(N(H)$SiMe_3$)(X)} (**4.3**), has not been isolated due to its transient nature and cannot be observed spectroscopically at room temperature. However, the existence of **4.3** is supported by extensive low temperature ^{1}H NMR studies, shown in Figure 4.3, that indicate the presence of an equilibrium in the solution mixture of **3.6** and XOH (X = $SiMe_3$, iPr, tBu).[46]

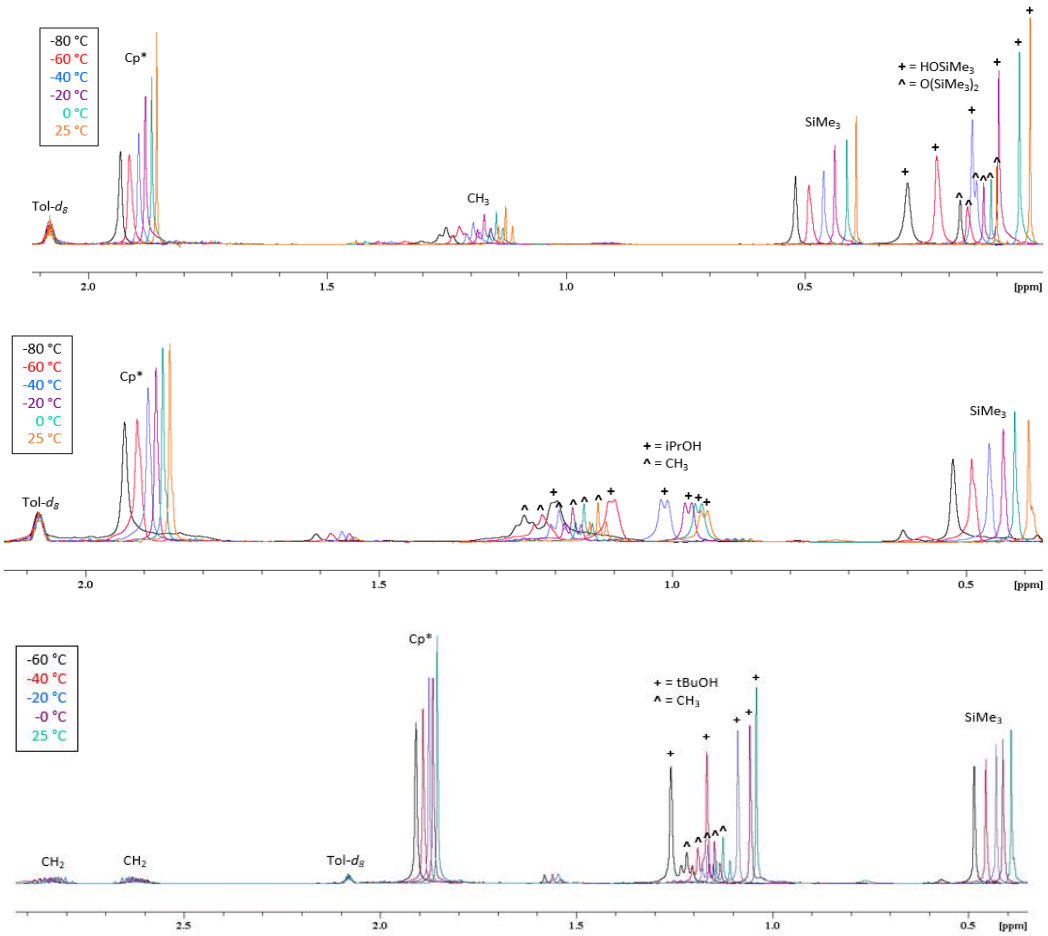

Figure 4.3. Partial ^{1}H NMR (500 MHz, C_7D_8) of **3.6** and (top) Me_3SiOH at temperatures ranging from -80 to 25 °C, (middle) iPrOH at temperatures ranging from -80 to 25 °C, or (bottom) tBuOH at temperatures ranging from -60 to 25 °C

In these experiments, toluene-d_8 solutions of **3.6** were prepared with an equal amount of XOH and the mixtures were cooled down to -80 or -60 °C in a pre-cooled and calibrated NMR. An initial ^{1}H NMR showed that the chemical shifts for the cooled mixture were much more downfield than those known for the mixture at room temperature. Spectra were taken as the temperature was increased by increments of 20 °C, allowing for temperature calibration and sample equilibration between each ^{1}H NMR collection. As the solution was allowed to warm slowly back towards 25 °C, the chemical shifts also began to move upfield until they were identical to the "unreacted" mixtures of **3.6** and XOH previously observed.

While temperature can account for some slight change in chemical shift, the extent of the downfield movement was more substantial than to be attributed to the temperature difference alone. This is substantiated by control experiments of **3.6** alone and the proton sources alone at low temperatures which reveal that the shifting peaks are *not* the result solely of the change in temperature but are in fact the result of the lower temperature favoring the formation of H-bonds.[50, 51] For instance, at 25 °C both free iPrOH and the mixture of **3.6** and iPrOH have a doublet for the methyl peaks which comes in at a chemical shift of δ = 0.94 ppm. At -80 °C, both are significantly

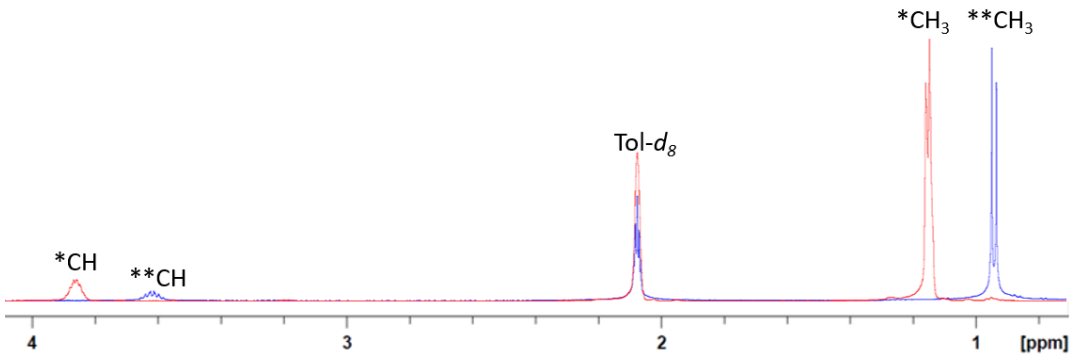

Figure 4.4: Partial ^{1}H NMR (500 MHz, C_7D_8) of iPrOH at 25 °C (blue, **) and -80 °C (red, *) showing the change in chemical shift due to temperature alone

more deshielded, but the free alcohol comes in at δ = 1.15 ppm while the corresponding methyl peaks of the **3.6** and iPrOH mixture come in at δ = 1.20 ppm, as shown in Figure 4.4. That these shifts are different at the same lower temperature is indicative of different chemical environments. As the changing temperature favors different ratios of free **3.6** and XOH vs the adduct **4.3**, the average chemical environment of the sample changes. In turn, the signal representing that average chemical environment (fast exchange and weak binding) moves accordingly in a phenomenon known as "marching".[52] At room temperature, the equilibrium favors the free, unassociated **3.6** and XOH and so these two species make up the vast majority of the solution and are seen cleanly in the ^{1}H NMR spectrum. At lower temperature, however, the equilibrium shifts to favor the association product **4.3**, for which the ^{1}H NMR signals are quite different – generally more deshielded – and so as the temperature drops, a greater ratio of **4.3** is present in the sample and the ^{1}H NMR spectra (which is a representation of the time average of the sample's composition) more closely resembles what an isolated sample of **4.3** would look like.

Finally, though these studies do indicate that there is an equilibrium at play, they do not rule out the possibility of a different reversible addition, such as the formation of a Mo(IV) alkoxy amido complex, {Cp*[N(Et)C(Ph)N(Et)]Mo(OR)(N(H)SiMe$_3$)(X)} (**4.4**), shown in Figure 4.5. However, several observations favor the proposal that the product more resembles the resonance hybrid **4.3** than it does **4.4**. As was noted above, **3.6** was found to engage in

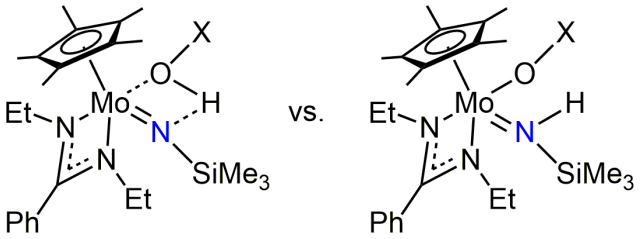

4.3 **4.4**

Figure 4.5. Potential structures of the product of addition of XOH to **3.6**

the same reversible process with silanols and alcohols alike (Me_3SiOH, iPrOH, and tBuOH (not illustrated) and did not seem to be affected by the steric bulk of the protic reagent – **4.3** is anticipated to have less sensitivity towards the steric bulk and electronic features of the X group than **4.4** would. Additionally, once formed, a new Mo-O bond would be expected to be stable and not necessarily engage in a reversible reaction, while a hydrogen bond is much more likely to be dynamic. There also appears to be no prescient for either the forward addition of RO-H across a Mo=N bond in a metal imido or for the formal reverse reaction. For these reasons, the 1 : 1 adduct, **4.3**, with N-atom acting as Hydrogen-bond acceptor, seems the most likely structure.

4.3.2 Step I: Variable Concentration ^{1}H NMR Studies and Equilibrium Constant

In an effort to quantify the relationship between free **3.6** with free XOH and the adduct **4.3**, a concentration study was designed with ^{1}H NMR experiments to obtain an equilibrium constant, K_{eq}. Just as lower temperatures favor the right side of the equilibrium shown in Step I of Scheme 4.6, according to Le Chatelier's Principle, increasing the amount of the **3.6** and XOH reagents should also increase formation of the association product, **4.3**. Therefore, a 0.1 M stock solution of **3.6** and iPrOH in toluene-d_8 was prepared in a 1.00 mL volumetric flask and serial dilutions were carried

out to create solutions at 0.01 M, 0.001 M, and 0.0001 M concentrations. At two temperatures, the change in chemical shift of the iPrOH methyl peaks as observed by ^{1}H NMR were measured with respect to the concentration of the prepared solutions, $[Mo]_0$. These data, presented in Figure 4.6, were fitted to a polynomial regression ($R^2 > 0.999$) to determine the K_{eq} for the association of Step I for **3.6** and iPrOH as shown in Scheme 4.7 and according to Equations 4.1 – 4.11.[53]

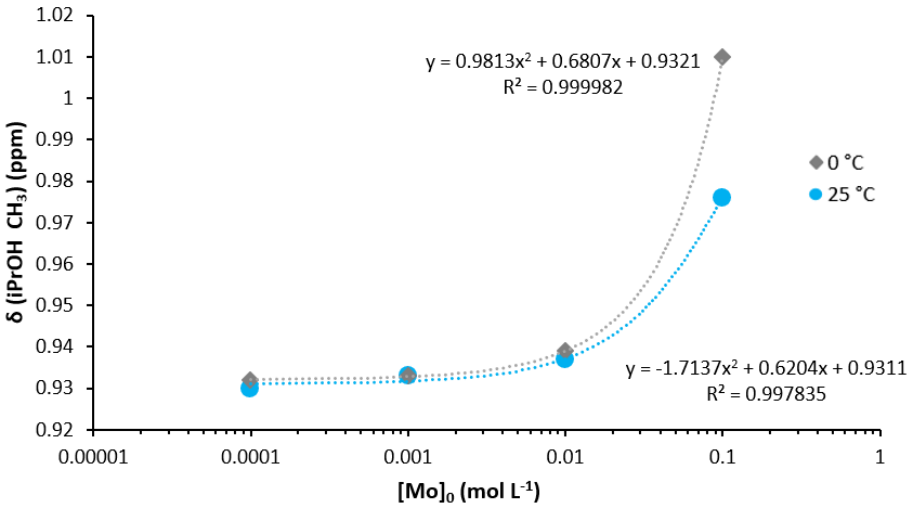

Figure 4.6. Comparison of observed chemical shift (δ) measured by ^{1}H NMR (500 MHz, C_7D_8, 0 °C or 25 °C) vs. the concentration of a prepared solutions of **3.6** and iPrOH ($[Mo]_0$)

Scheme 4.7

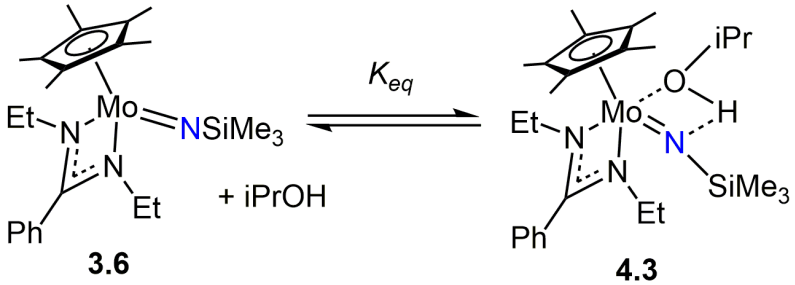

3.6 **4.3**

"Mo" + "iPrOH" **"Mo•iPrOH"**

According to the equilibrium shown in Scheme 4.7, K_{eq} is defined in Equation 4.1. Meanwhile, the mass balance of the equilibrium provides the total concentration of both species, $[Mo]_0$, as defined in Equation 4.2.

Equation 4.1

$$K_{eq} = \frac{[Mo][iPrOH]}{[Mo \bullet iPrOH]} = \frac{[Mo]^2}{[Mo \bullet iPrOH]}$$

Equation 4.2

$$[Mo]_0 = [Mo \bullet iPrOH] + [Mo]$$

Substituting Equation 4.1 with the solution to Equation 4.2 for [Mo] gives Equation 4.3, multiplication and rearrangement of which produces the quadratic Equation 4.4.

Equation 4.3

$$K_{eq} = \frac{([Mo]_0 - [Mo \bullet iPrOH])^2}{[Mo \bullet iPrOH]}$$

Equation 4.4

$$0 = [Mo \bullet iPrOH]^2 - (2[Mo]_0 + K_d)[Mo \bullet iPrOH]] + ([Mo]_0)^2$$

When solved for [Mo • iPrOH], Equation 4.4 gives Equation 4.5. Upon taking the negative root (since $[Mo]_0 \geq$ [Mo • iPrOH]) and simplifying, Equation 4.6 is produced.

Equation 4.5

$$[Mo \bullet iPrOH] = \frac{2[Mo]_0 \pm K_{eq}\sqrt{(2[Mo]_0 + K_{eq})^2 - 4([Mo]_0)^2}}{2}$$

Equation 4.6

$$[Mo \bullet iPrOH] = [Mo]_0 + \frac{K_{eq} - \sqrt{(K_d)^2 - 4K_{eq}[Mo]_0}}{2}$$

Since the observed chemical shift (δ_{obs}) of each of the concentration-dependent ^{1}H NMR signals is simply the weighted average of the chemical shifts of the free species (δ_{free}) (free **3.6** with free XOH) and associated species (δ_{assoc}) (adduct **4.3**) as shown in Equation 4.7, substituting for [Mo] gives Equation 4.8 and further simplification gives Equation 4.9.

Equation 4.7

$$\delta_{obs} = \frac{\delta_{obs}[Mo] + \delta_{assoc}[Mo \bullet iPrOH]}{[Mo]_0}$$

Equation 4.8

$$\delta_{obs} = \frac{\delta_{obs}([Mo]_0 - [Mo \bullet iPrOH]) + \delta_{assoc}[Mo \bullet iPrOH]}{[Mo]_0}$$

Equation 4.9

$$\delta_{obs} = \frac{(\delta_{assoc} - \delta_{free})[Mo \bullet iPrOH]}{[Mo]_0}$$

Setting the observed change in chemical shift upon association, Δδ, as $\delta_{assoc} - \delta_{free}$ gives the more manageable Equation 4.10. Finally, solving the quadratic Equation 4.6 for [*Mo • iPrOH*] and substituting this into Equation 4.10 provides Equation 4.11 that is fit to the experimental data from Figure 4.6 using a polynomial regression, Δδ, and K_{eq}.

Equation 4.10

$$\delta_{obs} = \delta_{free} + \Delta\delta\frac{[Mo \bullet iPrOH]}{[Mo]_0}$$

Equation 4.11*

$$\delta_{obs} = \delta_{free} + \Delta\delta\left(1 + \frac{K_{eq} - \sqrt{(K_{eq})^2 + 4K_{eq}[Mo]_0}}{2[Mo]_0}\right)$$

Using this determination, at 25 °C K_{eq} = 0.62 while at 0 °C K_{eq} = 0.68. The small, though not miniscule, magnitudes of the equilibrium constants corroborate what is experimentally observed by ^{1}H NMR; at equilibrium there is a higher concentration of reactants (free **3.6** and iPrOH) than of the association product (**4.3**). Under 100 mM solution conditions of each **3.6** and iPrOH in toluene-d_8, the concentration of **4.3** was determined to be only 6 mM at 0 °C. In all, the association of **3.6** and XOH in Step I

of Scheme 4.6 may be said therefore to favor the backwards direction under standard conditions.

4.3.3 Steps II and III: Addition of Me_3SiCl and Product Release

Upon addition of at least two equivalents of Me_3SiCl to a mixture of **3.6** and XOH (or more accurately, upon the addition of Me_3SiCl to the slight amount of **4.3** that exists in the solution at any given point in time) Steps II and III of Scheme 4.6 proceed immediately. First, in Step II, one equivalent of Me_3SiCl inserts into the four-membered ring of **4.3** though a formal "H-Cl" addition across the Mo=N bond, chemically trapping the now "activated" imido to create the six membered-ring of the proposed transition state {Cp*[N(Et)C(Ph)N(Et)]Mo((Cl)($SiMe_3$)($OSiMe_3$)(H)($NSiMe_3$))} (**4.5**). Formation of this transition state **4.5** is quickly followed by the loss of $O(SiMe_3)_2$ to produce a chloro, amido intermediate {Cp*[N(Et)C(Ph)N(Et)]Mo(Cl)(N(H)$SiMe_3$)} (**4.6**) that, in Step III, undergoes metathetical exchange with a remaining equivalent of Me_3SiCl to simultaneously produce **2.3** and $HN(SiMe_3)_2$. Neither **4.5** nor **4.6** is observed spectroscopically,[46] but this proposed pathway is in keeping with a similar intramolecular hydrogen-bonding assisted silylation of alcohols by Me_3SiCl.[54]

4.3.4 Dry Hydrolysis Control Experiments

Several control experiments were conducted to account for various observations from this series of "dry hydrolysis" studies and rule out alternate reaction pathways. For instance, relative to the formation of one equivalent of $HN(SiMe_3)_2$, some slight excess of X-O-$SiMe_3$ ether is usually observed spectroscopically. This

inequivalence is thought to be the result of the reactions between excess XOH with Me_3SiCl. To confirm this, a 2 : 1 mixture of iPrOH and Me_3SiCl in benzene-d_6 was observed to very gradually produce $iPrOSiMe_3$ when monitored by ^1H NMR and comparable reaction of tBuOH with Me_3SiCl produced $tBuOSiMe_3$ even more slowly. While this reaction would account for a very small inequivalence between the ratio of the organic products, the nearly instantaneous production and more pronounced excess of the ether suggests that the presence of the metal species plays a vital role, perhaps catalyzing faster reaction between XOH and Me_3SiCl than occurs in its absence.

The possibility of a residual amount of HCl being present in these silylation reactions, which might be catalyzing the production of the organic products and the conversion of **3.6** to **2.3** or both, also needed to be addressed. Therefore, reactions were run in the presence of a "proton sponge" (1,8-bis-(dimethylamino)-naphthalene) to absorb any adventitious HCl before it could cause a reaction. A 1 : 2 mixture of iPrOH and Me_3SiCl was added to a benzene-d_6 solution of **3.6** and proton sponge at room temperature (unreactive after 45 h) and rapidly yielded the expected quantitative production of $HN(SiMe_3)_2$ and a slight excess of iPrOSiMe, shown in Figure 4.7. Similarly, a 1 : 1 mixture of the same reaction using tBuOH yielded the dry hydrolysis but with only a 50% conversion of **3.6** and a 50% yield of $HN(SiMe_3)_2$ relative to a durene standard, which emphasizes the importance of the second equivalent of Me_3SiCl for the reaction to proceed to quantitive completion. These results confirm that it is the metal complex that facilitates the reaction and release of the N-containing product, though yield is, of course, limited by the appropriate amount of each reagent.

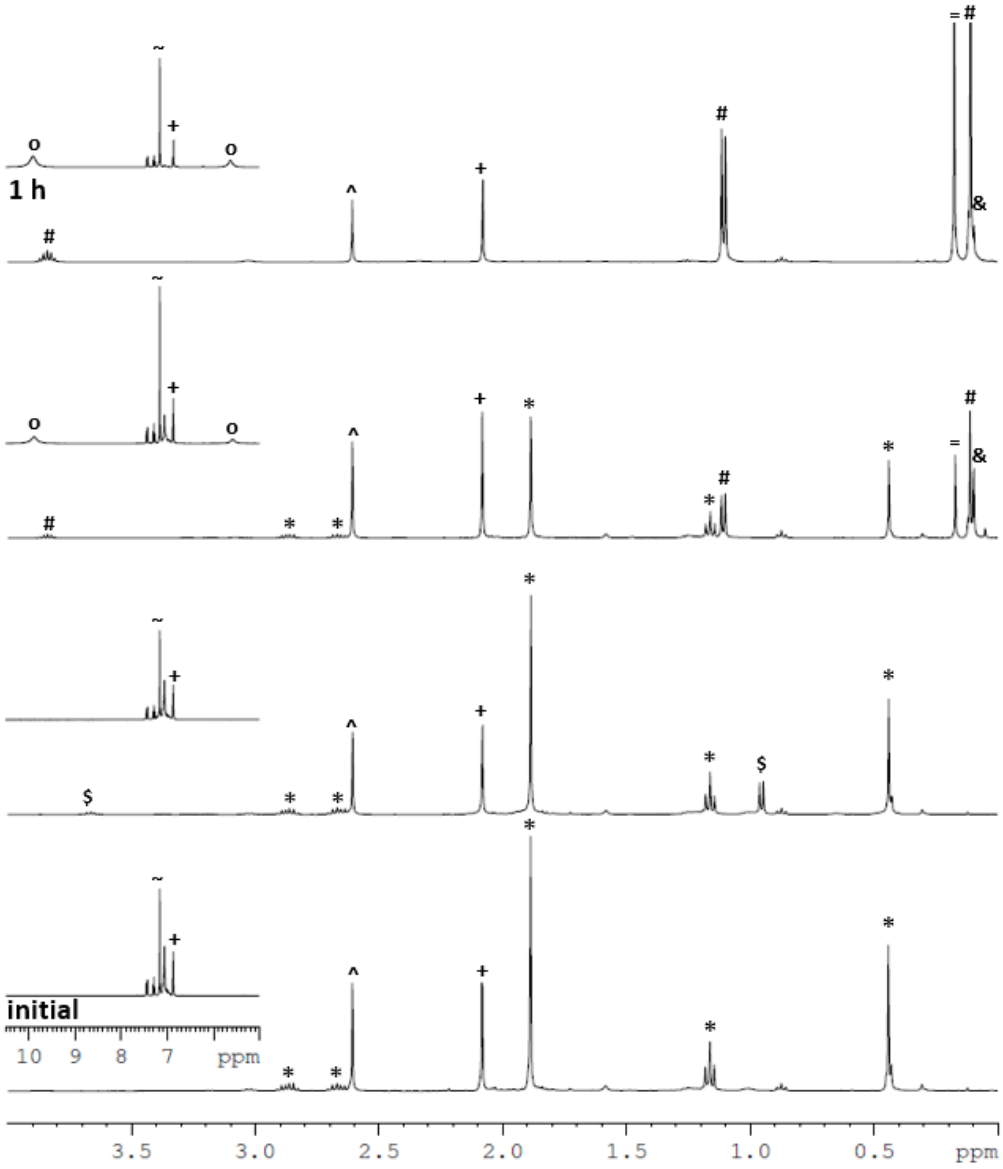

Figure 4.7. Partial ^{1}H NMR (400 MHz, C_6D_6, 25 °C) demonstrating the reaction of **3.6** (*****) with proton sponge (^) (bottom spectrum, stable after 45 h) upon the addition of iPrOH (**$**) (second from bottom spectrum) and Me_3SiCl (=) (second from top spectrum) to quickly form **2.3** (**o**), $Me_3SiOCH(CH_3)_2$ (#), and $(Me_3Si)_2NH$ (**&**) at 25 °C with durene (+) standard in benzene-d_6 (~)

4.4 Closing the Chemical Cycle

The dry hydrolysis reaction now completes the third and final step of a chemical cycle for the sterically reduced group 6 diethyl, phenyl CPAM system, the full loop of which is depicted in Scheme 4.8. This unique reactivity opens the possibility of efficient N_2 fixation with readily accessible and inexpensive proton sources, such as alcohols or silica gel, instead of the arduous stepwise processes of adding reductants and acids which currently dominates the literature. Furthermore, complexes **2.3** and **2.5** are both stable in the presence of a mixture of iPrOH over extended periods of time, and thus each step of the cycle seems to be compatible with the employed organic reagents.

Scheme 4.8

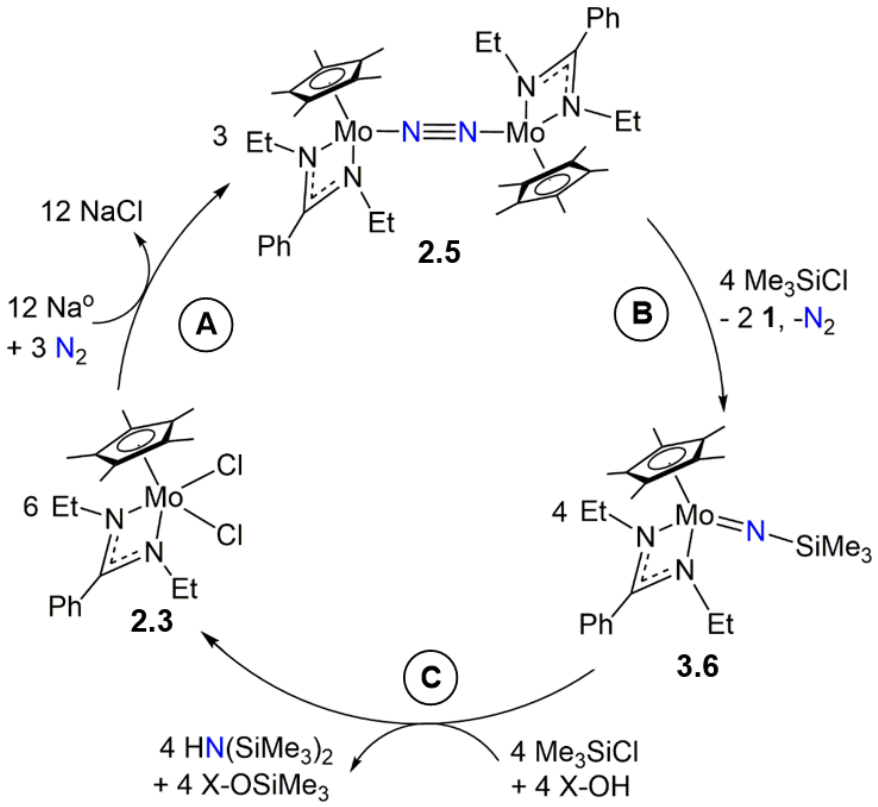

The dry hydrolysis reaction is also accessible to the Mo guanidinate derivative **3.10**, which is stable for 5 h in the presence of iPrOH and facilitates a dry hydrolysis reaction upon the addition of Me_3SiCl to yield **2.18** and the expected organic products $HN(SiMe_3)_2$ and $iPrOSiMe_3$ shown in Scheme 4.9. It should be noted, however, that the tungsten analogue **3.8** does not replicate the dry hydrolysis of the molybdenum **3.6**. These reactions (or lack thereof) further underscore the disparate reactivities of the group 6 congeners while demonstrating the versatility of the CPAM framework and the flexibility of the dry hydrolysis reaction as the vital and final step in the completion of the N_2 fixation cycle.

Scheme 4.9

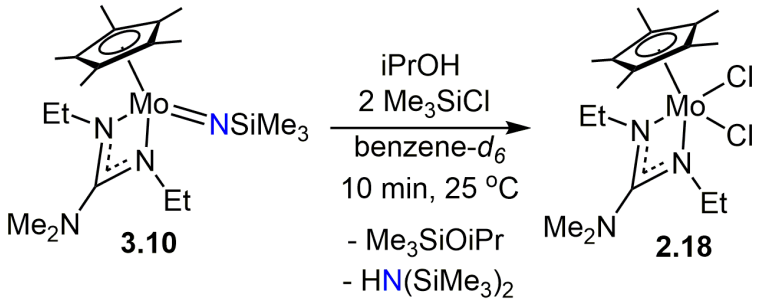

4.5 Conclusions

With the above results, Scheme 4.8 depicts a short and efficient chemical cycle that accomplishes dinitrogen fixation by well characterized group 6 complexes. Each step (A, B, and C) is well understood and requires only simple and accessible reagents. The N-containing product of hexamethyldisilazane is also interesting in its own right. $HN(SiMe_3)_2$ is a good silylating agent and can be used as a protecting group for amino acids or to silylated sugars prior to gas chromatographic separation,[55] and has also been shown be a useful drying agent for certain Scanning Electron Microscopy (SEM) applications.[56] Unlike all previous production of silylamines by dinitrogen fixation, this

is also the first chemoselective route to generating $HN(SiMe_3)_2$ which has the advantage of already containing a proton from a simple source and requiring fewer equivalents of acid to convert to ammonia (if that is the desired ultimate product) and which helps to obviate the need for more traditional, typically more energetically and environmentally costly H-atom sources (such as H_2 gas). All of these benefits together are promising for the eventual development of an efficient cycle which is not merely chemical, but catalytic.

4.6 Experimental Details

4.6.1 General Considerations

All manipulations of air and moisture sensitive compounds were carried out under an N_2 atmosphere with standard Schlenk or glovebox techniques. Et_2O and THF were distilled from Na/benzophenone under N_2 prior to use. Toluene and pentane were dried and deoxygenated by passage over activated alumina and GetterMax® 135 catalyst (purchased from Research Catalysts, Inc.) within a PureSolv solvent purification system manufactured by Innovative Technologies (model number PS-400-4-MD) and collected under N_2 prior to use. Benzene-d_6 and toluene-d_8 were dried over Na/K alloy and isolated by vacuum transfer prior to use. Celite© and silica gel were oven dried (150 °C for several days) prior to use. Cooling was performed in the internal freezer of a glovebox maintained at -30 °C. Trimethylsilyl chloride, hexamethydisiloxane, hexamethyldisilazane, trimethylsilanol, triethylsilanol, and triphenylsilanol were purchased from Sigma Aldrich and used as received. Phenol, pinacol, and proton sponge were purchased from Sigma Aldrich and dried under

vacuum prior to use. Alcohols were dried over $MgSO_4$ and distilled under N_2 prior to use (isopropyl alcohol was purchased from PHARMCO-AAPER and tert-butyl alcohol was purchased from J.T.Baker). All room temperature ^1H NMR spectra were recorded at 400 MHz and referenced to $SiMe_4$ using residual ^1H chemical shifts of benzene-d_6 or toluene-d_8. Variable temperature ^1H NMR studies were recorded at 500 MHz with low temperature calibration involving a methanol standard.

4.6.2 Supporting NMR and GC-MS Experiments

Reaction of 3.6 with iPrOH. A solution of **3.6** (5.0 mg, 10 µmol) and iPrOH (2.0 µL, 26 µmol), added via micro syringe, was made up in 0.6 mL benzene-d_6 in a Teflon© sealed Pyrex© J. Young NMR tube with a durene (0.5 mg, 4 µmol) standard. Over 53 h at 25 °C, the sample of **3.6** was observed by ^1H NMR to remain unchanged.

Reaction of 3.6 with pinacol. A solution of **3.6** (5.5 mg, 11 µmol) and pinacol (3.3 mg, 28 µmol) was prepared in 0.6 mL toluene-d_8 with a durene (0.5 mg, 4 µmol) internal standard in a Teflon© sealed Pyrex© J. Young NMR tube. Observed by ^1H NMR over 53 h at 25 °C, the sample of **3.6** was unchanged.

Reaction of 3.6 with Me_3SiOH. A solution of **3.6** (5.2 mg, 11 µmol) in 0.6 mL benzene-d_6 was prepared in a Teflon© sealed Pyrex© J. Young NMR tube with a durene (1.0 mg, 7.5 µmol) internal standard and an initial ^1H NMR was taken. To this was added Me_3SiOH (1.3 µL, 12 µmol) via micro syringe and the sample was left to sit for 17 h at 25 °C eliciting no change in the signal of the **3.6**, though $(Me_3Si)_2O$ was noted as a slight impurity in the Me_3SiOH.

Reaction of 3.6 with phenol. A solution of **3.6** (10.8 mg, 21.9 µmol) in 0.6 mL benzene-d_6 was prepared in a Teflon© sealed Pyrex© J. Young NMR tube to which was

added phenol (5.3 mg, 56 µmol). ^{1}H NMRs were taken after 10 minutes and 16 h at room temperature, showing the decrease in both **3.6** and phenol signals and the growth unidentified diamagnetic and paramagnetic peaks.

Reaction of 3.6 with Me_3SiCl. A solution of **3.6** (10.1 mg, 20.5 µmol) in 0.6 mL benzene-d_6 was prepared in a Teflon© sealed Pyrex© J. Young NMR tube with a durene (1.0 mg, 7.5 µmol) internal standard. Me_3SiCl (8.0 µL, 63.1 µmol) was added to the solution via micro syringe and spectra were taken after 10 minutes and 20 h at 25 °C, showing no change in the spectrum, and an additional ^{1}H NMR spectrum taken after heating at 70 °C for 12 h showed no further change to **3.6**.

Reaction of 3.6 with Me_3SiOH and Me_3SiCl followed by ^{1}H NMR. A solution of **3.6** (5.2 mg, 11 µmol) in 0.5 mL benzene-d_6 was prepared in a Teflon© sealed Pyrex© J. Young NMR tube with a durene (1.0 mg, 7.5 µmol) internal standard to which was added Me_3SiOH (1.3 µL, 12 µmol) via micro syringe and an initial ^{1}H NMR spectrum was taken. Me_3SiCl (2.9 µL, 23 µmol) was added to the mixture via micro syringe and ^{1}H NMR spectra were taken after 10 minutes, 3 h, and 16 h, showing the rapid and complete consumption of **3.6** and the concomitant production of **2.3**, $(Me_3Si)_2O$, and $(Me_3Si)_2NH$. See Figure 4.1 for corresponding spectra.

Preparatory scale reaction of 3.6 with Me_3SiOH and Me_3SiCl. A solution of **3.6** (45.5 mg, 92.2 µmol) in 0.5 mL benzene-d_6 was prepared in a Teflon© sealed Pyrex© J. Young NMR tube, to which was added Me_3SiOH (15.3 µL, 13.8 µmol) via micro syringe and an initial ^{1}H NMR was taken. To this was added Me_3SiCl (25.8 µL, 20.3 µmol) and the sample was allowed to sit for 17 h at 25 °C while precipitate crashed out of the brown solution, and periodic ^{1}H NMR showed production of $(Me_3Si)_2O$,

$(Me_3Si)_2NH$, and **2.3**. The reaction was rinsed into a vial with toluene and the solvent, with organic products, was removed *in vacuo* to yield dark brown solid **2.3** (41.2 mg, 94 %) confirmed by ^1H NMR to be pure.

Reaction of 3.6 with iPrOH and Me_3SiCl for GC/MS analysis. 3.6 (4.8 mg, 9.7 mmol) was dissolved in 1 mL pentane in a vial, to which was added iPrOH (0.8 µL, 11 mmol) via micro syringe to no visible effect. Upon the addition of Me_3SiCl (2.7 µL, 21 mmol) via micro syringe, brown precipitate (**2.3**, which is insoluble in pentane) began to form immediately. The vial was capped and the reaction let sit for 18 h at 25 °C. Finally, the solution was removed from the vial and filtered through a pipet with a kimwipe and celite plug with an additional 1 mL pentane to remove the solid **2.3** and to yield a brown solution amenable to analysis by GC/MS, which confirmed the presence of the products $Me_3SiOCH(CH_3)_2$ and $(Me_3Si)_2NH$ as well as $(Me_3Si)_2O$. Gas chromatography measurements were performed on an Agilent 6890N system coupled with a JEOL high resolution magnetic sector mass spectrometer (JMS-700 MStation) with the EI ion source (70 eV). The mass spectrometer was operated in the mode of high scan speed and low resolution (1000) with the mass range from 50 to 400 Daltons. The silica capillary column (Agilent VF-5MS, 30 m length, 250 µm I.D.) was used in the experiments with helium (at 1 mL/min) as the carrier gas. Analysis was performed as follows: injection volume = 1 µL, split mode (ratio=10), the front inlet temperature = 220 C, the column temperature was programmed from 30 °C at 1.5 min, then increased to 250 °C at the rate of 18 °C/min and then held at 250 °C for another 1.28 minutes. Fragmentation patterns obtained by EI were used to identify the

structures of the ions observed in the mass spectra based on the NIST Spectral Database. See Figure 4.2 for corresponding spectra.

Reaction of 3.6 with Et_3SiOH and Me_3SiCl. A solution of **3.6** (7.0 mg, 14 μmol) in 0.6 mL benzene-*d*$_6$ was prepared in a Teflon© sealed Pyrex© J. Young NMR tube with a durene (0.5 mg, 4 μmol) internal standard and to which was added Et_3SiOH (2.5 μL, 16 μmol) via micro syringe. An initial ^{1}H NMR was taken after which Me_3SiCl (3.9 μL, 30 μmol) was added via micro syringe and ^{1}H NMR showed the immediate production of **2.3** and $(Me_3Si)_2NH$ along with peaks presumed to be $Et_3SiOSiMe_3$. The sample was left to sit for 3 h at 25 °C during which time it grew orange in color and all **3**, Et_3SiOH, and Me_3SiCl were completely consumed.

Reaction of 3.6 with Ph_3SiOH and Me_3SiCl. A solution of **3.6** (4.6 mg, 9.3 μmol) in 0.6 mL benzene-*d*$_6$ was prepared in a Teflon© sealed Pyrex© J. Young NMR tube with a durene (1.0 mg, 7.5 μmol) internal standard. To this was added Ph_3SiOH (3.0 mg, 12 μmol) and Me_3SiCl (3.0 μL, 24 μmol) via micro syringe causing **2.3** to appear immediately with $(Me_3Si)_2NH$ and what is presumed to be $Ph_3SiOSiMe_3$. The conversion of **3.6** and Ph_3SiOH was judged to be complete after 7 h at 25 °C.

Reaction of 3.6 with iPrOH and Me_3SiCl followed by ^{1}H NMR. A solution of **3.6** (9.2 mg, 19 μmol) in 0.6 mL benzene-*d*$_6$ was prepared in a Teflon© sealed Pyrex© J. Young NMR tube with a durene (0.5 mg, 4 μmol) internal standard. To this was added iPrOH (1.5 μL, 20 μmol) via micro syringe and an initial ^{1}H NMR was taken. Me_3SiCl (4.8 μL, 38 μmol) was added via micro syringe and a ^{1}H NMR spectra was taken after 10 minutes at room temperature, showing the near compete conversion of **3.6** to **2.3** and the rapid consumption of all the iPrOH. After 1.5 h, only **2.3**,

$Me_3SiOCH(CH_3)_2$, $(Me_3Si)_2NH$, and a slight excess of Me_3SiCl remained. See Figure 4.8 for corresponding spectra.

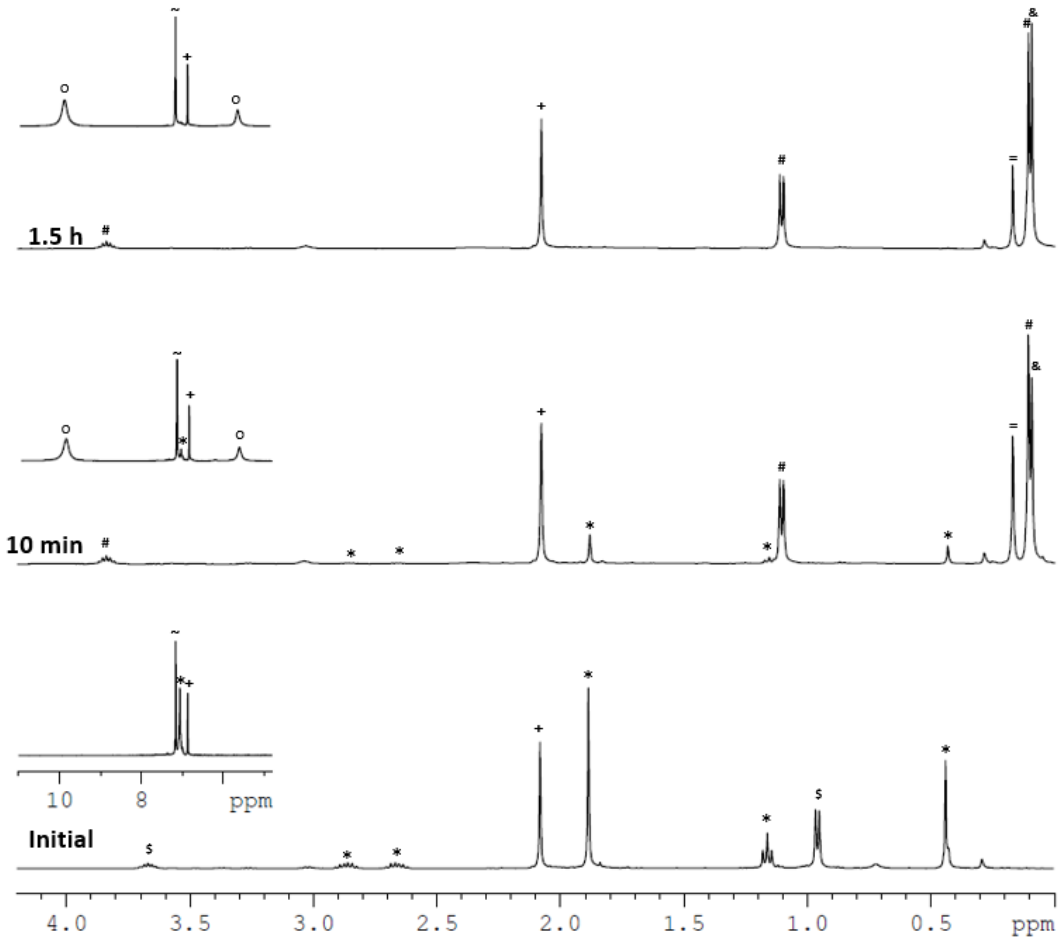

Figure 4.8. Partial ^{1}H NMR (400 MHz, C_6D_6, 25 °C) demonstrating the conversion of **3.6** (*****) and iPrOH (**$**) to **2.3** (**o**), $Me_3SiOCH(CH_3)_2$ (**#**), and $(Me_3Si)_2NH$ (**&**) upon the addition of Me_3SiCl (**=**) at 25 °C with durene (**+**) standard in benzene-*d*$_6$ (**~**)

Reaction of 3.6 with tBuOH and Me_3SiCl followed by ^{1}H NMR. A solution of **3.6** (11.0 mg, 22.3 µmol) in 0.6 mL benzene-*d*$_6$ was prepared in a Teflon© sealed Pyrex© J. Young NMR tube with a durene (0.5 mg, 4 µmol) internal standard and tBuOH (2.7 µL, 23 µmol) after which an initial ^{1}H NMR was taken. Me_3SiCl (6.3 µL, 62 µmol) was added via micro syringe and ^{1}H NMR spectra were taken at 10 minutes, 1 h, and 18 h at 25 °C showing the rapid and complete consumption of the starting

materials and production of **2.3**, $(CH_3)_3COSiMe_3$, and $(Me_3Si)_2NH$. See Figure 4.9 for corresponding spectra.

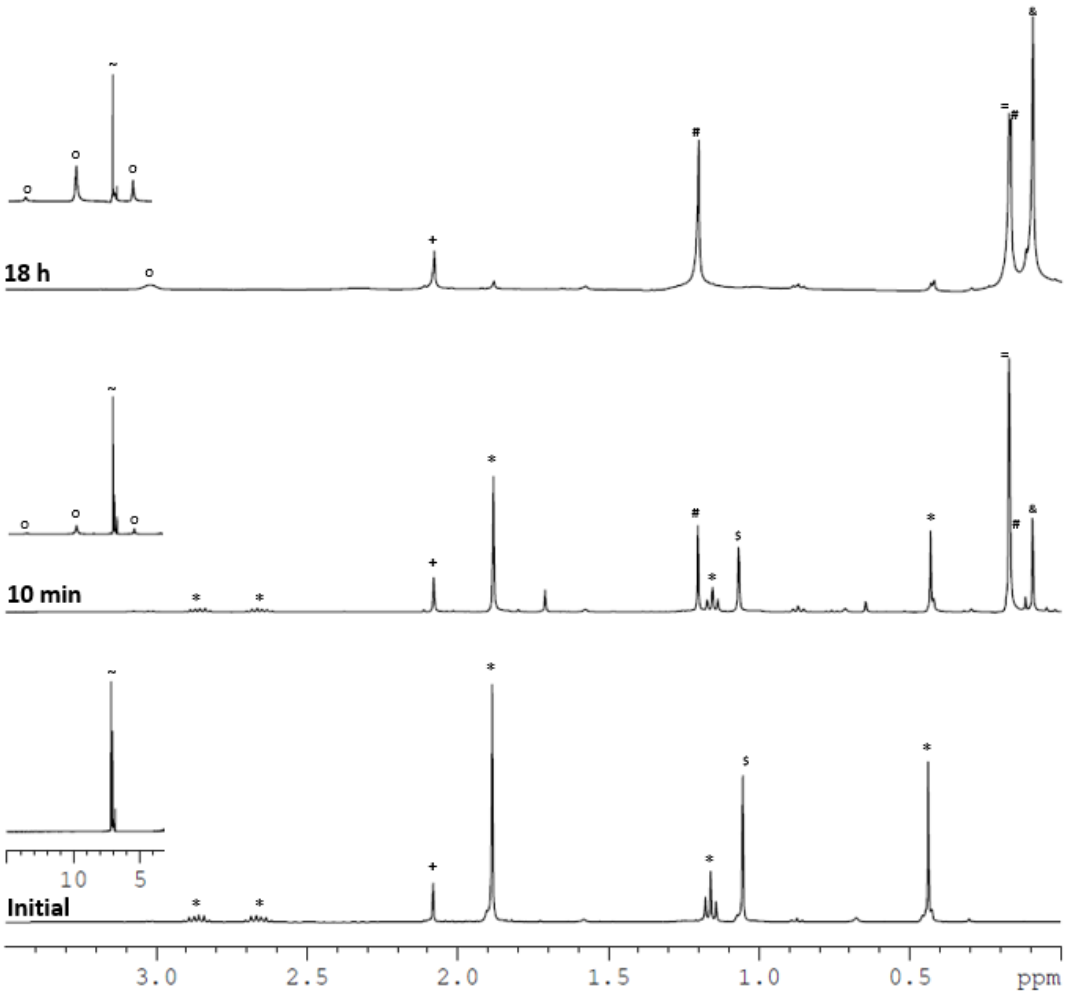

Figure 4.9. Partial ^{1}H NMR (400 MHz, C_6D_6, 25 °C) demonstrating the reaction of **3.6** (*****) and tBuOH (**$**) (bottom spectrum) to which Me_3SiCl (**=**) is added (middle and top spectra) to yield **2.3** (**o**), $(CH_3)_3COSiMe_3$ (**#**), and $(Me_3Si)_2NH$ (**&**) at 25 °C with durene (**+**) standard in benzene-d_6 (**~**)

Reaction of 3.6 with Me_3SiOH and Me_3SiCl for GC/MS analysis. 3.6 (4.9 mg, 9.9 mmol) was dissolved in 1 mL pentane in a vial, to which was added Me_3SiOH (1.5 µL, 14 mmol) via micro syringe to no visible effect. Upon the addition of Me_3SiCl (2.7 µL, 21 mmol) via micro syringe, brown precipitate (**2.3**, which is insoluble in pentane) began to form immediately. The vial was capped and the reaction let sit for

17 h at 25 °C. Finally, the solution was removed from the vial and filtered through a pipet with a kimwipe and celite plug with an additional 1 mL pentane to remove the solid **2.3** and to yield a brown solution amenable to analysis by GC/MS, which confirmed the presence of the products $(Me_3Si)_2O$ and $(Me_3Si)_2NH$. Gas chromatography measurements were performed on an Agilent 6890N system coupled with a JEOL high resolution magnetic sector mass spectrometer (JMS-700 MStation) with the EI ion source (70 eV). The mass spectrometer was operated in the mode of high scan speed and low resolution (1000) with the mass range from 50 to 400 Daltons. The silica capillary column (Agilent VF-5MS, 30 m length, 250 μm I.D.) was used in the experiments with helium (at 1 mL/min) as the carrier gas. Analysis was performed as follows: injection volume = 1 μL, split mode (ratio=10), the front inlet temperature = 220 C, the column temperature was programmed from 30 °C at 1.5 min, then increased to 250 °C at the rate of 18 °C/min and then held at 250 °C for another 1.28 minutes. Fragmentation patterns obtained by EI were used to identify the structures of the ions observed in the mass spectra based on the NIST Spectral Database. See Figure 4.10 for corresponding spectra.

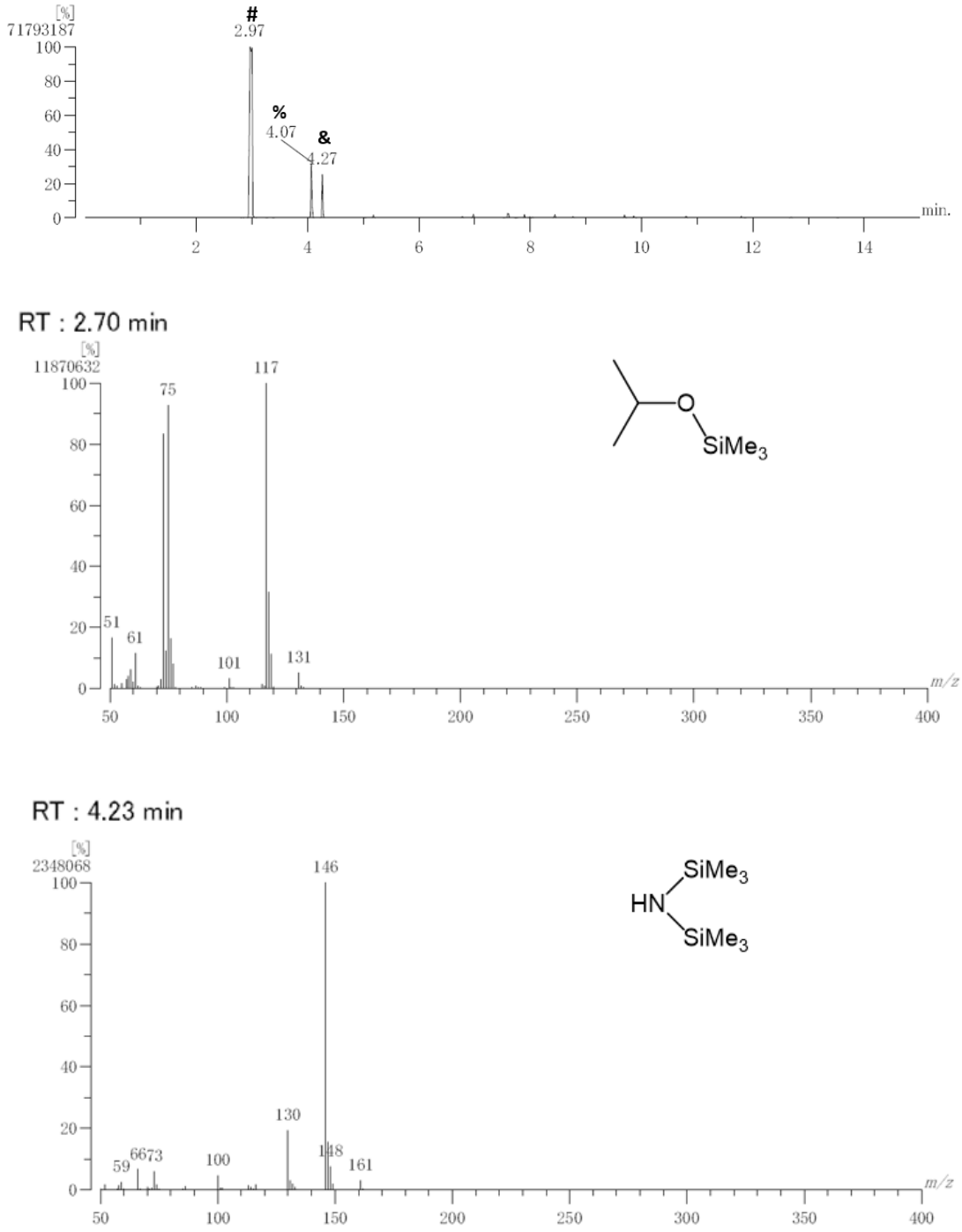

Figure 4.10. (Top) Chromatograph of the pentane solution from the reaction of **3.6** with iPrOH and Me_3SiCl at 25 °C to produce **2.3**, $Me_3SiOC(CH_3)_3$ (#) at 2.97 min, and $(Me_3Si)_2NH$ (**&**) at 4.23 min. Slight toluene **(%)** impurity noted at 4.07 min. (Bottom) Mass spectra for $Me_3SiOCH(CH_3)_2$ (retention time 2.97 min) and $(Me_3Si)_2NH$ retention time 4.23 min) from the pentane solution of the reaction of **3.6** with iPrOH and Me_3SiCl at 25 °C

Reaction of 3.6 with Me_3SiCl and PhOH followed by ^1H NMR. A solution of **3.6** (7.0 mg, 14 µmol) in 0.6 mL benzene-d_6 was prepared in a Teflon© sealed Pyrex© J. Young NMR tube with a durene (0.5 mg, 4 µmol) internal standard and Me_3SiCl (2.7 µL, 21 µmol), added via micro syringe. An initial ^1H NMR was taken, after which a small of phenol (4.6 mg, 21 mmol) was added to the tube, causing the solution to immediately change from brown to more orange in color, and periodic monitoring by ^1H NMR showed the immediate production of **2.3**, $PhOSiMe_3$, and $(Me_3Si)_2NH$ while sitting at 25 °C and complete after 3h. See Figure 4.11 for corresponding spectra.

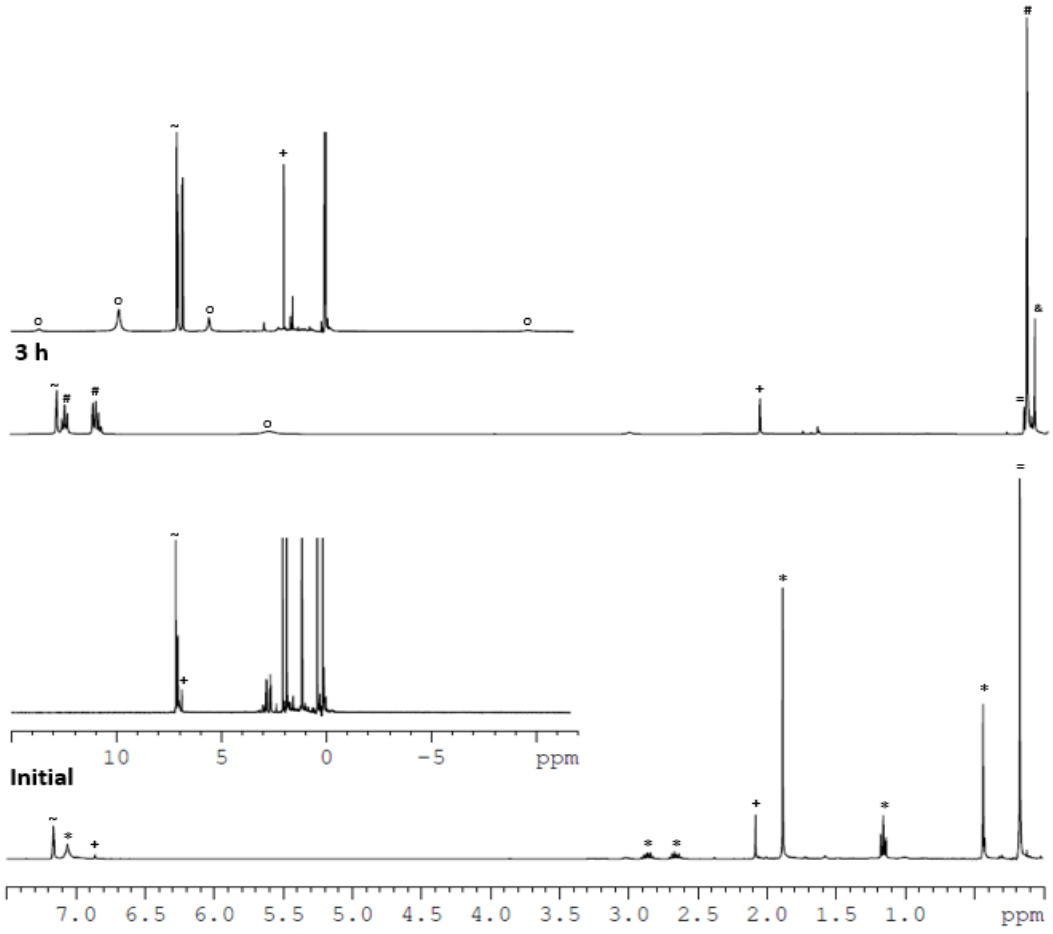

Figure 4.11. Partial ^1H NMR (400 MHz, C_6D_6, 25 °C) demonstrating the reaction of **3.6** (*****) and Me_3SiCl (=) (bottom spectrum) to which phenol (**$**) is added (top spectra) to yield **2.3** (**o**), $PhOSiMe_3$ (#), and $(Me_3Si)_2NH$ (**&**) at 25 °C with durene (+) standard in benzene-d_6 (~)

Reaction of 3.6 with silica gel and Me_3SiCl followed by ^1H NMR. A solution of **3** (4.9 mg, 9.9 μmol) in 0.6 mL benzene-d_6 was prepared in a Teflon© sealed Pyrex© J. Young NMR tube with a durene (1.0 mg, 7.5 μmol) internal standard and Me_3SiCl (2.7 μL, 21 μmol), added via micro syringe. An initial ^1H NMR was taken, after which a small spatula full of silica gel (20.0 mg) was added to the tube, causing the solution to immediately change from brown in color to red, and periodic monitoring by ^1H NMR showed the immediate production of **2.3**, $(Me_3Si)_2O$, and $(Me_3Si)_2NH$ while reacting at 25 °C. After 44 h, an additional spatula of silica gel was added, and the reaction proceeded until **3.6** was completely consumed after a total of 140 h. See Figure 4.12 for corresponding spectra.

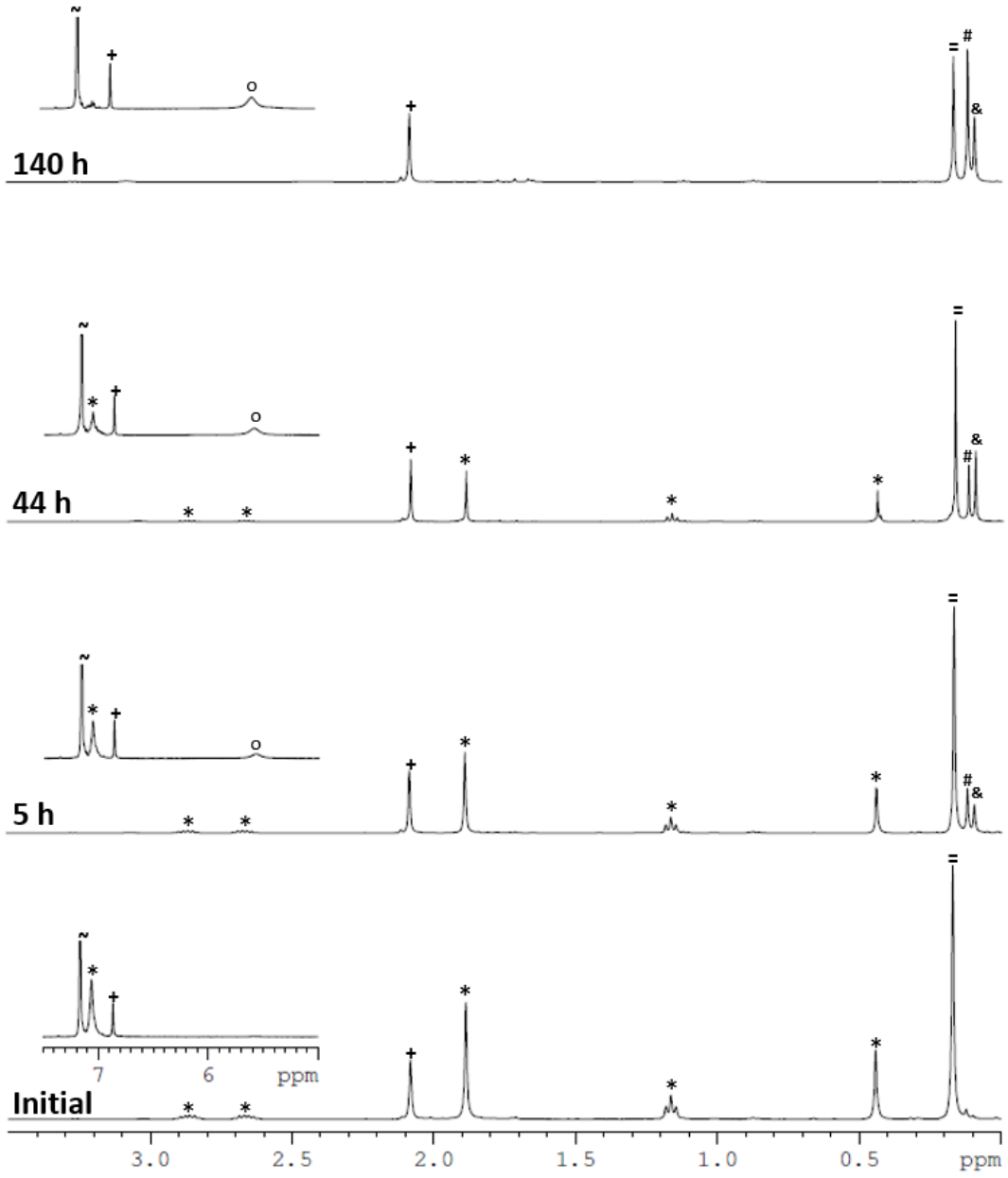

Figure 4.12. Partial ^{1}H NMR (400 MHz, C_6D_6, 25 °C) demonstrating the reaction of **3.6** (*****) and Me_3SiCl (**=**) in the presence of silica gel to yield **2.3** (**o**), $(Me_3Si)_2O$ (**#**), and $(Me_3Si)_2NH$ (**&**) at 25 °C with durene (+) standard in benzene-d_6 (~)

Preparatory scale reaction of 3.6 with silica gel and Me_3SiCl. A solution of **3.6** (49.0 mg, 99.3 µmol) in 5 mL THF was stirred in a round bottom flask with Me_3SiCl (26.0 µL, 205 µmol) added via micro syringe. Silica gel (196.7 mg) was added to the purple-brown solution which was stirred for 18 h at 25 °C becoming an orange-brown

in color. The reaction was filtered through a pipet with a kimwipe plug with additional THF to remove the silica gel. Finally, the solvent from the resulting filtrate was removed *in vacuo* to yield a brown solid **2.3** (38.0 mg, 80%). See Figure 4.13 for spectrum.

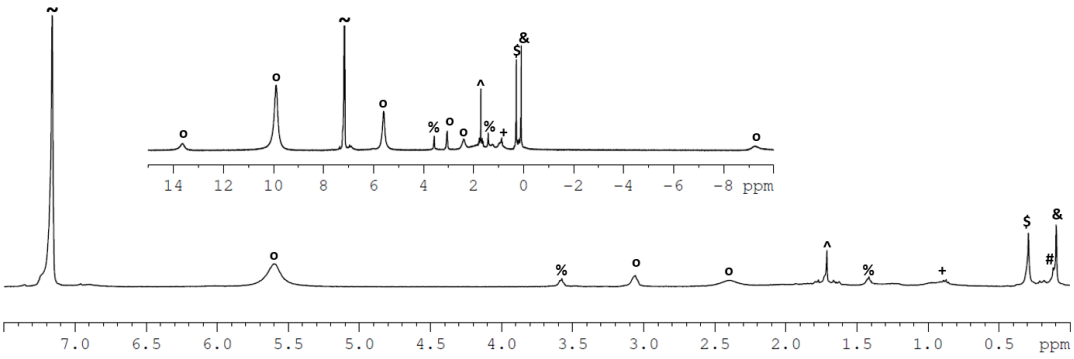

Figure 4.13. Partial ^{1}H NMR (400 MHz, C_6D_6, 25 °C) demonstrating the reaction of **3.6** and Me_3SiCl in the presence of silica gel to yield **2.3** (**o**) and residual signals for the $(Me_3Si)_2O$ (**#**) and $(Me_3Si)_2NH$ (**&**) products, THF (**%**) and pentane (**+**) solvents, as well as an unidentified impurity (**^**) and grease (**$**) at 25 °C in benzene-$d_6$ (**~**)

Filtration of 2.3 through silica gel. 2.3 (4.3 mg, 9.0 µmol) was dissolved in in 1.0 mL benzene-d_6 and filtered through a pad of silica gel supported by a kimwipe plug in a pipet, leaving a darker stain in the silica gel as the solution to bleached to a light orange upon collection of the filtrate. ^{1}H NMR showed only residual evidence of **2.3**.

Filtration of 2.3 with Me_3SiCl through silica gel. 2.3 (16.0 mg, 33.5 µmol) was dissolved in in 2 mL THF to which a micro syringe was used to add Me_3SiCl (8.5 µL, 67.0 µmol). The solution was mixed and filtered through a small column of silica gel supported on a kimwipe plug in a pipet. The brown filtrate was collected and the solvent removed in vacuo to yield **2.3** (14.8 mg, 93%) the identity of which was confirmed by ^{1}H NMR.

Low temperature ^{1}H NMR study of 3.6 and Me_3SiOH. A solution of **3.6** (5.5 mg, 11 mmol) in 0.6 mL toluene-d_8 was prepared in a Teflon© sealed Pyrex© J. Young NMR tube, to which was added Me_3SiOH (1.75 µL, 15.8 mmol) via micro syringe. The sample was placed in a pre-cooled NMR spectrometer where ^{1}H NMR spectra were taken at -80, -70, -60, -50, -40, -30, -20, -10, 0, 10, and 25 °C after equilibrating for 10 minutes at each temperature. The shifts for each reactant upfield to different degrees with respect to increasing temperature, indicating the presence of an equilibrium with very fast exchange. A control experiment of Me_3SiOH in toluene-d_8 at -80 °C demonstrated that the unbound silanol peak comes in at more upfield shifts than are depicted as the observed shifts for the mixture. See Figure 4.3 for corresponding spectra.

Low temperature ^{1}H NMR study of 3.6 and iPrOH. A solution of **3.6** (7.0 mg, 14 mmol) in 0.6 mL toluene-d_8 was prepared in a Teflon© sealed Pyrex© J. Young NMR tube, to which was added iPrOH (1.3 µL, 17 mmol) via micro syringe. The sample was placed in a pre-cooled NMR spectrometer where ^{1}H NMR spectra were taken at -80, -60, -40, -20, 0, and 25 °C after equilibrating for 10 minutes at each temperature. The shifts for each reactant moved upfield to different degrees with respect to increasing temperature, indicating the presence of an equilibrium with very fast exchange. A control experiment of iPrOH in toluene-d_8 at -80 °C demonstrated that the unbound alcohol comes in at more upfield shifts than are depicted as the observed shifts for the mixture. See Figure 4.3 for corresponding spectra.

Low temperature ^{1}H NMR study of 3.6 and tBuOH. A solution of **3.6** (24.3 mg, 49.2 mmol) in 0.6 mL toluene-d_8 was prepared in a Teflon© sealed Pyrex© J. Young

NMR tube, to which was added tBuOH (4.7 µL, 49.1 mmol) via micro syringe. The sample was placed in a pre-cooled NMR spectrometer where ^{1}H NMR spectra were taken at -60, -40, -20, 0, and 25 °C after equilibrating for 10 minutes at each temperature. The shifts for each reactant moved upfield to different degrees with respect to increasing temperature, indicating the presence of an equilibrium with very fast exchange. A control experiment of tBuOH in toluene-d_8 at -60 °C demonstrated that the unbound alcohol comes in at more upfield shifts than are depicted as the observed shifts for the mixture. See Figure 4.3 for corresponding spectra.

Concentration study of 3.6 and iPrOH by ^{1}H NMR. A 0.1 M stock solution of **3.6** (49.4 mg) was prepared in a 1.00 mL volumetric flask filled with toluene-d_8 and iPrOH (7.7 µL), via micro syringe, and mixed. Serial dilutions were then prepared at 0.01, 0.001, and 0.0001 M concentrations and of each solution, 0.6 mL was transferred to an individual a Teflon© sealed Pyrex© J. Young NMR tube. The samples were placed an NMR spectrometer precooled to 0 °C or calibrated to 25 °C and each sample was allowed 15 minutes to equilibrate in temperature before a ^{1}H NMR spectra were taken. The change in observed chemical shift of the methyl peaks of iPrOH (representing the weighted average of both the dissociated mixture, free **3.6** and iPrOH, and the proposed associated species, **4.3**) was measured with respect to the prepared concentration of the solution ($[Mo]_0$). These data (Figure 4.6) were fitted to a polynomial regression ($R^2 > 0.999$) to determine at 25 °C, $K_{eq} = 0.62$ while at 0 °C $K_{eq} = 0.68$ according to Equations 4.1 – 4.11.

Reaction of iPrOH and Me_3SiCl. iPrOH (5.0 µL, 65 µmol) was added via micro syringe to 0.6 mL benzene-d_6 in a Teflon© sealed Pyrex© J. Young NMR tube

with a durene (0.5 mg, 4 μmol) internal standard along with Me_3SiCl (17.0 μL, 130 μmol). The mixture was tracked by ^1H NMR over 51 h at 25 °C showing the slow appearance of $Me_3SiOCH(CH_3)_2$ as iPrOH and Me_3SiCl were consumed proportionally.

Reaction of tBuOH and Me_3SiCl. tBuOH (5.0 μL, 65 μmol) was added via micro syringe to 0.6 mL benzene-*d*$_6$ in a Teflon© sealed Pyrex© J. Young NMR tube with a durene (0.5 mg, 4 μmol) internal standard along with Me_3SiCl (17.0 μL, 130 μmol). The mixture was tracked by ^1H NMR over 51 h at 25 °C showing the very slow consumption of tBuOH and Me_3SiCl and the production of a very small amount of $Me_3SiOC(CH_3)_3$.

Reaction of 3.6 with iPrOH, proton sponge, and Me_3SiCl followed by ^1H NMR. A solution of **3.6** (4.6 mg, 9.3 μmol) in 0.6 mL benzene-*d*$_6$ was prepared in a Teflon© sealed Pyrex© J. Young NMR tube with proton sponge (1,8-bis(dimethylamino)naphthalene) (0.5 mg, 2 μmol) and a durene (0.5 mg, 4 μmol) internal standard. An initial ^1H NMR was taken and the mixture was left to sit at 25 °C for 45 h after which another ^1H NMR spectrum showed no change in the reaction mixture. iPrOH (0.8 μL, 10 μmol) was added via micro syringe and another ^1H NMR spectrum was taken. Me_3SiCl (2.5 μL, 20 μmol) was then added to the mixture via micro syringe and a ^1H NMR spectrum was taken after 10 minutes, showing immediate formation of **2.3**, $(Me_3Si)_2NH$, and $Me_3SiOCH(CH_3)_2$ with the partial consumption of **3.6** and Me_3SiCl and the full consumption of iPrOH. To this mixture, additional amounts of Me_3SiCl (7.5 μL, 60 μmol) and iPrOH (3.0 μL, 39 μmol) were added and an immediate and ^1H NMR spectrum showed no remaining **3.6** or iPrOH, only **2.3**,

$HN(Me_3Si)_2$, $Me_3SiOCH(CH_3)_2$, and excess Me_3SiCl. See Figure 4.7 for corresponding spectra.

Reaction of 3.6 with 1 : 1 ratio of tBuOH and Me_3SiCl followed by ^1H NMR. A solution of **3.6** (10.6 mg, 21.5 µmol) in 0.6 mL benzene-*d*$_6$ was prepared in a Teflon© sealed Pyrex© J. Young NMR tube with a durene (0.5 mg, 4 µmol) internal standard and Me_3SiCl (2.7 µL, 22 µmol) was added via micro syringe, after which an initial ^1H NMR was taken showing an even ratio of the two reagents. tBuOH (2.1 µL, 22 µmol) was added via micro syringe and ^1H NMR spectra were taken at 10 minutes and 30 minutes at 25 °C showing the immediate production of **2.3**, slight amounts of $(CH_3)_3COSiMe_3$, and very slight amounts of $HN(Me_3Si)_2$. After 18 h, the reaction was judged by ^1H NMR to have reached completion at which point just under half of the original amount of **3.6** and tBuOH remained unreacted. See Figure 4.14 for corresponding spectra.

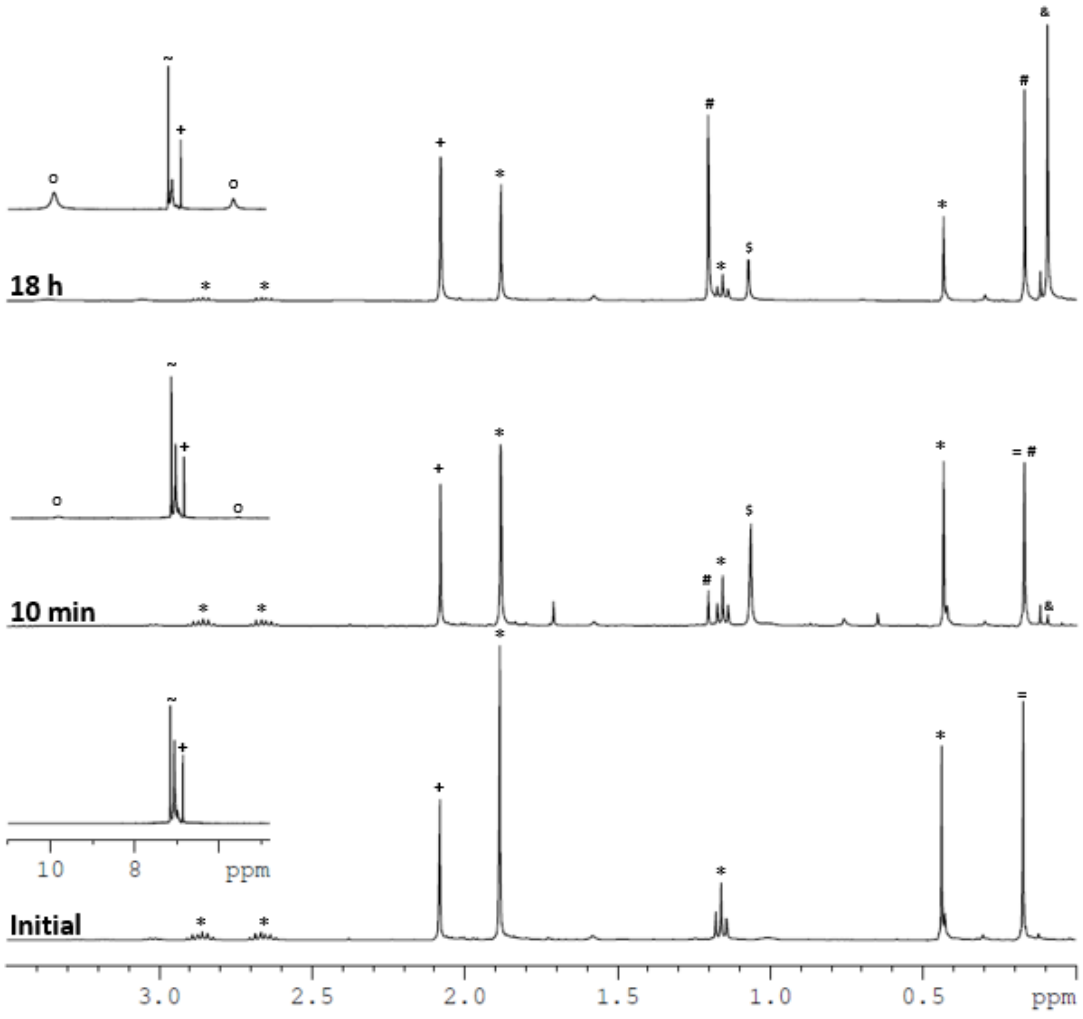

Figure 4.14. Partial ^{1}H NMR (400 MHz, C_6D_6, 25 °C) demonstrating the reaction of **3.6** (*****) and 1 equiv. Me_3SiCl (**=**) with tBuOH (**$**), converting half of **3.6** to **2.3** (**o**), $(CH_3)_3COSiMe_3$ (**#**), and $HN(Me_3Si)_2$ (**&**) at 25 °C with durene (**+**) standard in benzene-*d*$_6$ (**~**)

Reaction of 2.5 with iPrOH followed by ^{1}H NMR. A solution of **2.5** (4.5 mg, 5.4 µmol) in 0.6 mL benzene-*d*$_6$ was prepared in a Teflon© sealed Pyrex© J. Young NMR tube with a durene (0.5 mg, 4 µmol) internal standard and iPrOH (1.5 µL, 17 µmol). The mixture was allowed to sit at room temperature for 63 h and showed no significant change.

Reaction of 3.10 with Me_3SiCl and iPrOH followed by ^1H NMR. A solution of **3.10** (4.0 mg, 8.7 μmol) in 0.6 mL benzene-*d*$_6$ was prepared in a Teflon© sealed Pyrex© J. Young NMR tube with a durene (1.0 mg, 7.5 μmol) internal standard. An initial ^1H NMR was taken, after which a small of iPrOH (0.7 μ, 9.2 mmol) was added to the tube and a ^1H NMR showed no reaction after 5 h at room temperature. Upon the addition of Me_3SiCl (2.2 μL, 17 μmol) via micro syringe, the solution abruptly changed from a dark purple-brown to a pale brown and an immediate ^1H NMR showed the complete consumption of **3.10** and the production of **2.18**, $iPrOSiMe_3$, and $HN(Me_3Si)_2$. See Figure 4.15 for corresponding spectra.

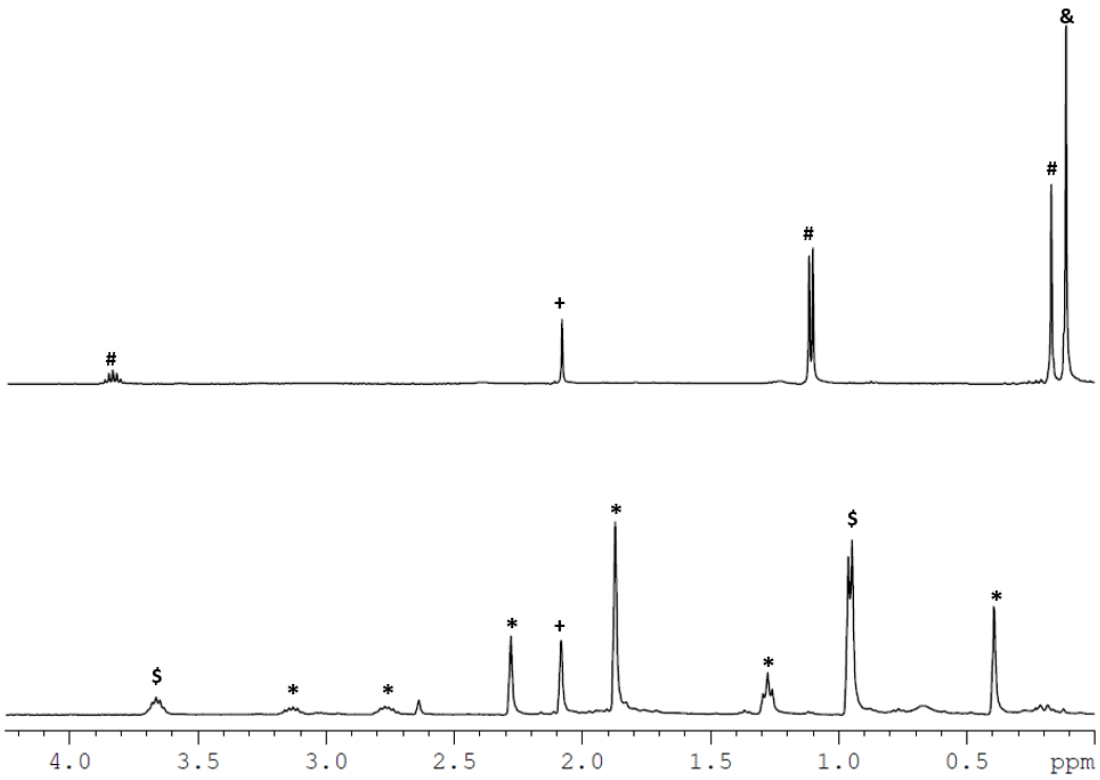

Figure 4.15. Partial ^1H NMR (400 MHz, C_6D_6, 25 °C) demonstrating (bottom) the reaction of **3.10** (*****) and iPrOH (**$**), stable after 5 h at 25 °C and (top) upon addition of Me_3SiCl, immediate conversion of **3.10** to **2.18**, $iPrOSiMe_3$ (#), and $HN(Me_3Si)_2$ (**&**) at with durene (**+**) standard in benzene-*d*$_6$ (**~**)

References

1. Tanabe, Y.; Nishibayashi, Y. Catalytic Dinitrogen Fixation to Form Ammonia at Ambient Reaction Conditions Using Transition Metal-Dinitrogen Complexes. **2016,** *16*, 1549-1577.
2. Nishibayashi, Y. E. *Topics in Organometallic Chemistry*. Springer Verlag: Berlin/Heidelberg, **2017**; Vol. 60.
3. MacLeod, K. C.; Holland, P. L. Recent Developments in Homogeneous Dinitrogen Reduction by Molybdenum and Iron. *Nat. Chem.* **2013,** *5*, 559-565.
4. Curley, J. J.; Sceats, E. L.; Cummins, C. C. A Cycle for Organic Nitrile Synthesis via Dinitrogen Cleavage. *J. Am. Chem. Soc.* **2006,** *128*, 14036-14037.
5. Keane, A. J. Early Transition Metal Studies of Dintrogen Cleavage and Metal-Nitrogen Bond Reactivity towards Catalytic N_2 Fixation. *Ph.D. Dissertation*, *University of Maryland*, College Park, MD, **2015**.
6. Keane, A. J.; Farrell, W. S.; Yonke, B. L.; Zavalij, P. Y.; Sita, L. R. Metal-Mediated Production of Isocyanates, $R_3EN{=}C{=}O$ from Dinitrogen, Carbon Dioxide, and R_3ECl. *Angew. Chem. Int. Ed.* **2015,** *54*, 10220-10224.
7. Shiina, K., Reductive silylation of molecular nitrogen via fixation to tris(trialkylsilyl)amine. *J. Am. Chem. Soc.* **1972,** *94*, 9266-9267.
8. Komori, K.; Oshita, H.; Mizobe, Y.; Hidai, M. Preparation and properties of molybdenum and tungsten dinitrogen complexes. 25. Catalytic conversion of molecular nitrogen into silylamines using molybdenum and tungsten dinitrogen complexes. *J. Am. Chem. Soc.* **1989,** *111*, 1939-1940.
9. Komori, K.; Sugura, S.; Mizobe, Y.; Yamada, M.; Hidai, M. Preparation and properties of molybdenum and tungsten dinitrogen complexes. 26. Syntheses and some reactions of trimethylsilylated dinitrogen complexes of tungsten and molybdenum. *Bull. Chem. Soc. Jpn.* **1989,** *62*, 2953-3959.
10. Oshita, H.; Mizobe, Y.; Hidai, M. Preparation and properties of molybdenum and tungsten dinitrogen complexes. XLI. Silylation and germylation of a coordinated dinitrogen in cis-$[M(N_2)_2(PMe_2Ph)_4]$ (M = Mo, W) using R_3ECl/NaI and R_3ECl/Na mixtures (E = Si, Ge). X-ray structure of trans-$[WI(NNGePh_3)(PMe_2Ph)_4]\cdot C_6H_6$. *Organomet. Chem.* **1993,** *456*, 213-220.
11. Kawaguchi, M.; Hamaoka, S.; Mori, M. Incorporation of molecular nitrogen into organic compounds. Titanium catalyzed nitrogenation. *Tetrahedron. Lett.* **1993,** *34*, 6907-6910.
12. Mori, M.; Kawaguchi, M.; Hori, M.; Hamaoka, S. Incorperation ofr Molecular Nitrogen into Organic-Compounds – Titanium Catalyzed Nitrogenation. *Heterocycles* **1994,** *39*, 729-739.
13. Hidai, M.; Mizobe, Y., Recent Advances in the Chemistry of Dinitrogen Complexes. *Chem. Rev.* **1995,** *95*, 1115-1133.
14. Mori, M. Activation of nitrogen for organic synthesis. *J. Organomet. Chem.* **2004,** *689*, 4210-4227.
15. Mori, M. Synthesis of Nitrgoen Heterocycles Utilizing Molecular Nitrogen as a Nitrogen Source and Attempt to use Air instead of Nitrogen Gas. *Heterocycles* **2009,** *78*, 281-318.

16. Tanaka, H.; Sasada, A.; Kouno, T.; Yuki, M.; Miyake, Y.; Nakanishi, H.; Nishibayashi, Y.; Yoshizawa, K. Molybdenum-Catalyzed Transformation of Molecular Dinitrogen into Silylamine: Experimental and DFT Study on the Remarkable Role of Ferrocenyldiphosphine Ligands. *J. Am. Chem. Soc.* **2011,** *133*, 3498-3506.
17. Yuki, M.; Tanaka, H.; Sasaki, K.; Miyake, Y.; Yoshizawa, K.; Nishibayashi, Y. Iron-catalysed transformation of molecular dinitrogen into silylamine under ambient conditions. *Nat. Commun.* **2012,** *3*.
18. Ogawa, T.; Kajita, Y.; Wasada-Tsutsui, Y.; Wasada, H.; Masuda, H. Preparation, Characterization, and Reactivity of Dinitrogen Molybdenum Complexes with Bis(diphenylphosphino)amine Derivative Ligands that Form a Unique 4-Membered P-N-P Chelate Ring. *Inorganic Chemistry* **2013,** *52*, 182-195.
19. Miyazaki, T.; Tanaka, H.; Tanabe, Y.; Yuki, M.; Nakajima, K.; Yoshizawa, K.; Nishibayashi, Y. Cleavage and Formation of Molecular Dinitrogen in a Single System Assisted by Molybdenum Complexes Bearing Ferrocenyldiphosphine. *Angew. Chem. Int. Ed.* **2014,** *53* (43), 11488-11492.
20. Liao, Q.; Saffon-Merceron, N.; Mezailles, N., Catalytic Dinitrogen Reduction at the Molybdenum Center Promoted by a Bulky Tetradentate Phosphine Ligand. *Angew. Chem. Int. Ed.* **2014,** *53*, 14206-14210.
21. Liao, Q.; Saffon-Merceron, N.; Mezailles, N. N_2 Reduction into Silylamine at Tridentate Phosphine/Mo Center: Catalysis and Mechanistic Study. *Acs Catal.* **2015,** *5*, 6902-6906.
22. Ung, G.; Peters, J. C. Low-Temperature N_2 Binding to Two-Coordinate L_2Fe0 Enables Reductive Trapping of L_2FeN_2- and NH_3 Generation. *Angew. Chem. Int. Ed.* **2015,** *54* (2), 532-535.
23. Imayoshi, R.; Tanaka, H.; Matsuo, Y.; Yuki, M.; Nakajima, K.; Yoshizawa, K.; Nishibayashi, Y. Cobalt-Catalyzed Transformation of Molecular Dinitrogen into Silylamine under Ambient Reaction Conditions. *Chem. - Eur. J.* **2015,** *21*, 8905-8909.
24. Siedschlag, R. B.; Bernales, V.; Vogiatzis, K. D.; Planas, N.; Clouston, L. J.; Bill, E.; Gagliardi, L.; Lu, C. C. Catalytic Silylation of Dinitrogen with a Dicobalt Complex. *J. Am. Chem. Soc.* **2015,** *137*, 4638-4641.
25. Cammarota, R. C.; Clouston, L. J.; Lu, C. C. Leveraging molecular metal-support interactions for H_2 and N_2 activation. *Coord. Chem. Rev.***2017,** *334*, 100-111.
26. Nishibayashi, Y.; Kuriyama, S.; Arashiba, K.; Nakajima, K.; Tanaka, H.; Yoshizawa, K. Azaferrocene-Based PNP-type Pincer Ligand: Synthesis of Molybdenum, Chromium, and Iron Complexes and Reactivity toward Nitrogen Fixation. *Eur. J. Inorg. Chem.* **2016,** *30*, 4856-4861.
27. Imayoshi, R.; Nakajima, K.; Nishibayashi, Y. Vanadium-catalyzed reduction of molecular dinitrogen into silylamine under ambient reaction conditions. *Chem. Lett.* **2017,** *46*, 466-468.
28. Araake, R.; Sakadani, K.; Tada, M.; Sakai, Y.; Ohki, Y. $[Fe_4]$ and $[Fe_6]$ Hydride Clusters Supported by Phosphines: Synthesis, Characterization, and Application in N_2 Reduction. *J. Am. Chem. Soc.* **2017,** *139*, 5596-5606.
29. Prokopchuk, D. E.; Wiedner, E. S.; Walter, E. D.; Popescu, C. V.; Piro, N. A.; Kassel, W. S.; Bullock, R. M.; Mock, M. T. Catalytic N_2 Reduction to Silylamines

and Thermodynamics of N_2 Binding at Square Planar Fe. *J. Am. Chem. Soc.* **2017,** *139*, 9291-9301.
30. Imayoshi, R.; Nakajima, K.; Takaya, J.; Iwasawa, N.; Nishibayashi, Y. Synthesis and Reactivity of Iron- and Cobalt-Dinitrogen Complexes Bearing PSiP-Type Pincer Ligands toward Nitrogen Fixation. *Eur. J. Inrog. Chem.* **2017,** *32*, 3769-3778.
31. Suzuki, T.; Fujimoto, K.; Takemoto, Y.; Wasada-Tsutsui, Y.; Ozawa, T.; Inomata, T.; Fryzuk, M.; Masuada, H. Efficient Catalytic Conversion of Dinitrogen to $N(SiMe_3)_3$ Using a Homogeneous Mononuclear Cobalt Complex. *ACS Catal.* **2018,** *8*, 3011-3015.
32. Kendall, A. J.; Johnson, S. I.; Bullock, R. M.; Mock, M. T. Catalytic Silylation of N_2 and Synthesis of NH_3 and N_2H_4 by Net Hydrogen Atom Transfer Reactions Using a Chromium P_4 Macrocycle. *J. Am. Chem. Soc.* **2018,** *140*, 2528-2536.
33. Gao, Y.; Li, G.; Deng, L. Bis(dinitrogen)cobalt(-1) Complexes with NHC Ligation: Synthesis, Characterization, and Their Dinitrogen Functionalization Reactions Affording Side-on Bound Diazene Complexes. *J. Am. Chem. Soc.* **2018,** *140*, 2239-2250.
34. Ferreira, R. B.; Cook, B. J.; Knight, B. J.; Catalano, V. J.; Garcia-Serres, R.; Murray, L. J. Catalytic Silylation of Dinitrogen by a Family of Triiron Complexes. *ACS Catal.* **2018,** *8*, 7208-7212.
35. Piascik, A. D.; Li, R.; Wilkinson, H. J.; Green, J. C.; Ashley, A. E. Fe-Catalyzed Conversion of N_2 to $N(SiMe_3)_3$ via an Fe-Hydrazido Resting State. *J. Am. Chem. Soc.* **2018,** *140*, 10691-10694.
36. Burford, R. J.; Fryzuk, M. D. Examining the relationship between coordination mode and reactivity of dinitrogen. *Nat. Rev. Chem.* **2017,** *1*, 26.
37. Yonke, B. Y.; Reeds, J. P.; Zavalij, P. Y.; Sita, L. R., Catalytic Degenerate and Nondegenerate Oxygen Atom Transfers Employing N_2O and CO_2 and a MII /MIV Cycle Mediated by Group 6 MIV Terminal Oxo Complexes. *Angew. Chem. Int. Ed.* **2011,** *50*, 12342-12346.
38. Wang, W. D.; Guzei, I. A.; Espenson, J. H. Hydrolysis, Hydrosulfidolysis, and Aminolysis of Imido(methyl)rhenium Complexes. *Inorg. Chem.* **2000,** *39*, 4107-4112.
39. Hayton, T. W.; Boncella, J. M.; Scott, B. L.; Batista, E. R. Exchange of an Imido Ligand in Bis(imido) Complexes of Uranium. *J. Am. Chem. Soc.* **2006,** *128*, 12622-12623.
40. Michelman, R. I.; Anderson, R. A.; Bergman, R. G. Preparation of monomeric (η^6-arene)OsNR complexes and their exchange reactions with amines, alcohols, and thiols. *J. Am. Chem. Soc.* **1991,** *113*, 5100-5102.
41. Swallow, D.; McInnes, J. M.; Mountford, P. Titanium imido complexes with tetraaza macrocyclic ligands. *J. Chem. Soc., Dalton. Trans.* **1998**, 2253-2260.
42. Chandrasekhar, V.; Boomishankar, R.; Nagendran, S. Recent Developments in the Synthesis and Structure of Organosilanols. *Chem. Rev.* **2004,** *104*, 5847-5910.
43. Lappert, M.; Protchenko, A.; Power, P.; Seeber, A. *Metal Amide Chemistry*. John Wiley & Sons: Chichester, **2009**.

44. Gray, M.; Snieckus, V.; Lebel, H. Lithium hexamethyldisilazane. In *Handbook of Reagents for Organic Synthesis: Reagents for Silocon-Mediated Organic Synthesis*, John Wiley & Sons: Chichester, **2011**.
45. Chandrasekhar, V.; Boomishankar, R.; Nagendran, S. Recent developments in the synthesis and structure of organosilanols. *Chem. Rev.* **2004,** *104*, 5847-5910.
46. Duman, L. M.; Sita, L. R. Closing the Loop on Transition-Metal-Mediated Nitrogen Fixation: Chemoselective Production of $HN(SiMe_3)_2$ from N_2, Me_3SiCl, and X—OH (X = R, R_3Si, or Silica Gel). *J. Am. Chem. Soc.* **2017,** *139*, 17241-17244.
47. van Look, G. *Silylating Agents Derivatization Reagents Protecting-Group Reagents Organosilicon Compounds Analytical Applications Synthetic Applications*. Fluka Chimie AG: Buchs, Switzerland, **1995**.
48. Cao, C.; Fadeev, A. Y.; McCarthy, T. J. Reactions of Organosilanes with Silica Surfaces in Carbon Dioxide. *Langmuir* **2001,** *17*, 757-561.
49. Eikey, R. A.; Abu-Omar, M. M. Nitrido and imido transition metal complexes of Groups 6-8. *Cood. Chem. Rev.* **2003,** *243*, 83-124.
50. Garcia-Viloca, M.; Gelabert, R.; Gonzales-Lafont, A.; Moreno, M.; Lluch, J. M. Temperature Dependence of Proton NMR Chemical Shift As a Criterion To Identify Low-Barrier Hydrogen Bonds. *J. Am. Chem. Soc.* **1998**, 10203-10209.
51. Muller, N.; Reiter, R. C., Temperature Dependence of Chemical Shifts of Protons in Hydrogen Bonds. *J. Chem. Phys.* **1965,** *42*, 3265-3269.
52. Kleckner, I. R.; Foster, M. P. An introduction to NMR-based approaches for measuring protein dynamics. *Biochimica et Biophysica Acta* **2011,** *1814*, 942-968.
53. von Kugelgen, S.; Bellone, D.; Cloke, R. R.; Perkins, W.; Fischer, F. R. Initiator Control of Conjugated Polymer Topology in Ring-Opening Alkyne Metathesis Polymerization. *J. Am. Chem. Soc.* **2016,** *138*, 6234 – 6239.
54. Park, S. Y.; Lee, J.-W.; Song, C. W. Parts-per-million level loading organocatalysed enantioselective silylation of alcohols. *Nat. Chem.* **2015,** *6*, 7512.
55. Armitage, D. A. Organosilanes. In *Comprehensive Organometallic Chemistry*, Queen Elizabeth College, University of London: London, **1982**.
56. Shively, S.; Miller, W. R. The use of HMDS (hexamethyldisilazane) to Replace Critical Point Drying (CPD) in the Preparation of Tardigrades for SEM (Scanning Electron Microscope) Imaging. *Trans. Kans. Acad. Sci.* **2009,** *112*, 198-200.

Chapter 5: Modifications to the Chemical Cycle

5.1 Variation of Reagents and Conditions towards Compatibility

Given the establishment of a completed chemical cycle illustrated in Scheme 4.8, there are significant reason to strive for improvement and optimize each step of the reaction in order achieve a catalytic cycle for N_2 fixation. Besides the modification of reaction conditions such as solvents, temperature, and time, there are two main avenues of exploration that will be discussed below as they relate to the established chemical cycle; substitution of the halogen within the cycle to promote more facile reaction, and modification of the reductant towards more environmentally benign, reagent-compatible, and efficient electron sources. The combination of these factors has led to further progress towards a catalytic cycle by exploring reaction and reagent compatibilities and in the process opened several intriguing avenues of research.

5.2 Halide Substitution, Iodo for Chloro

It is well known that the different reactivities of the halide group are a driving force in many different chemical reactions, and this holds true in organometallic chemistry. If a significant hurdle to N_2 fixation is the initial reduction of the N≡N bond, then determining ways to promote this reaction are of great import. Scheme 2.4 depicts the chemical reduction of the [Mo](VI) dichloride **2.3** by NaHg, passing through the [Mo](III) monochloride intermediate **2.7** to yield the dinuclear end-on-bridged dinitrogen [Mo](II) complex **2.5**; however, different dihalides have different reduction potentials and it was of interest to consider the substitution of the chloride ligands with other halides.[1, 2] Precedent exists for the reduction of early transition-metal diiodides to (μ-N_2) species under more favorable conditions than for analogous dichlorides[3-5]

and due do the larger radius of an I atom versus a Cl atom, a metal-iodo bond would be likely to be longer, and thus weaker, than a corresponding metal-chloro bond.[6] In addition, the Nishibayashi group has recently characterized a series of PNP-pincer ligand supported Mo trihalide and nirido, halide complexes, [(2,6-$(CH_2PtBu_2)_2C_5H_3N$)MoX_3] and [(2,6-$(CH_2PtBu_2)_2C_5H_3N$)Mo(N)X] (X = Br, I, Cl)), of which the iodide derivates demonstrated significant catalytic activity towards the formation of NH_3.[7] With this in mind, the synthesis and characterization of the sterically reduced CPAM iodo-analogues were investigated with the intent of creating a more labile metal-halide bond that might lower reaction barriers and allow for reaction under more mild conditions.

The first target of halide substitution was the Mo(IV) diiodide {Cp*[N(Et)C(Ph)N(Et)]MoI_2} (**5.1**). Initially, it was attempted to generate this species as shown in Scheme 5.1 by the reaction of benzene-d_6 solution of **2.5** and $SiMe_3I$ with N_2O, forming the proposed terminal oxo intermediate **4.1** *in situ* that was reacted with the Me_3SiI to produce **5.1** and $O(SiMe_3)_2$. The immediate product of this reaction displayed paramagnetic resonances by ^{1}H NMR, which were presumed to correspond to **5.1**, and the organic byproducts could easily be removed under reduced pressure. Still, while this did seem to be a promising avenue for a salt-free synthetic route to a diiodide, the synthesis remained somewhat unwieldy due to the multiple steps and

Scheme 5.1

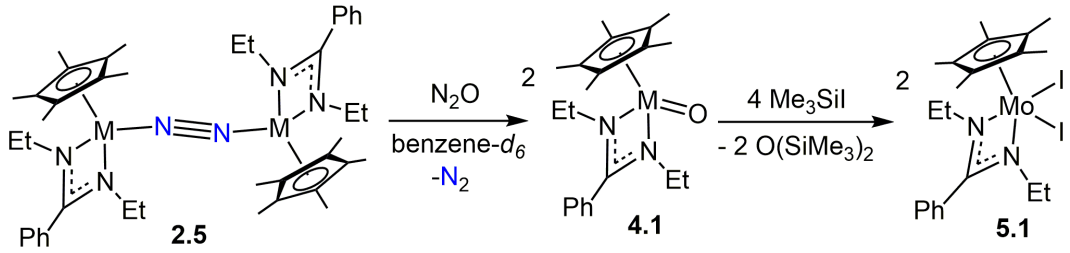

reagents. Exposure of **2.5** to excess I_2 cleanly yields **5.1** upon the displacement of N_2 as is shown in Scheme 5.2, however this is a somewhat counterproductive synthetic method since it discards a dinitrogen unit already coordinated to the metal centers. A more direct route was devised as is shown in Scheme 5.3 where **2.3** was reacted with a slight excess of Me_3SiI in toluene (or benzene-d_6 to follow by ^1H NMR, as is shown in Figure 5.1). Because Me_3SiCl is a more thermodynamically stable product than Me_3SiI, the latter reacts to produce the former by halide exchange between the trimethylsilyl and metal groups and the reaction proceeds in the forward direction,[5, 8] cleanly yielding **5.1** as a red oil which collects at the bottom of the reaction flask.

Unfortunately, due to both its insolubility (in both polar and non-polar solvents)

Scheme 5.2

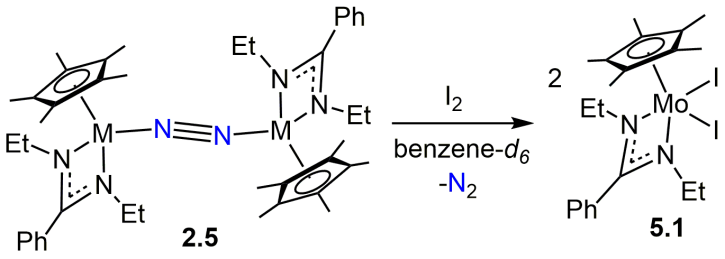

Scheme 5.3

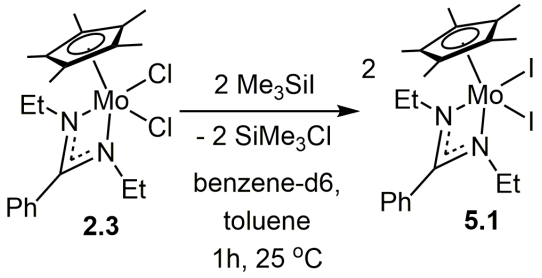

and its oily character, **5.1** could never be successfully isolated or recrystallized for complete characterization by XRD or EA. Still, evidence of its identity can be garnered through yet another synthetic approach, as is shown in Scheme 5.4. The dry hydrolysis reaction of **3.6** in benzne-d_6 using Me_3SiOH and two equivalents trimethylsilyl iodide (Me_3SiI) produces the same organic products, $O(SiMe_3)_2$ and $HN(SiMe_3)_2$, as are seen

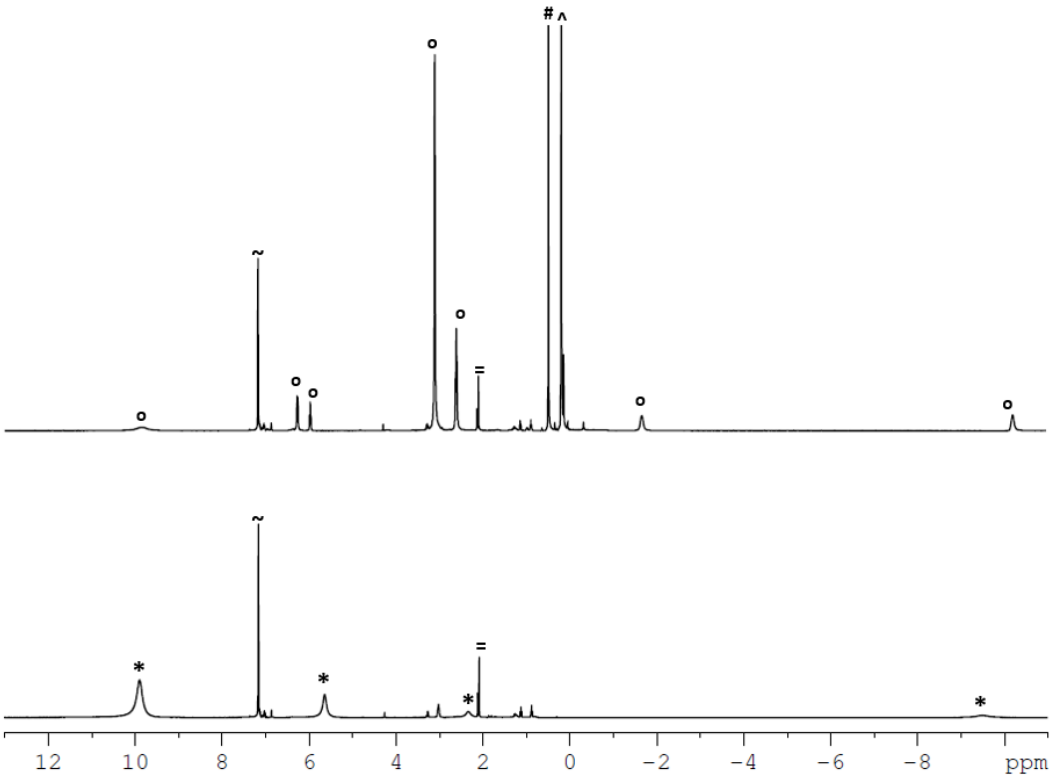

Figure 5.1. Partial ^{1}H NMR (400 MHz, C_6D_6, 25 °C) showing the reaction of **2.3** (*****) with excess Me_3SiI (^) converting to **5.1** (**o**) with the loss of Me_3SiCl (**#**) at room temperature over 1 h

from the Me_3SiCl reaction in Scheme 4.5 but now displays the appropriate ^{1}H NMR signals for diiodide **5.1** rather than the dichloride **2.3**. Mark Wallace was able to synthesize the iPr_2Me diiodide analogue {Cp*[N(iPr)C(Me)N(iPr)]MoI_2} (**5.2**) from the dichloride **1.24** under the same reaction conditions as Scheme 5.3. The success of this reaction also hints at the role that can be played by the silylating agent; substituting Me_3SiI for Me_3SiCl certainly proves success for Step C of Scheme 4.8, the dry hydrolysis, but more generally, it was of interest to investigate whether changing the identity of the halides on the metal centers might be a feasible way to increase the ease with which each portion of the cycle occurs.

In that vein, the substitution of the halide in the nitrido, chloride **3.4** was also investigated – because of the integral role that **3.4** plays in the production of silylimido **3.6** according to Scheme 3.1, could the nitrido, iodo **3.13** be generated that might affect the ease with which **3.6** could be synthesized? In exploratory work conducted by Jocelyn Baer,[9] an equimolar amount of I_2 was added to **2.8** in an ^{1}H NMR scale reaction in benzene-d_6, the result of which appeared to be a C_1 symmetric product with chemical shifts very similar to those of **3.6** as is shown in Figure 5.2. Specifically, the shifts of **3.13** are generally more downfield than those of **3.4** as would be expected for a more shielded chemical environment as a result of the substitution of chloro for iodo ligands. Unfortunately, attempts in to synthesize this material on a preparative scale from solutions of THF or toluene proved fruitless in terms of isolation – though positive results could be achieved for characterization by ^{1}H NMR, the product could not be isolated once solvent (benzene-d_6 for NMR scale reactions or toluene or THF for larger

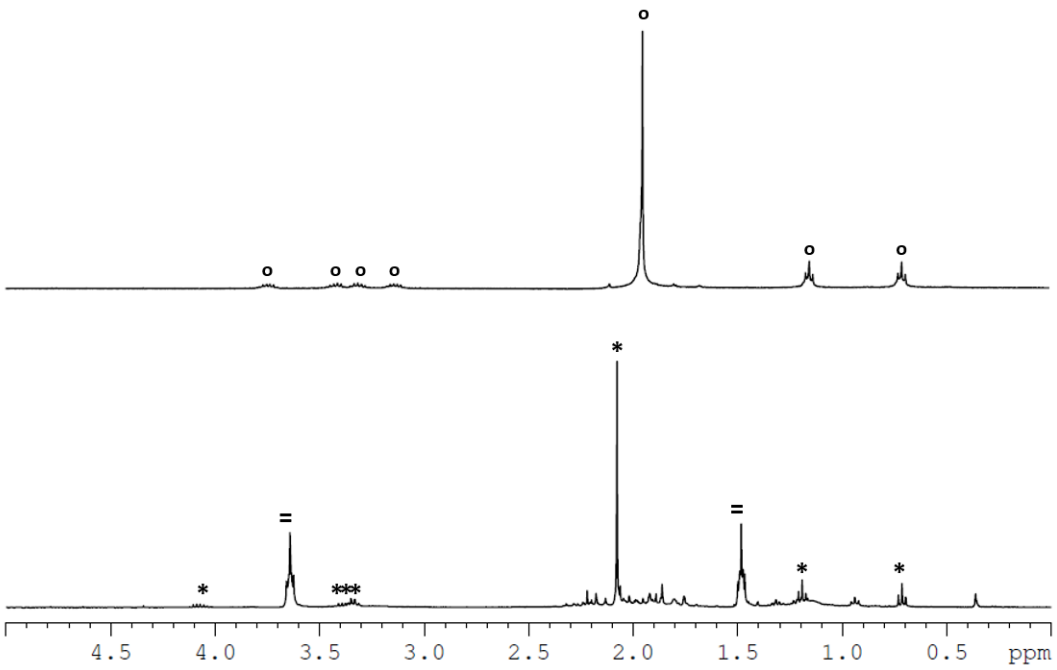

Figure 5.2. Partial ^{1}H NMR (400 MHz, C_6D_6, 25 °C) comparing solutions of (Top) **3.4** (*****) and (bottom) **3.13** (**o**) with THF (=) impurity noted

scale attempts) was removed *in vacuo*. It is possible that **3.13**, unlike the **3.4**, is actually an ion pair $\{Cp^*[N(Et)C(Ph)N(Et)]Mo(N)\}^+[I]^-$ as depicted in Figure 5.3. While in

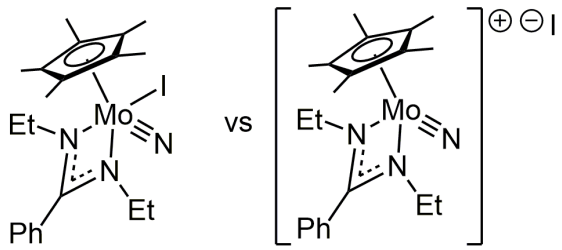

3.13

Figure 5.3. Potential on pair structure of the nitrido iodo **3.13**

solution, this pair might be stabilized by solvent, particularly the polar THF, however once the solvent is removed the molecule appears to decompose as indeed, it cannot be re-observed spectroscopically after the solvent has been removed a second time. Further corroboration of the identity of this product is found in Scheme 3.7 which produces the same shifts associated with **3.13** as a result of the addition of MeI to **2.8**.

Although both iodo-substituted complexes each **5.1** and **3.13** proved intractable and unsuitable for complete characterization for assorted reasons, however their *in situ* formation is still valuable. That they are not isolable is not a setback in the context of a potential catalytic cycle because in that case, each species would exist only transiently at best. Further, the existence of these species, which theoretically should have lower reduction potentials than their chloro analogues, [1-4] begs the question of what else can be done to ease or optimize other reduction steps in the cycle.

5.3 Alternative Reductants to NaHg

The process of reducing N_2, or other molecules in the CPAM chemical cycle, remains the lynchpin of the nitrogen fixation process. For instance, in the cleavage of the N≡N bond, all that is theoretically required are six electrons, but in practice, the

source of these reducing equivalents can vary widely from the transition-metal centers to supporting ligand sets to added chemical reductants. In many nitrogen fixation cycles, extremely harsh or exotic reagents are utilized, such as metallocenes (including cobaltocene, Cp_2Co, decamethyl cobaltocene, Cp^*_2Co, and decamethyl chromocene, Cp^*_2Cr) or KC_8 which often prove incompatible with the Brønsted acid proton sources (such as 2,6-lutidinium triflate, $[2,6\text{-}(CH_3)C_5H_3NH][CF_3SO_3]$, 2,6-lutidinium BArF, $[2,6\text{-}(CH_3)C_5H_3NH]$ $[B(3,5\text{-}(CF_3)_2C_6H_3)_4]$, or diphenylammonium triflate $[Ph_2NH_2]$ $[CF_3SO_3]$) that are necessary to functionalize and release the N-atom product. This incompatibility results in the need for laborious stepwise additions of electrons and protons as opposed to one-pot reactions, and even in instances where the reducing agents and proton sources are compatible, they cannot be recycled and must be used in at minimum stoichiometric amounts.[10-15]

The iPr_2Me CPAM ligand set has been shown to require the very strong reductant KC_8 for group 4 and 5 N_2 reduction[16-18] but the same reduction could be accomplished for group 6 complexes by either KC_8[18] or the somewhat more mild (but still strong)[19] reductant Na/Hg (0.5% w/w).[20] For the sterically reduced Et_2Ph CPAM system, NaHg was initially employed successfully in the conversion of **2.3** to **2.5** although as was noted in Chapter 2, the reaction time to produce **2.5** is one quarter of that required to produce **1.22**,[21] and if reacted longer in the presence of NaHg, **2.5** undergoes undesirable continued reaction to unidentifiable products. If NaHg is a sufficiently strong reductant to reduce the bulkier **1.24**, it may in reality be excessive for the more sensitive **2.3** and a chemical reductant with a lower reduction potential could be more appropriately employed with the same, or even more favorable, results.

To this end, the use of samarium metal (Sm°) was investigated as an abundant, accessible, and recyclable reducing agent and, upon activation by I_2, has been established to be compatible with the CPAM system.

5.3.1 Use of Sm° (2.5% I_2) as a Chemical Reducant

Samarium diiodide (SmI_2) was first reported as a single electron reducing agent by Kagan and co-workers.[22-25] It, and related lanthanide(II) dihalides, have been the subject of research facilitating organic transformations of substrates containing myriad functional groups and in the presence of other chemical reagents. For instance, SmI_2 can be used in tandem with Me_3SiCl in organic reductions such as pinacol couplings of carbonyls.[26, 27] In an example directly relevant to the cycle of Scheme 4.8, a recent system containing Sm°, SmI_2, Me_3SiCl, and DME, the Me_3SiCl was found to activate the surface of the metal to make it a more powerful reductant.[27] In fact, not only is SmI_2 compatible with a number of reagents, but based on the ratio of Sm° to SmI_2 and with the addition of activators such as hexamethylphosphoramide (HMPA), amides, LiX (X = Cl and Br), Me_3SiCl, water, and MeOH, the effective redox potential of the *in situ* generated Sm(II) species can be tuned to a noteworthy degree from -0.9 to -2.8 V (vs saturated calomel electrode) in THF relative to the measured redox potential of Sm° alone which is -2.0 V in 1,2-dimethoxyethane (DME).[28-36] Surprisingly, despite its uses in organic syntheses, SmI_2 and Sm° have only been reportedly used in a handful of instances for organometallic reactions.[37-41] Pointedly, there have been reports of dinuclear,[42, 43] trinuclear,[44] or even tetranuclear[45] Sm(II) (μ-N_2) complexes with at least somewhat reduced N_2 centers,[46] however the N_2 units of these complexes do not undergo N_2 cleavage and are either labile under vacuum or significantly supported by

the specific multiple metal centers and ligand features, so the formation of disamarium dinitrogen complexes in competition with the formation of CPAM dinitrogen complexes was not judged to be of significant concern. Taken together, the tuneability and compatibility of SmI_2 make it an ideal chemical reductant to investigate within the CPAM system that already employs Me_3SiCl and alcohols.[47]

Initial studies were undertaken to replace NaHg in step A of Scheme 4.8 with at least 2 equiv. SmI_2. Preliminary experiments, shown in Scheme 5.4 were conducted using the more sterically shielded iPr_2Me CPAM compound **1.24** with the goal of producing the end-on-bridged dinitrogen complex **1.22** as these compounds are more stable than the sterically un-encumbered Et_2Ph complexes **2.3** and **2.5**. SmI_2 in THF was freshly prepared *in situ* for each reaction by the pretreatment of Sm° with 1,2-diiodoethane according to Scheme 5.4, stirring until a vibrant blue, characteristic of SmI_2 was observed.[48-50] To this solution was then added a solution of **1.24** and reactions were attempted that varied in temperature (-30 °C – 25 °C, -30 °C), reaction time (2 h, 18 h), excess of reductant (3 equiv. SmI_2, 2 equiv. SmI_2), addition of excess Sm° to the reactions (3 equiv. SmI_2 / 3 equiv. Sm°, 2 equiv. SmI_2 / 2 equiv. Sm°), solvent of the

Scheme 5.4

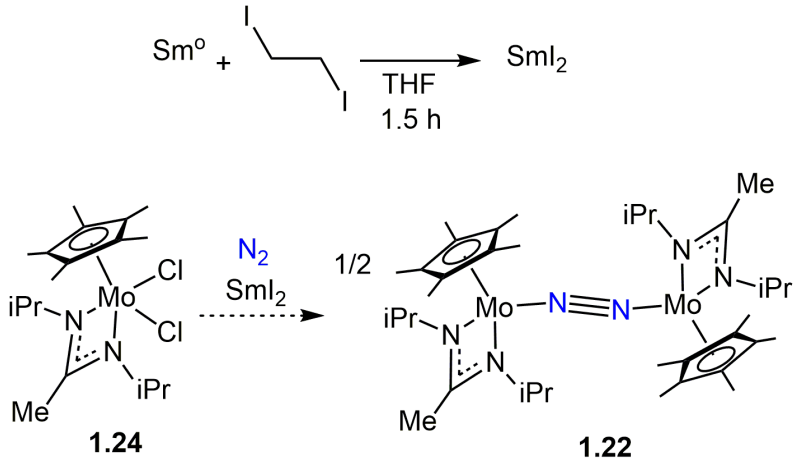

1.24 **1.22**

main reduction (THF, toluene, DME, Et_2O/THF), and even the addition of Me_3SiCl; however, no set of reaction conditions produced any evidence of **1.22**, or any other recognizable species as judged by ^1H NMR of the complex mixture of unidentifiable crude products.

It was hypothesized that, just as allowing the reaction of **2.3** with NaHg for longer than 30 minutes led to overreduction of the product, perhaps even equimolar amounts of SmI_2 could be too harsh of chemical reductant for **1.24**. Accordingly, for the more sensitive Et_2Ph CPAM framework, only substoichiometric amounts of I_2 were added to the Sm° to activate only a small portion of the metal in the reaction at any given time. To accomplish this, a fixed amount of Sm° was stirred at room temperature in THF and pretreated with 2.5 mole % of I_2 to generate Sm° (2.5% I_2). Upon the addition of a chilled THF solution of **2.3**, **2.5** was successfully produced as is shown in Scheme 5.5. Though the Sm° (2.5% I_2) reaction tool three times longer than NaHg to reach the final brown color, close monitoring of the duration of the reaction was still necessary in order to halt the reaction before it formed an unidentifiable mixture of products.

Scheme 5.5

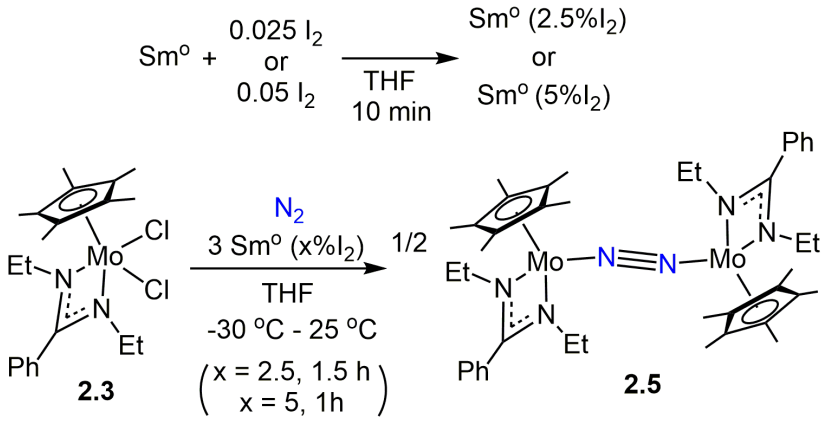

As Scheme 5.5 reveals, pretreating the Sm° with 5 mole % of I_2 (generating Sm° (5% I_2), also accomplished this transformation in a slightly shorter period of time, however a smaller amount of I_2 was preferred because it was thought to have the potential for fewer side reactions. The original conception of the I_2 activated Sm° was to form a small pool of active SmI_2 that would be continuously replenished by the remaining about of Sm° as it is sacrificially consumed to recycle Sm(III) trihalide co-products back to the active Sm(II) reducing species. Although the presence of at least some amount of SmI_2 is indicated by the diagnostic, vibrant blue of SmI_2 in the pre-treated reaction mixtures of Sm° and I_2, its actual mechanistic role remains uncertain. One possibility is that the initially generated SmI_2 does facilitate the reduction of **2.3** to **2.5**, but because it does so on such a small scale and consumes the available SmI_2 quickly, **2.5** does not immediately continue to react deleteriously, helping to control the rate or reduction. Alternatively, it is possible that the role of I_2 is actually very slight, serving only to remove a passivating oxide layer on the metal to expose a highly active Sm° surface at which the reduction occurs more readily. In any event, the attempted N_2 reduction of **2.3** by Sm° in the absence of any iodide, shown in Scheme 5.6, was not found to be successful, indicating that in whatever capacity, iodide *is* a necessary component of the reaction, at least for the Et_2Ph CPAM system.

Scheme 5.6

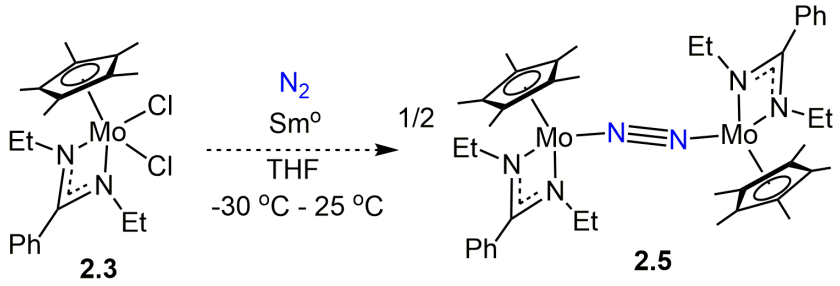

It is therefore conceivable that the use of the diiodide **5.1** as a starting material, instead of dichloride **2.3**, might eliminate the need to pre-treat the Sm° with I_2 altogether. Unfortunately, reactions of **5.1** with either Sm° (2.5%I_2) or Sm° alone, shown in Scheme 5.7, only resulted in the consumption of the starting material without

Scheme 5.7

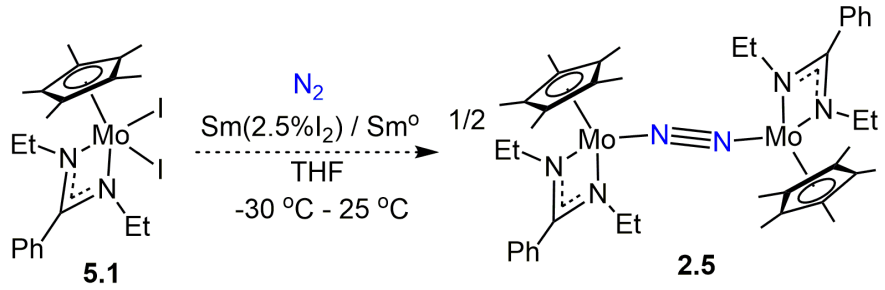

production of **2.5** as observed by ^{1}H NMR. Reactions carried out by Mark Wallace with the bulkier iPr$_2$Me ligand set, however, successfully produced **1.22** using Sm° (5%I_2) with the dichloride **1.24** or the diiodide **5.2**, the latter of which could also be reduced by Sm° in the absence of I_2 activation, as is shown in Scheme 5.8. These reactions were

Scheme 5.8

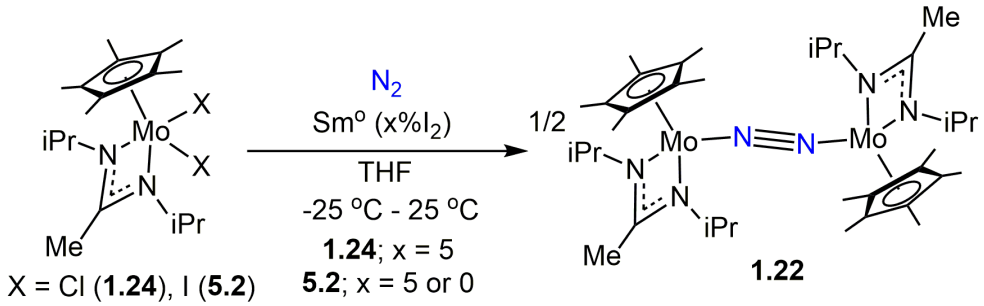

not time sensitive as running them overnight did not have any adverse effects on the formation of **1.22**. Mechanistically, it seems likely that the success of the reduction of **1.24** is a result of the increased steric shielding. The bulkier N-atom substituents of the iPr$_2$Me complexes allows N_2 to undergo coordination and reduction at the Mo centers. Conversely, the Mo centers of the Et$_2$Ph complexes may not shielded enough to

facilitate this coordination and reduction, especially with the greater reactivity of the iodo complexes. Finally, according to Scheme 5.9, Sm° (2.5%I_2) was shown to reduce **3.4** to **2.8** in even better yield than NaHg and, as an extension of this observation, **3.6** can be synthesized cleanly and quantitively from **3.4** via Sm° (2.5%I_2) and Me_3SiCl. Overall, this work represents a novel use of Sm° and SmI_2 reductants in organometallic chemistry and particularly in dinitrogen fixation.

Scheme 5.9

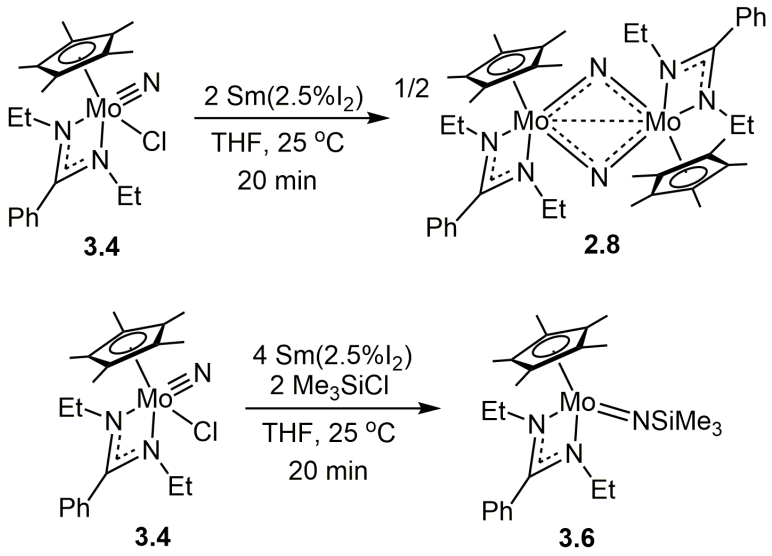

5.4. Attempted One-Pot Formation of the Silylimido

To convert the chemical cycle of Scheme 4.8 to a catalytic system, the compatibility of each step with the others is paramount. Additionally, in order to have perfect atom economy and increased chemical efficiency, it would be ideal to be able to convert **2.3** to **3.6** quantitively and *in situ*. Based on the established chemistry from Chapter 3.2.2, the heated reaction of a hydrocarbon solution of **3** with Me_3SiCl produces a 2 : 1 ratio of **3.6** : **2.3** with the overall loss of an N_2 unit. While **1** can in theory be recycled back to **2.5** and in a closed system, N_2 would not be lost to the atmosphere thus formally making up for the deficiency in atom economy, a one-pot

process that quantitively produces **3.6** without complicated or deleterious side reactions would be preferable over the current step-wise approach.

5.4.1 Via NaHg

A general pathway for this process is laid out in Scheme 5.10 which shows a combination of Steps A and B from Scheme 4.8. The initial N_2 reduction of **2.3** to **2.5** by NaHg was modified for temperature, reagent compatibility, and solvent based on the requirements of the next step, silylation of **2.5** by Me_3SiCl. It has been noted in Chapter 2.2 that the reaction can successfully be run at room temperature instead of requiring initial cooling to -30 °C. It was of interest then to run the reaction at an elevated temperature, something that would be required to facilitate step B in a reasonable period of time. Reacting a THF solution of **2.3** with NaHg at 40 °C for 15 minutes showed only unreacted starting material but running the reaction for longer did result in the formation of some **2.5**. This transformation was much faster than the

Scheme 5.10

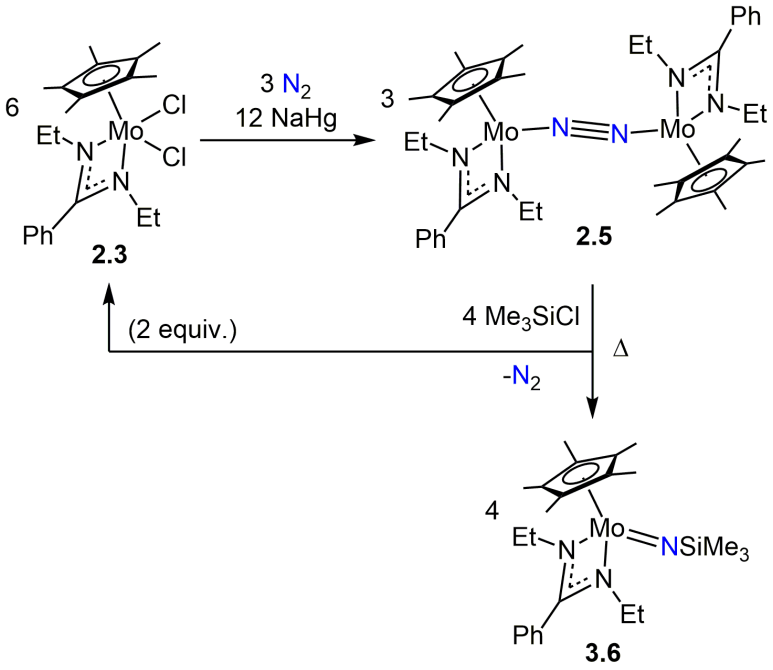

cooled or room temperature transformations and did not pass through an obvious blue color indicative of the formation of **2.7**. Furthermore, ^{1}H NMR of the crude product revealed a significant amount of what appears to be the amidine resulting from the loss of the amidinate, which is not ideal. Next, the reduction was attempted in the presence of Me_3SiCl because this compatibility is essential if a catalytic cycle is ever to be developed. Fortunately, the reaction was at least partially successful; warming from -30 °C to room temperature over 30 min, ^{1}H NMR of the crude products showed **2.5**, but **2.5** was accompanied by an unknown C_s species. Running the same reaction at room temperature increased the ratio of **2.5** but the new species remained, shown in Figure 5.4; the unknown product appears contain some kind of TMS group as judged by the presence of the large singlet in the upfield region of the spectra. These species could not be separated by recrystallization in pentane. As a control, a benzene-d_6 solution of Me_3SiCl was monitored by ^{1}H NMR in the presence of NaHg which only

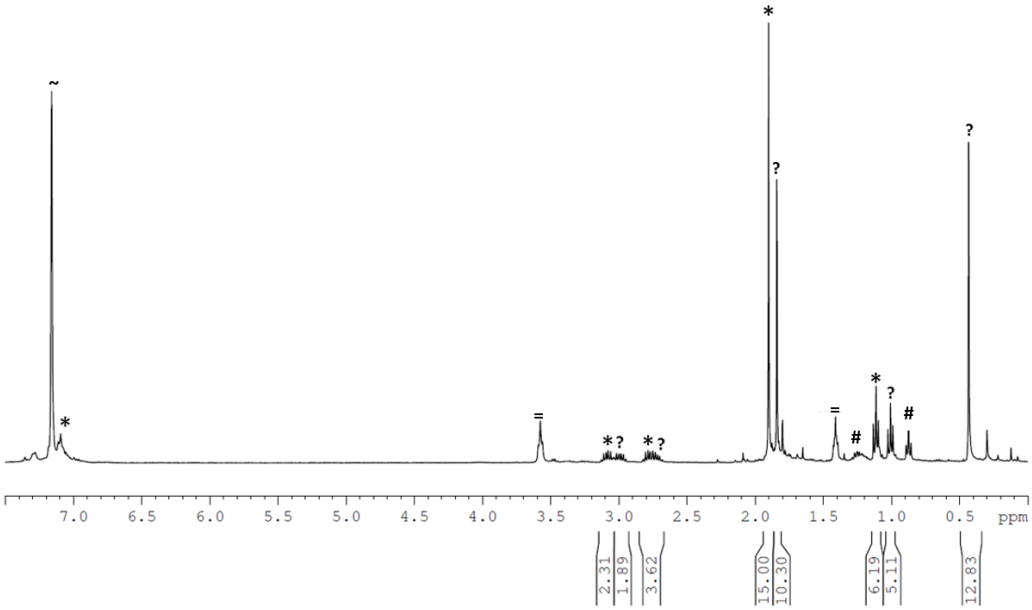

Figure 5.4. Partial ^{1}H NMR (400 MHz, C_6D_6, 25 °C) showing **2.5** (*****) and an unknown species (**?**) in in benzene-d_6 (**~**), the result of the N_2 reduction of **2.3** by NaHg in THF with Me_3SiCl. Pentane (**#**) and THF (**=**) residual solvent impurities noted

very slowly produced $O(SiMe_3)_2$ even at elevated temperature which indicates that the reagents are generally compatible and are not themselves responsible for these new species. As was discussed in Chapter 3.2.2, Step A of Scheme 4.8 has traditionally been run in the ethereal solvent THF, but this is known to impede the successful reaction of Step B which requires a hydrocarbon solvent to yield **3.6**. Therefore a 10 : 1 mixture of toluene : THF was utilized for the initial reduction (the reaction in pure toluene produced no recognizable products at all). Surprisingly, with the addition of Me_3SiCl, this reaction proceeded in the same way as the THF solution, albeit on a much slower time frame resulting in equal parts **2.5** and the unknown silylated product after stirring overnight. This again implies that NaHg in THF may be an unnecessarily strong reductant and solvent combination for this step. While each of these reactions were at least partially successful on their own, so far, reactions that combine the changes in these variables have not yet yielded **3.6**. This does not mean that such an *in situ* reduction and N-atom silylation is impossible, but simply that methodical study is advisable to continue to hone in on the optimal reaction conditions.

5.4.2 Via Sm° (2.5%I_2)

A related avenue of investigation was whether Sm° (2.5%I_2) could be employed to increase the efficiency of formation of **3.6** from Step B of Scheme 4.8; if **2.5** could be replaced by Sm° (2.5%I_2) as a sacrificial reductant in recycling **3.4** to **2.8**, then the loss of N_2, and perhaps even the issues of THF incompatibility, could be avoided altogether.[47] It was therefore necessary to determine if the thermal conversion of **2.5** with Me_3SiCl into a 2 : 1 mixture of **3.6** : **2.3** would be any different in the presence of Sm° (2.5%I_2). According to Scheme 5.11, there was no change in the amount of **3.6**

Scheme 5.11

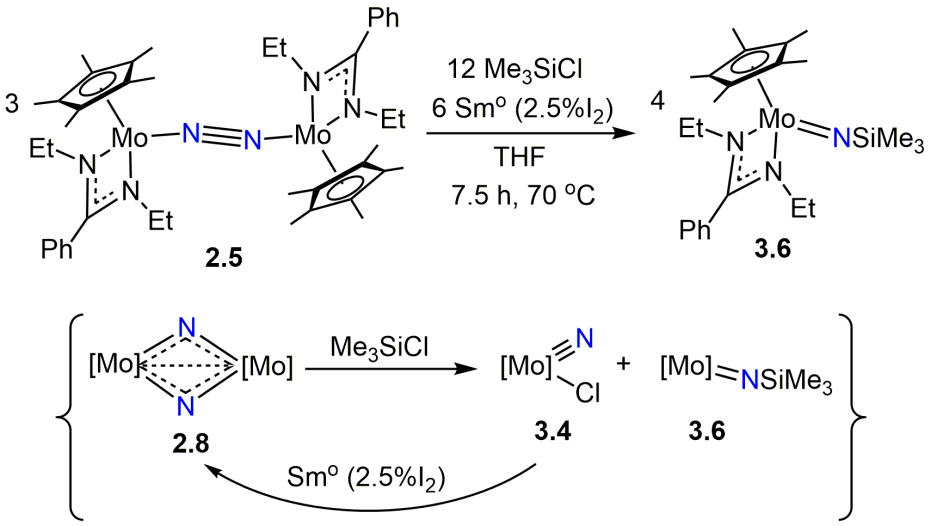

recovered which, at 64%, remains at 2/3, the same as Step B. This was surprising. (2.5%I_2) has already been described as an appropriate replacement for NaHg in the formation of quantitive amounts of **2.8** from **3.4** and this reaction occurs nearly instantaneously - certainly faster than the reduction of **3.4** by **2.5** which requires 21 h. Because of this, the reactivity depicted in the lower half of Scheme 5.11 was expected to take precedence, leading to the quantitive formation of **3.6** by reducing all **3.4** via Sm° (2.5%I_2) as soon as it was formed and thus precluding its reduction by **2.5** instead. While it is unfortunate that, based on the recovered yield of **3.6**, Sm° (2.5%I_2) does not, in fact, compete with **2.5** for the reduction of **3.4** under these conditions, is not to say that under *other* conditions (varying solvent, activator presence, and reagent concentrations) the redox potentials of the reductants might be modulated appropriately to accomplish the desired quantitive conversion to **3.6**. Furthermore, it is at least useful to confirm that the presence of Sm° (2.5%I_2) does not impede the formation of at least some **3.6** reaction and will not likely be detrimental to the complicated, cumulative N_2 fixation process.

5.5 Combining It All: One-Pot Dry Hydrolysis with Sm° (2.5%I_2)

With knowledge that Sm° (2.5%I_2) was likely to be compatible with the Me_3SiCl and protic reagents of Step C of Scheme 4.8, the dry hydrolysis reaction was coupled with the formation of **3.6** from the reduction of **3.4** to **2.8** by Sm° (2.5%I_2) according to Scheme 5.12.[47] The reaction was run in THF-d_8 on a preparative scale, an

Scheme 5.12

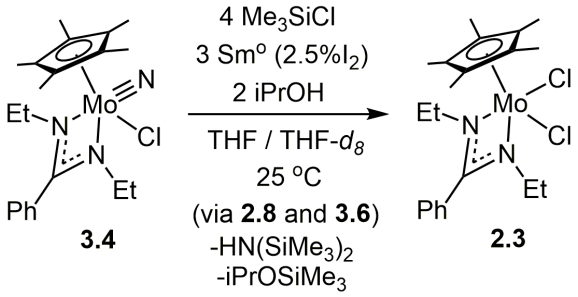

aliquot of which clearly showed the production of **3.6** as an intermediate prior to the dry hydrolysis process, and on an NMR scale as is shown in Figure 5.5 which allows for easy analysis of the reaction progress. An initial ^1H NMR established integrations of **3.4** and Me_3SiCl relative to the cyclododecane standard. Only 5 minutes after the addition of iPrOH to the mixture of **3.4**, Sm° (2.5%I_2), and Me_3SiCl, about half of the **3.4** had been consumed and trace amounts of the reactive intermediate **3.6** are visible along with significant amounts of **2.3**, $HN(SiMe_3)_2$, and $iPrOSiMe_3$. Intriguingly, one hour after the start of the reaction, the **2.3** has disappeared from the spectra (presumably having reacted unproductively with Sm° and Sm halide byproducts or having been converted briefly to **2.5** before undergoing undesirable reaction). Cyclododecane was chosen as the standard for this reaction to eliminate even the remote chance that durene could react with the Sm species and relative to this standard after 1h, $HN(SiMe_3)_2$ was observed in high (85%) yield relative to the amount of **3.4** from which the reaction

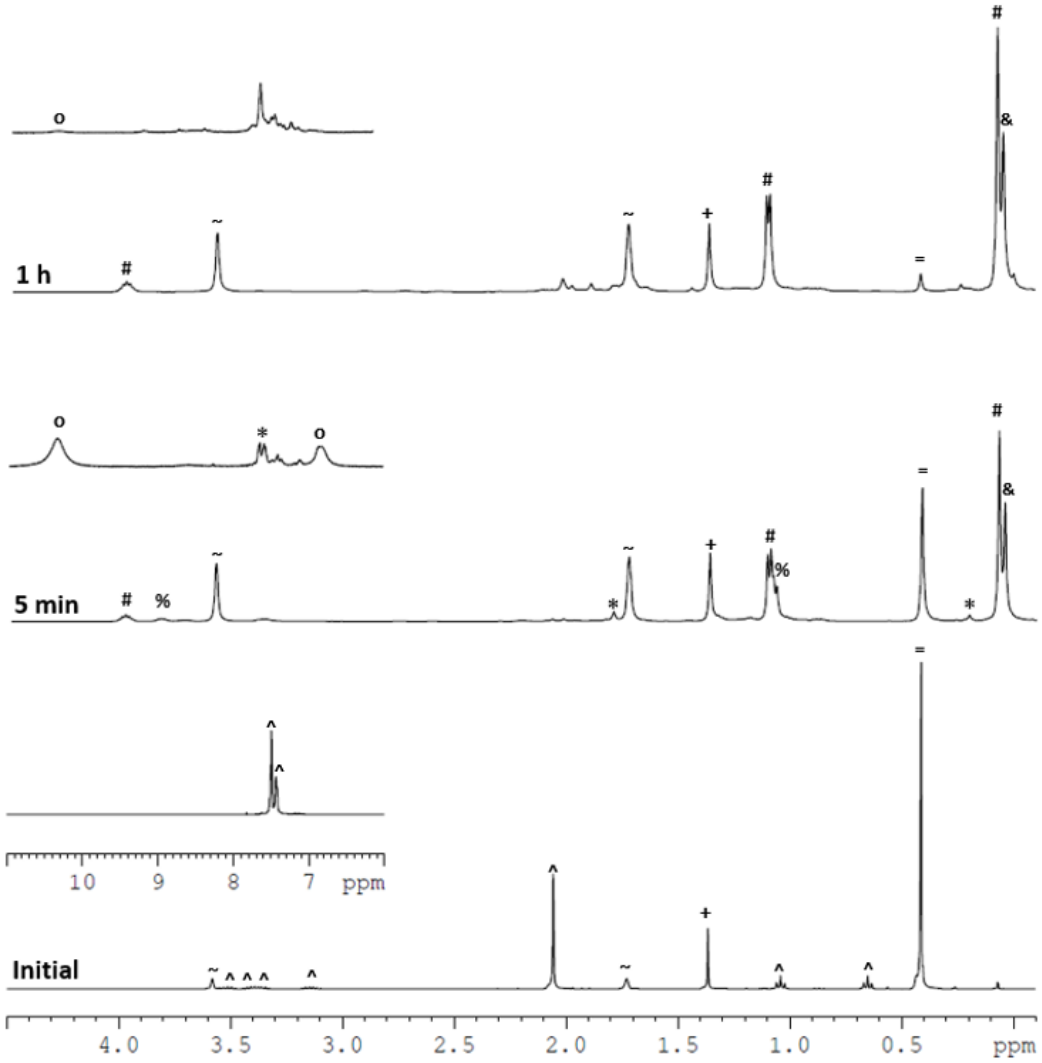

Figure 5.5. Partial ^{1}H NMR (400 MHz, THF-d_8, 25 °C) showing **3.4** (^) with Me_3SiCl (=) and a cyclododecane internal standard (+) (bottom) reacting with Sm° (2.5% I_2) in THF-d_8 (~) and iPrOH (**%**) to produce **3.6** (*) as an intermediate with $HN(SiMe_3)_2$ (**&**), $(CH_3)_2CHOSiMe_3$ (#), and **2.3** (**o**) (middle) before **2.3** is consumed by subsequent reaction leaving only the organic products (top)

began. A preparative scale version of this reaction was completed and the volatiles were vacuum transferred and analyzed by GC-MS to confirm the identities of the organic products. This reaction now demonstrates the compatibilities between the CPAM complexes **3.4**, **2.8**, **3.6**, the reductants Sm° and Sm° (2.5%I_2), the reagents Me_3SiCl and iPrOH, and the organic products $HN(SiMe_3)_2$ and $iPrOSiMe_3$.[47] This represents no

small feat in terms of reconciling each step of Scheme 4.8 and bodes very well for the continued progress towards eventual development of a catalytic N_2 fixation process.

5.6 Quantification of $HN(SiMe_3)_2$ as NH_4Cl

Finally, one of the most important aspects of a chemical process is the reliable quantification of the product formed relative to the starting material. For years, the analysis of NH_3 (either as the main product of catalysis or as a subsequent product of $N(SiMe_3)_3$) was carried out through a labor-intensive spectroscopic process known as the indophenol method. In this colorimetric determination, NH_3 or NH_4Cl is converted to indophenol ($OC_6H_4NC_6H_4OH$) which has a bright blue color (maximum absorbance = 625 nm) and its concertation can be determined based on the Beer Lambert Law.[14, 51-53] More recently, some groups including those of Schrock[14] and Nishibayshi,[54] have begun to acidify their $N(SiMe_3)_3$ products to NH_4Cl (or in some cases ^{15}N-labeled products) and judge the yield by ^1H NMR against an internal standard by integration. In order to improve the accuracy of judging overall $HN(SiMe_3)_2$ production for the CPAM system, a preliminary quantification method was developed merging the results of the reaction from Scheme 5.12 with the acid work-up depicted in Scheme 5.13.

Scheme 5.13

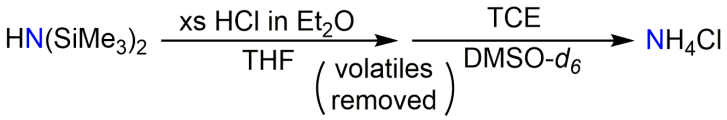

The first step was to confirm a method to convert known $HN(SiMe_3)_2$ to recognizable NH_4Cl. An authentic sample of $HN(SiMe_3)_2$ was prepared in a J Young NMR tube in 0.6 mL DMSO-d_6 which, by ^1H NMR, appeared as a singlet at $\delta = 0.01$ ppm. Directly to this sample was added an excess of HCl in Et_2O which caused a white

precipitate to appear immediately in the upper of the two immiscible solution layers. The upper, ethereal layer of solvent was carefully removed under reduced pressure and a subsequent ^{1}H NMR of the lower DMSO-*d*$_6$ layer revealed a very broad resonance at δ = 7.45 ppm. This broad singlet matched a control sample of authentic NH_4Cl in DMSO-*d*$_6$. Theoretically, despite some amount of quadripolar broadening, NH_4Cl should be a 1 : 1 : 1 triplet due to the spin of ^{14}N (I = 1), but the lack of distinction in the signal in this case was likely due to exchange with trace amounts of water or a slight excess of HCl in the sample. Finally, the addition of 1,1,2,2-tetrachloroethane (TCE) showed the addition of a sharp singlet at δ = 6.95 ppm by ^{1}H NMR but otherwise caused no further reaction, confirming that TCE is a suitable internal standard. A reaction was then carried out on an NMR scale in THF-*d*$_8$ according to Scheme 5.12 and upon confirmation by ^{1}H NMR that the reaction had run to completion, excess HCl in Et_2O was added to the sample initially causing white precipitate to form but quickly resolving to a muddy-looking solution. All of the volatiles were removed under reduced pressure, during which significant care was taken to avoid bumping, and the resulting brown solid was dissolved in DMSO-*d*$_6$ to which was added the 10.0 μL TCE standard. Unfortunately, ^{1}H NMR of the resulting inhomogeneous mixture (which contained solid Sm° in addition to various Mo and Sm byproducts) was broadened beyond recognition, much less quantification purposes, and so an *in situ* acidolysis process was abandoned for the reaction.

A vacuum transfer process was therefore developed to reliably separate out the organic products ($HN(SiMe_3)_2$ and $iPrOSiMe_3$) from the metal co-products. In an effort to minimize head space which could limit the success of such a transfer, a device was

assembled out of thick-walled hosing and glassware to facilitate vacuum transfer from one J Young NMR tube directly into another. As is shown in Figure 5.6, the THF reaction would be run in one tube, (A), and then the volatiles would be transferred to the next tube, (B), leaving solids in the first tube and isolating the organic products in the second for acid workup according to Scheme 5.13. The system was tested with a known amount of $HN(SiMe_3)_2$ and, following vacuum transfer for one tube to the other on the apparatus, acid workup by HCl, removal of volatiles *in vacuo*, preparation in DMSO-d_6, and addition of an equimolar amount of the TCE standard, a quantitive amount (99.5%) of NH_4Cl was found to be in the sample according to the integration

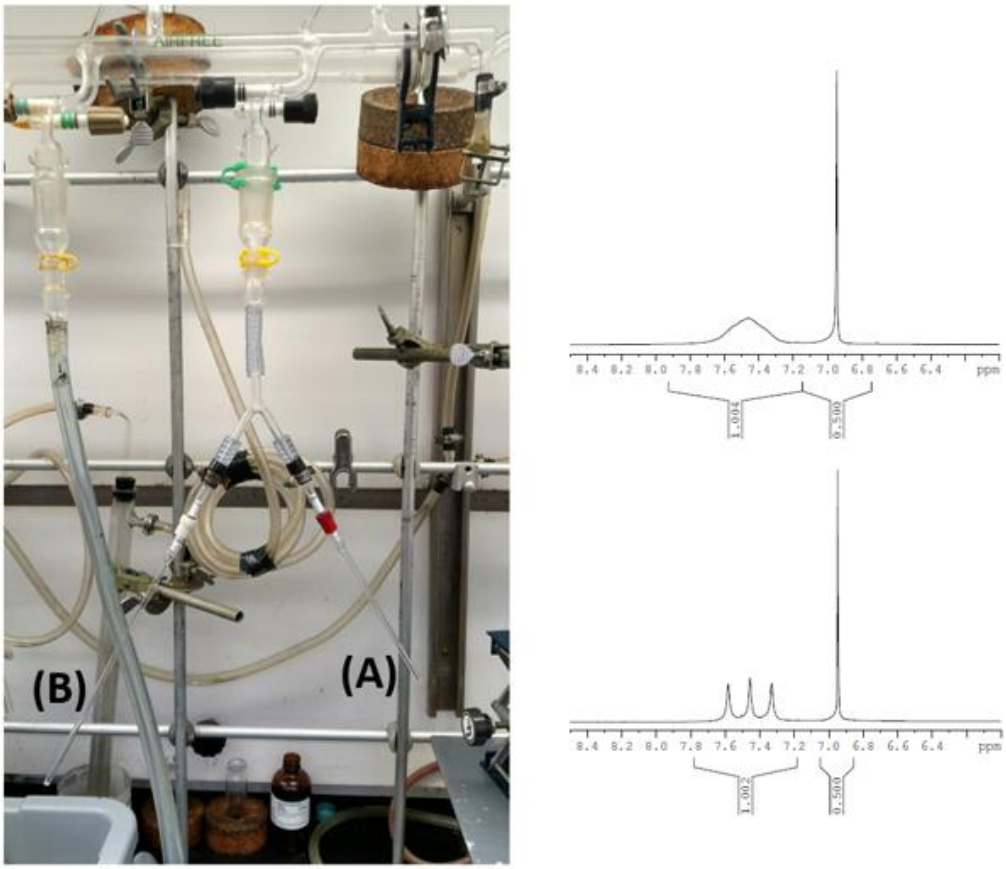

Figure 5.6. (Right) Vacuum transfer apparatus for transfer of organics from tube (A) to tube (B). (Left) Partial ^1H NMR (400 MHz, C_6D_6, 25 °C) showing the NH_4Cl signal relative to the TCE standard as a broad singlet due to exchange (top) and resolved to a triplet after vacuum (bottom)

shown in Figure 5.6. The NH_4Cl signal initially appeared again as a broad singlet, however after returning the sample to vacuum for 2 h (enough time to remove any residual water or HCl from the sample but not to significantly affect the amount of solvent or standard due to their high boiling points) the signal resolved into a triplet which did not affect the signal's integration.

Three trials of this process were carried out in total yielding an average quantification of 96.7% NH_4Cl quantified relative to the starting $HN(SiMe_3)_2$ and though there was some level on inconsistency in this transfer method, the process was deemed suitable to apply to the organometallic reaction. The reaction of Scheme 5.12 was again carried out in two identical NMR scale reactions in THF which were then vacuum transferred and acidified with excess HCl. Unfortunately, following the quantification process, the yields were determined at 50% and 23%. Not only are these yields much lower that the theoretical yield of the dry hydrolysis process (100%) and the experimental yield based on a cyclododecane standard (85%), but the magnitude of variation between these quantifications more than triple the variation of the trial vacuum transfer quantifications (± 27% compared to ± 7%). This could be explained at least partially by difficulties encountered in transferring the reaction transfer which were not present for the transfer of $HN(SiMe_3)_2$ alone; bumping of the inhomogeneous solution was more frequent and difficult to limit, it was much harder to determine when all of the volatiles had completely transferred due to the residue inside the reaction tube blocking visual assessment, and the oily residue could itself have been trapping some volatiles, delaying their transfer to the quantification tube. All told, although this process is clearly in need of further attention and optimization, it once again confirms

the presence of the silylamine product of Scheme 5.12 and, with further refinement, offers the beginnings of a new and eventually reliable way to quantitively assess the success of the CPAM N_2 fixation reactions.

5.7 Conclusions

In sum, modifications and improvements have been made for each step of Scheme 4.8 which again illustrate the unusual versatility and tuneability of the CPAM framework. The substitution of the halide in the CPAM products has been investigated with the exchange of iodide for chloride ligands which does seem to increase reactivity, although with the sterically reduced CPAM ligand framework, this increase may be too great to study the reactions in significant depth. Within the concepts of an iodo-based cycle, I_2 activated Sm° (Sm° (2.5%I_2)) has been introduced as a novel chemical reductant that can accomplish N_2 coordination and N-atom functionalization within the already established reactions. This reductant has the potential to be recycled and is significantly greener than alterative reductants such as NaHg. Furthermore, (Sm° (2.5%I_2) is appropriate not only for the initial reduction of N_2, but critically, *it is compatible* with the rest of the cycle including the silylating agent, Me_3SiCl, and most excitingly, the readily available proton source, alcohol. With these discoveries, a new chemical cycle is established as is shown in Scheme 5.14 in which each step is (theoretically, if not yet in practice), compatible with the others. Additionally, a process for the conversion of $HN(SiMe_3)_2$ into NH_4Cl was described which, although still in the nascent stage, promises to eventually be able to reliably quantify the results of the CPAM cycle's N_2 fixation. Upon the further investigation and variation of the solvents,

Scheme 5.14

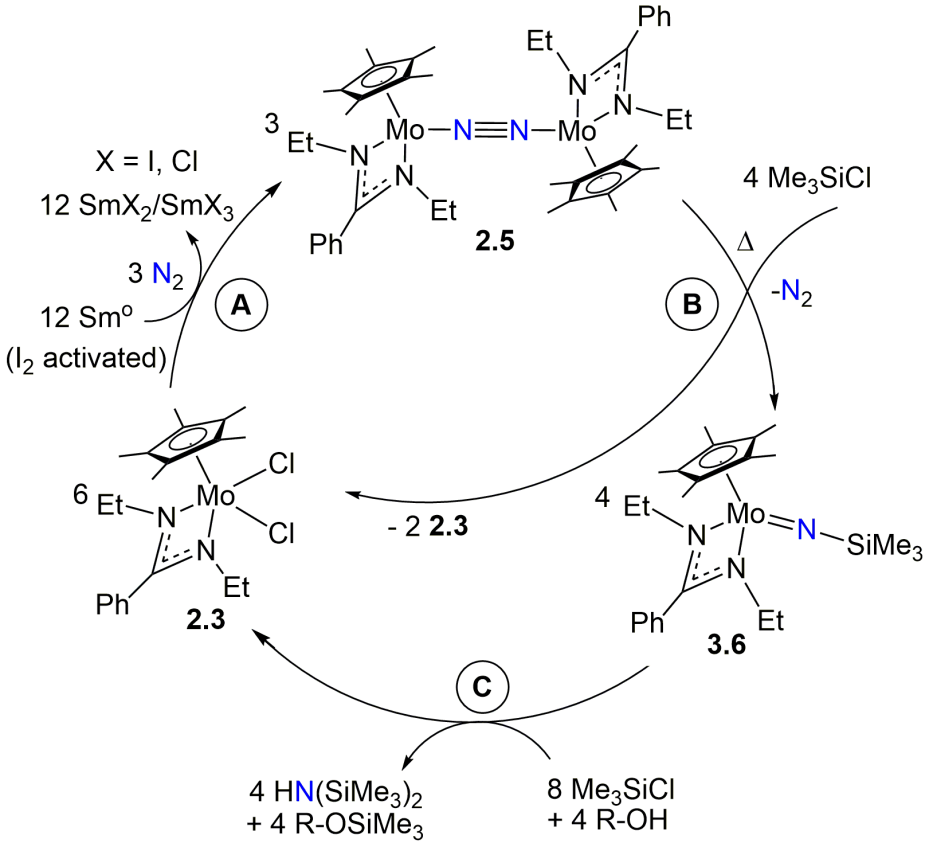

temperatures, and stoichiometries of reagents, the reactivities of each step may very well be tuned with enough specificity to accomplish a one-pot, catalytic process that requires minimal energy and proceeds with high atom economy.

5.8 Experimental Details

5.8.1 General Considerations

All manipulations of air and moisture sensitive compounds were carried out under an N_2 atmosphere with standard Schlenk or glovebox techniques. Et_2O and THF were distilled from Na/benzophenone under N_2 prior to use. Toluene and pentane were dried and deoxygenated by passage over activated alumina and GetterMax® 135

catalyst (purchased from Research Catalysts, Inc.) within a PureSolv solvent purification system manufactured by Innovative Technologies (model number PS-400-4-MD) and collected under N_2 prior to use. Benzene-d_6, toluene-d_8, and THF-d_8 were dried over Na/K alloy and isolated by vacuum transfer prior to use. DMSO-d_6 was dried over CaH, distilled under reduced pressure, and stored over activated 4 Å molecular sieves. Celite© was oven dried (150 °C for several days) prior to use. Cooling was performed in the internal freezer of a glovebox maintained at -30 °C. Trimethylsilyl chloride, trimethylsilyl iodide, trimethylsilanol, iodine, $HN(SiMe_3)_2$, NH_4Cl, and HCl/Et_2O were purchased from Sigma Aldrich and used as received. iPrOH was purchased from PHARMCO-AAPER, dried over $MgSO_4$, and distilled under N_2 prior to use. 1,1,2,2-tetrachloroethane was purchased from Sigma Aldrich, dried over $MgSO_4$, and distilled under reduced pressure prior to used. $[N(n\text{-}Bu)_4][B(C_6F_5)_4]$[60, 61] was prepared according to previous reports in similar yield and purity. All room temperature ^1H NMR spectra were recorded at 400 MHz and referenced to $SiMe_4$ using residual ^1H chemical shifts of benzene-d_6, toluene-d_8, THF-d_8, and DMSO-d_6. Gas chromatography measurements were performed on an Agilent 6890N system coupled with a JEOL high resolution magnetic sector mass spectrometer (JMS-700 MStation) with the EI ion source (70 eV). The mass spectrometer was operated in the mode of high scan speed and low resolution (1000) with the mass range from 50 to 500 daltons. The silica capillary column (Agilent DB-5, 60 m length, 250 μm I.D., 0.10 μm film) was used in the experiments with helium (at 1 mL/min) as the carrier gas. Analysis was performed as follows: injection volume = 1 μL, split mode (ratio=10), the front inlet temperature = 220 C, the column temperature was

programmed from 30 °C at 3.0 min, then increased to 250 °C at the rate of 10 °C/min and then held at 250 °C for another 5.0 minutes. Fragmentation patterns obtained by EI were used to identify the structures of the ions observed in the mass spectra based on the NIST Spectral Database.

5.8.2 Synthesis of New Compounds

Cp*[N(Et)C(Ph)N(Et)]MoI$_2$ (5.1). 2.3 (51.0 mg, 0.107 mmol) was dissolved in 5 mL toluene and stirred at 25 °C, to which was added Me_3SiI (45.6 μL, 0.321mmol) via micro syringe. After 16 hours, volatiles were removed *in vacuo* affording a dark maroon crystalline solid washed in pentane, **5.1** (64.1 mg, 91 % yield). ^{1}H NMR (400 MHz, C_7D_8, 25 °C) -10.23 (2H, br s, C*H*$_2$(CH$_3$)), -1.25 (2H, br s, C*H*$_2$(CH$_3$)), 2.57 (6H, br s, CH$_2$(C*H*$_3$)), 3.20 (15H, br s, C$_5$(C*H*$_3$)$_5$)), 6.00 (1H, t, J = 7.3, C(C$_6$*H*$_5$)), 6.32 (2H, d, J = 7.3, C(C$_6$*H*$_5$)), 9.78 (2H, br s, C(C$_6$*H*$_5$)).

Cp*[N(Et)C(Ph)N(Et)]Mo(N)I (3.13). 2.8 (49.2 mg, 0.0585 mmol) was dissolved in 3 mL THF to which was added a solution of I_2 (11.2 mg, 0.0884 mmol) in THF causing the dark brown solution to become immediately dark orange. The mixture was stirred for 1 h at 25 °C, after which volatiles were removed *in vacuo* to yield a dark brunneous-orange solid that was filtered through a kimwipe and celite plug in a pipet and washed in pentane, **3.13** (61.2 mg, 96 %). ^{1}H NMR (400 MHz, C_6D_6, 25 °C): 0.65 (3H, t, J = 7.0 Hz, CH$_2$(C*H*$_3$)) 1.13 (3H, t, J = 7.1 Hz, CH$_2$(C*H*$_3$)), 2.01 (15H, s, C$_5$(C*H*$_3$)$_5$), 3.23 – 3.32 (2H, m, C*H*$_2$(CH$_3$)), 3.26 – 3.36 (1H, m, C*H*$_2$(CH$_3$)), 3.96 – 4.06 (1H, m, C*H*$_2$(CH$_3$)), 6.86 – 7.13 (5H, m, C(C$_6$*H*$_5$)).

5.8.3 Supporting Syntheses, NMR, CV, and GC-MS Experiments

Reaction of 2.5 with N_2O and Me_3SiI. 2.5 (4.0 mg, 4.8 μmol) was dissolved in 0.6 mL of benzene-d_6 in an NMR tube with a durene standard (0.5 mg, 4 μmol) to which was added Me_3SiI (3.0 μL, 21 μmol) and an initial ^1H NMR was taken. As observed by ^1H NMR, no reaction occurred until the tube was charged with N_2O (10 psi) at which point the brown solution quickly became orange and an immediate ^1H NMR showed **5.1** had formed along with $O(SiMe_3)_2$.

Reaction of 2.5 with I_2. 2.5 (7.5 mg, 8.9 μmol) was dissolved in 0.6 mL of benzene-d_6 in an NMR tube to which was added I_2 (4.3 μL, 34 μmol) and the solution quickly changed from an orange brown to red as an oil began to settle on the bottom of the tube. ^1H NMR confirmed the presence of **5.1**.

Reaction of 2.3 with Me_3SiI followed by ^1H NMR. 2.3 (11.0 mg, 23.0 μmol) was dissolved in 0.6 mL of benzene-d_6 in an NMR tube with a durene (0.5 mg, 4 μmol) standard. To this was added Me_3SiI (10.0 μL, 70.3 μmol) and the orange solution grew vibrantly reddish-orange. After sitting at room temperature for 21 h, **5.1** was confirmed to have cleanly formed along with Me_3SiCl by ^1H NMR. See Figure 5.1 for relevant spectra.

Reaction of 3.6 with Me_3SiOH and Me_3SiI followed by ^1H NMR. 3.6 (3.0 mg, 6.1 μmol) was dissolved in 0.6 mL of benzene-d_6 in an NMR tube with a durene (1.0 mg, 7.5 μmol) standard and Me_3SiOH (1.0 μL, 9.0 mmol). To this was added Me_3SiI (2.0 μL, 14 μmol) causing the solution to change from a brown-purple to a marron- orange. ^1H NMR confirmed the consumption of the starting material and the production of **5.1**, $HN(SiMe_3)_2$, and $O(SiMe_3)_2$.

Reduction of 2.3 by Sm° (2.5% I_2). 2.3 (50.0 mg, 0.105 mmol) was dissolved in 4 mL THF and chilled to -30 °C. Sm^0 (48.0 mg, 0.319 mmol) was stirred in a Schlenk flask with 3 mL THF and I_2 (2.0 mg, 0.0080 mmol) at 25 °C for 10 minutes, until the very pale golden solution became a vibrant blue. The solution of **2.3** was added dropwise to the flask and the mixture was stirred for 1.5 h warming to 25 °C while changing from a deep green to a dark navy blue within 5 minutes and becoming browner within an hour, eventually coming to a deep golden brown. Volatiles were removed *in vacuo* and the resulting product was dissolved in pentane and filtered through a pipet with a kimwipe and celite plug before volatiles were again removed *in vacuo* to yield an oily brown solid that was recrystallized in pentane at -30 °C to yield **2.5** (20.9 mg, 48 % yield).

Reduction of 2.3 by Sm° (5% I_2). 2.3 (50.0 mg, 0.105 mmol) was dissolved in 4 mL THF and chilled to -30 °C. Sm° (48.0 mg, 0.319 mmol) was stirred in a Schlenk flask with 3 mL THF and I_2 (4.0 mg, 0.016 mmol) at 25 °C for 10 minutes, until the pale golden solution became a vibrant blue. The solution of **2.3** was added dropwise to the flask, causing the solution to become a deep green in color, and let stir coming to 25 °C over 1 h during which the solution grew to a deep golden brown. Volatiles were removed *in vacuo* and the resulting product was dissolved in pentane and filtered through a pipet with a kimwipe and celite plug before volatiles were again removed *in vacuo* to yield an oily brown solid that was recrystallized at -30 °C in pentane as **2.5** (25.0 mg, 57% yield).

Reduction of 3.4 by Sm° (2.5% I_2). 3.4 (49.9, 0.109 mmol) was dissolved 3 mL and chilled to -30 °C. Sm° (17.3 mg, 0.115 mmol) was stirred in a Schlenk flask

with 2 mL THF and I_2 (0.7 mg, 0.003 mmol) at 25 °C for 10 minutes, until the pale golden solution became a vibrant blue. The solution of **3.6** was added dropwise to the flask and the mixture was stirred for 20 min warming to 25 °C changing from a yellow-orange to a dark olive-brown. Volatiles were removed *in vacuo* the resulting product was washed in pentane to yield a greyish brown powder **2.8** (42.4 mg, 92% yield).

Reaction of 3.4 with Me_3SiCl and Sm° (2.5% I_2). Sm° (66.3 mg, 0.441 mmol) and I_2 (2.8 mg, 0.011) mmol) were placed in a Schlenk flask in 3 mL THF and stirred for 10 minutes until the orange solution became a vibrant blue in color. To this, a solution of **3.4** (50.2 mg, 0.110 mmol) and Me_3SiCl (28.0 μL, 0.220 mmol) in 3 mL THF that had been prechilled to -30 °C was added dropwise and let stir for 20 minutes, changing from an olive green in color to brown with a deep purple tinge. Volatiles were removed *in vacuo* the resulting product was dissolved in pentane and filtered through a pipet with a kimwipe and celite plug before being dried under reduced pressure to yield a purple-brown oil **3.6** (53.2 mg, 98 % yield).

Attempted Reduction of 2.3 by NaHg at 40 °C. **2.3** (18.8 mg, 0.0394 mmol) was dissolved in 4 mL THF in a 100 mL Schlenk flask. 0.5% (w/w) Na/Hg (0.5430 g, 0.118 mmol Na) and heated on an oil bath 40 °C for 15 minutes while stirred under a N_2 atmosphere. The mixture was allowed to cool to room temperature before solvents were removed *in vacuo*. The resulting solid was not soluble in pentane and was thus dissolved in toluene to filter through a pipet with a kimwipe and celite plug and determined by ^{1}H NMR to be unreacted **2.3**.

Reduction of 2.3 by NaHg at 40 °C. **2.3** (15.6 mg, 0.0327 mmol) was dissolved in 4 mL THF in a 100 mL Schlenk flask. 0.5% (w/w) Na/Hg (0.4445 g, 0.0967 mmol

Na) and heated on an oil bath 40 °C for 1 h while stirred under a N_2 atmosphere. The solution changed directly from an orange marron to a darker golden brown. The mixture was allowed to cool to room temperature before solvents were removed *in vacuo*. Crude ^{1}H NMR revealed **2.5** among a mixture of other peaks, some of which correspond to the amidine.

Reduction of 2.3 by NaHg with Me_3SiCl. **2.3** (53.3 mg, 0.112 mmol) was dissolved in 5 mL THF and chilled to -30 °C. Me_3SiCl (57.0 μL, 0.449 mmol) was added to the solution via micro syringe after which 0.5% (w/w) Na/Hg (1.5413 g, 0.335 mmol Na) was added. The solution was allowed to stir and warm to room temperature over 30 min and changed gradually from a maroon to a dark blue to a brown. Volatiles were removed *in vacuo* and ^{1}H NMR revealed **2.5** in a comparable amount to an unknown C_s symmetric product, neither of which could be recrystallized out in pentane.

Reduction of 2.3 by NaHg with Me_3SiCl. **2.3** (19.1 mg, 0.0400 mmol) was dissolved in 5 mL THF to which was added Me_3SiCl (10.5 μL, 0.0840 mmol) via micro syringe. 0.5% (w/w) Na/Hg (0.7483 g, 0.1627 mmol Na) was added. The solution was allowed to stir for 30 min and changed gradually from a maroon to a dark blue to a brown before volatiles were removed *in vacuo.* ^{1}H NMR revealed **2.5** in a slightly larger amount than the unknown C_s symmetric product.

Reaction of Me_3SiCl with NaHg. 0.5% (w/w) Na/Hg (0.0878 g, 0.0160 mmol Na) and Me_3SiCl (10.6 μL, 0.0835 mmol) were mixed together in 0.6 mL benzene-d_6 in a Teflon© sealed Pyrex© J. Young NMR tube and monitored at room temperature over 18 h which slowly resulted in the appearance of $O(SiMe_3)_2$. Heating the mixture

at 70 °C for 20 h resulted in the peak growing in slightly faster, but with significant amount of starting material remaining unreacted visually any by ^{1}H NMR.

Reduction of 2.3 by NaHg with Me_3SiCl in 10 : 1 toluene : THF. **2.3** (55.5 mg, 0.116 mmol) was dissolved in 2 mL toluene mixed with 0.2 mL THF and chilled to -30 °C. Me_3SiCl (60.0 μL, 0.473 mmol) was added to the chilled solution via micro syringe and 0.5% (w/w) Na/Hg (1.5943 g, 0.34674 mmol Na) was added after which the mixture was allowed to stir 18.5 h coming to room temperature. The originally maroon brown solution grew to a navy blue with brown undertones and volatiles were removed in vacuo after which the products were dissolved in pentane and filtered through pipet with a kimwipe and celite plug. The resulting brown solution was dried under vacuum and ^{1}H NMR revealed an even mixture of **2.5** the unknown C_s symmetric product.

Reaction of 2.5 with Me_3SiCl and Sm° (2.5% I_2). Sm° (18.0 mg, 0.120 mmol) and I_2 (0.007 mg, 0.03 mmol) were placed in a Teflon© sealed Pyrex© J. Young NMR tube with 0.6 mL THF and mixed by sonication for 30 seconds until the orange solution became a pale but vibrant blue in color. To this, Me_3SiCl (30.5 μL, 0.261 mmol) was added via micro syringe and **2.5** (50.4 mg, 0.059 mmol) was quantitively rinsed in with 1 mL THF. The mixture was heated on an oil bath at 70 °C for 7.5 h changing from an orange-brown to a darker, purple-tinged brown, after which the solution was filtered through a pipet with a kimwipe and celite plug and volatiles removed *in vacuo.* The resulting oil was dissolved in pentane before being filtered and dried under reduced pressure to yield a dark purple-brown oil **3.6** (37.9 mg, 64 % yield).

Reaction of 2.5 with Me_3SiCl and Sm° (2.5% I_2). Sm° (18.0 mg, 0.120 mmol) and I_2 (0.007 mg, 0.03 mmol) were placed in a Teflon© sealed Pyrex© J. Young NMR tube with 0.6 mL THF and mixed by sonication for 30 seconds until the orange solution became a pale but vibrant blue in color. To this, Me_3SiCl (30.5 μL, 0.261 mmol) was added via micro syringe and **2.5** (50.4 mg, 0.059 mmol) was quantitively rinsed in with 1 mL THF. The mixture was heated on an oil bath at 70 °C for 7.5 h changing from an orange-brown to a darker, purple-tinged brown, after which the solution was filtered through a pipet with a kimwipe and celite plug and volatiles removed *in vacuo.* The resulting oil was dissolved in pentane before being filtered and dried under reduced pressure to yield a dark purple-brown oil **3.6** (37.9 mg, 64 % yield).

Reaction of 3.4 with Me_3SiCl, Sm° (2.5% I_2), iPrOH followed by ^1H NMR. **3.4** (15.0 mg, 0.0329 mmol) was dissolved in 0.6 mL of THF-d_8 in an NMR tube with a cyclododecane standard (2.0 mg, 0.012 mmol) and Me_3SiCl (16.8 μL, 0.132 mmol) and an ^1H NMR was taken. Sm° (14.8 mg, 0.0984 mmol) and I_2 (0.6 mg, 0.002) mmol) were combined in a Teflon© sealed Pyrex© J. Young NMR tube in 0.3 mL THF-d_8 and mixed by sonication for one minute until the pale golden solution became a pale but vibrant blue, after which the NMR mixture was quantitively added to the J. Young tube with an additional 0.5 mL THF-d_8. iPrOH (5.0 μL, 0.065 mmol) was immediately added to the mixture via micro syringe and a ^1H NMR spectra showed immediate consumption of **3.4**, very slight evidence of intermediate **3.6**, and products **2.3**, $HN(SiMe_3)_2$, and $(CH_3)_2CHOSiMe_3$ in addition to a slight excess of excess Me_3SiCl and iPrOH. After 1 h at room temperature, **2.3** had mostly disappeared from the mixture by 1H NMR (as it was presumably reduced to **2.5** by the Sm° (2.5% I_2) which then

continued to react unproductively). Relative to the integration of the internal standard the yield of $HN(SiMe_3)_2$ was judged to be 85% compared to the starting amount of **3.4**. See Figure 5.6 for corresponding spectra.

Reaction of 3.4 with Me_3SiCl, Sm° (2.5% I_2), and iPrOH. 3.4 (24.5 mg, 0.0537 mmol) was dissolved in 0.6 mL of THF-d_8 in an NMR tube with a durene standard (0.5 mg, 4 mmol) and Me_3SiCl (41.0 μL, 0.323 mmol) and an initial ^1H NMR was taken. Sm° (33.0 mg, 0.219 mmol) was stirred in 3 mL THF-d_8 with I_2 (1.3 mg, 0.0051 mmol) at 25 °C for 15 minutes, until the pale golden solution became a vibrant blue. The mixture in the NMR tube was quantitively transferred to the round bottom flask with and an additional 1 mL THF-d_8 after which iPrOH (16.2 μL, 0.212 mmol) was added to the stirring mixture via micro syringe. After 1h of stirring, an aliquot was removed for ^1H NMR which showed no **3.4** remaining, a slight amount of diamagnetic intermediate **3.6**, as well as paramagnetic product **2.3** and organic products $HN(SiMe_3)_2$, and $(CH_3)_2CHOSiMe_3$. See Figure 5.7 for corresponding spectra.

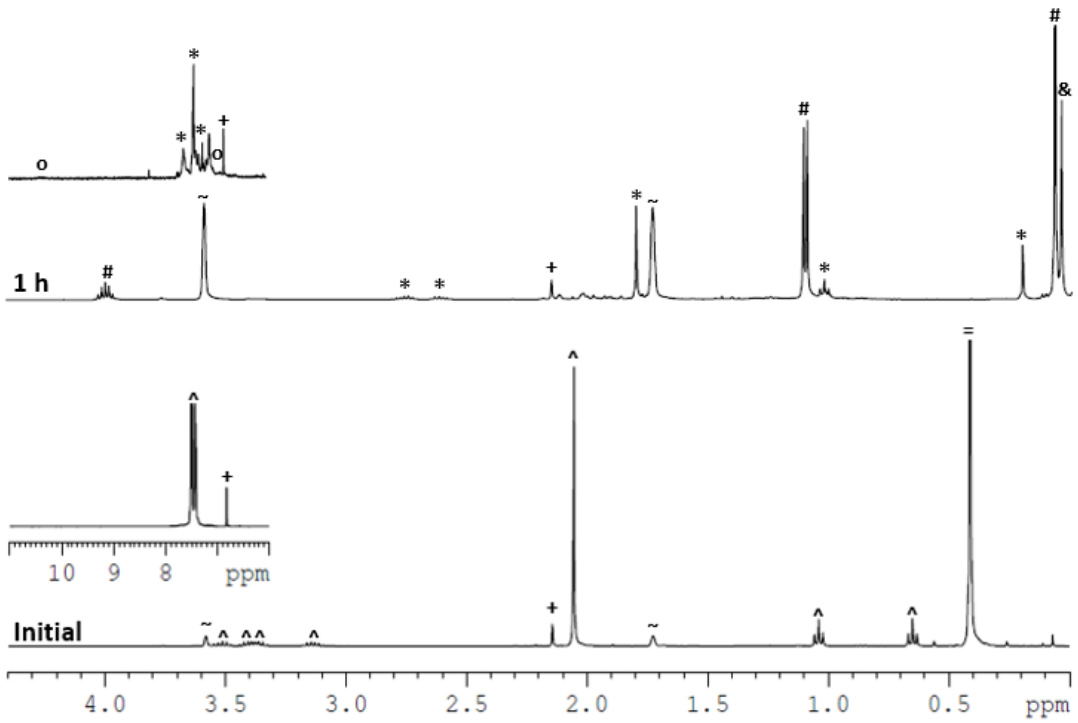

Figure 5.7. Partial ^{1}H NMR (400 MHz, THF-*d*$_8$, 25 °C) showing **3.4** (^) with Me_3SiCl (=) and durene standard (+) (bottom spectrum) upon reacting for 1 h with Sm° (2.5% I_2) in THF-*d*$_8$ (~) and iPrOH to produce the intermediate **3.6** (*****) as well as products **3.4** (**o**), $HN(SiMe_3)_2$ (**&**), and $(CH_3)_2CHOSiMe_3$ (#)

Confirmation of Organic Product Identity by GC/MS. Sm° (78.2 mg, 0.520 mmol) was stirred in a Schlenk tube in 3 mL THF with I_2 (3.5 mg, 0.0138 mmol) at 25 °C for 15 minutes, until the pale golden solution became a vibrant blue. **3.4** (82.2 mg, 0.180 mmol) was dissolved in 3 mL THF with a decane standard (35.1 μL, 0.180 mmol) and Me_3SiCl (91.5 μL, 0.721 mmol) added via micro syringe, and the resulting yellow solution was quantitively rinsed into the tube with the Sm° (2.5% I_2). iPrOH (27.6 μL, 0.361 mmol) was added to the stirring mixture via micro syringe and the reaction was let stir for 1 h at room temperature. The reaction tube was cycled onto a vacuum transfer line and the volatiles were vacuum transferred into a new Schlenk flask leaving all solid reside behind. This colorless solution was analyzed by GC/MS and shown to contain

the predicted organic products $HN(SiMe_3)_2$ and $(CH_3)_2CHOSiMe_3$. See Figure 5.8 for corresponding spectra.

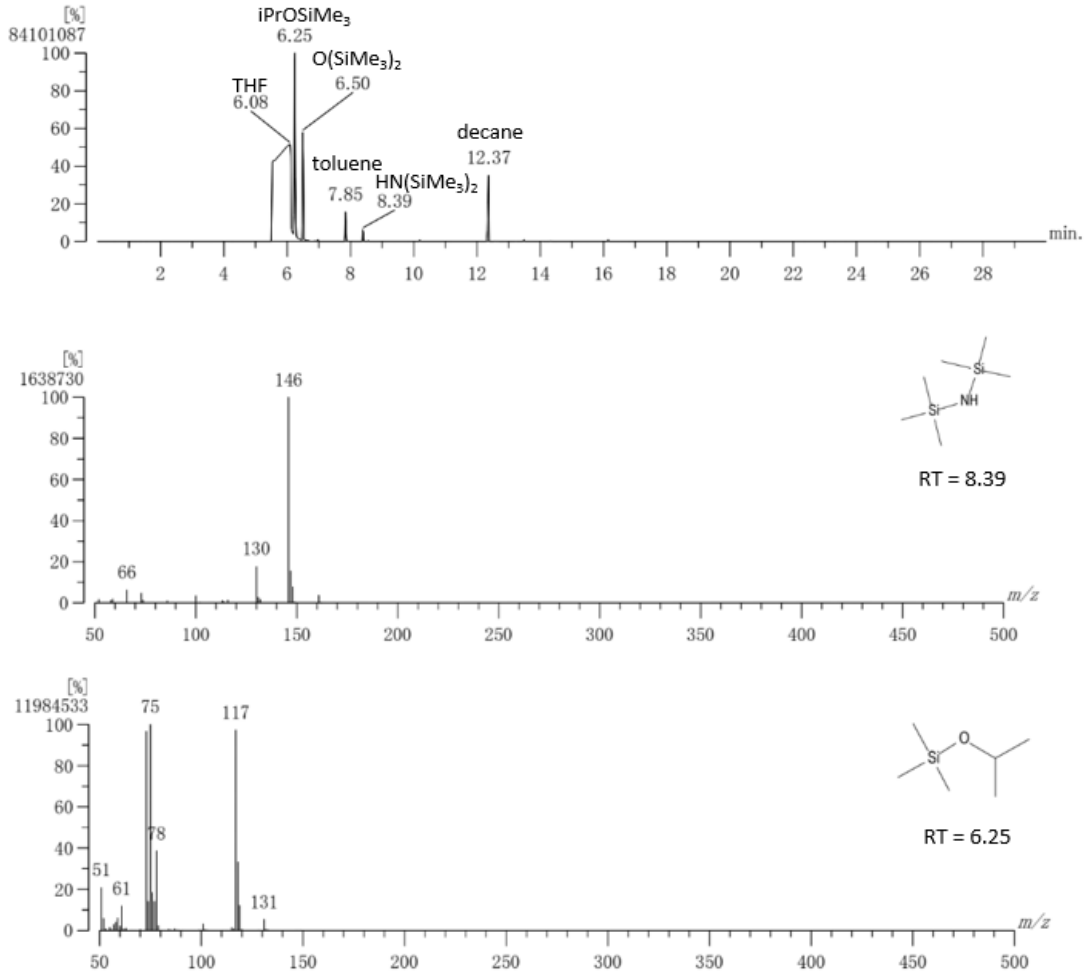

Figure 5.8. (Top) Chromatograph of the volatile results of the reaction of **3.4** with Sm° (2.5% I_2), Me_3SiCl, iPrOH, and a decane standard at 25 °C for 1h in THF to produce **2.3** as well as the noted organic products $HN(SiMe_3)_2$ at 8.39 min and $(CH_3)_2CHOSiMe_3$ at 6.25 min. Toluene and $O(SiMe_3)_2$ impurities are noted at 7.85 and 6.50 min respectively. (Bottom) Mass spectra for $HN(SiMe_3)_2$ (top, retention time 8.39 min) and $(CH_3)_2CHOSiMe_3$ (bottom, retention time 6.25 min) from the volatile THF solution of the reaction of **3.4** with Sm° (2.5% I_2), Me_3SiCl, iPrOH, and a decane standard at 25 °C for 1h

Conversion of $HN(SiMe_3)_2$ to NH_4Cl via HCl. $HN(SiMe_3)_2$ (23.0 μL, 0.0110 mmol) was prepared in 0.6 mL DMSO-*d*$_6$ in a Teflon© sealed Pyrex© J. Young NMR

tube. Following an initial ^{1}H NMR, HCl in Et_2O (2M, 0.55 mL, 0.11 mmol) was added into the tube causing white precipitate to form in the upper ethereal layer which was removed under reduced pressure until only the DMSO-*d*$_6$ layer remained. A ^{1}H NMR revealed the presence of NH_4Cl and the addition of 1,1,2,2-tetrachloroethane (10.0 μL, 0.0947 mmol) caused no observable change over 18 h.

Attempted ^{1}H NMR Quantification of $HN(SiMe_3)_2$ from 3.4 via conversion to NH_4Cl. **3.4** (15.0 mg, 0.0329 mmol) was dissolved in 0.6 mL of THF-d_8 in an NMR tube with a cyclododecane standard (2.0 mg, 0.012 mmol) and Me_3SiCl (16.8 μL, 0.132 mmol) and an ^{1}H NMR was taken. Sm° (14.8 mg, 0.0984 mmol) and I_2 (0.6 mg, 0.002) mmol) were combined in a Teflon© sealed Pyrex© J. Young NMR tube in 0.3 mL THF-d_8 and mixed by sonication for one minute until the pale golden solution became a pale but vibrant blue, after which the NMR mixture was quantitively added to the J. Young tube with an additional 0.5 mL THF-d_8. iPrOH (5.0 μL, 0.065 mmol) was immediately added to the mixture via micro syringe and a ^{1}H NMR spectra showed immediate consumption of **3.4**, very slight evidence of intermediate **3.6**, and products **2.3**, $HN(SiMe_3)_2$, and $(CH_3)_2CHOSiMe_3$ in addition to a slight excess of excess Me_3SiCl and iPrOH. After 1 h at room temperature, the reaction was judged to have run to completion. HCl in Et_2O (2M, 0.50 mL, 0.0987 mmol) was added and the solution agitated, initially showing signs of the formation of white precipitate but quickly settling to a muddy solution. Volatiles were removed *in vacuo* and the resulting brown coating was re-dissolved in DMSO-*d*$_6$ and spiked with TCE (10.0 μL, 0.0947 mmol), however the 1H NMR spectra was broadened almost to the point of being unrecognizable.

Representative ^{1}H NMR Quantification of $HN(SiMe_3)_2$ via conversion to NH_4Cl. $HN(SiMe_3)_2$ (20.0 μL, 0.00954 mmol) was prepared in 0.6 mL THF in a Teflon© sealed Pyrex© J. Young NMR tube and vacuum transferred to a new J. Young tube. To this tube was added HCl in Et_2O (2M, 0.15 mL, 0.030 mmol) causing white precipitate to immediately form. Volatiles were carefully removed *in vacuo* to leave a white coating in the tube that was dissolved in 0.6 mL DMSO-d_6. 1,1,2,2-tetrachloroethane (10.0 μL, 0.0947 mmol) was added via micro syringe and ^{1}H NMR comparison of the integrations confirmed a 99.5% yield of NH_4Cl (*Two more trials yielded results of 98.3% and 92.2% for an average of 96.7% yield*).

Representative ^{1}H NMR Quantification of $HN(SiMe_3)_2$ from 3.4 via conversion to NH_4Cl. Sm° (33.5 mg, 0.223 mmol) was placed in a Teflon© sealed Pyrex© J. Young NMR tube in 0.3 mL THF with I_2 (1.5 mg, 0.0059 mmol) and the ube was sonicated at 25 °C for 1 minute until the pale golden solution became a vibrant blue. **3.4** (34.0 mg, 0.0746 mmol) was dissolved in 30.2 mL THF with Me_3SiCl (38.0 μL, 0.299 mmol) and this mixture was quantitively rinsed into the Sm° (2.5%I_2) NMR tube with an additional 0.5 mL THF. To this was added iPrOH (11.5 μL, 0.150 mmol) and the mixture rapidly grew brown. After sitting for 2 h at room temperature, it was cycled onto the vacuum transfer apparatus and the volatiles were transferred to a new J Young tube over 3 h leaving an oily brown residue in the reaction tube. To this slightly foggy solution was added HCl in Et_2O (2M, 0.15 mL, 0.30 mmol) causing white precipitate to immediately form. Volatiles were carefully removed *in vacuo* to leave a white coating in the tube that was dissolved in 0.6 mL DMSO-d_6. 1,1,2,2-tetrachloroethane (10.0 μL, 0.0947 mmol) was added via micro syringe and ^{1}H NMR

comparison of the integrations determined a 50% yield of NH_4Cl. (*An identical reaction determined 23% yield upon repetition*). ^1H NMR (400 MHz, $(CD_3)_2SO$, 25 °C): 7.45 (4H, t, J_{NH} = 50.2 Hz, NH_4^+).

References

1. Shin, J. H.; Chruchill, D. G.; Bridgewater, B. M.; Pang, K.; Parkin, G. Hydride, halide, methyl, carbonyl, and chalcogenido derivatives of permethylmolybdenocene. *Inorg. Chim. Acta.* **2006,** *259*, 2942-2955.
2. Calhorda, J. M.; Carrondo, M. A. A. F. d. C. T.; Doas, A. R.; Galvao, A. M.; Garcia, A. M.; Martins, A. M.; Minas de Piedade, M. E.; Pinheiro, C. I.; Ramao, C. C.; Simoes, J. A. M.; Veiros, L. F. Syntheses, electrochemistry, and bonding of bis(cyclopentadienyl)molybdenum alkyl complexes. Molecular structure of $Mo(\eta^5\text{-}C_5H_5)_2(C_4H_9)_2$. Thermochemistry of $Mo(\eta^5\text{-}C_5H_5)_2R_2$and $Mo(\eta^5\text{-}C_5H_5)_2L$ (R = CH_3, C_2H_5, C_4H_9; L = ethylene, diphenylacetylene). *Organometallics* **1991,** *10*, 483 - 494.
3. Roddick, D. M.; Fryzuk, M. D.; Seidler, P. F.; Hillhouse, G. L.; Bercaw, J. E. Halide, Hydride, Alkyl, and Dinitrogen Complexes of Bis(pentamethylcyclopentadienyl)hafnium. *Organometallics* **1985,** *4*, 97-104.
4. Bernskoetter, W. H.; Olmos, A. V.; Lobkovsky, E.; Chirik, P. J. N_2 Hydrogenation Promoted by a Side-On Bound Hafnocene Dinitrogen Complex. *Organometallics* **2006,** *25*, 1021-1027.
5. Fryzuk, M. D.; Corkin, J. R.; Patrick, B. O. Reduction of hafnium(IV) complexes in the presence of molecular nitrogen: Attempts to form dinitrogen complexes of the heaviest group 4 element. *Can. J. Chem.* **2003,** *81*.
6. Uhl, W.; Appelt, C.; Wollschlanger, A.; Hepp, A.; Wurthwein, E. An Al/P-Based Frustrated Lewis Pair as an Efficient Ambiphilic Ligand: Coordination of Boron Trihalides, Rearrangement, and Formation of HBX_2 Complexes (X = Br, I). *Inorg. Chem.* **2014,** *53*, 8991-8999.
7. Arashiba, K.; Eizawa, A.; Tanaka, H.; Nakajima, K.; Yoshizawa, K.; Nishibayashi, Y. Catalytic Nitrogen Fixation via Direct Cleavage of Nitrogen – Nitrogen Triple Bond of Molecular Dinitrogen under Ambient Reaction Conditions. *Bull. Chem. Soc. Jpn.* **2017,** *90*, 1111-1118.
8. Chojnowski, J.; Crpryk, M.; Michalski, J. The mechanism of the reaction of organic phosphites with triakylsilyl iodide. Iodoanhydrides of P^{III} acids as intermediates. *215* **1981**, 355-365.
9. Baer, J. L. Investigating the Pentamethylcyclopentadienyl Amidinate (CPAM) Ligand Set via Synthesis and Characterization of a Variety of Group 4, 5, and 6 Metal-Organic Complexes for uses in Polymerization and Small Molecule Activation. *B.S. Dissertation, University of Maryland*, College Park, MD, **2018**.
10. Arashiba, K.; Miyake, Y.; Nishibayashi, Y. A molybdenum complex bearing PNP-type pincer ligands leads to the catalytic reduction of dinitrogen into ammonia. *Nat. Chem.* **2011,** *3*, 120-125.

11. Eizawa, A.; Arashiba, K.; Tanaka, H.; Kuriyama, S.; Matsuo, Y.; Nakajima, K.; Yoshizawa, K.; Nishibayashi, Y. Remarkable catalytic activity of dinitrogen-bridged dimolybdenum complexes bearing NHC-based PCP-pincer ligands toward nitrogen fixation. *Nat. Chem.* **2017,** *8*, 14874.
12. Anderson, J. S.; Rittle, J.; Peters, J. C. Catalytic conversion of nitrogen to ammonia by an iron model complex. *Nature* **2013,** *501*, 84-87.
13. Chalkley, M. J.; Del Castillo, T. J.; Matson, B. D.; Roddy, J. P.; Peters, J. C. Catalytic N_2-to-NH_3 Conversion by Fe at Lower Driving Force: A Proposed Role for Metallocene-Mediated PCET. *ACS Cent. Sci.* **2017,** *3*, 217-223.
14. Wickramasinghe, L. A.; Ogawa, T.; Schrock, R. R.; Müller, P. Reduction of Dinitrogen to Ammonia Catalyzed by Molybdenum Diamido Complexes. *J. Am. Chem. Soc.* **2017,** *139*, 9132-9135.
15. Yandulov, R. R.; Schrock, R. R. Catalytic Reduction of Dinitrogen to Ammonia at a Single Molybdenum Center. *Science* **2003,** *301*, 67-78.
16. Hirotsu, M.; Fontaine, P. P.; Zavalij, P. Y.; Sita, L. R. Extreme N equivalent to N bond elongation and facile N-atom functionalization reactions within two structurally versatile new families of group 4 bimetallic "Side-on-Bridged" dimitrogen complexes for zirconium and hafnium *J. Am. Chem. Soc.* **2007,** *129*, 12690-12692.
17. Keane, A. J.; Yonke, B. L.; Hirotsu, M.; Zavalij, P. Y.; Sita, L. R. Fine-Tuning the Energy Barrier for Metal-Mediated Dinitrogen N≡N Bond Cleavage. *J. Am. Chem. Soc.* **2014,** *136*, 9906-9909.
18. Fontaine, P. P.; Yonke, B. L.; Zavalij, P. Y.; Sita, L. R. Dinitrogen Complexation and Extent of N≡N Activation within the Group 6 "End-On-Bridged" Dinuclear Complexes, $\{(\eta^5\text{-}C_5Me_5)M\ N(i\text{-}Pr)C(Me)N(i\text{-}Pr)\}_2(\mu\text{-}\eta^1\text{:}\eta^1\text{-}N_2)$ (M = Mo and W). *J. Am. Chem. Soc.* **2010,** *132*, 12273-12285.
19. Connelly, N. G.; Gieger, W. E. Chemical Redox Agents for Organometallic Chemistry. *Chem. Rev.* **1996,** *96*, 877-910.
20. Keane, A. J.; Farrell, W. S.; Yonke, B. L.; Zavalij, P. Y.; Sita, L. R. Metal-Mediated Production of Isocyanates, $R_3EN{=}C{=}O$ from Dinitrogen, Carbon Dioxide, and R_3ECl. *Angew. Chem. Int. Ed.* **2015,** *54*, 10220-10224.
21. Duman, L. M.; Farrell, W. S.; Zavalij, P. Y.; Sita, L. R. Steric Switching from Photochemical to Thermal Reaction Pathways for Enhanced Efficiency in Metal-Mediated Nitrogen Fixation. *J. Am. Chem. Soc.* **2016,** *138*, 14856-14859.
22. Namy, J. L.; Girard, P.; Kagan, H. B. A new preparation of some divalent lanthanide iodides and their usefulness in organic synthesis *Nouv. J Chim.* **1977,** *1*.
23. Girard, P.; Namy, J. L.; Kagan, H. B. Divalent lanthanide derivatives in organic synthesis. 1. Mild preparation of samarium iodide and ytterbium iodide and their use as reducing or coupling agents. *J. Am. Chem. Soc.* **1980,** *102*, 2693-2698.
24. Kagan, H. B.; Namy, J. L. Lanthanides in organic synthesis. *Tetrahedron* **1986,** *42*, 6573-6614.
25. Gopalaiah, K.; Kagan, H. B. Use of samarium diiodide in the field of asymmetric synthesis. *New J. Chem.* **2008,** *32*, 607-637.
26. Nicalaou, K. C.; Ellery, S. P.; Chen, J. S. Samarium diiodide mediated reactions in total synthesis. *Angew. Chem. Int. Ed.* **2009,** *48*, 7140-7165.

27. Yoshimura, A.; Saeki, R.; Nomoto, A.; Ogawa, A. Pinacol couplings of a series of aldehydes and ketones with SmI_2/Sm/Me_3SiCl in DME. *Tetrahedron* **2015,** *71*, 5347-5355.
28. Inanaga, J.; Ishikawa, M.; Yamaguchi, M. A mild and convenient method for the reduction of organic halides by using a samarium diiodide-THF solution in the presence of hexamethylphosphoric triamide (HMPA). *Chem. Lett.* **1987**, 1485-1486.
29. Prasad, E.; Knettle, B. W.; Flowers, R. A., II. The Role of Ligand Displacement in Sm(II)-HMPA-Based Reductions. *J. Am. Chem. Soc.* **2004,** *126*, 6891-6894.
30. Lautens, M.; Ren, Y. Chlorotrimethylsilane as an Activating Reagent in the Samarium-Promoted Cyclopropanation of Allylic and α-Allenic Alcohols. *J. Org. Chem.* **1996,** *61*, 2210-2214.
31. Szostak, M.; Spain, M.; Procter, D. J. Determination of the Effective Redox Potentials of SmI_2, $SmBr_2$, $SmCl_2$, and their Complexes with Water by Reduction of Aromatic Hydrocarbons. Reduction of Anthracene and Stilbene by Samarium(II) Iodide-Water Complex. *J. Org. Chem.* **2014,** *79*, 2522-2537.
32. Maity, S.; Hoz, S. Deciphering a 20-Year-Old Conundrum: The Mechanisms of Reduction by the Water/Amine/SmI_2 Mixture. *Chem. Eur. J.* **2015,** *21*, 18394-18400.
33. Sun, L.; Mellah, M. Efficient Electrosynthesis of $SmCl_2$, $SmBr_2$, and Sm(OTf)$_2$ from a "Sacrificial" Samarium Anode: Effect of nBu_4NPF_6 on the Reactivity. **2014,** *33*, 4625-4628.
34. Huang, Y.; Zhang, Y.; Wang, Y., Facile reduction of azides to the corresponding amines with metallic samarium and catalytic amount of iodine. *Tetrahedron Lett.* **1997,** *38*, 1065-1066.
35. Ogawa, A.; Takami, N.; Sekiguchi, M.; Ryu, I.; Kambe, N.; Sonoda, N. The first deoxygenative coupling of amides by an unprecedented samarium/samarium diiodide system. *J. Am. Chem. Soc.* **1992,** *114*, 8729-8730.
36. Chauvin, Y.; Olivier, H.; Saussine, L. Addition reaction of some rare earth metals to unsaturated compounds in ethers. *Inorg. Chim. Acta.* **1989,** *161*, 45-47.
37. Hatita, H.; Anaka, Y.; Hiyama, T. A novel reduction of zinc(II) chloride with samarium metal and its application to silylation of 1-alkynes. *Synlett* **1996,** *7*, 637-639.
38. Li, Z.; Iida, K.; Tomisaka, Y.; Yoshimura, A.; Hiaro, T.; Nomoto, A.; Ogawa, A. New Entry to the Construction of Si-Si Linkages: Sm/SmI_2-Induced Efficient Reductive Coupling of Organochlorosilanes. *Organometallics* **2007,** *26*, 1212-1216.
39. Liu, Y.; Xiao, S.; Qi, Y.; Du, F. Reductive Homocoupling of Organohalides Using Nickel(II) Chloride and Samarium Metal. *Chem. Asian J.* **2017,** *12*, 673-678.
40. Lee, C. C.; Hu, Y.; Ribbe, M. W. Catalytic Reduction of CN-, CO, and CO_2 by Nitrogenase Cofactors in Lanthanide-Driven Reactions. *Angew. Chem. Int. Ed.* **2015,** *54*, 1219-1222.
41. Sickerman, N. S.; Tanifuji, K.; Lee, C. C.; Ohki, Y.; Tatsumi, K.; RIbbe, M. W.; Hu, Y. Reduction of C1 Substrates to Hydrocarbons by the Homometallic Precursor and Synthetic Mimic of the Nitrogenase Cofactor. *J. Am. Chem. Soc.* **2017,** *139*, 603-606.

42. Jubb, J.; Gambarotta, S. Dinitrogen Reduction Operated by a Samarium Macrocyclic Complex. Encapsulation of Dinitrogen into a Sm_2Li_4 Metallic Cage. *J. Am. Chem. Soc.* **1994,** *116*, 4477-4478.
43. Evans, W. J.; Ulibarri, T. A.; Ziller, J. W. Isolation and x-ray crystal structure of the first dinitrogen complex of an f-element metal, $[(C_5Me_5)_2Sm]_2N_2$. *J. Am. Chem. Soc.* **1988,** *110*.
44. Guillemot, G.; Castellano, B.; Prange, T.; Solari, E.; Floriani, C. Use of Calix[4]arenes in the Redox Chemistry of Lanthanides: the Reduction of Dinitrogen by a Calix[4]arene-Samarium Complex. *Inorg. Chem.* **2007,** *46*, 5152-5154.
45. Dube, T.; Conochi, S.; Gambarotta, S.; Yap, G. P.; Vasapollo, G. Tetrametallic reduction of dinitrogen: formation of a tetranuclear samarium dinitrogen complex. *Angew. Chem. Int. Ed.* **1999,** *38*, 3657-3659.
46. Evans, W. J.; Lee, D. S. Early developments in lanthanide-based dinitrogen reduction chemistry. *Can. J. Chem.* **2005,** *83*, 375-384.
47. Duman, L. M.; Sita, L. R., 'Greener' Nitrogen Fixation: Samarium Metal Reduction of CPAM Group 6 Metal Halides in the Presence of N_2, Me_3SiCl, and Alcohols. *ChemComm* **2018,** *In Preperation*.
48. Proctor, D. J.; Flowers, R. A. I.; Skrydstrup; T. *Organic Synthesis Using Samarium Diiodide: A Practical Guide*. RSC Publishing: Cambridge, 2009.
49. Szostak, M.; Procter, D. J. Beyond Samarium Diiodide: Vistas in Reductive Chemistry Mediated by Lanthanides(II). *Angew. Chem. Int. Ed.* **2012,** *51*, 9238-9256.
50. Szostak, M.; Spain, M.; Procter, D. J. Recent advances in the chemoselective reduction of functional groups mediated by samarium(II) iodide: a single electron transfer approach. *Chem. Soc. Rev.* **2013,** *42*, 9155-9183.
51. Chaney, A. L.; Marbach, E. P. Modified Reagents for Determination of Urea and Ammonia. *Clin. Chem.* **1962,** *8*, 130-132.
52. Bolleter, W. T.; Bushman, C. J.; Tidwell, P. W. Spectroscopic determination of ammonia as indophenol. *Anal. Chem.* **1961,** *33*, 592-594.
53. Verdouw, H.; Van Echteld, C. J. A.; Dekkers, E. M. J. Ammonia determination based on indophenol formation with sodium salicylate. *Water Research* **1978,** *12*, 399-402.
54. Sekiguchi, Y.; Arashiba, K.; Eizawa, A.; Nakajima, K.; Nishibayashi, Y.; Tanaka, H.; Yoshizawa, K. Catalytic Reduction of Molecular Dinitrogen to Ammonia and Hydrazine Using Vanadium Complexes. *Angew. Chem. Int. Ed.* **2818,** *57*, 9064-9068.

Chapter 6: Conclusions and Future Directions

6.1 Completed Work

The work described in this thesis represents the culmination of over ten years of research in small molecule activation and dinitrogen fixation supported by varied CPAM systems across the early transition metals. In summary, this thesis work describes a strategy employed to successfully lower the barriers to reactions N_2 fixation reaction by reducing the steric demands of the CPAM platform using a Et_2Ph amidinate. The increased space about the metal centers facilitates more facile chemical reduction and a groundbreaking, thermally mediated cleavage of N_2[1] which is intramolecular in nature[2] and from which the N-atoms may be effectively silylated under similarly mild conditions.[1] The subsequent chemoselective release of $HN(SiMe_3)_2$ is achieved by employing readily available alcohols or silanols as alternative proton sources.[3] Furthermore, the first use of Sm° (2.5%I_2) as a greener chemical reductant for the activation of N_2 is described and its compatibility for employment in a N_2 fixation cycle composed of the other reactions is demonstrated.[4] These are all important discoveries in that they break the boundaries of what has previously been achieved with group 6 dinitrogen complexes. The reactions have been investigated at length, resulting in a detailed mechanistic understanding and helping to illuminate the role that the metal identity, ligand architecture, and reaction conditions can play in such systems. By targeting compatible reactions, the project has progressed to final stages of developing a catalytic cycle for N_2 fixation that is capable of merging high atom economy with chemical efficiency under mild conditions – the ultimate goal of all synthetic N_2 fixation.

6.2 Future Directions

Continuing to move towards a catalytic cycle for N_2 fixation mediated by CPAM group 6 complexes, there are a series of studies based on the Et_2Ph CPAM complexes introduced in this document that would be of significant interest. The first is a through computation analysis of the N_2 cleavage, silylation, and $HN(SiMe_3)_2$ release processes. This could theoretically further corroborate the intramolecular nature of the N_2 cleavage (especially in the case of Mo which is experimentally inconclusive), help to elucidate the mechanism of Me_3SiCl silylation, and authenticate the proposed mechanism of dry hydrolysis. Several other research groups have expressed interest in such a study and collaborations are hoped to prove fruitful. Another area ripe for further investigation in the complete electrochemical characterization of the dichloride, (μ-N_2), and (μ-N)$_2$ species which will help to quantify the reduction potentials of the Mo and W complexes and determine the conditions under which electrochemically mediate reduction, or cleavage, might be possible, perhaps eventually leading to an electrochemically driven cycle. Further study is also proposed for the reactivities of disulfides with the (μ-N_2), and (μ-N)$_2$ complexes – such experiments and characterization would help to shore up the understanding of the relationship between Mo and the less reactive W based on their seemingly disparate reactivities. Continuing investigations into appropriate reaction conditions may also be used to determine compatibility for steps in the fixation cycle beyond those currently known. Finally, the acidolysis process to convert $HN(SiMe_3)_2$ to NH_4Cl for quantification purposes is in need of refinement to move beyond proof-of-concept. Fortunately, custom-designed

glassware should resolve the issues of inconsistency and return a valuable tool for measuring the success of N_2 fixation by CPAM systems.

This thesis work has verified the general correlation of decreasing CPAM steric demands and increasing reactivity but has also served to underline reality that the Et_2Ph CPAM framework may be located at the edge of practical stability; thus, to extend this project beyond the scope of what has been covered in this thesis, alternative ligand platforms and metal centers may be necessary to further refine reactivity. The sensitivity of the Et_2Ph complexes makes timing and reaction conditions particularly important and, in some cases (such as the chemical N_2 reductions by Mo) even hinders reactions that are known to proceed more robustly with the bulkier iPr_2Me CPAM set. Such instability being noted, ideally the CPAM system would be even more reactive than the Et_2Ph system, accomplishing N_2 cleavage, functionalization, and release very quickly and at ambient or sub-ambient temperatures. Therefore, further steric reductions of the CPAM framework are an important area of investigation despite probable challenges. Preliminary investigations into substitution of the distal Ph position for Me or H, the Cp* for Cp', and the amidinate for an iminocaprolactam-based ligand,[5] as are shown in Figure 6.1, have all been undertaken and though no conclusive results have yet been obtained, their continuing pursuit has the potential to

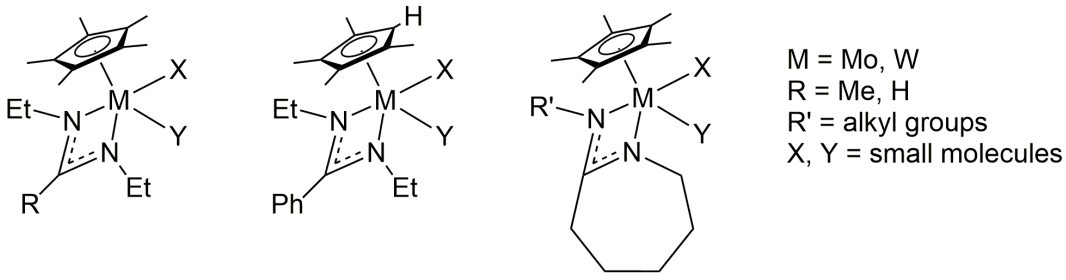

Figure 6.1. Potential CPAM derived structures with further steric reduction

drop reaction barriers even further and open still more potential reaction pathways. Additionally, as a means of further controlling the reactivity of these systems, the group 6 Mo or W center could be substituted for a later transition metal which may help to bolster the stability of the complexes. For instance, the group 7 metal Re has been shown to have a potential role in N_2 fixation by nitrogenase in the absence of Mo,[6] to support chemically-mediate N_2 cleavage and N-atom alkylation,[7] and may be amenable to the CPAM framework based on the existence of Cp*$ReCl_4$ precursors.[8] With these potential strategies in mind, new frontiers await and the systematic study of CPAM complexes that may be tuned to an exacting degree based on ligand design and extended further across the periodic table.

6.3 Relevance and Societal Impact

In sum, this work makes a significant contribution not only to the mapping of group 6 CPAM dinitrogen complexes and their subsequent reactivity, but also to the broader field of efficient N_2 fixation. The unconventional approach of closely studying congeners and closely-related analogues has allowed for the discovery of unconventional solutions to long-standing challenges. For one, this system is centered upon the cleavage of the inert N_2 bond which is accomplished under mild conditions and in such a way that does not inhibit subsequent functionalization of the N-atoms. Contrary to the proverb of "if it ain't broke, don't fix it," this successful approach prescribes instead that when it comes to dinitrogen, "if it ain't broke, you can't fix it". The selectively produced silylamine product released at the end of the cycle is also of significant novelty because the proton source can be any of a number of commercially available alcohols or even silica gel, meaning that neither costly, exotic acids nor H_2

are necessary. The product itself can easily be converted to the general N-product precursor of ammonia, or can be utilized directly "as-is" for industrial and academic applications, directly synthesizing a valuable chemical without having to go through the intermediate of ammonia. Finally, the specificity with which this CPAM system is coming to be understood bodes very well for the continued mapping and tuneability of N_2 activation and reactivity as future studies progress. The trends and relationships between ligand design and metal identity that have been identified can potentially be applied to other N_2 fixation processes, or at least may inspire other researchers to apply a similar systematic approach to the design of their complexes in pursuit of a similar depth of understanding.

The challenges and necessity of synthetic nitrogen fixation remain as substantial as ever. With the global population predicted to reach nearly 10 billion by 2050,[9] there is a continuing need for ever more food, fertilizer, and specialty chemicals to maintain and advance society. However, while the world's continually growing appetite for N-containing products may be understandable, it is not without consequence. High energy consumption and the production of undesirable byproducts mar the sustainability of the currently employed Haber-Bosch process.[10] There are also unanticipated results of the massive scale of synthetic N_2 fixation: Changes to the Earth's nitrogen cycle rival those of man-made alteration to the carbon cycle[11] and the overuse of fertilizers in agriculture causes nitrate pollution which has led to new problems such as potentially dangerous levels of nitrate and nitrite in ground-water supplies[12] and so-called "dead zones" in bodies of water.[12] These ramification make it even more imperative that chemists are responsible stewards of synthetic N_2 fixation.

The more that high atom economy and energy efficiency is targeted in the development of N_2 fixation processes, the more such undesirable consequences can be offset, and viable, contentious approaches to the thermodynamically demanding and mechanistically challenging process of N_2 fixation will continue to be advanced sustainably.

References

1. Duman, L. M.; Farrell, W. S.; Zavalij, P. Y.; Sita, L. R. Steric Switching from Photochemical to Thermal Reaction Pathways for Enhanced Efficiency in Metal-Mediated Nitrogen Fixation. *J. Am. Chem. Soc.* **2016,** *138*, 14856-14859.
2. Duman, L. M.; Zavalij, P. Y.; Sita, L. R. An Intramolecular Mechanism for N_2 Cleavage in Dinuclear Mo and W CPAM/CPGU Complexes. *J. Am. Chem. Soc.* **2018,** *In Preperation*.
3. Duman, L. M.; Sita, L. R. Closing the Loop on Transition-Metal-Mediated Nitrogen Fixation: Chemoselective Production of $HN(SiMe_3)_2$ from N_2, Me_3SiCl, and X-OH (X = R, R_3Si, or Silica Gel). *J. Am. Chem. Soc.* **2017,** *139*, 17241-17244.
4. Duman, L. M.; Sita, L. R., 'Greener' Nitrogen Fixation: Samarium Metal Reduction of CPAM Group 6 Metal Halides in the Presence of N_2, Me_3SiCl, and Alcohols. *Chem. Commun.* **2018,** *In Preperation*.
5. Wei, J.; Duman, L. M.; Redman, D. W.; Yonke, B., Zavalij P. Y.; Sita, L. R. N-Substituted Iminocaprolactams as Versatile and Low Cost Ligands in Group 4 Metal Initiators for the Living Coordinative Chain Transfer Polymerization of α-Olefins. *Organometallics* **2017,** *36*, 4202-4207.
6. Bishop, P. E.; Jarlenski, D. M. L.; Hetheringtons, D. R. Expression of an alternative nitrogen fixation system in Azotobacter vinelandii. *J. Bacteriol.* **1982,** *150*, 1244-1251.
7. Klopsch, I.; Finger, M.; Wurtele, C.; Milde, B.; Werz, D. B.; Schneider, S., Dinitrogen Splitting and Functionalization in the Coordination Sphere of Rhenium. *J. Am. Chem. Soc.* **2014,** *136*, 6881-6883.
8. Herrmann, W. A.; Floel, M.; Kulpe, J.; Felixberger, J. K.; Herdtweck, E. Organorhenium oxides and halides of the π -aromatic series: Syntheses and structures of important key compounds. *J. Organomet. Chem.* **1998**, 297-313.
9. *2017 Revision of World Population Prospects*; United Nations Population Division: **2017**.
10. Smil, V. *Enriching the Earth: Fritz Haber, Carl Bosch, and the Transformation of World Food Production*. MIT Press: Cambridge, MA, **2001**.
11. Galloway, J. N.; Townsend, A. R.; Erisman, J. W.; Bekunda, M.; Cai, Z.; Freney, J. R.; Matinelli, L. A.; Seitzinger, S. P.; Sutton, M. A. Transformation of the Nitrogen Cycle: Recent Trends, Questions, and Potential Solutions. *Science* **2008,** *320*, 889-892.
12. Hansen, B.; Thorling, L.; Schullehner, J.; Termansen, M.; Dalgaard, R. Groundwater nitrate response to sustainable nitrogen management. *Scientific Reports* **2017,** *7*, 1-12.

References Chapter 1

1. Darwent, B. d. *Bond Dissociation Energies in Simple Molecules*. National Bureau of Standards: Washington, D. C, 1970.
2. Jia, H. P.; Quadrelli, E. A. Mechanistic aspects of dinitrogen cleavage and hydrogenation to produce ammonia in catalysis and organometallic chemistry: relevance of metal hydride bonds and dihydrogen. *Chem. Soc. Rev.* **2014,** *43*, 547-564.
3. Chatt, J. Molecular Nitrogen as a Ligand. *Pure. Appl. Chem.* **1970,** *24*, 425-441.
4. Simon, J.; Kroneck, P. M. H. The production of ammonia by multiheme cytochromes c. *Met Ions Life Sci.* **2014,** *14*, 211-236.
5. Navarro-González, R. M., M. J.; Molina, L. T. Nitrogen fixation by volcanic lightning in the early Earth. *Geophys. Res. Lett.* **1998,** *25*, 3123-3126.
6. Hill, R. D.; Rinker, R. G.; Wilson, H. D. Atmospheric Nitrogen Fixation by Lightining. *J. Atmospheric Sci.* **1980,** *37*, 179-192.
7. Drapcho, D. L.; Sisterson, D.; Kumar, R. Nitrogen fixation by lightning activity in a thunderstorm. *Atmospheric Environ.* **1983,** *17*, 729-734.
8. Aizawa, K.; Cimarelli, C.; Alatorre-Ibargüengoitia, M. A.; Yokoo, A.; Dingwell, D. B.; Iguchi, M. Physical properties of volcanic lightning: Constraints from magnetotelluric and video observations at Sakurajima volcano, Japan. *Earth Planet. Sci. Lett.* **2016,** *444*, 45-55.
9. Einsle, O.; Tezcan, F. A.; Andrade, S. L. A.; Schmid, D.; Yoshida, M.; Howard, J. B.; Rees, D. C. Nitrogenase MoFe-protein at 1.16 Å resolution: A central ligand in the FeMo-cofactor *Science* **2002,** *298*, 1696-1700.
10. Spatzal, T.; Aksoyoglu, M.; Zhang, L.; Andrade, S. L. A.; Schleicher, E.; Weber, S.; Rees, D. C.; Einsle, O. Evidence for interstitial carbon in nitrogenase FeMo cofactor. *Science* **2011,** *334*, 940.
11. Spatzal, T.; Perez, K. A.; Einsle, O.; Howard, J. B.; C., R. D. Ligand binding to the FeMo-cofactor: Structures of CO-bound and reactivated nitrogenase. *Science* **2014,** *345*, 1620-1623.
12. Burgess, B. K.; Lowe, D. J. Mechanism of Molybdenum Nitrogenase. *Chem. Rev.* **1996,** *96*, 2983-3011.
13. Pickett, C. J. The Chatt cycle and the mechanism of enzymic reduction of molecular nitrogen. *J. Biol. Inorg. Chem.* **1996,** *1*, 601-606.
14. Seefeldt, L. C.; Hoffman, B. M.; Dean, D. R. Mechanism of Mo-Dependent Nitrogenase. *Annual Review of Biochemistry* **2009,** *78*, 701-722.
15. Lukayanov, D.; Yang, Z. Y.; Barney, B. M.; Dean, D. R.; Seefeldt, L. C.; Hoffman, B. M. Unification of reaction pathway and kinetic scheme for N_2 reduction catalyzed by nitrogenase. *Proc. Natl. Acad. Sci. U.S.A.* **2012,** *109*, 5583-5587.
16. Howard, J. B.; Rees, D. C. How many metals does it take to fix N_2? A mechanistic overview of biological nitrogen fixation. *Proc. Natl. Acad. Sci. U.S.A.* **2014,** *103*, 17088-17093.
17. Lukayanov, D.; Khadka, N.; Yang, Z. Y.; Dean, D. R.; Seefeldt, L. C.; Hoffman, B. M., Reductive Elimination of H_2 Activates Nitrogenase to Reduce

the N≡N Triple Bond: Characterization of the E4(4H) Janus Intermediate in Wild-Type Enzyme *J. Am. Chem. Soc.* **2016,** *138*, 10674-10683.
18. Mus, F.; Alleman, A. B.; Pence, N.; Seefeldt, L. C.; Peters, J. W. Exploring the alternatives of biological nitrogen fixation. *Metallomics* **2018,** *10*, 523-538.
19. Farcau, B. W. *The ten cents war*. Praeger: Westprot, CT, **2000**.
20. Crookes, W. *The Wheat Problem*. Longmans, Green, and Co.: London, **1917**.
21. Smil, V. Detonator of the population explosion. *Nature* **1999,** *400*, 415.
22. Nørskov, J.; Chen, J. Sustainable Ammonia Synthesis: Exploring the scientific challenges associated with discovering alternative, sustainable processes for ammonia production. U.S. Department of Energy: Dulles, VA, **2016**.
23. Smil, V. *Enriching the Earth: Fritz Haber, Carl Bosch, and the Transformation of World Food Production*. MIT Press: Cambridge, MA, 2001.
24. Schlögl, R. Ammonia Synthesis. In *Handbook of Heterogeneous Catalysis*, Wiley Online Library: 2008.
25. MacKay, B. A.; Fryzuk, M. D. Dinitrogen Coordination Chemistry: On the Biomimetic Borderlands. *Chem. Rev.* **2004,** *104*, 385-401.
26. Bezdek, M. J.; Chirik, P. J. Expanding Boundaries: N_2 Cleavage and Functionalization beyond Early Transition Metals. *Angew. Chem. Int. Ed.* **2016,** *55*, 7892-7896.
27. Gruber, N.; Galloway, J. N. An Earth-system perspective of the global nitrogen cycle. *Nature* **2008,** *451*, 293-296.
28. *2017 Revision of World Population Prospects*; United Nations Population Division: **2017**.
29. Bortells, H. Molybdenum as a catalyst in biological nitrogen bonding. *Arch. Mikrobiol.* **1930,** *1*, 333-342.
30. Allen, A. D.; Senoff, C. W. Nitrogenpentammineruthenium(II) complexes. *Chem. Commun.* **1965**, 621-622.
31. Shilov, A. E.; Shilova, A.; Borod'ko, Y. G. *Kinetik i Kataliz* **1966,** *7*, 768.
32. Allen, A. D.; Senoff, C. V. Nitrogenopentammineruthenium(II) complexes. *Chem. Commun.* **1965,** *0*, 621-622.
33. Tanabe, Y.; Nishibayashi, Y. Catalytic Dinitrogen Fixation to Form Ammonia at Ambient Reaction Conditions Using Transition Metal-Dinitrogen Complexes. **2016,** *16*, 1549-1577.
34. Stucke, N.; Flöser, B. M.; Weirich, T.; Tuczek, F. Nitrogen Fixation Catalyzed by Transition Metal Complexes: Recent Developments. *Eur. J. Inorg. Chem.* **2018**, 1337–1355.
35. Y., R.; Duboc, C.; Gennari M. Molecular Catalysts for N_2 Reduction :State of the Art, Mechanism, and Challenges. *Chem. Phys. Chem.* **2017,** *18*, 2606-2617.
36. Fryzuk, M. D.; Johnson, S. A. The continuing story of dinitrogen activation. *Coord. Chem. Rev.* **2000,** *200-202*, 379-409.
37. Tanabe, Y.; Nishibayashi, Y. Developing more sustainable processes for ammonia synthesis. *Coord. Chem. Rev.* **2013,** *257*, 2551-2564.
38. Ohki, Y.; Fryzuk, M. D. Dinitrogen activation by group 4 metal complexes. *Angew. Chem. Int. Ed.* **2007,** *46*, 3180-3183.

39. Duman, L. M.; Sita, L. R. Group 5 transition metal-dinitrogen complexes. In *Transition Metal-Dinitrogen Complexes: Preparation and Reactivity*, Nishibayashi, Y., Ed. Wiley-VCH: Weinheim, **2018**; Vol. Accepted.
40. Nishibayashi, Y. E. *Topics in Organometallic Chemistry*. Springer Verlag: Berlin/Heidelberg, **2017**; Vol. 60.
41. Poveda, A.; Perilla, I. C.; Perez, C. R. Review: Some considerations about coordination compounds with end-on dinitrogen. *J. Coord. Chem.* **2001,** *54*, 427-440.
42. Zhang, W. C.; Tang, Y. H.; Lei, M.; Morokuma, K.; Musaev, D. G. Ditantalum Dinitrogen Complex: Reaction of H2 Molecule with "End-on-Bridged" [Ta(IV)2(μ-η(1): η(1)-N2) and Bis(μ-nitrido) [Ta(V)]2(μ-N)2 Complexes. *Inorganic Chemistry* **2011,** *50* (19), 9481-9490.
43. Burford, R. J.; Fryzuk, M. D. Examining the relationship between coordination mode and reactivity of dinitrogen. *Nat. Rev. Chem.* **2017,** *1*, 26.
44. Burford, R. J.; Yeo, A.; Fryzuk, M. D. Dinitrogen activation by group 4 and group 5 metal complexes supported by phosphine-amido containing ligand manifolds. *Coord. Chem. Rev.* **2017,** *334*, 84-99.
45. Hirotsu, M.; Fontaine, P. P.; Zavalij, P. Y.; Sita, L. R. Extreme N equivalent to N bond elongation and facile N-atom functionalization reactions within two structurally versatile new families of group 4 bimetallic "Side-on-Bridged" dimitrogen complexes for zirconium and hafnium. *J. Am. Chem. Soc.* **2007,** *129*, 12690-12692.
46. Keane, A. J.; Yonke, B. L.; Hirotsu, M.; Zavalij, P. Y.; Sita, L. R. Fine-Tuning the Energy Barrier for Metal-Mediated Dinitrogen N≡N Bond Cleavage. *J. Am. Chem. Soc.***2014,** *136*, 9906-9909.
47. Chatt, J.; Dilworth, J. R.; Richards, R. L. Recent advances in the chemistry of nitrogen fixation. *Chem. Rev.* **1978,** *78*, 589-625.
48. Mock, M. T.; Chen, S.; Rousseau, R.; O'Hagan, M. J.; Dougherty, W. G.; Kassel, W. S.; DuBois, D. L.; Bullock, R. M. A rare terminal dinitrogen complex of chromium. *Chem. Commun.* **2011,** *47*, 12212-12214.
49. Vidyaratne, I.; Scott, J.; Gambarotta, S.; Budzelaar, P. H. M. Dinitrogen Activation, Partial Reduction, and Formation of Coordinated Imide Promoted by a Chromium Diiminepyridine Complex. *Inorg. Chem.* **2007,** *46*, 7040-4049.
50. Sellman, D. M., G. Systematic Synthesis of N_2-Complexes: Further N_2-Complexes of Chromium. *Z. Naturforsch.* **1972,** *27B*, 718-719.
51. Denholm, S.; Hunter, G.; Weakley, T. J. R. Dinitrogen complexes derived from tricarbonyl(η^6-hexaethylbenzene)chromium(0): crystal and molecular structure of μ-dinitrogenbis[dicarbonyl(η^6-hexaethylbenzene)chromium(0)]-toluene (1/1). *J. Chem. Soc., Dalton Trans* **1987**, 2789-2792.
52. Monillas, W. H.; Yap, G. P. A.; MacAdams, L. A.; Theopold, K. H. Binding and Activation of Small Molecules by Three-Coordinate Cr(I). *J. Am. Chem. Soc.* **2007,** *129*, 8090-8091.
53. Berben, L. A.; Kozimor, S. A. Dinitrogen and Acetylide Complexes of Low-Valent Chromium. *Inorg. Chem.* **2008,** *47*, 6438-4647.
54. Hoffert, W. A.; Rappe, A. K.; Shores, M. P. Unusual Electronic Effects Imparted by Bridging Dinitrogen: an Experimental and Theoretical Investigation. *Inorg. Chem.* **2010,** *49*, 9497-9507.

55. López-Alcalá, J. M.; Puerta, M. C.; González-Vílchez, F. Dinitrogen complexes of chromium(III) with chelating agents. *Transition Met. Chem.* **1985,** *10*, 247-248.
56. Kendall, A. J.; Johnson, S. I.; Bullock, R. M.; Mock, M. T. Catalytic Silylation of N_2 and Synthesis of NH_3 and N_2H_4 by Net Hydrogen Atom Transfer Reactions Using a Chromium P_4 Macrocycle. *J. Am. Chem. Soc.* **2018,** *140*, 2528-2536.
57. Chatt, J.; Pearman, A. J.; Richards, R. L. The reduction of mono-coordinated molecular nitrogen to ammonia in a protic environment. *Nature* **1975,** *253*, 39-40.
58. Leigh, G. J.; Prietoalcon, R.; Sanders, J. R. The Protonation of Bridging Dinitrogen to Yield Ammonia. *ChemComm.* **1991,** *0*, 921-922.
59. Leigh, G. J. Protonation of coordinated dinitrogen. *Acc. Chem. Res.* **1992,** *25*, 177-181.
60. Hidai, M. Chemical nitrogen fixation by molybdenum and tungsten complexes. *Coord. Chem. Rev.* **1999,** *185-186*, 99-108.
61. Hidai, M.; Mizobe, Y. Recent Advances in the Chemistry of Dinitrogen Complexes. *Chem. Rev.* **1995,** *95*, 1115-1133.
62. Yandulov, R. R.; Schrock, R. R. Catalytic Reduction of Dinitrogen to Ammonia at a Single Molybdenum Center. *Science* **2003,** *301*, 67-78.
63. Anderson, J. S.; Rittle, J.; Peters, J. C. Catalytic conversion of nitrogen to ammonia by an iron model complex. *Nature* **2013,** *501*, 84-87.
64. Del Castillo, T. J.; Thompson, N. B.; Peters, J. C. A Synthetic Single-Site Fe Nitrogenase: High Turnover, Freeze-Quench 57Fe Mössbauer Data, and a Hydride Resting State. *J. Am. Chem. Soc.* **2016,** *138*, 5341–5350.
65. Arashiba, K.; Miyake, Y.; Nishibayashi, Y. A molybdenum complex bearing PNP-type pincer ligands leads to the catalytic reduction of dinitrogen into ammonia. *Nat. Chem.* **2011,** *3*, 120-125.
66. Arashiba, K.; Kinoshita, E.; Kuriyama, S.; Eizawa, A.; Nakajima, K.; Tanaka, H.; Yoshizawa, K.; Nishibayashi, Y. Catalytic Reduction of Dinitrogen to Ammonia by Use of Molybdenum–Nitride Complexes Bearing a Tridentate Triphosphine as Catalysts. *J. Am. Chem. Soc.* **2015,** *137*, 5666–5669.
67. Eizawa, A.; Arashiba, K.; Tanaka, H.; Kuriyama, S.; Matsuo, Y.; Nakajima, K.; Yoshizawa, K.; Nishibayashi, Y. Remarkable catalytic activity of dinitrogen-bridged dimolybdenum complexes bearing NHC-based PCP-pincer ligands toward nitrogen fixation. *Nat. Commun.* **2017,** *8*, 14874.
68. Laplaza, C. E.; Cummins, C. C. Dintrogen Cleavage by a 3-Coordinate Molybdenum(III) Complex. *Science* **1995,** *268*, 861-863.
69. Laplaza, C. E.; Johnson, M. J. A.; Peters, J. C.; Odom, A. L.; Kime, E.; Cummins, C. C.; George, G. N.; Pickering, I. J. *J. Am. Chem. Soc.* **1996,** *118*, 8623-8638.
70. Curley, J. J.; Sceats, E. L.; Cummins, C. C. A Cycle for Organic Nitrile Synthesis via Dinitrogen Cleavage. *J. Am. Chem. Soc.* **2006,** *128*, 14036-14037.
71. Solari, E.; Da Silva, C.; Iacono, B.; Hesschenbrouck, J.; Rizzoli, C.; Scopelliti, R.; Floriani, C. Photochemical activation of the N≡N bond in a dimolybdenum - dinitrogen complex: formation of a molybdenum nitride. *Angew. Chem. Int. Ed.* **2001,** *40*, 3907-3909.

72. Curley, J. J.; Cook, T. R.; Reece, S. Y.; Muller, P.; Cummins, C. C. Shining Light on Dinitrogen Cleavage: Structural Features, Redox Chemistry, and Photochemistry of the Key Intermediate Bridging Dinitrogen Complex. *J. Am. Chem. Soc.* **2008,** *130*, 9394-9405.
73. Miyazaki, R.; Tanaka, H.; Tanabe, Y.; Yuki, M.; Nakajima, K.; Yoshizawa, K.; Nishibayashi, Y. Cleavage and Formation of Molecular Dinitrogen in a Single System Assisted by Molybdenum Complexes Bearing Ferrocenyldiphosphine. *Angew. Chem. Int. Ed.* **2014,** *53*, 11488-11492.
74. Rebreyend, C.; de Bruin, B. Photolytic N_2 Splitting: A Road to Sustainable NH_3 Production? A*ngew. Chem. Int. Ed.* **2015,** *54*, 42-44.
75. Krewald, V. Dinitrogen photoactivation: status quo and future perspectives. *Dalton Trans.* **2018,** *47*, 10320-10329.
76. Hanna, T. E.; Lobkovsky, E.; Chirik, P. J. Dinitrogen Complexes of Bis(cyclopentadienyl) Titanium Derivatives: Structural Diversity Arising from Substituent Manipulation. *Organometallics* **2009,** *28*, 4079-4088.
77. Chirik, P. J. Group 4 Transition Metal Sandwich Complexes: Still Fresh after Almost 60 Years. *Organometallics* **2010,** *29*, 1500-1517.
78. Tanaka, H.; Arashiba, K.; Kuriyama, S.; Sasada, A.; Nakajima, K.; Yoshizawa, K.; Nishibayashi, Y. Unique behaviour of dinitrogen-bridged dimolybdenum complexes bearing pincer ligand towards catalytic formation of ammonia. *Nat. Commun.* **2014,** *5*, 3737.
79. Imayoshi, R.; Nakajima, K.; Takaya, J.; Iwasawa, N.; Nishibayashi, Y. Synthesis and Reactivity of Iron- and Cobalt-Dinitrogen Complexes Bearing PSiP-Type Pincer Ligands toward Nitrogen Fixation. *Eur. J. Inrog. Chem.* **2017,** *32*, 3769-3778.
80. Kinoshita, E.; Arashiba, K.; Kuriyama, S.; Miyake, Y.; Shimazaki, R.; Nakanishi, H.; Nishibayashi, Y. Synthesis and Catalytic Activity of Molybdenum–Dinitrogen Complexes Bearing Unsymmetric PNP-Type Pincer Ligands. *Organometallics* **2012,** *31*, 8437-8443.
81. Nishibayashi, Y.; Kuriyama, S.; Arashiba, K.; Nakajima, K.; Tanaka, H.; Yoshizawa, K. Azaferrocene-Based PNP-type Pincer Ligand: Synthesis of Molybdenum, Chromium, and Iron Complexes and Reactivity toward Nitrogen Fixation. *Eur. J. Inorg. Chem.* **2016,** *30*, 4856-4861.
82. Pool, J. A.; Lubkovsky, E.; Chirik, P. J. Hydrogenation and cleavage of dinitrogen to ammonia with a zirconium complex. *Nature* **2004,** *327*, 527-530.
83. Peng, Y.; Ramos-Garces, M. V.; Lionetti, D.; Blakemore, J. D. Structural and Electrochemical Consequences of [Cp*] Ligand Protonation. *Inorg. Chem.* **2017,** *56*, 10824-10831.
84. Berno, P.; Hao, S. K.; Minhas, R.; Gambarotta, S. Dinitrgen Fixation versus Metal-Metal Bond Formation in the Chemistry of Vanadium(II) Amidinates. *J. Am. Chem. Soc.* **1994,** *116*, 7417-7418.
85. Barry, S. T. Amidinates, guanidinates and iminopyrrolidinates: Understanding precursor thermolysis to design a better ligand. *Coord. Chem. Rev.* **2013,** *257*, 3192-3201.
86. Barker, J.; Kilner, M. The coordination chemistry of the amidine ligand. *Coord. Chem. Rev.* **1994,** *133*, 219-300.

87. MacLeod, K. C.; Holland, P. L. Recent Developments in Homogeneous Dinitrogen Reduction by Molybdenum and Iron. *Nat. Chem.* **2013,** *5*, 559-565.
88. Sita, L. R. Ex Uno Plures ("Out of One, Many"): New Paradigms for Expanding the Range of Polyolefins through Reversible Group Transfers. *Angew. Chem. Int. Ed.* **2009,** *48*, 2464-2472.
89. Babcock, J. R.; Sita, L. R. Facile Preparation of Unsymmetric Carbodiimides via i*n Situ* Tin(II)-Mediated Heterocumulene Metathesis. *Organometallics* **1998,** *120*, 5585-5586.
90. Koterwas, L. A.; Fettinger, J. C.; R., S. L. Stereospecific Syntheses, Metal Configurational Stabilities, and conformational Analyses of m*eso*-(R,*S)*- and (R,*R)*-(η^5-C_5R_5)Ti(CH_3)$_2$-N,*N'*-bis(1-phenylethyl)acetamidinates for R = H and Me. *Organometallics* **1999,** *18*, 4183-4190.
91. Jayaratne, K. C.; Keaton, R. J.; Henningsen, D. A.; Sita, L. R. Living Ziegler−Natta Cyclopolymerization of Nonconjugated Dienes: New Classes of Microphase-Separated Polyolefin Block Copolymers via a Tandem Polymerization/Cyclopolymerization Strategy. *J. Am. Chem. Soc.* **200,** *122*, 10490-10491.
92. Jayaratne, K. C.; Sita, L. R. Stereospecific Living Ziegler−Natta Polymerization of 1-Hexene. *J. Am. Chem. Soc.* **2000,** *122*, 958-959.
93. Fontaine, P. P.; Yonke, B. L.; Zavalij, P. Y.; Sita, L. R. Dinitrogen Complexation and Extent of N≡N Activation within the Group 6 "End-On-Bridged" Dinuclear Complexes, {(η^5-C_5Me_5)M N(i-Pr)C(Me)N(i-Pr)}$_2$(μ-η^1:η^1-N_2) (M = Mo and W). *J. Am. Chem. Soc.* **2010,** *132*, 12273-12285.
94. Production of Isocyanates, $R_3EN{=}C{=}O$ from Dinitrogen, Carbon Dioxide, and R_3ECl. *Angew. Chem. Int. Ed.* **2015,** *54*, 10220-10224.
95. Duman, L. M.; Farrell, W. S.; Zavalij, P. Y.; Sita, L. R. Steric Switching from Photochemical to Thermal Reaction Pathways for Enhanced Efficiency in Metal-Mediated Nitrogen Fixation. *J. Am. Chem. Soc.* **2016,** *138*, 14856-14859.
96. Hirotsu, M.; Fontaine, P. P.; Epshteyn, A.; Zavalij, P. Y.; Sita, L. R. Dinitrogen activation at ambient temperatures: New modes of H(2) and PhSiH(3) additions for an "End-on-bridged" [Ta(IV)] (2)(μ-η(1):η(1)-N(2) complex and for the bis(μ-nitrido) [Ta(V)(μ-N)](2) product derived from facile N=N bond cleavage. *J. Am. Chem. Soc.* **2007,** *129*, 9284-9285.

References Chapter 2

1. Hirotsu, M.; Fontaine, P. P.; Zavalij, P. Y.; Sita, L. R. Extreme N equivalent to N bond elongation and facile N-atom functionalization reactions within two structurally versatile new families of group 4 bimetallic "Side-on-Bridged" dimitrogen complexes for zirconium and hafnium. *J. Am. Chem. Soc.* **2007,** *129*, 12690-12692.
2. Keane, A. J.; Yonke, B. L.; Hirotsu, M.; Zavalij, P. Y.; Sita, L. R. Fine-Tuning the Energy Barrier for Metal-Mediated Dinitrogen N≡N Bond Cleavage. *J. Am. Chem. Soc.***2014,** *136*, 9906-9909.
3. Fontaine, P. P.; Yonke, B. L.; Zavalij, P. Y.; Sita, L. R. Dinitrogen Complexation and Extent of N≡N Activation within the Group 6 "End-On-Bridged"

Dinuclear Complexes, {(η^5-C_5Me_5)M N(i-Pr)C(Me)N(i-Pr)}$_2$(μ-η^1:η^1-N_2) (M = Mo and W). *J. Am. Chem. Soc.* **2010,** *132*, 12273-12285.
4. Duman, L. M.; Farrell, W. S.; Zavalij, P. Y.; Sita, L. R. Steric Switching from Photochemical to Thermal Reaction Pathways for Enhanced Efficiency in Metal-Mediated Nitrogen Fixation. *J. Am. Chem. Soc.* **2016,** *138*, 14856-14859.
5. Keane, A. J.; Farrell, W. S.; Yonke, B. L.; Zavalij, P. Y.; Sita, L. R., Metal-Mediated Production of Isocyanates, $R_3EN{=}C{=}O$ from Dinitrogen, Carbon Dioxide, and R_3ECl. *Angew. Chem. In. Ed.* **2015,** *54*, 10220-10224.
6. Duman, L. M.; Zavalij, P. Y.; Sita, L. R. An Intramolecular N2 Cleavage Mechanism for G6 CPAM/CPAM Dinuclear Complexes. *J. Am. Chem. Soc.* **2018,** *In Preperation*.
7. Zhang, W. C.; Tang, Y. H.; Lei, M.; Morokuma, K.; Musaev, D. G. Ditantalum Dinitrogen Complex: Reaction of H2 Molecule with "End-on-Bridged" [Ta(IV)2(μ-η(1): η(1)-N2) and Bis(μ-nitrido) [Ta(V)]2(μ-N)2 Complexes. *Inorganic Chemistry* **2011,** *50* (19), 9481-9490.
8. Wickramasinghe, L. A.; Ogawa, T.; Schrock, R. R.; Müller, P. Reduction of Dinitrogen to Ammonia Catalyzed by Molybdenum Diamido Complexes. *J. Am. Chem. Soc.* **2017,** *139*, 9132-9135.
9. Y., R.; Duboc, C.; Gennari, M. Molecular Catalysts for N_2 Reduction: State of the Art, Mechanism, and Challenges. *Chem. Phys. Chem.* **2017,** *18*, 2606-2617.
10. Yandulov, R. R.; Schrock, R. R. Catalytic Reduction of Dinitrogen to Ammonia at a Single Molybdenum Center. *Science* **2003,** *301*, 67-78.
11. Smythe, N. C.; Schrock, R. R.; Muller, P.; Weare, W. W. Synthesis of [(HIPTNCH$_2$CH$_2$)$_3$N]V compounds (HIPT=3,5-(2,4,6-i-Pr$_3$C$_6$H$_2$)$_2$C$_6$H$_3$) and an evaluation of vanadium for the reduction of dinitrogen to ammonia. *Inorganic Chemistry* **2006,** *45*, 9197-9205.
12. Arashiba, K.; Miyake, Y.; Nishibayashi, Y. A molybdenum complex bearing PNP-type pincer ligands leads to the catalytic reduction of dinitrogen into ammonia. *Nat. Chem.* **2011,** *3*, 120-125.
13. Kiriyama, S.; Arashiba, K.; Nakajima, K.; Tanaka, H.; Kamaru, N.; Youshizawa, K.; Nishibayashi, Y. Catalytic Formation of Ammonia from Molecular Dinitrogen by Use of Dinitrogen-Bridged Dimolybdenum–Dinitrogen Complexes Bearing PNP-Pincer Ligands: Remarkable Effect of Substituent at PNP-Pincer Ligand. *J. Am. Chem/. Soc.* **2014,** *27*, 9719-9731.
14. Tanaka, H.; Arashiba, K.; Kuriyama, S.; Sasada, A.; Nakajima, K.; Yoshizawa, K.; Nishibayashi, Y. Unique behaviour of dinitrogen-bridged dimolybdenum complexes bearing pincer ligand towards catalytic formation of ammonia. *Nat. Commun.* **2014,** *5*, 3737.
15. Tanaka, H.; Arashiba, K.; Kuriyama, S.; Sasada, A.; Nakajia, K.; Yoshizawa, K.; Nishibayashi, Y. Catalytic Nitrogen Fixation via Direct Cleavage of Nitrogen–Nitrogen Triple Bond of Molecular Dinitrogen under Ambient Reaction Conditions. *Bull. Chem. Soc. Jpn.* **2014,** *90*, 1111-1118.
16. Kinoshita, E.; Arashiba, K.; Kuriyama, S.; Miyake, Y.; Shimazaki, R.; Nakanishi, H.; Nishibayashi, Y. Synthesis and Catalytic Activity of Molybdenum–Dinitrogen Complexes Bearing Unsymmetric PNP-Type Pincer Ligands. *Organometallics* **2012,** *31*, 8437-8443.

17. Eizawa, A.; Arashiba, K.; Tanaka, H.; Kuriyama, S.; Matsuo, Y.; Nakajima, K.; Yoshizawa, K.; Nishibayashi, Y. Remarkable catalytic activity of dinitrogen-bridged dimolybdenum complexes bearing NHC-based PCP-pincer ligands toward nitrogen fixation. *Nat. Chem.* **2017,** *8*, 14874.
18. Holland, P. L. Metal–dioxygen and metal–dinitrogen complexes: where are the electrons? *Dalton Trans.* **2010,** *39*, 5415-5425.
19. Pauling, L.; Kamb, B. A revised set of values of single-bond radii derived from the observed interatomic distances in metals by correction for bond number and resonance energy. *Proc. Natl. Acad. Sci. U.S.A.* **1986,** *83*, 3569-3571.
20. Laplaza, C. E.; Cummins, C. C., Dinitrogen Cleavage by a 3-Coordinate Molybdenum9III) Complex. *Science* **1995,** *268*, 861-863.
21. Laplaza, C. E.; Johnson, M. J. A.; Peters, J. C.; Odom, A. L.; Kime, E.; Cummins, C. C.; George, G. N.; Pickering, I. J. *J. Am. Chem. Soc.* **1996,** *118*, 8623 - 8638.
22. Morrey, J. R. Isosbestic Points in Absorbance Spectra. *Phys. Chem.* **1963,** *67*, 1569–1569.
23. Hinrichsen, S.; Broda, H.; Gradert, C.; Söncksen, L.; Tucsek, F. Recent developments in synthetic nitrogen fixation. *Annu. Rep. Prog. Chem., Sect. A: Inorg. Chem.* **2012,** *108*.
24. Slater, J. C. Atomic Radii in Crystals. *J. Chem. Phys.* **1964,** *41*, 3199-3204.
25. Kepp, K. P. A Quantitative Scale of Oxophilicity and Thiophilicity. *Inorg. Chem.* **2016,** *55*, 9461–9470.
26. Hammett, L. P. The Effect of Structure upon the Reactions of Organic Compounds. Benzene Derivatives. *J. Am. Chem. Soc.* **1937,** *59*, 96-103.
27. Jaffé, H. H. A Reëxamination of the Hammett Equation. *Chem. Rev.* **1953,** *53*, 191–261.
28. Caro, C. A.; Cabello, G.; Landaeta, E.; Pérez, J.; González, M.; Zagal, J. H.; Lillo, L. Preparation, spectroscopic, and electrochemical characterization of metal(II) complexes with Schiff base ligands derived from chitosan: correlations of redox potentials with Hammett parameters. *J. Coord. Chem.* **2014,** *67*, 4114-4124.
29. Duman, L. M.; Sita, L. R., Closing the Loop on Transition-Metal-Mediated Nitrogen Fixation: Chemoselective Production of $HN(SiMe_3)_2$ from N_2, Me_3SiCl, and X—OH (X = R, R_3Si, or Silica Gel). *J. Am. Chem. Soc.* **2017,** *139*, 17241-17244.
30. Duman, L. M.; Zavalij, P. Y.; Sita, L. R. An Intramolecular Mechanism for N_2 Cleavage in Dinuclear Mo and W CPAM/CPGU Complexes. *J. Am. Chem. Soc.* **2018,** *In Preperation*.
31. Murray, R. C.; Blum , L.; Liu, A. H.; Schrock, R. R. Simple routes to mono(μ^5-pentamethylcyclopentadienyl) complexes of molybdenum(V) and tungsten(V). **1985,** *4*, 953-954.
32. Sal, P. G.; Jiménez, I.; Martín, A.; Pedraz, T.; Royo, P.; Sellés, A.; Vazquez de Miguel, A. Synthesis of chloro and methyl imido cyclopentadienyl molybdenum and tungsten complexes. X-ray molecular structures of [WCp^*Cl_3(NtBu)], [$MoCp^*C1Me_2$(NtBu)] and [WCp^*C1Me_2(NtBu)]. *Inrog. Chim. Acta.* **1998,** *273*, 270-278.

33. King, R. B.; Iqbal, M. Z.; King, A. J., Jr. Pentamethylcyclopentadienyl derivatives of transition metals: VI. Carbonylation of metal-metal tripple bonds: a high pressure infrared spectroscopic study. *J. Organomet. Chem.* **1979,** *15*, 53-63.

References Chapter 3

1. Laplaza, C. E.; Cummins, C. C. Dintrogen Cleavage by a 3-Coordinate Molybdenum(III) Complex. *Science* **1995,** *268*, 861-863.
2. Curley, J. J.; Sceats, E. L.; Cummins, C. C. A Cycle for Organic Nitrile Synthesis via Dinitrogen Cleavage. *J. Am. Chem. Soc.* **2006,** *128*, 14036-14037.
3. MacLeod, K. C.; Holland, P. L. Recent Developments in Homogeneous Dinitrogen Reduction by Molybdenum and Iron. *Nat. Chem.* **2013,** *5*, 559-565.
4. Nishibayashi, Y. E. *Topics in Organometallic Chemistry*. Springer Verlag: Berlin/Heidelberg, 2017; Vol. 60.
5. Buss, J. A.; Cheng, C.; Agapie, T. A Low-Valent Molybdenum Nitride Complex: Reduction Promotes Carbonylation Chemistry. *Angew. Chem. Int. Ed.* **2018,** *57*, 9670-9674.
6. Y., R.; Duboc, C.; Gennari M. Molecular Catalysts for N_2 Reduction :State of the Art, Mechanism, and Challenges. *Chem. Phys. Chem.* **2017,** *18*, 2606-2617.
7. Stucke, N.; Flöser, B. M.; Weirich, T.; Tuczek, F. Nitrogen Fixation Catalyzed by Transition Metal Complexes: Recent Developments. *Eur. J. Inorg. Chem.* **2018**, 1337–1355.
8. Liao, Q.; Cavaillé, A.; Saffon-Merceron, N.; Mézailles, N. Direct Synthesis of Silylamine from N_2 and a Silane Mediated by a Tridentate Phosphine Molybdenum Fragment. *Angew. Chem. Int. Ed.* **2016,** *55*, 11212-11216.
9. Shaver, M. P.; Fryzuk, M. D. Activation of molecular nitrogen: Coordination, cleavage and functionalization of N_2 mediated by metal complexes. *Adv. Synth. Catal.* **2003,** *345*, 1061-1076.
10. Gade, L. H.; P., M. New transition metal imido chemistry withdiamido-donor ligands. *Coord. Chem. Rev.* **2001,** *216-217*, 65–97.
11. Bezdek, M. J.; Chirik, P. J. Interconversion of Molybdenum Imido and Amido Complexes by Proton-Coupled Electron Transfer. *Angew. Chem. Int. Ed.* **2018,** *57*, 2224-2228.
12. Ishii, Y.; Tokunaga, S.; Seino, H.; Hidai, M. Synthesis of Tungsten (1-Pyridinio)imido Complexes: Facile N-N Bond Cleavage To Form Pyridine from Coordinated Dinitrogen. *Inorg. Chem.* **1996,** *35*, 5118-5119.
13. Dreher, A.; Meyer, S.; Näther, C.; Westphal, A.; Broda, H.; Sarkar, B.; Kiam, W.; Kurz, P.; Tuczek, F. Reduction and Protonation of Mo(IV) Imido Complexes with depe Coligands: Generation and Reactivity of a S = 1/2 Mo(III) Alkylnitrene Intermediate. *Inrog. Chem.* **2013,** *52*, 2335-2352.
14. Chatt, J.; Dilworth, J. R.; Richards, R. L. Recent advances in the chemistry of nitrogen fixation. *Chem. Rev.* **1978,** *78*, 589-625.
15. Stephan, G. C.; Sivasankar, C.; Studt, F.; Tuczek, F. Energetics and Mechanism of Ammonia Synthesis through the Chatt Cycle: Conditions for a Catalytic Mode and Comparison with the Schrock Cycle. *Chem. Eur. J.* **2007,** *14*, 644-652.

16. Chatt, J.; Pearman, A. J.; Richards, R. L. The reduction of mono-coordinated molecular nitrogen to ammonia in a protic environment. *Nature* **1975,** *253*, 39-40.
17. Alias, Y.; Ibrahim, S. K.; Queiros, M. A.; Fonseca, A.; Talarmin, J.; Volant, F.; Pickett, C. J. Electrochemistry of molybdenum imides: cleavage of molybdenum–nitrogen triple bonds to release ammonia or amines. *J. Chem. Soc. Dalton. Trans.* **1997,** *26*, 4807-4815.
18. Yandulov, R. R.; Schrock, R. R. Catalytic Reduction of Dinitrogen to Ammonia at a Single Molybdenum Center. *Science* **2003,** *301*, 67-78.
19. Suess, D. L. M.; Peters, J. C., H–H and Si–H Bond Addition to Fe≡NNR$_2$ Intermediates Derived from N$_2$. *J. Am. Chem. Soc.* **2013,** *135*, 4938-4941.
20. Klopsch, I.; Finger, M.; Wurtele, C.; Milde, B.; Werz, D. B.; Schneider, S. Dinitrogen Splitting and Functionalization in the Coordination Sphere of Rhenium. *J. Am. Chem. Soc.* **2014,** *136*, 6881-6883.
21. MacLeod, K. C.; McWilliams, S. F.; Mercado, B. Q.; Holland, P. L. Stepwise N-H bond formation from N2-derived iron nitride, imide and amide intermediates to ammonia. *Chem. Sci.* **2016,** *7*, 5736-5746.
22. Keane, A. J.; Farrell, W. S.; Yonke, B. L.; Zavalij, P. Y.; Sita, L. R. Metal-Mediated Production of Isocyanates, R$_3$EN=C=O from Dinitrogen, Carbon Dioxide, and R$_3$ECl. *Angew. Chem. Int. Ed.* **2015,** *54*, 10220-10224.
23. Yonke, B. L.; Reeds, J. P.; Fontaine, P. P.; Zavalij, P. Y.; Sita, L. R. Catalytic Production of Isocyanates via Orthogonal Atom and Group Transfers Employing a Shared Formal Group 6 M(II)/M(IV) Redox Cycle. *Organometallics* **2014,** *33*, 3239-3242.
24. Keane, A. J. Early Transition Metal Sutdies of Dintirogen Cleavage and Metal-Nitrogen Bond Reactivity towards catalytic N$_2$ Fixation. Ph.D. Dissertation, *University of Maryland*, College Park, MD, **2015**.
25. Duman, L. M.; Farrell, W. S.; Zavalij, P. Y.; Sita, L. R. Steric Switching from Photochemical to Thermal Reaction Pathways for Enhanced Efficiency in Metal-Mediated Nitrogen Fixation. *J. Am. Chem. Soc.* **2016,** *138*, 14856-14859.
26. Yonke, B. L.; Reeds, J. P.; Zavalij, P. Y.; Sita, L. R. Atom- and Group Transfers to M^{IV} Oxo and Imido Complexes, (η^5-C$_5$Me$_5$)M[N(*i*Pr)C(Me)N(*i*Pr)](E) (M = Mo, W; E = O, NSiMe$_3$): Orthogonal Generation of a M^{VI} Terminal Nitride via Inter-ligand Silyl Group Migration. *Z. Anorg. Allg. Chem.* **2014,** *641*, 61 - 64.
27. Duman, L. M.; Zavalij, P. Y.; Sita, L. R. An Intramolecular Mechanism for N$_2$ Cleavage in Dinuclear Mo and W CPAM/CPGU Complexes. *J. Am. Chem. Soc.* **2018,** *In Preperation*.
28. Connelly, N. G.; Gieger, W. E. Chemical Redox Agents for Organometallic Chemistry. *Chem. Rev.* **1996,** *96*, 877-910.
29. Eaborn, C.; Jackson, R. A.; Walsingham, R. W. Organosilicon compounds. Part XLI. The reaction of bis(trimethylsilyl)mercury with some ethers. *J. Chem. Soc. C.* **1967,** *0*, 2188-2191
30. Blayney, M. B.; Winn, J. S.; Nierenberg, D. W. Handling dimethylmercury. *Chemical and Engineering News* **1997**.
31. Fontaine, P. P.; Yonke, B. L.; Zavalij, P. Y.; Sita, L. R. Dinitrogen Complexation and Extent of N≡N Activation within the Group 6 "End-On-Bridged"

Dinuclear Complexes, {(η^5-C_5Me_5)M N(i-Pr)C(Me)N(i-Pr)}$_2$(μ-η^1:η^1-N_2) (M = Mo and W). *J. Am. Chem. Soc.* **2010,** *132*, 12273-12285.
32. Tarkhanova, I. G.; Gantman, M. G.; Chizhov, A. O.; Smirnov, V. V. Addition of tetrachloromethane to oct-1-ene initiated by amino alcohols. *Russ. Chem. Bull., Int. Ed.* **2006,** *55*, 1624-1630.
33. Saeki, A.; Yamamoto, N.; Yoshida, Y.; Kozawa, T., Geminate Charge Recombination in Liquid Alkane with Concentrated CCl_4: Effects of CCl_4 Radical Anion and Narrowing of Initial Distribution of Cl-. *J. Phys. Chem. A.* **2011,** *115*, 10166-10173.
34. Nair, R. P.; Kim, T. H.; Frost, B. J., Atom Transfer Radical Addition Reactions of CCl_4, $CHCl_3$, and p-Tosyl Chloride Catalyzed by Cp′Ru(PPh_3)(PR_3)Cl Complexes. **2009,** *28*, 4681-4688.
35. Zanella, R.; Ros, R.; Grazian, M. Sulfur-sulfur bond cleavage promoted by palladium(0) and Platinum(0) triphenylphosphine complexes. *Inorg. Chem.* **1973,** *12*, 2736-2738.
36. Blower, P. J.; Dilworth, J. R. Thioalto-Complexes of the Transition Metals. *Coord. Chem. Rev.* **1987,** *76*, 121-185.
37. Hossain, M. M.; Lin, H.-M.; Zhu, J.; Lin, Z.; Shyu, S.-G. Activation of the S-S Bonds of Alkyl Disulfides RSSR (R) Me, Et, Pr, Bun) by Heterodinuclear Phosphido-Bridged CpW$(CO)_2$(μ-PPh_2)Mo$(CO)_5$. *Organometallics* **2006,** *25*, 440-446.
38. Aubart, M. A.; Bergman, R. G. Reaction of Organic Disulfides with Cobalt-Centered Metal Radicals. Use of the E- and C-Based Dual-Parameter Substituent Model and Quantitative Solvent Effect Analyses To Compare Outer-Sphere and Inner-Sphere Electron-Transfer Processes. *J. Am. Chem. Soc.* **1998,** *120*, 8755-8766.
39. Eaborn, C.; Jackson, R. A.; Walsingham, R. Organosilicon compounds. Part XLI. The reaction of bis(trimethylsilyl)mercury with some ethers. **1967,** *0*, 2188-2191.

References Chapter 4

1. Tanabe, Y.; Nishibayashi, Y. Catalytic Dinitrogen Fixation to Form Ammonia at Ambient Reaction Conditions Using Transition Metal-Dinitrogen Complexes. **2016,** *16*, 1549-1577.
2. Nishibayashi, Y. E. *Topics in Organometallic Chemistry*. Springer Verlag: Berlin/Heidelberg, **2017**; Vol. 60.
3. MacLeod, K. C.; Holland, P. L. Recent Developments in Homogeneous Dinitrogen Reduction by Molybdenum and Iron. *Nat. Chem.* **2013,** *5*, 559-565.
4. Curley, J. J.; Sceats, E. L.; Cummins, C. C. A Cycle for Organic Nitrile Synthesis via Dinitrogen Cleavage. *J. Am. Chem. Soc.* **2006,** *128*, 14036-14037.
5. Keane, A. J. Early Transition Metal Studies of Dintrogen Cleavage and Metal-Nitrogen Bond Reactivity towards Catalytic N_2 Fixation. *Ph.D. Dissertation, University of Maryland*, College Park, MD, **2015**.
6. Keane, A. J.; Farrell, W. S.; Yonke, B. L.; Zavalij, P. Y.; Sita, L. R. Metal-Mediated Production of Isocyanates, $R_3EN{=}C{=}O$ from Dinitrogen, Carbon Dioxide, and R_3ECl. *Angew. Chem. Int. Ed.* **2015,** *54*, 10220-10224.

7. Shiina, K., Reductive silylation of molecular nitrogen via fixation to tris(trialkylsilyl)amine. *J. Am. Chem. Soc.* **1972,** *94*, 9266-9267.
8. Komori, K.; Oshita, H.; Mizobe, Y.; Hidai, M. Preparation and properties of molybdenum and tungsten dinitrogen complexes. 25. Catalytic conversion of molecular nitrogen into silylamines using molybdenum and tungsten dinitrogen complexes. *J. Am. Chem. Soc.* **1989,** *111*, 1939-1940.
9. Komori, K.; Sugura, S.; Mizobe, Y.; Yamada, M.; Hidai, M. Preparation and properties of molybdenum and tungsten dinitrogen complexes. 26. Syntheses and some reactions of trimethylsilylated dinitrogen complexes of tungsten and molybdenum. *Bull. Chem. Soc. Jpn.* **1989,** *62*, 2953-3959.
10. Oshita, H.; Mizobe, Y.; Hidai, M. Preparation and properties of molybdenum and tungsten dinitrogen complexes. XLI. Silylation and germylation of a coordinated dinitrogen in cis-$[M(N_2)_2(PMe_2Ph)_4]$ (M = Mo, W) using R_3ECl/NaI and R_3ECl/Na mixtures (E = Si, Ge). X-ray structure of trans-$[WI(NNGePh_3)(PMe_2Ph)_4]\cdot C_6H_6$. *Organomet. Chem.* **1993,** *456*, 213-220.
11. Kawaguchi, M.; Hamaoka, S.; Mori, M. Incorporation of molecular nitrogen into organic compounds. Titanium catalyzed nitrogenation. *Tetrahedron. Lett.* **1993,** *34*, 6907-6910.
12. Mori, M.; Kawaguchi, M.; Hori, M.; Hamaoka, S. Incorperation ofr Molecular Nitrogen into Organic-Compounds – Titanium Catalyzed Nitrogenation. *Heterocycles* **1994,** *39*, 729-739.
13. Hidai, M.; Mizobe, Y., Recent Advances in the Chemistry of Dinitrogen Complexes. *Chem. Rev.* **1995,** *95*, 1115-1133.
14. Mori, M. Activation of nitrogen for organic synthesis. *J. Organomet. Chem.* **2004,** *689*, 4210-4227.
15. Mori, M. Synthesis of Nitrgoen Heterocycles Utilizing Molecular Nitrogen as a Nitrogen Source and Attempt to use Air instead of Nitrogen Gas. *Heterocycles* **2009,** *78*, 281-318.
16. Tanaka, H.; Sasada, A.; Kouno, T.; Yuki, M.; Miyake, Y.; Nakanishi, H.; Nishibayashi, Y.; Yoshizawa, K. Molybdenum-Catalyzed Transformation of Molecular Dinitrogen into Silylamine: Experimental and DFT Study on the Remarkable Role of Ferrocenyldiphosphine Ligands. *J. Am. Chem. Soc.* **2011,** *133*, 3498-3506.
17. Yuki, M.; Tanaka, H.; Sasaki, K.; Miyake, Y.; Yoshizawa, K.; Nishibayashi, Y. Iron-catalysed transformation of molecular dinitrogen into silylamine under ambient conditions. *Nat. Commun.* **2012,** *3*.
18. Ogawa, T.; Kajita, Y.; Wasada-Tsutsui, Y.; Wasada, H.; Masuda, H. Preparation, Characterization, and Reactivity of Dinitrogen Molybdenum Complexes with Bis(diphenylphosphino)amine Derivative Ligands that Form a Unique 4-Membered P-N-P Chelate Ring. *Inorganic Chemistry* **2013,** *52*, 182-195.
19. Miyazaki, T.; Tanaka, H.; Tanabe, Y.; Yuki, M.; Nakajima, K.; Yoshizawa, K.; Nishibayashi, Y. Cleavage and Formation of Molecular Dinitrogen in a Single System Assisted by Molybdenum Complexes Bearing Ferrocenyldiphosphine. *Angew. Chem. Int. Ed.* **2014,** *53* (43), 11488-11492.

20. Liao, Q.; Saffon-Merceron, N.; Mezailles, N., Catalytic Dinitrogen Reduction at the Molybdenum Center Promoted by a Bulky Tetradentate Phosphine Ligand. *Angew. Chem. Int. Ed.* **2014,** *53*, 14206-14210.
21. Liao, Q.; Saffon-Merceron, N.; Mezailles, N. N_2 Reduction into Silylamine at Tridentate Phosphine/Mo Center: Catalysis and Mechanistic Study. *Acs Catal.* **2015,** *5*, 6902-6906.
22. Ung, G.; Peters, J. C. Low-Temperature N_2 Binding to Two-Coordinate L_2Fe0 Enables Reductive Trapping of L_2FeN_2- and NH_3 Generation. *Angew. Chem. Int. Ed.* **2015,** *54* (2), 532-535.
23. Imayoshi, R.; Tanaka, H.; Matsuo, Y.; Yuki, M.; Nakajima, K.; Yoshizawa, K.; Nishibayashi, Y. Cobalt-Catalyzed Transformation of Molecular Dinitrogen into Silylamine under Ambient Reaction Conditions. *Chem. - Eur. J.* **2015,** *21*, 8905-8909.
24. Siedschlag, R. B.; Bernales, V.; Vogiatzis, K. D.; Planas, N.; Clouston, L. J.; Bill, E.; Gagliardi, L.; Lu, C. C. Catalytic Silylation of Dinitrogen with a Dicobalt Complex. *J. Am. Chem. Soc.* **2015,** *137*, 4638-4641.
25. Cammarota, R. C.; Clouston, L. J.; Lu, C. C. Leveraging molecular metal-support interactions for H_2 and N_2 activation. *Coord. Chem. Rev.***2017,** *334*, 100-111.
26. Nishibayashi, Y.; Kuriyama, S.; Arashiba, K.; Nakajima, K.; Tanaka, H.; Yoshizawa, K. Azaferrocene-Based PNP-type Pincer Ligand: Synthesis of Molybdenum, Chromium, and Iron Complexes and Reactivity toward Nitrogen Fixation. *Eur. J. Inorg. Chem.* **2016,** *30*, 4856-4861.
27. Imayoshi, R.; Nakajima, K.; Nishibayashi, Y. Vanadium-catalyzed reduction of molecular dinitrogen into silylamine under ambient reaction conditions. *Chem. Lett.* **2017,** *46*, 466-468.
28. Araake, R.; Sakadani, K.; Tada, M.; Sakai, Y.; Ohki, Y. $[Fe_4]$ and $[Fe_6]$ Hydride Clusters Supported by Phosphines: Synthesis, Characterization, and Application in N_2 Reduction. *J. Am. Chem. Soc.* **2017,** *139*, 5596-5606.
29. Prokopchuk, D. E.; Wiedner, E. S.; Walter, E. D.; Popescu, C. V.; Piro, N. A.; Kassel, W. S.; Bullock, R. M.; Mock, M. T. Catalytic N_2 Reduction to Silylamines and Thermodynamics of N_2 Binding at Square Planar Fe. *J. Am. Chem. Soc.* **2017,** *139*, 9291-9301.
30. Imayoshi, R.; Nakajima, K.; Takaya, J.; Iwasawa, N.; Nishibayashi, Y. Synthesis and Reactivity of Iron- and Cobalt-Dinitrogen Complexes Bearing PSiP-Type Pincer Ligands toward Nitrogen Fixation. *Eur. J. Inrog. Chem.* **2017,** *32*, 3769-3778.
31. Suzuki, T.; Fujimoto, K.; Takemoto, Y.; Wasada-Tsutsui, Y.; Ozawa, T.; Inomata, T.; Fryzuk, M.; Masuada, H. Efficient Catalytic Conversion of Dinitrogen to $N(SiMe_3)_3$ Using a Homogeneous Mononuclear Cobalt Complex. *ACS Catal.* **2018,** *8*, 3011-3015.
32. Kendall, A. J.; Johnson, S. I.; Bullock, R. M.; Mock, M. T. Catalytic Silylation of N_2 and Synthesis of NH_3 and N_2H_4 by Net Hydrogen Atom Transfer Reactions Using a Chromium P_4 Macrocycle. *J. Am. Chem. Soc.* **2018,** *140*, 2528-2536.
33. Gao, Y.; Li, G.; Deng, L. Bis(dinitrogen)cobalt(-1) Complexes with NHC Ligation: Synthesis, Characterization, and Their Dinitrogen Functionalization

Reactions Affording Side-on Bound Diazene Complexes. *J. Am. Chem. Soc.* **2018,** *140*, 2239-2250.
34. Ferreira, R. B.; Cook, B. J.; Knight, B. J.; Catalano, V. J.; Garcia-Serres, R.; Murray, L. J. Catalytic Silylation of Dinitrogen by a Family of Triiron Complexes. *ACS Catal.* **2018,** *8*, 7208-7212.
35. Piascik, A. D.; Li, R.; Wilkinson, H. J.; Green, J. C.; Ashley, A. E. Fe-Catalyzed Conversion of N_2 to $N(SiMe_3)_3$ via an Fe-Hydrazido Resting State. *J. Am. Chem. Soc.* **2018,** *140*, 10691-10694.
36. Burford, R. J.; Fryzuk, M. D. Examining the relationship between coordination mode and reactivity of dinitrogen. *Nat. Rev. Chem.* **2017,** *1*, 26.
37. Yonke, B. Y.; Reeds, J. P.; Zavalij, P. Y.; Sita, L. R., Catalytic Degenerate and Nondegenerate Oxygen Atom Transfers Employing N_2O and CO_2 and a MII /MIV Cycle Mediated by Group 6 MIV Terminal Oxo Complexes. *Angew. Chem. Int. Ed.* **2011,** *50*, 12342-12346.
38. Wang, W. D.; Guzei, I. A.; Espenson, J. H. Hydrolysis, Hydrosulfidolysis, and Aminolysis of Imido(methyl)rhenium Complexes. *Inorg. Chem.* **2000,** *39*, 4107-4112.
39. Hayton, T. W.; Boncella, J. M.; Scott, B. L.; Batista, E. R. Exchange of an Imido Ligand in Bis(imido) Complexes of Uranium. *J. Am. Chem. Soc.* **2006,** *128*, 12622-12623.
40. Michelman, R. I.; Anderson, R. A.; Bergman, R. G. Preparation of monomeric (η^6-arene)OsNR complexes and their exchange reactions with amines, alcohols, and thiols. *J. Am. Chem. Soc.* **1991,** *113*, 5100-5102.
41. Swallow, D.; McInnes, J. M.; Mountford, P. Titanium imido complexes with tetraaza macrocyclic ligands. *J. Chem. Soc., Dalton. Trans.* **1998**, 2253-2260.
42. Chandrasekhar, V.; Boomishankar, R.; Nagendran, S. Recent Developments in the Synthesis and Structure of Organosilanols. *Chem. Rev.* **2004,** *104*, 5847-5910.
43. Lappert, M.; Protchenko, A.; Power, P.; Seeber, A. *Metal Amide Chemistry*. John Wiley & Sons: Chichester, **2009**.
44. Gray, M.; Snieckus, V.; Lebel, H. Lithium hexamethyldisilazane. In *Handbook of Reagents for Organic Synthesis: Reagents for Silocon-Mediated Organic Synthesis*, John Wiley & Sons: Chichester, **2011**.
45. Chandrasekhar, V.; Boomishankar, R.; Nagendran, S. Recent developments in the synthesis and structure of organosilanols. *Chem. Rev.* **2004,** *104*, 5847-5910.
46. Duman, L. M.; Sita, L. R. Closing the Loop on Transition-Metal-Mediated Nitrogen Fixation: Chemoselective Production of $HN(SiMe_3)_2$ from N_2, Me_3SiCl, and X—OH (X = R, R_3Si, or Silica Gel). *J. Am. Chem. Soc.* **2017,** *139*, 17241-17244.
47. van Look, G. *Silylating Agents Derivatization Reagents Protecting-Group Reagents Organosilicon Compounds Analytical Applications Synthetic Applications*. Fluka Chimie AG: Buchs, Switzerland, **1995**.
48. Cao, C.; Fadeev, A. Y.; McCarthy, T. J. Reactions of Organosilanes with Silica Surfaces in Carbon Dioxide. *Langmuir* **2001,** *17*, 757-561.
49. Eikey, R. A.; Abu-Omar, M. M. Nitrido and imido transition metal complexes of Groups 6-8. *Cood. Chem. Rev.* **2003,** *243*, 83-124.
50. Garcia-Viloca, M.; Gelabert, R.; Gonzales-Lafont, A.; Moreno, M.; Lluch, J. M. Temperature Dependence of Proton NMR Chemical Shift As a Criterion To Identify Low-Barrier Hydrogen Bonds. *J. Am. Chem. Soc.* **1998**, 10203-10209.

51. Muller, N.; Reiter, R. C., Temperature Dependence of Chemical Shifts of Protons in Hydrogen Bonds. *J. Chem. Phys.* **1965,** *42*, 3265-3269.
52. Kleckner, I. R.; Foster, M. P. An introduction to NMR-based approaches for measuring protein dynamics. *Biochimica et Biophysica Acta* **2011,** *1814*, 942-968.
53. von Kugelgen, S.; Bellone, D.; Cloke, R. R.; Perkins, W.; Fischer, F. R. Initiator Control of Conjugated Polymer Topology in Ring-Opening Alkyne Metathesis Polymerization. *J. Am. Chem. Soc.* **2016,** *138*, 6234 – 6239.
54. Park, S. Y.; Lee, J.-W.; Song, C. W. Parts-per-million level loading organocatalysed enantioselective silylation of alcohols. *Nat. Chem.* **2015,** *6*, 7512.
55. Armitage, D. A. Organosilanes. In *Comprehensive Organometallic Chemistry*, Queen Elizabeth College, University of London: London, **1982**.
56. Shively, S.; Miller, W. R. The use of HMDS (hexamethyldisilazane) to Replace Critical Point Drying (CPD) in the Preparation of Tardigrades for SEM (Scanning Electron Microscope) Imaging. *Trans. Kans. Acad. Sci.* **2009,** *112*, 198-200.

References Chapter 5

1. Shin, J. H.; Chruchill, D. G.; Bridgewater, B. M.; Pang, K.; Parkin, G. Hydride, halide, methyl, carbonyl, and chalcogenido derivatives of permethylmolybdenocene. *Inorg. Chim. Acta.* **2006,** *259*, 2942-2955.
2. Calhorda, J. M.; Carrondo, M. A. A. F. d. C. T.; Doas, A. R.; Galvao, A. M.; Garcia, A. M.; Martins, A. M.; Minas de Piedade, M. E.; Pinheiro, C. I.; Ramao, C. C.; Simoes, J. A. M.; Veiros, L. F. Syntheses, electrochemistry, and bonding of bis(cyclopentadienyl)molybdenum alkyl complexes. Molecular structure of $Mo(\eta^5\text{-}C_5H_5)_2(C_4H_9)_2$. Thermochemistry of $Mo(\eta^5\text{-}C_5H_5)_2R_2$and $Mo(\eta^5\text{-}C_5H_5)_2L$ (R = CH_3, C_2H_5, C_4H_9; L = ethylene, diphenylacetylene). *Organometallics* **1991,** *10*, 483 - 494.
3. Roddick, D. M.; Fryzuk, M. D.; Seidler, P. F.; Hillhouse, G. L.; Bercaw, J. E. Halide, Hydride, Alkyl, and Dinitrogen Complexes of Bis(pentamethylcyclopentadienyl)hafnium. *Organometallics* **1985,** *4*, 97-104.
4. Bernskoetter, W. H.; Olmos, A. V.; Lobkovsky, E.; Chirik, P. J. N_2 Hydrogenation Promoted by a Side-On Bound Hafnocene Dinitrogen Complex. *Organometallics* **2006,** *25*, 1021-1027.
5. Fryzuk, M. D.; Corkin, J. R.; Patrick, B. O. Reduction of hafnium(IV) complexes in the presence of molecular nitrogen: Attempts to form dinitrogen complexes of the heaviest group 4 element. *Can. J. Chem.* **2003,** *81*.
6. Uhl, W.; Appelt, C.; Wollschlanger, A.; Hepp, A.; Wurthwein, E. An Al/P-Based Frustrated Lewis Pair as an Efficient Ambiphilic Ligand: Coordination of Boron Trihalides, Rearrangement, and Formation of HBX_2 Complexes (X = Br, I). *Inorg. Chem.* **2014,** *53*, 8991-8999.
7. Arashiba, K.; Eizawa, A.; Tanaka, H.; Nakajima, K.; Yoshizawa, K.; Nishibayashi, Y. Catalytic Nitrogen Fixation via Direct Cleavage of Nitrogen – Nitrogen Triple Bond of Molecular Dinitrogen under Ambient Reaction Conditions. *Bull. Chem. Soc. Jpn.* **2017,** *90*, 1111-1118.

8. Chojnowski, J.; Crpryk, M.; Michalski, J. The mechanism of the reaction of organic phosphites with triakylsilyl iodide. Iodoanhydrides of P^{III} acids as intermediates. *215* **1981**, 355-365.
9. Baer, J. L. Investigating the Pentamethylcyclopentadienyl Amidinate (CPAM) Ligand Set via Synthesis and Characterization of a Variety of Group 4, 5, and 6 Metal-Organic Complexes for uses in Polymerization and Small Molecule Activation. *B.S. Dissertation, University of Maryland,* College Park, MD, **2018**.
10. Arashiba, K.; Miyake, Y.; Nishibayashi, Y. A molybdenum complex bearing PNP-type pincer ligands leads to the catalytic reduction of dinitrogen into ammonia. *Nat. Chem.* **2011,** *3*, 120-125.
11. Eizawa, A.; Arashiba, K.; Tanaka, H.; Kuriyama, S.; Matsuo, Y.; Nakajima, K.; Yoshizawa, K.; Nishibayashi, Y. Remarkable catalytic activity of dinitrogen-bridged dimolybdenum complexes bearing NHC-based PCP-pincer ligands toward nitrogen fixation. *Nat. Chem.* **2017,** *8*, 14874.
12. Anderson, J. S.; Rittle, J.; Peters, J. C. Catalytic conversion of nitrogen to ammonia by an iron model complex. *Nature* **2013,** *501*, 84-87.
13. Chalkley, M. J.; Del Castillo, T. J.; Matson, B. D.; Roddy, J. P.; Peters, J. C. Catalytic N_2-to-NH_3 Conversion by Fe at Lower Driving Force: A Proposed Role for Metallocene-Mediated PCET. *ACS Cent. Sci.* **2017,** *3*, 217-223.
14. Wickramasinghe, L. A.; Ogawa, T.; Schrock, R. R.; Müller, P. Reduction of Dinitrogen to Ammonia Catalyzed by Molybdenum Diamido Complexes. *J. Am. Chem. Soc.* **2017,** *139*, 9132-9135.
15. Yandulov, R. R.; Schrock, R. R. Catalytic Reduction of Dinitrogen to Ammonia at a Single Molybdenum Center. *Science* **2003,** *301*, 67-78.
16. Hirotsu, M.; Fontaine, P. P.; Zavalij, P. Y.; Sita, L. R. Extreme N equivalent to N bond elongation and facile N-atom functionalization reactions within two structurally versatile new families of group 4 bimetallic "Side-on-Bridged" dimitrogen complexes for zirconium and hafnium *J. Am. Chem. Soc.* **2007,** *129*, 12690-12692.
17. Keane, A. J.; Yonke, B. L.; Hirotsu, M.; Zavalij, P. Y.; Sita, L. R. Fine-Tuning the Energy Barrier for Metal-Mediated Dinitrogen N≡N Bond Cleavage. *J. Am. Chem. Soc.* **2014,** *136*, 9906-9909.
18. Fontaine, P. P.; Yonke, B. L.; Zavalij, P. Y.; Sita, L. R. Dinitrogen Complexation and Extent of N≡N Activation within the Group 6 "End-On-Bridged" Dinuclear Complexes, $\{(\eta^5\text{-}C_5Me_5)M\ N(i\text{-}Pr)C(Me)N(i\text{-}Pr)\}_2(\mu\text{-}\eta^1\text{:}\eta^1\text{-}N_2)$ (M = Mo and W). *J. Am. Chem. Soc.* **2010,** *132*, 12273-12285.
19. Connelly, N. G.; Gieger, W. E. Chemical Redox Agents for Organometallic Chemistry. *Chem. Rev.* **1996,** *96*, 877-910.
20. Keane, A. J.; Farrell, W. S.; Yonke, B. L.; Zavalij, P. Y.; Sita, L. R. Metal-Mediated Production of Isocyanates, $R_3EN{=}C{=}O$ from Dinitrogen, Carbon Dioxide, and R_3ECl. *Angew. Chem. Int. Ed.* **2015,** *54*, 10220-10224.
21. Duman, L. M.; Farrell, W. S.; Zavalij, P. Y.; Sita, L. R. Steric Switching from Photochemical to Thermal Reaction Pathways for Enhanced Efficiency in Metal-Mediated Nitrogen Fixation. *J. Am. Chem. Soc.* **2016,** *138*, 14856-14859.

22. Namy, J. L.; Girard, P.; Kagan, H. B. A new preparation of some divalent lanthanide iodides and their usefulness in organic synthesis *Nouv. J Chim.* **1977,** *1*.
23. Girard, P.; Namy, J. L.; Kagan, H. B. Divalent lanthanide derivatives in organic synthesis. 1. Mild preparation of samarium iodide and ytterbium iodide and their use as reducing or coupling agents. *J. Am. Chem. Soc.* **1980,** *102*, 2693-2698.
24. Kagan, H. B.; Namy, J. L. Lanthanides in organic synthesis. *Tetrahedron* **1986,** *42*, 6573-6614.
25. Gopalaiah, K.; Kagan, H. B. Use of samarium diiodide in the field of asymmetric synthesis. *New J. Chem.* **2008,** *32*, 607-637.
26. Nicalaou, K. C.; Ellery, S. P.; Chen, J. S. Samarium diiodide mediated reactions in total synthesis. *Angew. Chem. Int. Ed.* **2009,** *48*, 7140-7165.
27. Yoshimura, A.; Saeki, R.; Nomoto, A.; Ogawa, A. Pinacol couplings of a series of aldehydes and ketones with SmI_2/Sm/Me_3SiCl in DME. *Tetrahedron* **2015,** *71*, 5347-5355.
28. Inanaga, J.; Ishikawa, M.; Yamaguchi, M. A mild and convenient method for the reduction of organic halides by using a samarium diiodide-THF solution in the presence of hexamethylphosphoric triamide (HMPA). *Chem. Lett.* **1987**, 1485-1486.
29. Prasad, E.; Knettle, B. W.; Flowers, R. A., II. The Role of Ligand Displacement in Sm(II)-HMPA-Based Reductions. *J. Am. Chem. Soc.* **2004,** *126*, 6891-6894.
30. Lautens, M.; Ren, Y. Chlorotrimethylsilane as an Activating Reagent in the Samarium-Promoted Cyclopropanation of Allylic and α-Allenic Alcohols. *J. Org. Chem.* **1996,** *61*, 2210-2214.
31. Szostak, M.; Spain, M.; Procter, D. J. Determination of the Effective Redox Potentials of SmI_2, $SmBr_2$, $SmCl_2$, and their Complexes with Water by Reduction of Aromatic Hydrocarbons. Reduction of Anthracene and Stilbene by Samarium(II) Iodide-Water Complex. *J. Org. Chem.* **2014,** *79*, 2522-2537.
32. Maity, S.; Hoz, S. Deciphering a 20-Year-Old Conundrum: The Mechanisms of Reduction by the Water/Amine/SmI_2 Mixture. *Chem. Eur. J.* **2015,** *21*, 18394-18400.
33. Sun, L.; Mellah, M. Efficient Electrosynthesis of $SmCl_2$, $SmBr_2$, and $Sm(OTf)_2$ from a "Sacrificial" Samarium Anode: Effect of nBu_4NPF_6 on the Reactivity. **2014,** *33*, 4625-4628.
34. Huang, Y.; Zhang, Y.; Wang, Y., Facile reduction of azides to the corresponding amines with metallic samarium and catalytic amount of iodine. *Tetrahedron Lett.* **1997,** *38*, 1065-1066.
35. Ogawa, A.; Takami, N.; Sekiguchi, M.; Ryu, I.; Kambe, N.; Sonoda, N. The first deoxygenative coupling of amides by an unprecedented samarium/samarium diiodide system. *J. Am. Chem. Soc.* **1992,** *114*, 8729-8730.
36. Chauvin, Y.; Olivier, H.; Saussine, L. Addition reaction of some rare earth metals to unsaturated compounds in ethers. *Inorg. Chim. Acta.* **1989,** *161*, 45-47.
37. Hatita, H.; Anaka, Y.; Hiyama, T. A novel reduction of zinc(II) chloride with samarium metal and its application to silylation of 1-alkynes. *Synlett* **1996,** *7*, 637-639.

38. Li, Z.; Iida, K.; Tomisaka, Y.; Yoshimura, A.; Hiaro, T.; Nomoto, A.; Ogawa, A. New Entry to the Construction of Si-Si Linkages: Sm/SmI_2-Induced Efficient Reductive Coupling of Organochlorosilanes. *Organometallics* **2007,** *26*, 1212-1216.
39. Liu, Y.; Xiao, S.; Qi, Y.; Du, F. Reductive Homocoupling of Organohalides Using Nickel(II) Chloride and Samarium Metal. *Chem. Asian J.* **2017,** *12*, 673-678.
40. Lee, C. C.; Hu, Y.; Ribbe, M. W. Catalytic Reduction of CN-, CO, and CO_2 by Nitrogenase Cofactors in Lanthanide-Driven Reactions. *Angew. Chem. Int. Ed.* **2015,** *54*, 1219-1222.
41. Sickerman, N. S.; Tanifuji, K.; Lee, C. C.; Ohki, Y.; Tatsumi, K.; RIbbe, M. W.; Hu, Y. Reduction of C1 Substrates to Hydrocarbons by the Homometallic Precursor and Synthetic Mimic of the Nitrogenase Cofactor. *J. Am. Chem. Soc.* **2017,** *139*, 603-606.
42. Jubb, J.; Gambarotta, S. Dinitrogen Reduction Operated by a Samarium Macrocyclic Complex. Encapsulation of Dinitrogen into a Sm_2Li_4 Metallic Cage. *J. Am. Chem. Soc.* **1994,** *116*, 4477-4478.
43. Evans, W. J.; Ulibarri, T. A.; Ziller, J. W. Isolation and x-ray crystal structure of the first dinitrogen complex of an f-element metal, $[(C_5Me_5)_2Sm]_2N_2$. *J. Am. Chem. Soc.* **1988,** *110*.
44. Guillemot, G.; Castellano, B.; Prange, T.; Solari, E.; Floriani, C. Use of Calix[4]arenes in the Redox Chemistry of Lanthanides: the Reduction of Dinitrogen by a Calix[4]arene-Samarium Complex. *Inorg. Chem.* **2007,** *46*, 5152-5154.
45. Dube, T.; Conochi, S.; Gambarotta, S.; Yap, G. P.; Vasapollo, G. Tetrametallic reduction of dinitrogen: formation of a tetranuclear samarium dinitrogen complex. *Angew. Chem. Int. Ed.* **1999,** *38*, 3657-3659.
46. Evans, W. J.; Lee, D. S. Early developments in lanthanide-based dinitrogen reduction chemistry. *Can. J. Chem.* **2005,** *83*, 375-384.
47. Duman, L. M.; Sita, L. R., 'Greener' Nitrogen Fixation: Samarium Metal Reduction of CPAM Group 6 Metal Halides in the Presence of N_2, Me_3SiCl, and Alcohols. *ChemComm* **2018,** *In Preperation*.
48. Proctor, D. J.; Flowers, R. A. I.; Skrydstrup; T. *Organic Synthesis Using Samarium Diiodide: A Practical Guide*. RSC Publishing: Cambridge, 2009.
49. Szostak, M.; Procter, D. J. Beyond Samarium Diiodide: Vistas in Reductive Chemistry Mediated by Lanthanides(II). *Angew. Chem. Int. Ed.* **2012,** *51*, 9238-9256.
50. Szostak, M.; Spain, M.; Procter, D. J. Recent advances in the chemoselective reduction of functional groups mediated by samarium(II) iodide: a single electron transfer approach. *Chem. Soc. Rev.* **2013,** *42*, 9155-9183.
51. Chaney, A. L.; Marbach, E. P. Modified Reagents for Determination of Urea and Ammonia. *Clin. Chem.* **1962,** *8*, 130-132.
52. Bolleter, W. T.; Bushman, C. J.; Tidwell, P. W. Spectroscopic determination of ammonia as indophenol. *Anal. Chem.* **1961,** *33*, 592-594.
53. Verdouw, H.; Van Echteld, C. J. A.; Dekkers, E. M. J. Ammonia determination based on indophenol formation with sodium salicylate. *Water Research* **1978,** *12*, 399-402.
54. Sekiguchi, Y.; Arashiba, K.; Eizawa, A.; Nakajima, K.; Nishibayashi, Y.; Tanaka, H.; Yoshizawa, K. Catalytic Reduction of Molecular Dinitrogen to Ammonia

and Hydrazine Using Vanadium Complexes. *Angew. Chem. Int. Ed.* **2818,** *57*, 9064-9068.

References Chapter 6

1. Duman, L. M.; Farrell, W. S.; Zavalij, P. Y.; Sita, L. R. Steric Switching from Photochemical to Thermal Reaction Pathways for Enhanced Efficiency in Metal-Mediated Nitrogen Fixation. *J. Am. Chem. Soc.* **2016,** *138*, 14856-14859.
2. Duman, L. M.; Zavalij, P. Y.; Sita, L. R. An Intramolecular Mechanism for N_2 Cleavage in Dinuclear Mo and W CPAM/CPGU Complexes. *J. Am. Chem. Soc.* **2018,** *In Preperation*.
3. Duman, L. M.; Sita, L. R. Closing the Loop on Transition-Metal-Mediated Nitrogen Fixation: Chemoselective Production of $HN(SiMe_3)_2$ from N_2, Me_3SiCl, and X-OH (X = R, R_3Si, or Silica Gel). *J. Am. Chem. Soc.* **2017,** *139*, 17241-17244.
4. Duman, L. M.; Sita, L. R., 'Greener' Nitrogen Fixation: Samarium Metal Reduction of CPAM Group 6 Metal Halides in the Presence of N_2, Me_3SiCl, and Alcohols. *Chem. Commun.* **2018,** *In Preperation*.
5. Wei, J.; Duman, L. M.; Redman, D. W.; Yonke, B., Zavalij P. Y.; Sita, L. R. N-Substituted Iminocaprolactams as Versatile and Low Cost Ligands in Group 4 Metal Initiators for the Living Coordinative Chain Transfer Polymerization of α-Olefins. *Organometallics* **2017,** *36*, 4202-4207.
6. Bishop, P. E.; Jarlenski, D. M. L.; Hetheringtons, D. R. Expression of an alternative nitrogen fixation system in Azotobacter vinelandii. *J. Bacteriol.* **1982,** *150*, 1244-1251.
7. Klopsch, I.; Finger, M.; Wurtele, C.; Milde, B.; Werz, D. B.; Schneider, S., Dinitrogen Splitting and Functionalization in the Coordination Sphere of Rhenium. *J. Am. Chem. Soc.* **2014,** *136*, 6881-6883.
8. Herrmann, W. A.; Floel, M.; Kulpe, J.; Felixberger, J. K.; Herdtweck, E. Organorhenium oxides and halides of the π -aromatic series: Syntheses and structures of important key compounds. *J. Organomet. Chem.* **1998**, 297-313.
9. *2017 Revision of World Population Prospects*; United Nations Population Division: **2017**.
10. Smil, V. *Enriching the Earth: Fritz Haber, Carl Bosch, and the Transformation of World Food Production*. MIT Press: Cambridge, MA, **2001**.
11. Galloway, J. N.; Townsend, A. R.; Erisman, J. W.; Bekunda, M.; Cai, Z.; Freney, J. R.; Matinelli, L. A.; Seitzinger, S. P.; Sutton, M. A. Transformation of the Nitrogen Cycle: Recent Trends, Questions, and Potential Solutions. *Science* **2008,** *320*, 889-892.
12. Hansen, B.; Thorling, L.; Schullehner, J.; Termansen, M.; Dalgaard, R. Groundwater nitrate response to sustainable nitrogen management. *Scientific Reports* **2017,** *7*, 1-12.

I figure I've done what I could do, more or less, and now I'm going back to being a chemical; all we are is a lot of talking nitrogen you know….

-Arthur Miller, *Danger: Memory!*